

**FUNCTIONAL CHARACTERIZATION AND SPATIAL AND TEMPORAL
PATTERNS OF EXPRESSION OF GENES INVOLVED IN GIBBERELLIN AND
DITERPENE RESIN ACID BIOSYNTHESIS IN WHITE SPRUCE**

by

Kathryn Madeleine Storey

B.Sc., The University of Ottawa, 2007

A THESIS SUBMITTED IN PARTIAL FULFILLMENT OF
THE REQUIREMENTS FOR THE DEGREE OF

DOCTOR OF PHILOSOPHY

in

The Faculty of Graduate and Postdoctoral Studies

(Botany)

THE UNIVERSITY OF BRITISH COLUMBIA
(Vancouver)

February 2016

©Kathryn Madeleine Storey, 2016

Abstract

Conifers produce large quantities of diterpene resin acids (DRAs) as major components of the constitutive and induced oleoresin defense system. Like all vascular plants, conifers also produce gibberellin (GA) diterpene phytohormones, which influence growth and development. Conifers thus provide an interesting biological system for comparing the GA and DRA diterpene biosynthetic pathways. Despite serving different functions in growth and defense, respectively, the GA and DRA biosynthetic pathways are biochemically similar, utilizing the same isoprenoid precursors, evolutionarily related diterpene synthases (diTPSs), and functionally similar cytochrome P450 monooxygenases (CYP450s) to produce structurally similar diterpene intermediates and diterpene acid products. Functional characterization of central diTPS genes (*ent*-copalyl diphosphate synthase [CPS], *ent*-kaurene synthase [KS], levopimaradiene/abietadiene synthase [LAS]) and CYP450 genes (*ent*-kaurene oxidase [CYP701] and CYP720B4) in white spruce (*Picea glauca*), described in this thesis, allowed for comparative analysis of GA and DRA pathway genes. This thesis characterized the DXS (1-deoxy-D-xylulose 5-phosphate synthase) gene family in white spruce as additional analysis of the isoprenoid biosynthetic pathway producing the common precursor to both GAs and DRAs. Transcript expression of genes was analyzed to understand their seasonal (year-long time course of apical bud and shoot development), sample-specific (e.g. needle, stem, bud, bark/phloem, wood/xylem), and stress-specific (methyl jasmonate [MeJA] exposure) spatial and temporal patterns. Functionality of the DRA pathway was also assessed via quantification of DRA products.

Expression of DRA and GA pathway genes was generally spatially separated. Expression of DRA genes was low in photosynthetic tissues but up-regulated during the time

of year when trees are most likely to encounter seasonal attack from insect pests; expression declined sharply well before dormancy showing a strong seasonality to DRA production. GA related genes had broader expression across sample types and throughout the year, but spatially were mainly allocated to photosynthetic tissues. GA and DRA pathway genes all showed differential responses to MeJA treatment, and within corresponding sample types, age also played a role in expression. These studies improve our understanding of the organization of conifer chemical defenses, showing distinct differences compared with GA gene expression, and providing information on the spatial, seasonal and stress-responsive expression of DRA pathway genes.

Preface

Plant material collection and treatment application in the experiment “Effects of methyl jasmonate treatment on diterpenoid production and gene expression over time”, detailed in section 2.6, was completed as a larger team effort with postdoctoral fellows: Katrin Geisler, Melissa Mageroy, Jose Celedon and Justin Whitehill of the Bohlmann laboratory. Diterpene resin acid extractions in wood/xylem samples were completed in tandem with Katrin Geisler. RNA extractions from wood/xylem samples were completed by Jose Celedon and Katrin Geisler. Volunteer undergraduate student Simone Asselin aided in completion of remaining diterpene resin acid extractions for this experiment.

The remaining work in this dissertation is original, unpublished, independent work by the author K.M. Storey.

Table of Contents

Abstract.....	ii
Preface	iv
Table of Contents.....	v
List of Tables	ix
List of Figures.....	xi
List of Abbreviations and Symbols	xiv
Acknowledgements.....	xviii
Dedication.....	xx
Chapter 1: Introduction.....	1
1.1. Diterpenoids in plant general and specialized metabolism.....	1
1.2. Enzymes involved in GA and DRA biosynthesis	7
1.2.1. Diterpene synthases	7
1.2.2. Cytochrome P450 monooxygenases	8
1.2.3. 1-Deoxy-D-xylulose 5-phosphate synthases.....	9
1.3. Characterized GA and DRA related genes & evolutionary relationships.....	12
1.4. Thesis objectives & hypotheses	16
Chapter 2: Materials and methods	21
2.1. Functional characterization of <i>PsCPS</i> , <i>PsKS</i> and <i>PgLAS</i>	21
2.1.1. Isolation of <i>LAS</i> cDNA sequence from white spruce, PCR amplification & preparation of protein construct	21
2.1.2. Preparation of Sitka spruce <i>CPS</i> and <i>KS</i> protein constructs	23
2.1.3. Heterologous protein expression and purification of <i>PsCPS</i> , <i>PsKS</i> and <i>PgLAS</i>	23
2.1.4. Gel electrophoresis and protein immunoblotting.....	24
2.1.5. DiTPS enzyme assays	25
2.1.6. GC-MS analysis of diTPS assay products	26
2.1.7. LC-MS analysis of <i>PgLAS</i> assay products.....	27
2.1.8. Phylogenetic analysis of diTPSs.....	28
2.2. Functional characterization of <i>PgCYP701</i>	28
2.2.1. Isolation of <i>CYP701</i> full-length cDNA from white spruce	28
2.2.2. Preparation of <i>PgCYP701</i> protein construct and yeast transformation	29
2.2.3. Preparation and purification of yeast microsomes.....	30
2.2.4. CYP450 carbon monoxide spectrum assay.....	31
2.2.5. <i>In vitro</i> CYP450 enzyme assays	31
2.2.6. GC-MS analysis	32
2.2.7. Diterpene standards and substrates	33
2.3. Functional characterization of <i>PgCYP720B4</i>	33
2.3.1. Isolation of <i>CYP720B4</i> full-length cDNA from white spruce	33
2.3.2. Preparation of <i>PgCYP720B4</i> protein construct and yeast transformation ...	33

2.3.3. Protein expression and <i>in vivo</i> enzyme assays.....	34
2.3.4. GC-MS analysis	35
2.3.5. Diterpene standards and substrates	35
2.3.6. Phylogenetic analysis of CYP450s.....	36
2.4. Functional characterization of <i>PgDXS1</i> , <i>PgDXS2A</i> and <i>PgDXS2B</i>	36
2.4.1. Isolation of <i>DXS1</i> , <i>DXS2A</i> and <i>DXS2B</i> cDNA from white spruce, PCR amplification & preparation of protein constructs	36
2.4.2. Heterologous <i>PgDXS</i> protein expression and purification.....	38
2.4.3. Gel electrophoresis and protein immunoblotting.....	38
2.4.4. <i>DXS in vitro</i> enzyme assays	38
2.4.5. LC-MS analysis	39
2.4.6. Phylogenetic analysis of <i>DXS</i> s.....	39
2.5. Vegetative white spruce apical bud development time course	40
2.5.1. Plant materials.....	40
2.5.2. Experimental treatment of plant materials.....	40
2.5.3. Extraction of diterpene resin acids (DRAs).....	44
2.5.4. Analysis of DRA metabolites by GC-MS.....	44
2.5.5. Statistical analysis of changes in DRA concentrations.....	46
2.5.6. Total RNA isolation.....	47
2.5.7. cDNA synthesis	48
2.5.8. Quantitative real-time PCR (qPCR) analysis.....	48
2.5.9. Statistical analysis of gene expression data	49
2.6. Effects of methyl jasmonate treatment on diterpenoid production and gene expression over time.....	51
2.6.1. Experimental treatment of plant materials.....	51
2.6.2. Extraction of DRAs	54
2.6.3. Analysis of DRA metabolites by GC-MS.....	54
2.6.4. Statistical analysis of changes in DRA concentrations.....	55
2.6.5. Total RNA isolation and cDNA synthesis	55
2.6.6. Quantitative real-time PCR analysis.....	56
2.6.7. Reference gene stability testing	58
2.6.8. Statistical analysis of gene expression data	61
Chapter 3: Functional characterization and comparison of expression of genes involved in gibberellin and diterpene resin acid biosynthesis in white spruce	62
3.1. Introduction.....	62
3.2. Results.....	66
3.2.1. Cloning, sequencing and identification of spruce diTPSs: CPS, KS and LAS.....	66
3.2.2. Heterologous expression and functional characterization of spruce diTPSs: CPS, KS and LAS.....	72

3.2.3. Cloning and identification of white spruce CYP450s: CYP701 and CYP720B4	80
3.2.4. Heterologous expression and functional characterization of white spruce CYP701 and CYP720B4.....	86
3.2.5. DRA concentrations in white spruce apical bud and developing apical shoots over time	91
3.2.6. DRA concentrations in dissected apical buds and shoots from selected times during apical bud development.....	94
3.2.7. Relative expression of GA and DRA biosynthetic genes in whole samples of developing spruce apical buds and shoots	98
3.2.8. Expression of genes involved in GA and DRA biosynthesis in stems, needles and new buds in spruce during apical bud and shoot development	103
3.2.9. Effect of MeJA treatment and time on DRA concentration in specific samples of white spruce	113
3.2.10. Effect of MeJA treatment and time on transcript abundance of DRA and GA biosynthetic genes in specific sample types of white spruce	125
3.3. Discussion	153
Chapter 4: Functional characterization and comparison of expression of <i>DXS</i> genes involved in gibberellin and diterpene resin acid biosynthesis in white spruce	169
4.1. Introduction	169
4.2. Results.....	171
4.2.1. Cloning and identification of spruce <i>DXS</i> genes	171
4.2.2. Heterologous expression and functional characterization of spruce <i>DXS</i> genes.....	176
4.2.3. Relative expression of general and specialized related <i>DXS</i> genes in whole samples of developing spruce apical buds and shoots.....	180
4.2.4. Expression of <i>DXS</i> genes in white spruce stems, needles and new buds during apical bud and shoot development	183
4.2.5. Effect of MeJA treatment and time on transcript abundance of <i>DXS</i> genes in different sample types of white spruce.....	190
4.3. Discussion	208
Chapter 5: Concluding discussion	218
5.1. Overview of thesis work	218
5.1.1. Development of apical buds and apical shoots over a calendar year of growth	220
5.1.2. Response of GA and DRA biosynthetic pathways to MeJA	222
5.2. Future research.....	224
References	228

Appendix 1.....	242
-----------------	-----

List of Tables

Table 2.1. Oligonucleotide primers used for <i>Pg</i> diTPS and CYP450 gene mining, cloning and qPCR analysis.	22
Table 2.2. Oligonucleotide primers used for <i>PgDXS</i> gene mining, cloning and qPCR analysis.	37
Table 2.3. Dates and corresponding time points for white spruce (<i>Pg653</i>) apical bud and shoot samples collected over a year-long period of vegetative bud development.....	43
Table 2.4. Oligonucleotide primers used for reference gene stability testing.	60
Table 3.1. Relative transcript abundance of diTPS and CYP450 genes related to DRA and GA biosynthesis in white spruce developing apical buds and shoots over a one-year time course.	100
Table 3.2. Statistical results based on analysis of relative transcript abundance of diTPS and CYP450 genes related to DRA and GA biosynthesis in white spruce developing apical buds and apical shoots over a year-long time course.	108
Table 3.3. Relative transcript abundance of diTPS and CYP450 genes related to DRA and GA biosynthesis in white spruce developing apical buds and shoots over a year-long time course.....	109
Table 3.4. Statistical results based on analysis of DRA abundance in control or MeJA-treated samples from white spruce over a time course.	115
Table 3.5. Mean DRA concentrations and statistical results in different samples from white spruce over time.	117
Table 3.6. Mean DRA concentrations in control and MeJA-treated samples from white spruce.	120
Table 3.7. DRA concentrations in control and MeJA-treated samples from white spruce.	124
Table 3.8. Statistical results based on analysis of relative transcript abundance of diTPS and CYP450 genes related to DRA and GA biosynthesis in control or MeJA-treated samples from white spruce.	127
Table 3.9. Relative transcript abundance of <i>PgCPS</i> in control or MeJA-treated samples from white spruce.	132
Table 3.10. Relative transcript abundance of <i>PgKS</i> in control or MeJA-treated samples from white spruce.	136
Table 3.11. Relative transcript abundance of <i>PgLAS</i> in control or MeJA-treated samples from white spruce.	141

Table 3.12. Relative transcript abundance of <i>PgCY701</i> in control or MeJA-treated samples from white spruce.	146
Table 3.13. Relative transcript abundance of <i>PgCYP720B4</i> in control or MeJA-treated samples from white spruce.	151
Table 4.1. Relative transcript abundance of <i>DXS</i> genes related to DRA and GA biosynthesis in white spruce developing apical buds and shoots over a year-long time course.	182
Table 4.2. Statistical results based on analysis of relative transcript abundance of <i>DXS</i> genes in white spruce developing apical buds and apical shoots over a year-long time course.	187
Table 4.3. Relative transcript abundance of <i>DXS</i> genes in white spruce developing apical buds and shoots over a year-long time course.	188
Table 4.4. Statistical results based on analysis of relative transcript abundance of <i>DXS</i> genes in control or MeJA-treated samples from white spruce.	193
Table 4.5. Relative transcript abundance of <i>PgDXS1</i> in control or MeJA-treated samples from white spruce.	197
Table 4.6. Relative transcript abundance of <i>PgDXS2A</i> in control or MeJA-treated samples from white spruce.	201
Table 4.7. Relative transcript abundance of <i>PgDXS2B</i> in control or MeJA-treated samples from white spruce.	207
Supplemental Table S1. Phenotypic observations of white spruce (<i>Pg653</i>) apical buds and shoots sampled during a year-long period of vegetative bud development.	243

List of Figures

Figure 1.1. Comparison of gibberellin biosynthesis and diterpene resin acid biosynthesis of conifer specialized metabolism.	4
Figure 1.2. The MEP pathway, as characterized in angiosperms, leads to isoprenoid precursor substrates for both gibberellin and diterpene resin acid biosynthesis pathways in conifers.	11
Figure 2.1. White spruce (<i>Pg653</i>) apical buds and shoots sampled during a year-long period of vegetative bud development.	42
Figure 2.2. White spruce <i>Pg653</i> samples for transcript and metabolite analysis in the MeJA treatment experiment.	53
Figure 3.1. Comparison of the amino acid sequence of <i>PgLAS</i> with characterized orthologs <i>PsLAS</i> , <i>PaLAS</i> and closely related <i>PaISO</i>	68
Figure 3.2. Comparison of the amino acid sequences of <i>PsCPS</i> , and <i>PsKS</i> with respective characterized orthologs <i>PgCPS</i> , <i>AtCPS</i> , <i>PgKS</i> and <i>AtKS</i>	69
Figure 3.3. Phylogenetic maximum-likelihood tree of full-length amino acid diTPS sequences from angiosperms and gymnosperms characterized as or like CPS, KS or involved in the conifer specific TPS-d3 family.	71
Figure 3.4. Polyacrylamide gel electrophoresis and corresponding Western blots showing the expression of three His-tag purified recombinant proteins from expression of recombinant Sitka and white spruce diTPS genes in <i>E. coli</i> : <i>PsCPS</i> , <i>PsKS</i> , and <i>PgLAS</i>	73
Figure 3.5. GC-MS analysis of <i>in vitro</i> assays with purified recombinant CPS proteins.	75
Figure 3.6. GC-MS analysis of the reaction product of recombinant <i>PsKS</i> protein.	76
Figure 3.7. GC-MS analysis of the reaction products of recombinant LAS proteins.	78
Figure 3.8. LC-MS analysis of assay products from <i>PgLAS</i> and <i>PaLAS</i>	79
Figure 3.9. Comparison of the amino acid sequence of <i>PgCYP701</i> with characterized orthologs from <i>Pisum sativum</i> (Pissa), <i>Arabidopsis thaliana</i> (At) and <i>Stevia rebaudiana</i> (Sr).	82
Figure 3.10. Comparison of the amino acid sequence of <i>PgCYP720B4</i> with characterized ortholog <i>PsCYP720B4</i> and closely related <i>PtCYP720B1</i>	83
Figure 3.11. Phylogenetic maximum-likelihood tree of full-length amino acid CYP450 sequences from angiosperms and gymnosperms characterized as CYP701 and CYP720.	85

Figure 3.12. CO-difference spectra.	87
Figure 3.13. GC-MS analysis of the reaction product of recombinant <i>PgCYP701</i> protein.	88
Figure 3.14. GC-MS analysis of <i>in vivo</i> enzyme assays of recombinant <i>PgCYP720B4</i> expressed in a yeast recombinant system.	90
Figure 3.15. Total DRA concentration (mg g^{-1} DW) in white spruce vegetative apical bud and apical shoot samples over a year-long time course.....	92
Figure 3.16. Total DRA concentration (mg g^{-1} DW) in white spruce vegetative apical buds and apical shoots over a time course, focusing on biological time points that correspond with shoot development and new bud set.	95
Figure 3.17. Mean concentrations of DRA (mg g^{-1} DW) in white spruce over a vegetative apical bud developmental time course separated by time point and sample part.	97
Figure 3.18. Relative transcript abundance of diTPS and CYP450 genes in white spruce developing apical buds and shoots over a one-year time course.....	99
Figure 3.19. Relative transcript abundance of diTPS and CYPs related to DRA and GA biosynthesis in different parts of white spruce developing vegetative apical buds and apical shoots.	105
Figure 3.20. Mean relative transcript abundance diTPS and CYP450 genes in a white spruce developing vegetative apical buds and apical shoots over a time course separated by time point and sample part.....	107
Figure 3.21. Mean concentration of DRA (mg g^{-1} DW) over sample type and time point in white spruce.....	116
Figure 3.22. Mean concentrations of DRA (mg g^{-1} DW) over MeJA treatment and sample type in white spruce.....	119
Figure 3.23. Total DRA concentration in MeJA-treated white spruce samples over a time course.....	122
Figure 3.24. Mean relative transcript abundance over MeJA treatment and sample type in white spruce.	129
Figure 3.25. Relative transcript abundance of <i>PgCPS</i> in white spruce samples in response to MeJA treatment over a time course.	131
Figure 3.26. Relative transcript abundance of <i>PgKCS</i> in white spruce samples in response to MeJA treatment over a time course.	135
Figure 3.27. Relative transcript abundance of <i>PgLAS</i> in white spruce samples in response to MeJA treatment over a time course.	140

Figure 3.28. Relative transcript abundance of <i>PgCYP701</i> in white spruce samples in response to MeJA treatment over a time course.	145
Figure 3.29. Relative transcript abundance of <i>PgCYP720B4</i> in white spruce samples in response to MeJA treatment over a time course.	150
Figure 4.1. Comparison of the amino acid sequences of <i>PgDXS1</i> , <i>PgDXS2A</i> and <i>PgDXS2B</i> with characterized orthologs from <i>Picea abies</i> and <i>Zea mays</i>	173
Figure 4.2. Phylogenetic maximum-likelihood tree of full-length amino acid DXS sequences from angiosperms and gymnosperms.	175
Figure 4.3. Polyacrylamide gel electrophoresis and corresponding Western blots showing the expression of three His-tag purified recombinant proteins from expression of recombinant white spruce DXS genes in <i>E. coli</i> : <i>PgDXS1</i> , <i>PgDXS2A</i> , and <i>PgDXS2B</i>	177
Figure 4.4. LC-MS analysis of <i>in vitro</i> assays with purified recombinant DXS proteins.	179
Figure 4.5. Relative transcript abundance of <i>DXS</i> genes in white spruce developing apical buds and shoots over a one-year time course.	181
Figure 4.6 Relative transcript abundance of <i>PgDXS</i> in different parts of white spruce developing apical buds and apical shoots.	185
Figure 4.7. Mean relative transcript abundance of <i>PgDXS</i> genes in a white spruce developing apical buds and apical shoots over a time course separated by time point and sample part.	186
Figure 4.8. Mean relative transcript abundance over MeJA treatment and sample type in white spruce.	194
Figure 4.9. Relative transcript abundance of <i>PgDXS1</i> in white spruce samples in response to MeJA treatment over a time course.	196
Figure 4.10. Relative transcript abundance of <i>PgDXS2A</i> in white spruce samples in response to MeJA treatment over a time course.	200
Figure 4.11. Relative transcript abundance of <i>PgDXS2B</i> in white spruce samples in response to MeJA treatment over a time course.	206

List of Abbreviations and Symbols

aa	Amino acids
ACT2	Actin 2
APCI	atmospheric pressure chemical ionization
<i>At</i>	<i>Arabidopsis thaliana</i>
BAC	Bacterial artificial chromosome
BSA	Bovine serum albumin
BSTFA	bis(trimethylsilyl)trifluoroacetamide
Cdc2	Cell division cycle protein 2
cDNA	Complimentary deoxyribonucleic acid
CIAP	Calf intestinal alkaline phosphatase
CPP	Copalyl diphosphate
CPR	cytochrome P450 monooxygenase reductase
CPS	<i>ent</i> -copalyl diphosphate synthase
CYP450	cytochrome P450 monooxygenase
dATP	deoxyadenosine triphosphate
dCTP	deoxycytidine triphosphate
DEPC	Diethylpyrocarbonate
dGTP	deoxyguanosine triphosphate
DiTPS	Diterpene synthase
DL-G3P	DL-glyceraldehyde 3-phosphate
DNA	Deoxyribonucleic acid
dNTP	deoxyribonucleotide triphosphate
DO	Drop-out

DRA	Diterpene resin acid
DTT	Dithiothreitol
dTTP	deoxythymidine triphosphate
DW	Dry weight
DXR	1-deoxy-D-xylulose-5-phosphate reductoisomerase
DXS	1-deoxy-D-xylulose-5-phosphate synthase
EDTA	Ethylenediaminetetraacetic acid
eEF1 α	Eukaryotic elongation factor 1 alpha
eIF4E	Translation initiation factor 4E
eIF5A	Translation initiation factor 5A
EI	Electron ionization
ESI	Electrospray ionization
FL	Full-length
GA	Gibberellin (Gibberellic acid)
GA ₁	Gibberellin A ₁
GA ₃	Gibberellin A ₃
GA ₄	Gibberellin A ₄
GA ₇	Gibberellin A ₇
GA ₉	Gibberellin A ₉
GA ₁₂	Gibberellin A ₁₂
<i>Gb</i>	<i>Ginkgo biloba</i>
GC	Gas chromatography
GGPP	Geranyl geranyl diphosphate
H3	Core histone protein 3
HEPES	4-(2-Hydroxyethyl)piperazine-1-ethanesulfonic acid

i.d.	internal diameter
intPA	integrated peak area
IPTG	isopropyl- β -D-thiogalactopyranoside
IRC	Inter-run calibrator
IS	internal standard
ISO	Isopimaradiene synthase p13
KA	Kaurenoic acid
KS	<i>ent</i> -Kaurene synthase
LAS	Levopimaradiene-abietadiene synthase
LC	Liquid chromatography
m/z	mass-to-charge ratio
MEP	2-C-methyl-D-erythritol 4-phosphate
MeJA	Methyl jasmonate
mRNA	Messenger ribonucleic acid
MS	Mass spectrometer
NADPH	β -Nicotinamide adenine dinucleotide 2'-phosphate reduced tetrasodium salt
NTC	No template control
OD	optical density
p.s.i.	Pounds per square inch
<i>Pa</i>	<i>Picea abies</i> ; Norway spruce
<i>Pc</i>	<i>Pinus contorta</i> ; lodgepole pine
<i>Pd</i>	<i>Pinus densiflora</i> ; Japanese red pine
<i>Pg</i>	<i>Picea glauca</i> ; white spruce
<i>Pp</i>	<i>Physcomitrella patens</i>
<i>Ps</i>	<i>Picea sitchensis</i> ; Sitka spruce

<i>Pt</i>	<i>Pinus taeda</i> ; loblolly pine
qPCR	Quantitative real-time PCR
RF	Response factor
RNA	Ribonucleic acid
RPL3	Ribosomal protein L3
<i>Sc</i>	<i>Saccharomyces cerevisiae</i>
SD	Synthetic defined
SEM	Standard error of the mean
SST	synthetic standard
TPP	Thiamine pyrophosphate
TPS	Terpene synthase
UBE2	Ubiquitin-conjugating enzyme E2
YPD	yeast extract peptone dextrose
YPD-E	yeast extract peptone dextrose ethanol
YPG	yeast extract peptone galactose
<i>Zm</i>	<i>Zea mays</i> ; maize

Acknowledgements

I am very grateful for the unending assistance of many outstanding people. I would like to thank my academic supervisor, Dr. Jörg Bohlmann, for giving me the opportunity to study and complete my PhD in his lab. I would also like to express my gratitude for the great amount of support, scientific guidance and knowledge provided to me throughout my degree.

Many thanks also to our lab managers, Karen Reid and Angela Chiang; I would not have survived without you both. To have such helpful and knowledgeable people supporting such a huge lab was beneficial in countless ways; thank you both for always answering questions and offering friendly support.

To my project advisor, Dr. Philipp Zerbe, I'd like to thank you for your advice and specific brand of tough but fair encouragement; it helped more than I ever would like to admit. Thanks also to past project advisors and senior colleagues, Dr. Björn Hamberger and Dr. Toshi Ohnishi, who were essential in the creation of my final project.

I am so thankful to my committee members Dr. Colette Breuil and Dr. Carl Douglas for their advice, guidance, and support during my research and thesis writing.

To every member of the Bohlmann group, I would like to extend my gratitude; being a part of such a large group of amazing people is an experience like no other. I am thankful for the inviting environment that our group offers as well as the unending fount of knowledge. I have learned more from impromptu casual scientific conversations than I ever thought possible. Specific thanks goes to those postdocs who toiled with me to prepare our collective white spruce MeJA time trial experiment: Katrin Geisler, Melissa Mageroy, Jose Celedon and Justin Whitehill. Thanks also to my volunteer student, Simone Asselin, who

was an extremely diligent worker and impressed me greatly. Thanks to our hard working and all-around amazing research technicians: Angela Chiang, Hannah Henderson, Sharon Janscik and Harpreet Dullat. I learned so much from each of you and am glad that we became friends along the way. To Lina Madilao and Mack Yuen, my work would have been exponentially harder without your expertise; thank you for help and for teaching me aspects of your specific knowledge, learning hands-on about GC-/LC-MS technology and bioinformatics was infinitely useful. And a special thanks to Baillie Redfern, Natalia Koloslova and Tina Chou, three graduate student friends, from each of you I have taken away very different and useful lessons that I will always remember.

I would also like to extend a thank you to the Botany graduate office staff for help with every aspect of my studies that happened outside of a lab. I am also most grateful for the salary support from NSERC and UBC postgraduate fellowships.

Thanks to Dr. Reuben Peters, Iowa State University USA, for providing the *ZmAN2* constructs. Thanks to John Tyson & The Snutch Laboratory (MSL) for use of their 384-well plate qPCR machine. Thanks to Hitoshi Sakakibara of the RIKEN Plant Science Center (Japan), and Dr. Thomas Moritz of the Umeå Plant science Center (Sweden) for analysis of gibberellin metabolites.

Finally to my mom, my dad and my sister Jennifer, thank you for your love and support.

Dedication

To my family,

I smile because you are always there for me,

I laugh because there is nothing I can do about it.

Chapter 1: Introduction

1.1. Diterpenoids in plant general and specialized metabolism

As a characteristic associated with their sessile nature, plants have developed complex and dynamic metabolic pathways to respond to changes in their environment. In plants we recognize two major types of metabolism: primary, or general, metabolism and secondary, or specialized, metabolism. General metabolism is comprised of pathways that are essential for plant development, growth and reproduction. The genes of these pathways are generally highly conserved across species and are often restricted from expansion with the result that they are frequently present as single or small copy number of genes. In their environment, plants are forced to respond to biotic and abiotic stresses, and do so using specialized metabolic pathways. In specialized metabolism tens of thousands of distinct metabolites are produced by functionally diverse gene families to deal with specific environmental challenges. Specialized metabolites are typically restricted to distinct and narrow taxonomic groups, for example within a single species, genus or family. Specialized metabolites offer a specific ecological function in a plant's interaction with other organisms in its environment (Peters, 2006; Keeling and Bohlmann, 2006; Gershenzon and Dudareva, 2007).

The largest and most diverse class of known natural metabolites are the terpenoids, with approximately 50,000 distinct molecules known (Buckingham, 2011), they are particularly widespread among plant species. Plants synthesize a huge array of terpenoids that play essential roles in diverse functions within the plant. In general metabolism, terpenoids have functions in photosynthesis (e.g. carotenoids, plastoquinone), respiration

(e.g. ubiquinone), and plant growth and reproduction (e.g. gibberellins, cytokinins, abscisic acid). Terpenoids involved in specialized metabolism include many kinds of volatiles and non-volatile compounds that allow the plant to interact with other organisms. Many specialized terpenoids also have been shown to have therapeutic uses for humans (e.g. taxol, artemisinin, menthol) (Bohlmann and Keeling, 2008; Lange et al., 1999). In conifers, an example of the diversity of specialized terpenoid metabolites is seen in the production of oleoresin that is composed of a mixture of monoterpenoids, sesquiterpenoids and diterpene resin acids (DRAs). Oleoresin offers not only a physical barrier against attack by invasive organisms but its constituent chemical compounds can also affect the physiology and behavior of pests (Keeling et al., 2008).

Terpenoid precursors arise via two independent biosynthetic pathways in plants that produce isopentyl diphosphate (IPP) and dimethylallyl diphosphate (DMAPP), the common precursors to all isoprenoid molecules. Although some cross-talk between pathways has been observed in plant species, generally the cytosolic mevalonic acid pathway is known to provide IPP and DMAPP precursors for sesqui- (C₁₅) and triterpenes (C₃₀) (Eisenreich et al., 2001; Lichtenthaler, 2010), whereas the 2-C-methyl-D-erythritol 4-phosphate (MEP) pathway operates in the plastids of plants and photosynthetic eukaryotes and provides precursors for the biosynthesis of mono- (C₁₀) and diterpenes (C₂₀). In conifers, monoterpenes are present in large volumes in the volatile fraction of the oleoresin, while diterpenoids encompass gibberellin phytohormones, photosynthetic pigments and non-volatile oleoresin compounds among others (Eisenreich et al., 2004).

Gibberellins (GAs) and DRAs are diterpenoids, specifically belonging to a group of more than 7,000 labdane (or bicyclic) and labdane-related metabolites (Peters, 2010). A

specific step in their biosynthesis is distinguished by the bicyclization of geranylgeranyl diphosphate (GGPP) to the labdadienyl/copalyl diphosphate (CPP) intermediate produced by a class II reaction of a diterpene synthase (diTPS). This reaction is either catalyzed by copalyl diphosphate synthase (CPS), which is considered the first committed step in gibberellin biosynthesis, or one of several bifunctional diTPS (e.g. levopimaradiene/abietadiene synthase, LAS) in the production of DRAs.

Bioactive GAs are ubiquitous phytohormones that are involved in many developmental processes ranging from plant growth and cell elongation, to flowering, germination, dormancy and senescence, among others (Fleet and Sun, 2005; Yamaguchi, 2008). Gibberellins are tetracyclic diterpenes and since their discovery in 1926 (Kurosawa 1926; Phinney, 1983), 136 GAs have been identified although only a small number have known biological activities (Olszewski et al., 2002). The biosynthesis of GAs in vascular plants begins with the cyclization of GGPP to *ent*-kaurene, the monofunctional diTPSs *ent*-CPS and *ent*-KS performing this sequential reaction with *ent*-copalyl diphosphate (*ent*-CPP) as intermediate (Figure 1.1). Following this, two cytochrome P450 (CYP450) enzymes, each performing 3-step oxidation reactions, catalyze the next steps in the pathway from *ent*-kaurene to gibberellin A₁₂ (GA₁₂), the committed precursor of all GAs. *Ent*-kaurene oxidase (CYP701) oxidizes *ent*-kaurene at the C-19 position to produce *ent*-kaurenoic acid; following this *ent*-kaurenoic acid oxidase (CYP88) catalyzes the formation of GA₁₂. GA₁₂ is further modified to produce either bioactive or non-bioactive forms of gibberellins, the latter existing mainly as deactivated metabolites or as precursors to active forms. These reactions are catalyzed through the actions of 2-oxoglutarate-dependent dioxygenase enzymes (Hedden and Phillips, 2000; Yamaguchi, 2008).

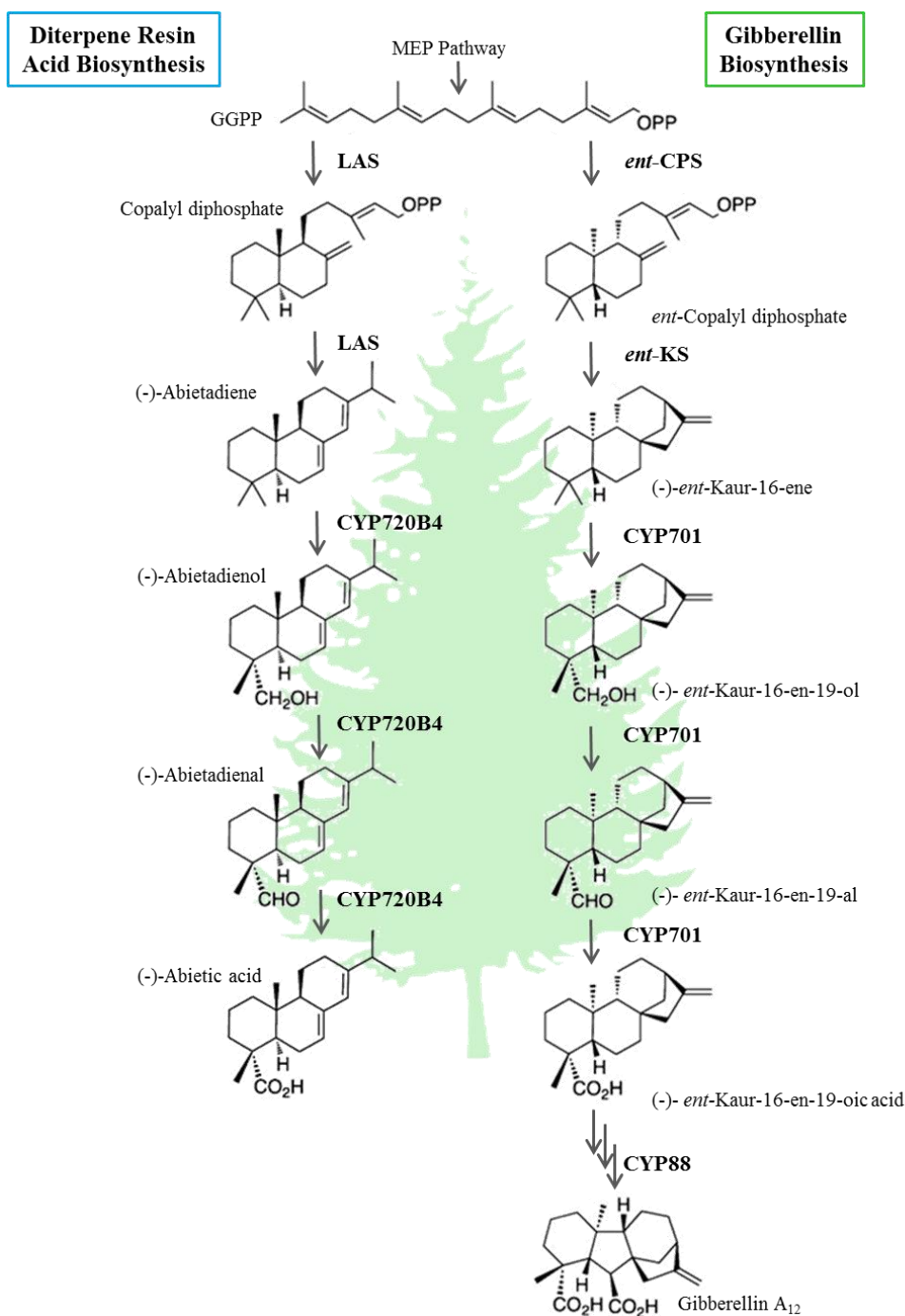


Figure 1.1. Comparison of gibberellin biosynthesis and diterpene resin acid biosynthesis of conifer specialized metabolism. In both pathways there is an initial diTPS cyclization step, using GGPP (C20) as precursor. LAS is a bifunctional enzyme using GGPP as a substrate and ultimately producing several diterpene olefins (not shown) as products. This initial step is performed by two monofunctional diterpene synthases in the GA pathway, *ent-CPS* and *ent-KS*. These products, in both pathways, are oxidized by cytochromes P450, CYP720B4 or CYP701, in a three step oxidation to arrive at either *ent*-kaurenoic acid in the GA pathway or one or possibly several diterpene resin acids; pictured here is abietic acid. (Figure adapted from Keeling et al., 2010)

DRAs are bi- or tricyclic diterpenoids that are well characterized in conifer species. Conifer trees have developed complex physical and chemical defenses to combat herbivore or pathogen attack, and these defenses are either present constitutively within the plant or induced after attack or wounding. Oleoresin is a prominent chemical and physical defense system of conifers, and is comprised mainly of a large array of monoterpenes, sesquiterpenes and DRAs (Martin et al., 2002; Miller et al., 2005; Zulak et al., 2009). Oleoresin serves both as a constitutive and inducible defense, being sequestered in specialized resin ducts, resin glands, resin blisters or resin cells, as well as an inducible defense that can be localized to traumatic resin ducts developed in the cambial zone and developing xylem (Martin et al., 2002; Franceschi et al., 2005; McKay et al., 2003). The volatile mono- and sesquiterpenoid oleoresin components play a multitude of roles in response to pest and pathogen attack; for example, acting as feeding deterrents, pest toxins, or stimulating chemical modification of insect physiology by interfering with ovary or egg development (Lindgren et al., 1996; Leal et al., 1997; Keeling and Bohlmann, 2006). In response to insect attack, the resin can act as a physical barrier by ‘pitching out’ and trapping the invader while sealing the wound. Some DRAs present in the oleoresin are known to possess anti-microbial activity (Raffa et al., 2005, Kopper et al., 2005). As well, DRAs within the extruded resin help to strengthen this physical barrier by polymerization after the volatile terpenoids have dissipated (Keeling and Bohlmann, 2006).

The biosynthesis of DRAs in conifers can be best described as a metabolic system with several nodes, resembling a matrix, rather than a simple linear pathway. Figure 1.1 describes the steps of a selected path of DRA biosynthesis, simplified to highlight the types of enzymes involved in the process. DRAs are synthesized from GGPP precursor and are

cyclized by a set of bifunctional diTPS to form diterpene olefin intermediates (in jack and lodgepole pine, monofunctional class I diTPS are also potentially involved (Hall et al., 2013)). One such bifunctional diTPS, LAS, produces a thermally unstable diterpenol intermediate that spontaneously dehydrates to give rise to the diterpenes abietadiene, levopimaradiene, neoabietadiene, and palustradiene which can be characterized *in planta* via GC-MS analysis (Keeling et al., 2011a). These diterpenes are initially hydroxylated by CYP450 enzymes from the conifer specific CYP720B family; Sitka spruce (*Picea sitchensis*) CYP720B4 performs a 3-step oxidation reaction at the C-18 position, through alcohol and aldehyde intermediates, to produce a resin acid corresponding to the initial diterpene substrate, i.e. abietic acid, levopimaric acid, neoabietic acid and palustric acid (Hamberger et al., 2011).

The diversity of diterpenes is mainly the result of the functional plasticity of diterpene synthase enzymes. Indeed, it has been shown via mutagenesis studies that as little as one amino acid substitution at selected positions of the diTPS active site can alter enzyme catalytic specificity (Roach et al., 2014; Keeling et al., 2008; Zerbe et al., 2012; Kawaide et al 2011; Morrone et al., 2008, Xu et al., 2007a). Following the formation of terpenoid olefins by diTPSs, cytochrome P450 monooxygenases further contribute to the structural and functional diversity of terpenoids (Hamberger and Bak, 2013, Zhao et al., 2014, Mizutani and Sato, 2011).

1.2. Enzymes involved in GA and DRA biosynthesis

1.2.1. Diterpene synthases

Diterpene synthases perform multi-step cyclo-isomerization reactions of GGPP or CPP to form diterpene metabolites. The diterpene synthases known to date have variations of three α -helical conserved domains: α , β and γ (Chen et al., 2011; Köksal et al., 2011; Zhou et al., 2012; Peters, 2010; Keeling et al., 2010) and depending on their function, can be separated into two functional classes. Class II diTPS enzymes catalyze the initial cyclization of GGPP to a bicyclic diphosphate intermediate. They contain a signature D-X-D-D motif which lies in the $\gamma\beta$ -domain in the N-terminal of the protein (Bohlmann et al., 1998; Wendt et al., 1997; Prisic et al., 2007) and is required for protonation-initiated carbocation formation (Christianson, 2006). By contrast, the activity of class I diTPSs resides in the C-terminal half of the protein with the active site located in the α -domain where two motifs, D-D-X-X-D and N-D-X-X-T-X-X-X-E, are conserved; these are required for the Mg^{2+} -dependent ionization of the diphosphate group and subsequent cyclization and rearrangement reactions (Christianson, 2006; Keeling et al., 2010; Zerbe et al., 2012).

In angiosperms, the diterpene synthases that are active in general and specialized biosynthesis are monofunctional class I or class II enzymes (Yamaguchi, 2008; Sakamoto et al., 2004). In gymnosperms, diTPSs of GA biosynthesis also exist as monofunctional class I and class II enzymes. In contrast, diTPSs of conifer DRA biosynthesis (specialized metabolism) exist typically as bifunctional enzymes that contain active sites for both class I and class II reactions. These bifunctional diTPSs are a part of the TPS-d3 family (Stofer Vogel et al., 1996; Peters et al., 2000; Martin et al., 2004; Keeling et al., 2011a). Recently,

the first class I monofunctional diTPSs involved in specialized metabolism were characterized from jack and lodgepole pines (Hall et al., 2013).

1.2.2. Cytochrome P450 monooxygenases

Cytochromes P450 are heme-thiolate enzymes and are known to perform a wide variety of reactions in general and specialized metabolism in plants. Most catalyze the insertion of oxygen, and hence their more formal nomenclature is CYP450 monooxygenases (Bernhardt, 2006). Microsomal CYP450 monooxygenases function with cytochrome P450 reductases as coenzymes, which utilize electrons from NADPH or NADH to cleave atmospheric oxygen to hydroxylate the substrate. The diversity of CYP450s in land plants has increased massively through evolutionary time to the point where it is suggested that in angiosperms, CYP450s now represent 1% of the functional gene space (Nelson et al., 2004; Nelson et al., 2008). Indeed, this is not surprising when the large variety of CYP450 involvement in plant metabolism is considered. CYP450s are involved in phytohormone biosynthesis and catabolism (e.g. gibberellins, brassinosteroids, abscisic acid), and they also contribute to core metabolic processes such as the biosynthesis of pigments (e.g. carotenoids), structural components (e.g. lignin, suberin), and UV protectants (e.g. flavonoids), among others. They are also involved in specialized metabolic pathways such as in the biosynthesis of taxol, benzyloquinoline alkaloids, and DRAs (Bak et al., 2011; Mizutani, 2012).

Sequence identity between CYP450s can often be quite low, sometimes falling below 20% identity at the amino acid level. Nomenclature guidelines state that CYP450s need 40%

identity or more to fall within the same family and 55% for a subfamily (Nelson, 2006; Werck-Reichhart and Feyereisen, 2000). Commonly found CYP450 motifs include a proline-rich region and the oxygen binding motif (A/G-G-X-D/E-T-T/S) (Durst and Nelson, 1995; Danielson, 2002) as well as the universally conserved E-X-X-R motif which interacts with the heme iron center to help stabilize the core structure, and the heme binding motif F-X-X-G-X-R-X-C-G where the conserved cysteine residue forms a thiolate ligand that tethers the iron to the CYP450 (Werck-Reichhart and Feyereisen, 2000; Graham and Peterson, 1999).

1.2.3. 1-Deoxy-D-xylulose 5-phosphate synthases

The 1-deoxy-D-xylulose 5-phosphate synthase (DXS) enzymes catalyze the first rate-limiting step in the cytosolic MEP pathway (Estévez et al., 2001; Lois et al., 2000; Cordoba et al., 2009). In photosynthetically active leaf tissue of *Arabidopsis thaliana*, DXS has been shown to be the major flux controlling enzyme of the MEP pathway (Wright et al., 2014). DXSs are members of the transferase family of enzymes, specifically catalyzing the thiamin-dependent condensation of glyceraldehyde-3-phosphate (G3P) and pyruvate to form 1-deoxy-D-xylulose-5-phosphate (DXP) (Lichtenhaler, 1999), as shown in Figure 1.2. DXSs are usually encoded by a small gene family in a given plant species. Across plant species, DXSs are clustered into three independent clades (type I, type II and type III) that are differentially expressed during growth and development as well as in specific organs. Type I *DXS* genes are associated with general metabolism and housekeeping functions (Kim et al. 2005), whereas genes identified as type II are thought to be involved in defense responses and specialized metabolism and genes of the third type are not found in all plant species, their roles are not yet completely clear (Phillips et al., 2007; Cordoba et al. 2009).

DXS enzymes contain a universally conserved transketolase-like domain that is essential for thiamine pyrophosphate binding and in addition, certain key residues have been reported to be crucial for enzyme catalysis and binding to G3P substrate (Xiang et al., 2007; Cordoba et al., 2011). These residues were first identified from the crystal structures of prokaryotic DXSs but are conserved in angiosperm models.

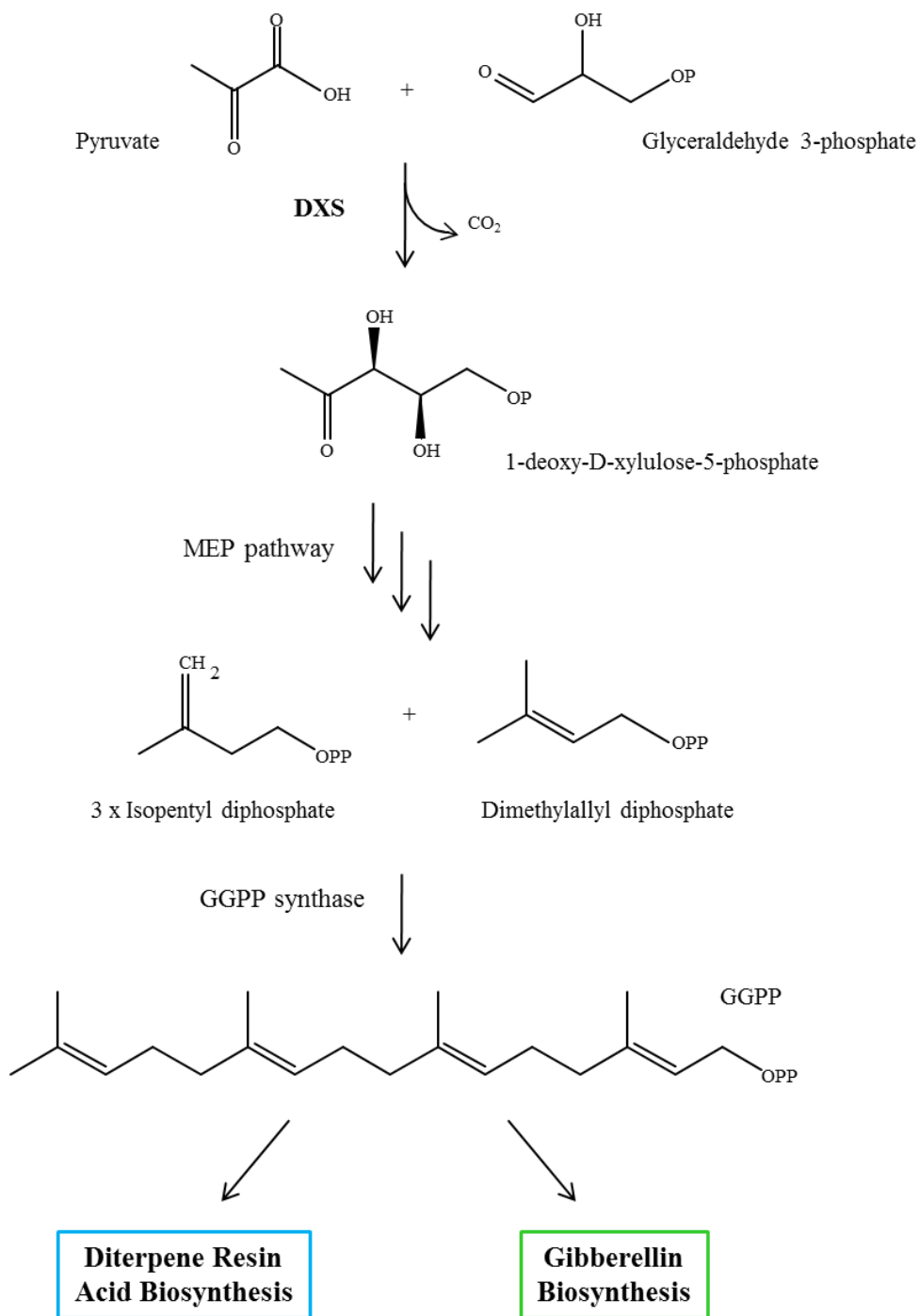


Figure 1.2. The MEP pathway, as characterized in angiosperms, leads to isoprenoid precursor substrates for both gibberellin and diterpene resin acid biosynthesis pathways in conifers.

1.3. Characterized GA and DRA related genes & evolutionary relationships

Within conifer diterpene biosynthesis, two pathways coexist and possibly compete for resources. These serve very different functions within the plant: the pathway of GA biosynthesis in general metabolism and the pathway of DRA biosynthesis of specialized metabolism. Even though they are disparate in function, sequence data show that the enzymes in these pathways share a common evolutionary ancestry.

Diterpene synthases that function in generalized metabolism in angiosperms and gymnosperms are monofunctional, including those associated with GA biosynthesis: CPS and KS. CPS and KS have been identified and functionally characterized in numerous angiosperm species including *Arabidopsis thaliana*, *Oryza sativa*, *Cucurbita maxima* and *Stevia rebaudiana* (Yamaguchi, 2006; Sakamoto et al., 2004; Smith et al. 1998; Yamaguchi et al. 1996; Richman et al., 1999), as well as recently in the conifer, Sitka spruce (*Picea sitchensis*) (Keeling et al., 2010). On the other hand, a more basal land plant, *Physcomitrella patens*, contains only a single diTPS that encodes for a bifunctional CPS/KS enzyme (*PpCPS/KS*) (Hayashi et al., 2006). Through sequence and gene structure analysis, it appears that extant monofunctional CPS and KS enzymes evolved from the duplication of an ancestral bifunctional CPS/KS enzyme followed by a subsequent subfunctionalization with each derived enzyme losing one of the two active domains (Keeling et al., 2010; Trapp and Croteau, 2001). Phylogenetically, both *PpCPS/KS* and the monofunctional CPS enzymes belong to the TPS-c family, with known KS enzymes being characterized in the closely related TPS-e family (Trapp and Croteau, 2001; Keeling et al., 2010; Chen et al., 2011).

This same model of duplication of an ancestral bifunctional CPS/KS can be extended to support the claim that in conifers the bifunctional and monofunctional diTPSs share a common ancestor (Bohlmann et al., 1998; Trapp and Croteau, 2001; Keeling et al., 2010). The modern bifunctional diTPSs of DRA specialized metabolism have undergone a duplication of the ancestral *CPS/KS* gene and subsequent neofunctionalization, retaining both active sites, to introduce the specialized metabolism pathway.

In the DRA pathway, two bifunctional diTPSs, LAS and isopimaradiene synthase (ISO), have been characterized in a number of species including Norway spruce (*Picea abies*) (Martin et al., 2004), Sitka spruce (Keeling et al., 2011b), and balsam fir (*Abies balsamea*) (Zerbe et al. 2012). LAS has also been characterized in loblolly pine (*Pinus taeda*) (Ro and Bohlmann 2006) as well as in jack pine (*Pinus banksiana*) and lodgepole pine (*Pinus contorta*) (Hall et al., 2013) with lodgepole pine carrying two copies of *LAS* genes. An abietadiene synthase was characterized from grand fir (*Abies grandis*) (Stofer Vogel et al., 1996; Peters et al., 2000). The first monofunctional class I diTPSs involved in DRA specialized biosynthesis in conifers were recently discovered in jack pine and lodgepole pine, each with single copies of monofunctional pimaradiene synthase (producing mainly pimaradiene) and ISO (producing mainly isopimaradiene with trace amounts of sandaracopimaradiene). Hall et al. (2013) showed that they formed a new group within the TPS-d3 family having evolved from bifunctional diTPSs rather than the ancestral diTPSs of GA metabolism.

This situation in conifers, where specialized bifunctional diTPSs have arisen from bifunctional diTPS in GA biosynthesis is unique. However, the general patterns of diTPSs of specialized metabolism having evolved from genes of general metabolism have parallels in

angiosperms, such as in rice (*Oryza sativa*) where gene duplication and neofunctionalization of gibberellin-related genes has formed specialized pathways. Indeed, rice is one of the best characterized systems in angiosperms with respect to diterpene biosynthesis in both general and specialized metabolism. The rice genome contains two monofunctional CPS-like and seven KS-like enzymes that have been diverted to labdane-related specialized metabolism, with single copies of *CPS* and *KS* remaining that are devoted to general GA metabolism (Prisic et al., 2004; Xu et al., 2004; Sakamoto et al., 2004; Xu et al., 2007b, Chen et al. 2011). These CPS-like and KS-like enzymes have been recruited to specialized pathways producing over 20 labdane-related diterpenoids that act as phytoalexins or allelochemicals to defend the rice plant from microbial pests or inhibit the growth of nearby plants (Kato et al., 1994; Kato-Noguchi and Ino, 2003; Peters, 2006).

Similarly, the rice genome also contains five paralogs of *ent*-kaurene oxidase (*CYP701*), only one of which is reported to have kept its ancestral function in GA metabolism (Sakamoto et al., 2004). In other vascular plants *CYP701* is thought to be a single-copy gene. In rice, transcripts of two *ent*-kaurene oxidase-like genes are inducible upon treatment with methyl jasmonate (MeJA) or fungal cell wall components, and neither of these enzymes are able to complement the function of *CYP701* when transformed into a *CYP701* mutant. In fact, rather than acting at C-19 of *ent*-kaurene as *CYP701* does in the formation of *ent*-kaurenoic acid, one *ent*-kaurene oxidase-like enzyme catalyzes hydroxylations at C-3 of *ent*-sandaracopimaradiene and *ent*-cassadiene, which are predicted intermediates in the early steps of biosynthetic pathways for certain phytoalexins in rice (Wang et al., 2012).

To date, CYP450s involved in GA biosynthesis have not been characterized in any conifer species, however from putative CYP701 sequences it is known that Sitka spruce and loblolly pine sequences group correctly into the CYP71 clan along with the characterized CYP701 enzymes from angiosperms. The second CYP450 dedicated to gibberellin metabolism is CYP88, *ent*-kaurenoic acid oxidase, which catalyzes the 3-step oxidation from *ent*-kaurenoic acid to GA₁₂. CYP88 falls into the CYP85 clan in which the oldest evolutionary families contain CYP450s involved in terpenoid phytohormone biosynthesis (such as CYP707 enzymes encoding abscisic acid hydroxylases and CYP85, CYP90 and CYP724 enzymes involved in early brassinosteroid biosynthesis) (Hamberger and Bohlmann, 2006; Hamberger and Bak, 2013). Members of the CYP720B family in conifers (*Pt*CYP720B1, Ro et al., 2005; *Ps*CYP720B4, Hamberger et al. 2011) also group within the CYP85 clan and they catalyze 3-step oxidation reactions from multiple diterpene olefins to produce DRAs. The pathways of GA and DRA biosynthesis are similar (Figure 1.1.), in that both begin with the diterpenoid precursor GGPP, share evolutionarily related diTPSs, have CYP450s that perform 3-step hydroxylation reactions on a methyl group of the A-ring of their diterpenoid substrate, and share structurally similar metabolite intermediates and end products (*ent*-kaurenoic acid vs DRAs). In contrast to the diTPSs involved in these pathways, and their evolutionary origins by diversification and sub-or neofunctionalization, it is believed that the presence of the CYP720Bs in the CYP85 clan indicates convergent evolution of function with the CYP701 enzymes (Hamberger and Bohlmann, 2006; Hamberger et al., 2011; Hamberger and Bak, 2013).

Both GA and DRA biosynthetic routes draw GGPP precursors from the MEP pathway. Within this pathway, DXS catalyzes the first rate-limiting step. *DXS* genes are

highly conserved, essential genes across plant and bacterial species; in bacteria, they have been well studied in species such as *Escherichia coli* and *Deinococcus radiodurans* (Xiang et al., 2007). DXS type I, II or III have been characterized to varying degrees within angiosperm species, with some examples being the enzymes from *Arabidopsis thaliana* (Estévez et al., 2000; Araki et al., 2000), *Medicago trunculata* (Walter et al., 2002), *Oryza sativa* (rice; Kim et al., 2005), *Vitis vinifera* (grape vine; Battilana et al., 2011), *Zea mays* (maize; Cordoba et al., 2011), and *Catharanthus roseus* (Madagascar periwinkle; Chahed et al., 2000; Han et al., 2013). Less is known for gymnosperm species, with characterized DXSs reported only for Norway spruce (Phillips et al., 2007), *Pinus densiflora* (Japanese red pine; Kim et al., 2009), and *Ginkgo biloba* (Gong et al., 2006; Kim et al., 2006). In most of these characterized examples, one or two DXS type I or type II proteins were identified, suggesting roles for the enzymes in both general and specialized metabolism pathways. Although the evolutionary relationships of *DXS* genes are not completely understood it is thought that the different clades of DXS enzymes arose from duplications of *DXS* type I genes and persisted in the genomes of higher plants through relaxed purifying selection or positive selection due to an advantage of retaining multiple copies dedicated to different metabolic pathways (Carretero-Paulet et al., 2013).

1.4. Thesis objectives & hypotheses

Conifers provide an interesting experimental system in which to analyze and compare enzymes pathways that share structurally similar intermediates and products, and follow similar mechanistic paths but that perform in general versus specialized metabolism.

Studying these pathways could give insight into the evolution of pathways that are part of a

resource allocation system between growth (influenced by GAs) and defense (as a function of DRAs). This knowledge is relevant given that conifer trees (as crucial components of the vast northern boreal forests) are ecologically important as carbon sinks and natural habitats, as well as being of great economic importance to major industries centered on the uses of wood, wood fiber/pulp and combustible energy. The conifers of boreal forests are also hosts of pest/pathogen attacks that can disrupt or destroy their ecological and/or economic value; examples include the damage done by spruce budworm (*Choristoneura fumiferana*), white pine/spruce weevil (*Pissodes strobi*) and mountain pine beetle (*Dendroctonus ponderosae*). As such, a thorough understanding of the biochemistry of conifer chemical defenses, their expression across the seasons, and the influence of stress on their expression could be extremely valuable for devising engineered solutions that improve conifer tree defenses.

Previous studies, using either white spruce (*Picea glauca*), Sitka spruce or Norway spruce, have identified individual conifer DXS, diTPS and CYP450 enzymes involved in isoprenoid precursor biosynthesis, the GA biosynthetic pathway (with the exception of the *ent*-kaurene oxidase, CYP701), and the production of an array of diterpenoids in the DRA pathways (Phillips et al., 2007, Keeling et al., 2010, Keeling et al., 2011b, Hamberger et al., 2011). My thesis builds on this work with one section of my studies focused on the characterization of selected additional enzymes involved in these pathways, primarily those from white spruce.

The main goal of my thesis was to compare and contrast the pathways of general and specialized metabolism in a spruce species to gain a better understanding of the seasonal, sample-specific, and stress-specific (via MeJA exposure) expression of DXS, diTPS and CYP450 genes involved in GA and DRA biosynthetic pathways in white spruce. This goal

was enhanced by evaluating the functionality of the DRA pathway via analysis of DRA product biosynthesis.

In my thesis the following questions have been addressed:

Question 1: How do coexisting diterpene pathways of general and specialized metabolism compare within a conifer species?

Hypothesis 1: Genes involved in GA metabolism in white and Sitka spruce have conserved functions for GA genes across plant species, while genes of DRA metabolism have functions that are specialized for DRA biosynthesis in conifer species.

Chapter 3 explored this hypothesis with the functional characterization of selected diTPS and CYP450 genes involved in GA and DRA biosynthesis in white spruce and Sitka spruce providing data that ultimately lead to the first full and direct comparison of these biochemically similar pathways of general versus specialized metabolism. Chapter 4 includes identification and functional characterization of *DXS* genes from the MEP pathway in white spruce as an example of a representative rate-limiting step in early isoprenoid biosynthesis.

Question 2: What differences are observed in the expression of white spruce GA and DRA related genes, as well as pathway metabolites, over a year of vegetative apical bud and shoot growth?

Hypothesis 2: Expression of genes encoding enzymes of the specialized DRA defense pathway show markedly different expression patterns than those of GA biosynthesis with maximal expression in times and places when defensive chemicals are needed most.

Chapters 3 and 4 explored this hypothesis by assessing the gene expression of selected white spruce diTPS, CYP450 (Chapter 3) and *DXS* (Chapter 4) genes involved in DRA versus GA biosynthesis over a year-long time course (31 sampled time points) of vegetative apical bud and shoot development. Furthermore, DRA metabolite levels were also measured over the time course, providing a functional context to changes in gene expression. Sample-specific gene expression (stem, needles and new buds) was also analyzed at selected time points in spring, summer and autumn to help determine which samples were most important for GA or DRA biosynthesis as well as where DRA metabolites were being sequestered.

Question 3: What patterns emerge in the expression of *DXS*, diTPS and CYP450 genes associated with GA or DRA metabolism in response to methyl jasmonate induced stress? How do these responses differ within sample types? Does the gene expression response to chemically induced stress fit with the results of the studies of spatial and temporal accumulation of DRA metabolites?

Hypothesis 3: MeJA treatment affects gene expression of enzymes involved in the defense (specialized) pathway of DRA biosynthesis but has little or no effect on genes involved in GA biosynthesis.

Chapters 3 and 4 explored this hypothesis through comparative studies of the gene expression response of selected diTPS, CYP450 (Chapter 3) and DXS (Chapter 4) enzymes involved in DRA versus GA biosynthesis to elicitor (MeJA) induced stress with targeted sampling over a 30-day time course. Gene expression and DRA metabolite levels were measured over the time course in five sample types (mature needles, young needles, bark/phloem, wood/xylem and young stems) to determine how MeJA treatment affected DRA metabolite levels and how induction/up-regulation patterns of GA or DRA related genes correlate with changes in DRA metabolite levels.

Chapter 2: Materials and methods

2.1. Functional characterization of *PsCPS*, *PsKS* and *PgLAS*

2.1.1. Isolation of *LAS* cDNA sequence from white spruce, PCR amplification & preparation of protein construct

The *PgLAS* cDNA was amplified from white spruce (clonal line *Pg653*) xylem and phloem cDNA by PCR using Phusion Hot Start II Polymerase (Thermo). Sequence mining primers were based on an N-terminal truncated sequence [76 amino acids (aa) removed] of the Sitka spruce sequence (*PsLAS*) reported by Keeling et al. (2011b) (Table 2.1) that produces a protein that is more active than that from the full-length native sequence. *PgLAS* cDNA was ligated into pJET1.2 cloning vector using CloneJET PCR cloning Kit (Clontech) and the sequence was verified. The *PgLAS* sequence was amplified by PCR using In-Fusion based primers and was subcloned into an NdeI-digested pET28b(+) expression vector (Novagen, Merck) using the In-Fusion HD EcoDry Cloning Kit (Clontech). The resulting recombinant protein contained an N-terminal His tag. See Table 2.1 for primer sequences.

Table 2.1. Oligonucleotide primers used for *Pg* diTPS and CYP450 gene mining, cloning and qPCR analysis.

Gene	Primer Direction	Sequence (5' → 3')
Sequence mining		
<i>PgLAS</i>	Forward	GCTAGCAAACGAGAATTCCTCCAGGT
	Reverse	CTCGAGCTAAGCAACCGGATGGAAGA
<i>PgCYP701</i>	Forward	CTCGAGATGGAAGACGTTGAAGCAATGTTAAGGGTTTTTCTC
	Reverse	GCTAGCTTAAGTGTGGACATGGAGATATTGCTAGGGATATG C
<i>PgCYP720B4</i>	Forward	CTCGAGATGGCGCCCATGGCAGACCAAATATCATTAC
	Reverse	GCTAGCTTATTCACTCTCTACTCTACCATGAAGGCTAATGGG
cDNA cloning		
<i>PsCPS</i>	Forward	<u>CGCGCGGCAGCCATATG</u> ATGAAAATGTCAAAATCGGTGGAAG TTCAACACTGCGCCG
	Reverse	<u>GTCATGCTAGCCATATG</u> TTAATACTGGCTGGAAGAGAACC GTCTCCACG
<i>PsKS</i>	Forward	<u>CGCGCGGCAGCCATATG</u> ATGAAGCGTGAGCAATACACAATTC TGAATGAGAAAGAAAGC
	Reverse	<u>GTCATGCTAGCCATATG</u> TTACAGAATAGGATCAACAATGACT GCATTAACATACCCAAGC
<i>PgLAS</i>	Forward	<u>CGCGCGGCAGCCATATG</u> AAACGAGAATTCCTCCAGG
	Reverse	<u>GTCATGCTAGCCATATG</u> CTAAGCAACCGGATGGAAG
<i>PgCYP701</i>	Forward	<u>CTAAATTACCGGATCAAAAATG</u> GGAAGACGTTGAAGCAATG
	Reverse	<u>GATCCCCCGCGAATTTTA</u> AGTGTGGACATGGAGATATTG
<i>PgCYP720B4</i>	Forward	CTCGAGATGGCGCCCATGGCAGACCAAATATCATTAC
	Reverse	GCTAGCTTATTCACTCTCTACTCTACCATGAAGGCTAATGGG
qPCR analysis		
<i>PgCPS</i>	Forward	TCAAGCGGTGTTTCCAGTGTGT
	Reverse	AAGCTGGAACCACTGCTATCCAT
<i>PgKS</i>	Forward	TTCAGATTCAGAGCCGCGAGTTG
	Reverse	CATTGTGGAACTGTGGCTGTTGAG
<i>PgLAS</i>	Forward	GGACGATCTCAAGTTGTTTTCCGATTC
	Reverse	CACTCTGCTTCTTTCTGTATACGCTTCT
<i>PgCYP701</i>	Forward	CTGAAGGAAGCCCCACAGTTGA
	Reverse	ATCGCAGTGGAAGGATCGGTACAG
<i>PgCYP720B4</i>	Forward	TTTCAAGCCCAATACCCAAAGGCACTG
	Reverse	CTCGTCTCTTTGGAAGGAGATAAATCC

Bold text corresponds to a restriction enzyme site, single underlined text is the target vector sequence, text with double underline is a yeast kozak-like initiation sequence

2.1.2. Preparation of Sitka spruce *CPS* and *KS* protein constructs

Picea sitchensis (clonal line FB3-425) *ent*-copalyl diphosphate synthase (*PsCPS*) and *ent*-kaurene synthase (*PsKS*) were previously cloned, from flushing bud and 1st interwhorl phloem cDNA, into pJET1.2 (CloneJET, Thermo Scientific) by Keeling et al. (2010; GenBank Accession *PsCPS*: GU045757, and *PsKS*: GU045758). A full-length *PsCPS* sequence and a pseudomature sequence of *PsKS*, lacking its putative transit peptide (Keeling et al., 2010; Zerbe et al., 2012), were amplified by PCR using In-Fusion based primers and subcloned into individual NdeI-digested pET28b(+) plasmids (Novagen, Merck) using the In-Fusion HD EcoDry Cloning Kit (Clontech), resulting in recombinant proteins that were N-terminal His tagged. See Table 2.1 for primer sequences.

2.1.3. Heterologous protein expression and purification of *PsCPS*, *PsKS* and *PgLAS*

pET28b(+) plasmid constructs containing *PsCPS*, *PsKS* or *PgLAS* were each transformed into C43(DE3) *Escherichia coli* cells (OverExpress, Lucigen corp.) containing the pRARE2 plasmid (which codes for seven rare tRNAs in the *E. coli* host) prepared from Rosetta 2 cells (EMD Biosciences). Luria-Bertani medium containing kanamycin (50 mg L⁻¹) and chloramphenicol (30 mg L⁻¹) was inoculated with one individual colony and cultured overnight at 37°C and 200 rpm. Terrific broth medium containing kanamycin (50 mg L⁻¹) and chloramphenicol (30 mg L⁻¹) was inoculated with a 1:100 dilution of the overnight culture and then grown at 37°C and 180 rpm until an optical density at 600nm (OD₆₀₀) of between 0.6 to 0.8 was reached. Cultures were then cooled to 16°C, induced with 0.2 mM IPTG (isopropyl-β-D-thiogalactopyranoside; Fisher), and cultured for an additional 18 h at 16°C and 180 rpm before pelleting and freezing at -20°C.

For protein purification, cell pellets were resuspended in 2 mL g⁻¹ lysis buffer containing 20 mM HEPES (pH 7.5), 350 mM NaCl, 20 mM imidazole, 5 mM dithiothreitol (DTT), 1.0 mg mL⁻¹ lysozyme (Sigma) and 5 mM protease inhibitor cocktail (Roche). Harvested cells were incubated with gentle shaking for 30 min at 4°C in lysis buffer, sonicated for 1 min on ice (Branson Sonifier S-250A, Branson Ultrasonics), and clarified by centrifugation for 30 min at 2000g, 4°C. Recombinant proteins were purified by affinity chromatography using HisSpinTrap columns (GE Healthcare). The columns were washed with 600 µL binding buffer (20 mM HEPES, 350 mM NaCl and 20 mM imidazole, pH 7.5) before loading harvested cell lysate in 600 µL aliquots, eluting by centrifugation for 30 s at 100g. After lysate had been loaded, columns were washed three times with binding buffer, with elution by centrifugation. His-tagged protein was then eluted in 400 µL elution buffer containing 20 mM HEPES, 350 mM NaCl, and 350 mM imidazole, pH 7.5. Protein eluates were desalted against desalting buffer containing 20 mM HEPES, 350 mM NaCl, 5 mM DTT, and 10% glycerol, pH 7.5 using PD MiniTrap G-25 desalting columns (GE Healthcare). Desalting columns were washed 3 times with desalting buffer, then purified protein eluate was applied to columns dropwise and eluted by centrifugation at 1000g for 2 min, 4°C. Protein concentration was quantified by direct measurement of A₂₈₀ with a NanoDrop spectrophotometer (NanoDrop Technologies) and used directly in *in vitro* assays.

2.1.4. Gel electrophoresis and protein immunoblotting

Denaturing gel electrophoresis and immunoblotting was performed to confirm the presence and size of expressed recombinant diTPS proteins for future enzyme assays. Approximately 5-10 µg protein from each sample were mixed 4:1 v:v with 5X SDS buffer

(0.5M Tris-base, pH 6.8, 4% w/v SDS, 10% v/v β -mercaptoethanol, 10% w/v sucrose, 0.01% w/v bromophenol blue), and boiled for 10 min. Samples were loaded onto SDS-polyacrylamide gels, together with prestained molecular weight standards (Thermo Scientific, PageRuler Plus), made based on a discontinuous system (Laemmli, 1970) consisting of 4% stacking gels and 10% resolving gels. Gels were run in a Mini-PROTEAN 3 apparatus (Bio-Rad) at a constant voltage of 100V. The resolved proteins were electrophoretically transferred to PVDF membranes at 20V for 40 min, as described by Towbin et al. (1979). Blots were blocked for 2 h at room temperature in Tris-Buffered Saline (50 mM Tris base, 150 mM NaCl, 0.01% Tween-20, pH7.2; TBST) containing 5% milk (to reduce non-specific binding). The blots were then incubated with a monoclonal mouse anti-polyHistidine-alkaline phosphatase antibody (Sigma), diluted 1:4000 v/v, for 1 h at room temperature. After incubation, blots were washed three times with TBST and developed using 4-nitrotetrazolium blue and 5-bromo-4-chloro-3-indolyl phosphate as substrates.

2.1.5. DiTPS enzyme assays

Assays to confirm activity of *PsCPS* and *PsKS* were based on previous work by Keeling et al. (2010) using single-vial coupled assays as described previously (O'Maille et al., 2004; Keeling et al., 2008; Hall et al., 2011; Zerbe et al., 2012). Assays analyzed both the pair of recombinant spruce enzymes (*PsCPS* and *PsKS*) and a combination of *PsKS* with a monofunctional angiosperm CPS enzyme, *Zea mays* CPS (*ZmAn2*; provided by Dr. R. Peters, Iowa State University; Harris et al., 2005). Assays were completed in 2 mL amber glass GC sample vials. Assay buffer (500 μ L) consisted of 50 mM HEPES, 100 mM KCl, 7.5 mM $MgCl_2$, 5% v:v glycerol, 5 mM DTT, and 0.1 mg mL⁻¹ bovine serum albumin

(BSA), pH 7.2. To start the assay, the substrate geranylgeranyl diphosphate (GGPP; Sigma) was added to the assay buffer at 15 μ M along with approximately 50 μ g of each purified protein. Assays were overlaid with 500 μ L pentane containing 2 μ M 1-eicosene (Sigma) as an internal standard, and incubated at 100 rpm for 1 h at 30°C. Subsequently, the vials were vortexed for 20 s to stop the reaction (by denaturing the protein) and extract the assay products from the aqueous layer. Assay vials were then centrifuged at 1000g for 20 min at 4°C to separate the phases.

Assays containing solely 50 μ g monofunctional CPS enzyme were set up as above, however before the addition of the pentane overlay and protein denaturation, assay products were enzymatically dephosphorylated by the addition of 10 U CIAP (Calf Intestinal Alkaline Phosphatase; Invitrogen) with incubation overnight at 37°C. Pentane overlay (500 μ L) containing 2 μ M 1-eicosene as an internal standard was then added, and assays were vortexed and centrifuged as above for the coupled CPS/KS assays.

Assays to test the bifunctional white spruce LAS (*PgLAS*) were set up as the above coupled assays, but using only 50 μ g of *PgLAS* recombinant enzyme.

2.1.6. GC-MS analysis of diTPS assay products

GC-MS analysis for single enzyme *PgLAS* *in vitro* assays as well as coupled *PsCPS*, *ZmAn2*, and *PsKS* enzyme assays was performed by electron ionization (EI) after injection of the pentane overlay into an Agilent 7890A Series GC system with an Agilent 7683 autosampler, coupled to an Agilent 7000B MSD Triple Quadrupole system (Agilent Technologies) in scan/selected ion monitoring (SIM) mode (scan, mass-to charge ratio [m/z]

40-500, SIM, m/z 83, 229, 257, 272 [dwell time 50]). Compounds were separated using an Agilent HP5ms column (5% phenyl methyl siloxane, 30 m x 250 μ m internal diameter (i.d.), 0.25 μ m film thickness). Samples of 1 μ L were injected in pulsed splitless mode at 250°C with a column flow of 1.2 mL helium min^{-1} and 25 pounds per square inch (p.s.i.) pulse pressure, and the following GC temperature program was used: 40°C for 2 min, ramp at 20°C min^{-1} to a final temperature of 300°C, hold for 2 min for a total run time of 17 min.

GC-MS analysis for single enzyme *PsCPS* assays was performed similarly by EI after injection of the pentane overlay into an Agilent 6890A series GC system, with an Agilent 7683B autosampler, coupled to an Agilent 5973N MSD system (Agilent Technologies) in scan/SIM mode (scan, m/z 40-400, SIM, m/z 69, 83, 257, 272, 275, 290 [dwell time 40]). Compounds were separated using a Solgel-Wax (30 m x 250 μ m i.d., 0.25 μ m film thickness; SGE Incorporated) capillary column. Samples of 1 μ L were injected in pulsed splitless mode at 250°C with a column flow of 1.0 mL helium min^{-1} and 50 p.s.i. pulse pressure, and the following GC temperature program was used: 40°C for 2 min, ramp at 25°C min^{-1} to a final temperature of 250°C, hold for 5 min for a total run time of 15.40 min.

2.1.7. LC-MS analysis of *PgLAS* assay products

Work by Keeling et al. (2011a) suggests that the *Picea abies* LAS produces epimeric thermally unstable allylic tertiary alcohols, 13-hydroxy-8(14)-abietene as an initial product which spontaneously dehydrates under high temperature GC-MS conditions to the apparent LAS products abietadiene, levopimaradiene, neoabietadiene and palustradiene which can be analyzed via GC-MS. Therefore, metabolite products from *in vitro* single enzyme *PgLAS*

assays were analyzed by LC-MS on a LC-MSD-Trap-XCT Plus (1100 series device, Agilent) in APCI (atmospheric pressure chemical ionization) mode. Chromatography was achieved using 10 μ L assay volume injections on an Agilent Zorbax Rx-SIL silica column (4.6 mm i.d. \times 150 mm \times 5 μ m; Agilent) with isocratic elution of pentane/ether (80:20) at 30°C at 1.4 mL min⁻¹. Post-column, via T-fitting, 0.1 mL min⁻¹ 0.2% formic acid in pentane/ether (80:20) was added by syringe pump for ionization. APCI-MS conditions were as follows: APCI temperature, 350°C; dry temperature, 325°C; nebulizer, 60 p.s.i.; dry gas flow, 7 L min⁻¹; high voltage capillary, 3 kV; and positive mode, 40-350 atomic mass unit scan range.

2.1.8. Phylogenetic analysis of diTPSs

Amino acid sequence alignments were carried out using MUSCLE (<http://www.ebi.ac.uk/Tools/msa/muscle/>; Edgar, 2004). Maximum-likelihood phylogenetic trees were constructed using the PhyML 3.0 platform (<http://atgc.lirmm.fr/phyml/>; Guidon et al., 2010) with four rate substitution categories, LG substitution model, BIONJ starting tree and 500 bootstrap replicates. Phylogenetic trees were visualized using Interactive Tree of Life v2 (iTOL) web server (<http://itol.embl.de/>; Letunic and Bork, 2011).

2.2. Functional characterization of *PgCYP701*

2.2.1. Isolation of *CYP701* full-length cDNA from white spruce

The full-length cDNA of *P. glauca* ent-kaurene oxidase (*PgCYP701*) was amplified from white spruce (clonal line *Pg653*) mature needle cDNA by PCR using Phusion Hot Start II DNA Polymerase (Thermo Scientific). *PgCYP701* cDNA was ligated into pJET1.2 cloning

vector using CloneJET PCR cloning Kit (Clontech) and sequence verified. Gene specific primers (Table 2.1) were based on available bacterial artificial chromosome (BAC) libraries (Hamberger et al., 2009) and genomic sequences from in-house databases.

2.2.2. Preparation of *PgCYP701* protein construct and yeast transformation

PgCYP701 cDNA sequence amplified by PCR from the above pJET1.2 cloning vector and was subcloned into BamHI and EcoRI digested yeast expression vector pYeDP60 (Pompon et al., 1996) using the In-Fusion HD EcoDry Cloning Kit (Clontech) with gene specific, In-Fusion based primers (Table 2.1), designed to include a yeast Kozak-like nucleotide sequence “AAAA” (Romanos et al., 1992) directly 5’ to the native ATG start site of *PgCYP701*. The yeast *Saccharomyces cerevisiae* (*Sc*) strain used in this experiment was BY4741 (MATa his3 Δ 1; leu2 Δ 0; met15 Δ 0; ura3 Δ 0) (Brachmann et al., 1998). In the Bohlmann laboratory a *Pinus contorta* (*Pc*; lodgepole pine) cytochrome P450 monooxygenase reductase (*PcCPR1*), under the control of the GAL10-cyc1 promoter, was genomically integrated into the BY4741 yeast strain for use in the functional analysis of recombinant cytochrome P450 monooxygenases (CYP450s). The prepared expression vector was transformed into BY4741 following the LiAc method (Gietz and Schiestl, 2007). To prepare yeast competent cells, strain BY4741:*PcCPR1* was inoculated into YPD medium (1% yeast extract, 2% bacto-peptone, 2% dextrose) and grown at 30°C to an OD₆₀₀ of 0.6-0.8 nm. Cells were harvested by centrifugation and washed in sterile water. Yeast cells were then resuspended in 100 mM LiAc (lithium acetate) and dispensed into 50 μ L samples to be used for single transformation reactions. To the 50 μ L yeast cell aliquots was added 240 μ L polyethylene glycol (MW3350, 50% w/v), 36 μ L 1.0 M LiAc, 25 μ L salmon sperm DNA

(2.0 mg mL⁻¹; Life Technologies) and 0.5 µg prepared plasmid DNA. Transformation reactions were incubated at 200 rpm at 30°C for 30 min, then heat shocked at 42°C for 20 min. Lastly, transformed yeast cells were pelleted by centrifugation at 200g for 1 minute and resuspended in 500 µL sterile water. Aliquots of 50 µL of these reactions were plated onto appropriate synthetic complete drop-out (DO) selective medium plates and incubated at 30°C for 3-4 days.

2.2.3. Preparation and purification of yeast microsomes

To prepare yeast microsomes for use in *in vitro* enzyme assays, three transformant BY4741:*PcCPR1* colonies were grown in 50 mL cultures at 28°C in appropriate liquid synthetic defined (SD) drop-out selective media (2% dextrose) until an OD₆₀₀ of 0.2 nm was reached. These cells were then transferred to 200 mL cultures in YPD-E (1% yeast extract, 2% bacto-peptone, 2% dextrose, 5% ethanol) medium and grown for 24-30 h at 28°C shaking at 180 rpm, and 50 mL of this culture transferred again to 200 mL YPG (1% yeast extract, 2% bacto-peptone, 2% galactose) medium for 12-16 h at 28°C and 180 rpm for induction of cells. To isolate microsomes from the yeast, cells were first sedimented at 3000g for 10 min at 4°C and resuspended in TEK buffer (50 mM Tris-HCl, 1 mM EDTA, 100 mM KCl, pH 7.5). They were centrifuged again as above and then transferred to TES2 buffer (50 mM Tris-HCl, 1 mM EDTA, 600 mM sorbitol, 5 mM DTT, 0.25 mM phenylmethylsulfonyl fluoride, pH 7.5). The resuspended cells were mixed with acid-washed glass beads (425-600 mm, Sigma) and broken by vigorous hand shaking for a total of 2 min, then the supernatant was collected and centrifuged at 10,000g for 15 min at 4°C to remove unbroken cells and residual glass beads. The cell homogenate was ultracentrifuged at 100,000g for 1 h at 4°C to

sediment the microsomes containing the recombinant CYP450 and *PcCPR1* proteins.

Microsomes were then homogenized with a hand-held Potter-Elvehjem homogenizer (pestle and glass tube; Sigma-Aldrich), resuspended in TEG buffer (50 mM Tris-HCl, 1 mM EDTA, 30% v/v glycerol, pH 7.5) and used directly in CO spectrum and *in vitro* enzyme assays.

2.2.4. CYP450 carbon monoxide spectrum assay

Activity of recombinant *PgCYP701* enzyme was assayed using a CO difference spectrum assay modified from Omura and Sato (1964). Purified microsomal fractions were diluted ten-fold in 0.1 M potassium phosphate buffer pH 7.5, aliquoted into 500 μ L glass cuvettes (Starna Scientific, type 18/B path length 10mm), and reduced by addition of a few milligrams of sodium dithionite for 2 min. Absorbance between 400-500 nm was measured in a UV-VIS spectrophotometer (Shimadzu) to obtain an absorbance reading of the reduced CYP450. Then, carbon monoxide gas was bubbled into the solution for approximately 30 sec and absorbance of the solution was measured once more. To obtain the difference spectrum the absorbance reading from the reduced CYP450 was subtracted from that of the CYP450-CO complex. Concentrations of CYP450 were calculated using the extinction coefficient 91 $\text{mM}^{-1} \text{cm}^{-1}$ (Omura and Sato, 1964) and equation 1 below (Guengerich, 2009):

$$\text{nmol mL}^{-1} \text{ CYP450} = \Delta\text{Abs}(450-490) / 0.091 \quad (1)$$

2.2.5. *In vitro* CYP450 enzyme assays

Isolated microsomes containing *PgCYP701* and *PcCPR1* were assayed to test for CYP450 activity. To generate the substrate, *ent*-kaurene, needed for CYP701 activity a 2-

step *in vitro* assay was used. The first reaction step combined 150 µg of *ZmAn2* and 100 µg *PgKS* enzymes with 15 µM GGPP as substrate, and assay buffer containing 50 mM HEPES, 100 mM KCl, 7.5 mM MgCl₂, 5% v:v glycerol, 5 mM DTT, 0.1 mg mL⁻¹ BSA, pH 7.2 in a total volume of 450 µL. The reaction was incubated at 100 rpm for 1.5 h at 30°C. The second reaction step involved the addition of 45 µL prepared microsomes and 5 µL 10 mM reduced β-nicotinamide adenine dinucleotide 2'-phosphate (NADPH; Sigma-Aldrich tetrasodium salt) to the first reaction mixture, followed by incubation at 100 rpm for 1.5 h at 30°C. To extract enzymatic products a 500 µL aliquot of 2:1 pentane:diethyl ether solvent containing 2 µM 12,14-dichlorodehydroabietic acid as an internal standard, was overlaid on the reaction mixture. The vials were then vigorously vortexed for 40 sec, and centrifuged at 1000g for 20 min to separate organic and aqueous phases. A 40 µL aliquot of the organic layer was transferred to a new glass vial insert and then derivatized by the addition of 5 µL bis(trimethylsilyl)trifluoroacetamide (BSTFA; derivatization grade, Sigma-Aldrich) with incubation overnight.

2.2.6. GC-MS analysis

GC-MS analysis for *PgCYP701* enzyme assays was performed by EI after injection of the pentane overlay into an Agilent 7890A Series GC system with an Agilent GC sampler 80 combipal autosampler, coupled to an Agilent 5975C MSD system (Agilent Technologies) in scan/SIM mode (scan, *m/z* 40-500, SIM, *m/z* 83, 229, 257, 272, 374 [dwell time 40]). Compounds were separated using an Agilent HP5ms column (5% phenyl methyl siloxane, 30 m x 250 µm i.d., 0.25 µm film thickness). Samples of 1 µL were injected in pulsed splitless mode at 250°C with a column flow of 1 mL helium min⁻¹ and 25 p.s.i. pulse pressure, and the

following GC temperature program was used: 70°C for 1 min, ramp at 20°C min⁻¹ to a final temperature of 300°C, hold for 3 min for a total run time of 15.5 min.

2.2.7. Diterpene standards and substrates

Authentic *ent*-kaurene standard was provided by Dr. Tomonobu Toyomasu, Yamagata University, Japan. *Ent*-kaurenol, *ent*-kaurenal, and *ent*-kaurenoic acid (90% purity) were purchased from Olchemim Ltd. (<http://www.olchemim.cz>).

2.3. Functional characterization of *PgCYP720B4*

2.3.1. Isolation of *CYP720B4* full-length cDNA from white spruce

Primers to amplify *PgCYP720B4* were designed based on the *PsCYP720B4* sequence identified by Hamberger et al. (2011) (Table 2.1). The *PgCYP720B4* sequence was amplified from a mixture of young and mature needle cDNA of white spruce (clonal line *Pg653*) with Phusion hot start II polymerase (Life Technologies). The PCR amplified *PgCYP720B4* cDNA was ligated into pJET1.2 cloning vector using CloneJET PCR cloning Kit (Clontech) and the sequence was verified.

2.3.2. Preparation of *PgCYP720B4* protein construct and yeast transformation

The *PgCYP720B4* sequence was excised from the pJET1.2 cloning vector by digestion with *NheI* and *XhoI* (NEB) and ligated into *NheI* and *XhoI* digested yeast dual expression vector pESC-Leu (Stratagene) by traditional cloning. The prepared expression

vector was transformed, alongside a previously prepared pESC-His vector from the Bohlmann Lab containing a *S. cerevisiae* GGPP synthase (*ScGGPPS*) and *P. abies* *LAS* (*PaLAS*; Martin et al., 2004; Hamberger et al., 2011), into yeast cell strain BY4741 with a chromosomally integrated *PcCPR1* gene following the LiAc method (Gietz and Schiestl, 2007) as detailed previously for *PgCYP701* (section 2.2.2.). Transformed yeast cells were selected on appropriate SD-DO-selective medium plates and grown at 30°C for 72 h to 96 h.

2.3.3. Protein expression and *in vivo* enzyme assays

As a test for function, *PgCYP720B4* was co-expressed with *ScGGPPS*, *PaLAS* and *PcCPR1* for *in vitro* assays. Single colonies of transformed yeast cells were grown at 30°C and 180 rpm in appropriate liquid SD-DO-selective medium containing 2% dextrose to an OD₆₀₀ of 0.6-0.8. Cultures were spun at 2000g for 5 min (to pellet cells and remove media) and resuspended in liquid SD-DO-selective medium containing 2% galactose and incubated again at 30°C and 180 rpm for 16 h to induce protein expression. Yeast cells were pelleted as above, washed with 5 mL ddH₂O, and transferred to a glass test tube. Metabolites from yeast cells were extracted twice by vortexing for 1 min 30 sec with 2 mL diethyl ether (inhibitor-free, Fisher), with 2 µM 12,14-dichlorodehydroabietic acid as internal standard, and approximately 250 µL acid-washed glass beads (425-600 µm, Sigma). The extracted solvent layer was transferred to a clean glass test tube containing anhydrous Na₂SO₄, and evaporated by N₂ gas until approximately 500 µL remained. Solvent samples were transferred to amber glass GC vials and derivatized by the addition of 150 µL trimethylsilyl-diazomethane (TMS-diazomethane; 2.0 M in diethyl ether; Sigma-Aldrich) and 150 µL methanol. Derivatization

reactions were allowed to react for 30 min, samples were dried to completion under N₂ gas and resuspended in 200 µL diethyl ether for GC-MS analysis.

2.3.4. GC-MS analysis

GC-MS analysis for metabolite extracts from yeast *in vitro* PgCYP720B4 assays was performed by EI after injection of the pentane overlay into an Agilent 7890A Series GC system with an Agilent 7683 autosampler, coupled to an Agilent 7000B MSD Triple Quadrupole system (Agilent Technologies) in scan/SIM mode (scan, m/z 40-500, SIM, m/z 270, 272, 307, 314, 316 [dwell time 50]). Compounds were separated using an Agilent HP5ms column (5% phenyl methyl siloxane, 30 m x 250 µm i.d., 0.25 µm film thickness). Samples of 1 µL were injected in pulsed splitless mode at 250°C with a column flow of 0.85 mL helium min⁻¹ and 50 p.s.i. pulse pressure, and the following GC temperature program was used: 60°C for 3 min, ramp at 10°C min⁻¹ to a final temperature of 300°C, hold for 5 min for a total run time of 32 min.

2.3.5 Diterpene standards and substrates

Diterpene resin acids (DRAs) were purchased from Orchid Cellmark. Diterpenoid olefins, alcohols, and aldehydes were synthesized from the corresponding acids by Best West Laboratories.

2.3.6. Phylogenetic analysis of CYP450s

Phylogenetic analysis was carried out as in section 2.1.8.

2.4. Functional characterization of *PgDXS1*, *PgDXS2A* and *PgDXS2B*

2.4.1. Isolation of *DXS1*, *DXS2A* and *DXS2B* cDNA from white spruce, PCR amplification & preparation of protein constructs

Full-length cDNA sequences of three *P. glauca* 1-deoxy-D-xylulose 5-phosphate synthase (*DXS*) genes, *PgDXS1*, *PgDXS2A*, and *PgDXS2B*, were amplified from white spruce (clonal line *Pg653*) mature needle, young needle, and phloem cDNA respectively by PCR using Phusion Hot Start II DNA Polymerase (Thermo Scientific) and gene specific primers (Table 2.2) based on in-house databases and previously characterized Norway spruce (*Picea abies*, *Pa*) *DXS* sequences (*PaDXS1*, EF688331.1; *PaDXS2A*, EF688332.1; *PaDXS2B*, EF688333; Phillips et al., 2007). Each gene family member was ligated into a pJET1.2 cloning vector using CloneJET PCR cloning Kit (Clontech) and sequence verified. Using predictions from the ChloroP (Emanuelsson et al., 1999) and TargetP (Emanuelsson et al., 2000) servers, pseudomature forms of each *PgDXS* gene, lacking a putative transit peptide (*PgDXS1*, 54 aa removed; *PgDXS2A*, 48 aa removed; *PgDXS2B*, 18 aa removed), were amplified by PCR using In-Fusion based primers and subcloned into separate NdeI-digested pET28b(+) expression vectors (Novagen, Merck) using the In-Fusion HD EcoDry Cloning Kit (Clontech). The resulting recombinant proteins each contained an N-terminal His tag. See Table 2.2 for primer sequences.

Table 2.2. Oligonucleotide primers used for *PgDXS* gene mining, cloning and qPCR analysis.

Gene	Direction	Sequence (5'→3')
Sequence mining		
<i>PgDXS1</i>	Forward	ATGGCGACGACGATGGC
	Reverse	TCAAGACATTACTTGAAGTGCTTCTCTTG
<i>PgDXS2A</i>	Forward	ATGGCCATAACAAGCAGGGC
	Reverse	TTATCGGTGCTTGAGAAGAGCATC
<i>PgDXS2B</i>	Forward	ATGGCATCACTGGGAGTGG
	Reverse	TCAAATCAAGGAAGAATATTCAATCACTG
cDNA In-Fusion cloning		
<i>PgDXS1</i>	Forward	<u>CGCGCGGCAGCC</u> CATAT GGCCGCTGCTTTATCTGAC
	Reverse	GTCATGCTAGCC CATAT GTCAAGACATTACTTGAAGTGCTTC
<i>PgDXS2A</i>	Forward	<u>CGCGCGGCAGCC</u> CATAT GGCAGCCACTAAAAGAAAGC
	Reverse	GTCATGCTAGCC CATAT GTTATCGGTGCTTGAGAAGAG
<i>PgDXS2B</i>	Forward	<u>CGCGCGGCAGCC</u> CATAT GGGGAGTAATATATCTCAACCAAGC
	Reverse	GTCATGCTAGCC CATAT GTCAAATCAAGGAAGAATATTCAATC
qPCR analysis		
<i>PgDXS1</i>	Forward	AAGGGAGCACGAGGTAATAATAAC
	Reverse	CGATGTAGTGGTCAGGAAGAAC
<i>PgDXS2A</i>	Forward	GTTGACAGTGGAGGAAGG
	Reverse	ATTATGGTAGCCGCAATATG
<i>PgDXS2B</i>	Forward	TGGTTGTAATGGCTCCTTC
	Reverse	GGGTTCCCTTTGTTGTTTGG

Bold text corresponds to a restriction enzyme site, single underlined text is the target vector sequence, text with double underline is a yeast kozak-like initiation sequence

2.4.2. Heterologous *PgDXS* protein expression and purification

Heterologous expression of *PgDXS* proteins was carried out as described in section 2.1.3 (Heterologous *PsCPS*, *PsKS* and *PgLAS* protein expression and purification) with changes to buffer preparations. Here, lysis buffer contained: 20 mM HEPES (pH 7.5), 350 mM NaCl, 40 mM imidazole, 5 mM DTT, 1.0 mg mL⁻¹ lysozyme (Sigma) and 5 mM protease inhibitor cocktail (Roche); binding buffer contained: 20 mM HEPES (pH 7.5), 350 mM NaCl and 40 mM imidazole; lastly desalting buffer contained 20mM HEPES (pH 7.5), 350 mM NaCl, 2 mM MgCl₂, 10% glycerol, 1.8 mM TPP (thiamine pyrophosphate) and 5 mM DTT.

2.4.3. Gel electrophoresis and protein immunoblotting

SDS-PAGE and Western blotting was carried out as in section 2.1.4.

2.4.4. DXS *in vitro* enzyme assays

Assays to confirm the functional activity *PgDXS1*, *PgDXS2A* and *PgDXS2B* were based on previous work by Battilana et al. (2011). *In vitro* enzyme assays were completed in 2 mL amber glass GC sample vials and performed by mixing 50 µL of purified enzyme with 50 µL assay buffer containing: 50 mM HEPES (pH7.2), 2 mM MgCl₂, 5% glycerol, 5 mM DTT, and 0.1 mg mL⁻¹ BSA, with 1.8 mM sodium pyruvate and 1.86 mM DL-G3P (DL-glyceraldehyde 3-phosphate) as substrate and 1.8mM TPP as a DXS enzyme cofactor. To start the assays, the substrates and enzyme cofactor were added to the enzyme and buffer mix and incubated for 1 h at 30°C, shaking at 100 rpm. The assays were terminated with the

addition of 20 μL acetonitrile and vigorous vortexing for a total of 40 s. The assays were then transferred to 250 μL glass vial inserts (Agilent) and centrifuged at 130g for 10 min at 4°C to precipitate protein.

2.4.5. LC-MS analysis

Metabolite products from *in vitro* assays using recombinant DXS proteins were identified by LC-MS analysis using an LC-MSD-Trap-XCD plus 1100 series device (Agilent) on an Agilent Zorbax SB-C18 (4.6 mm x 150 mm, 3.5 μm pore size) in negative electrospray ionization (ESI) mode (dry temperature 350°C, nebulizer pressure 60 p.s.i., dry gas 12 L min⁻¹). Assay samples of 2.0 μL were injected with a column flow of 0.8 mL min⁻¹, the mobile phases used were: 95% H₂O + 0.2% formic acid (solvent A) and 5% acetonitrile + 0.2% formic acid (solvent B). Samples were subjected to an elution gradient program as follows: 5% solvent B for 3 min to 95% solvent B over 5 min holding for 0.1 min. Compounds were identified by comparison with a synthesized 1-deoxy-D-xylulose 5-phosphate (DXP) authentic standard (Sigma-Aldrich).

2.4.6. Phylogenetic analysis of DXSs

Phylogenetic analysis was carried out as in section 2.1.8, however using a JTT substitution model in place of an LG substitution model.

2.5. Vegetative white spruce apical bud development time course

2.5.1. Plant materials

White spruce (*Picea glauca*; clone Pg653) seedlings were propagated by somatic embryogenesis and purchased from Laurentian Forestry Center (Natural Resources Canada). Seedlings were acquired in August 2006, grown in individual cone pots in a mixture of forestry sand and perennial mix and were acclimated to natural light and environmental conditions outside of the University of British Columbia horticulture greenhouse for at least a year prior to the experiment. Two months prior to the beginning of the experiment, 140 five-year old trees were repotted to 2-gallon pots with 4 trees in each pot using perennial soil mix from West Creek Farms which is a high peat content soil mix combined with vermiculite and composted bark and aggregates (<http://www.westcreekfarms.com/>, Fort Langley, BC). Each 2-gallon pot was fertilized with 13g Professional Horticulture “ProHort” Premium 20-10-10 controlled release fertilizer (<http://www.directsolutions.com/canada/prohort-premium-20-10-10>; Direct Solutions, Delta, BC); trees and seedlings were previously treated with this fertilizer approximately once per year. After repotting and during the year of experimental collection, trees were again kept outside at the University of British Columbia horticulture greenhouse in natural conditions and watered 3-4 times per week.

2.5.2. Experimental treatment of plant materials

Vegetative apical buds and shoots of white spruce (clonal line Pg653) were collected based on a time course designed to generally follow the known growth stages of *P. glauca* trees (Alfaro et al., 2000; previous collection unpublished). The collection consisted of 31

time points, with 4 trees sampled per time point. Collection points were spaced at minimum 1 week apart to as long as 1 month apart (Figure 2.1; Table 2.3), based on known phenology and expected growth stages under local climatic conditions. Apical buds and shoots were consistently collected around the same time of day, between noon and 2pm. In most cases, apical buds or shoots were cut from trees using a razor blade, flash frozen in liquid nitrogen and stored at -80°C prior to analyses. For eight selected time points during spring and summer, apical buds or apical shoots were first dissected into 2 or 3 distinct sample parts (needles, stem, new buds) before flash freezing. Dissection included removal of needles and visible new bud growth from each fresh stem with a razor blade. Stem refers to the entirety of the apical shoot stem section including developing bark/phloem and wood/xylem material; needles consists of all needles present in the apical bud or shoot sample; new buds are buds that were set on the apical shoot/stem after the initial bud flush and were large enough to be seen by eye. “Whole” apical bud and apical shoot samples refer to a biologically proportional recreation of the entire sample by combining finely ground tissue from stem, needles and new buds (where applicable).

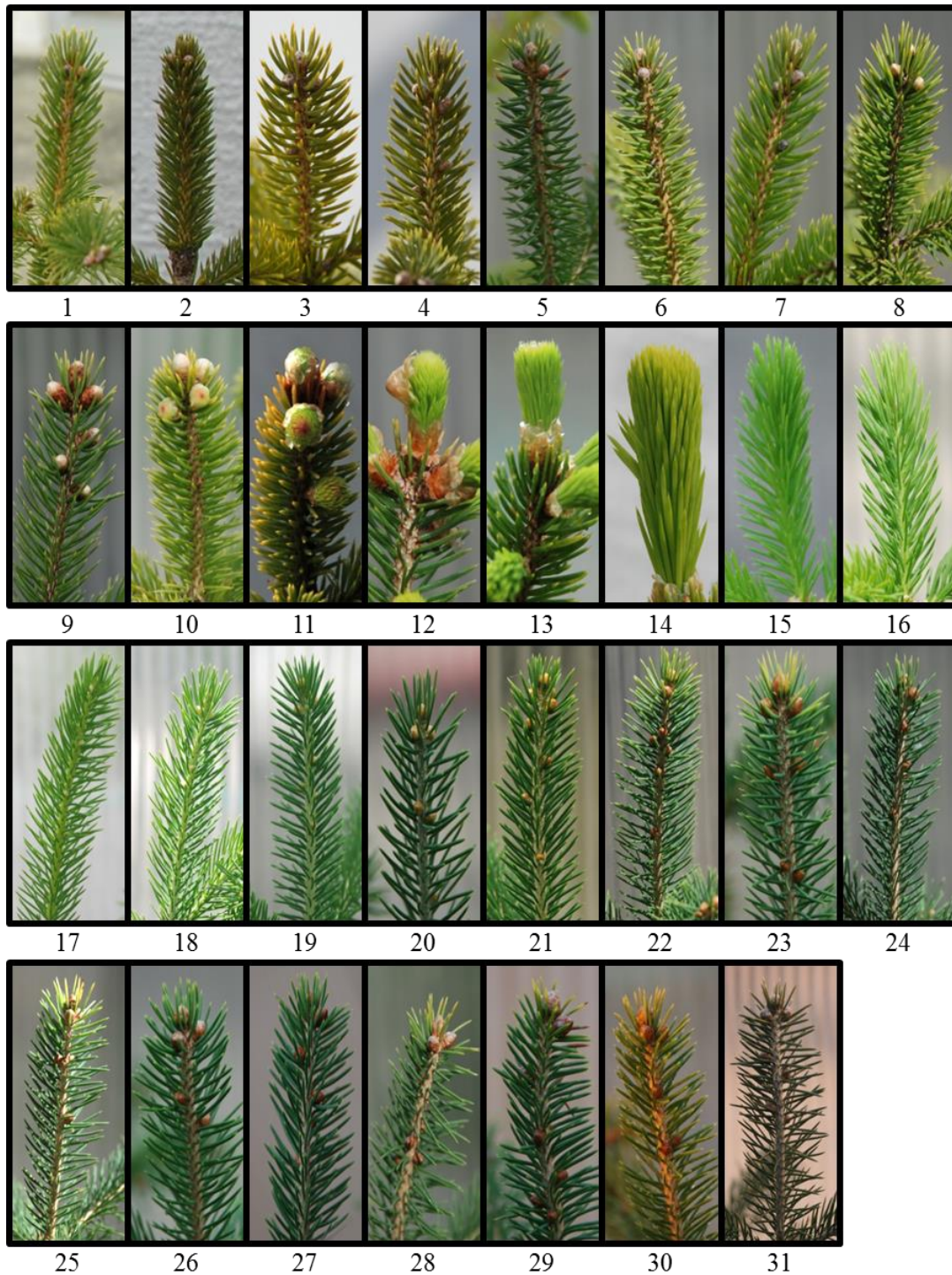


Figure 2.1. White spruce (*Pg653*) apical buds and shoots sampled during a year-long period of vegetative bud development. Images shown are of apical leader with 1 being the first time point collected beginning in January 2011 and 31 the last in December 2011. The period of time between each time point is as follows: time points 1-2, 4 weeks; 2-3, 2 weeks; 3-4 and onwards to 20, 1 week; 20-21 and onwards to 30, 2 weeks; 30-31, 4 weeks. For specific dates, see Table 2.3. Specific time points were chosen based upon phenotypic development based on Alfaro et al. (2000). Photos by K.M. Storey.

Table 2.3. Dates and corresponding time points for white spruce (*Pg653*) apical bud and shoot samples collected over a year-long period of vegetative bud development. Time points were spaced 1-4 weeks apart based on the growing season. At each time point 4-5 trees were collected.

Month	Time Point	Date ^a	Day of the Year ^b
January	1	Jan 19	19
February	2	Feb 16	47
March	3	Mar 2	61
	4	Mar 9	68
	5	Mar 16	74
	6	Mar 23	82
	7	Mar 30	89
April	8	Apr 6	96
	9	Apr 13	103
	10	Apr 20	110
	11	Apr 27	117
May	12	May 4	124
	13	May 11	131
	14	May 18	138
	15	May 25	145
June	16	Jun 1	152
	17	Jun 8	159
	18	Jun 15	166
	19	Jun 22	173
	20	Jun 29	180
July	21	Jul 13	194
	22	Jul 27	208
August	23	Aug 10	222
	24	Aug 24	236
September	25	Sept 7	250
	26	Sept 21	264
October	27	Oct 5	278
	28	Oct 19	292
November	29	Nov 2	306
	30	Nov 16	320
December	31	Dec 14	348

^a Collection occurred in 2011, ^b January 1st as day 1, December 31st as day 365

2.5.3 Extraction of diterpene resin acids (DRAs)

Methods for the extraction, derivatization and GC-MS analysis of diterpenoids were adapted from Lewinsohn et al. (1993) and Hamberger et al. (2011). Time points 1-11 were pooled samples consisting of 4 individual biological samples (pooled due to sample limitations), whereas time points 12-31 consisted of two technical replicates and four biological replicates. All steps were carried out in 2 mL amber vials (Agilent). Samples weighing 5-25 mg were ground to a fine powder with mortar and pestle under liquid nitrogen and extracted by shaking overnight in 750 μL of tert-butyl methyl ether with 100.3 $\mu\text{g mL}^{-1}$ 12,14-dichlorodehydroabietic acid as the internal standard (IS). The organic extract and the insoluble sample residue were allowed to separate by gravity and 400 μL of the organic supernatant was moved to a new vial and derivatized by mixing with 120 μL methanol and 120 μL trimethylsilyl-diazomethane (2.0 M in diethyl ether; Sigma-Aldrich). Samples were then incubated at room temperature for at least 20 minutes, dried to completion under N_2 gas and resolved in 400 μL diethyl ether before GC/MS analysis. The residual sample from the original 750 μL extraction was dried at room temperature for 2 days prior to weighing to determine dry weight (DW) of the sample.

2.5.4. Analysis of DRA metabolites by GC-MS

Diterpene resin acids from sample extracts were analyzed by GC-MS with an AT-1000 capillary column (30 m x 250 μm i.d., 0.25 μm film thickness; Alltech) in scan/SIM mode (scan, m/z 40-500; SIM, m/z 270, 272, 284, 286, 288, 307, 314, 316 [dwell time 35]) on an Agilent 6890N series GC-MS system, with an Agilent 7683B autosampler, coupled to an Agilent 5975 MSD system (Agilent Technologies). Samples of 0.1 μL , 0.2 μL , or 0.5 μL

were injected in pulsed splitless mode at 250°C with a column flow of 0.8 mL helium min⁻¹ and 25 p.s.i. pulse pressure. The following GC temperature program was used: 150°C for 1 min, ramp at 1.65°C min⁻¹ to 200°C, ramp again at 25°C min⁻¹ to 240°C, hold for 12 min, for a run time of 47.9 min.

GC-MS-generated peaks from extracted DRAs and synthesized standards (SST) (pimaric acid, sandaracopimaric acid, levopimaric acid, palustric acid, isopimaric acid, abietic acid, dehydroabietic acid and neoabietic acid), as well as the IS, were integrated using Hewlett-Packard Chemstation software. A response factor (RF) was calculated for each SST based on a comparison with a known concentration of the IS. DRA concentrations were calculated using equation 2 below:

$$\begin{aligned} &[(\text{DRA}_{\text{intPA}}/\text{IS}_{\text{intPA}}) * (\text{ng IS injected}) / (\text{SST.DRA}_{\text{RF}}/\text{IS}_{\text{RF}}) * \\ &(\mu\text{L extraction vol.} / \mu\text{L injected vol.})] / \text{g DW} / 1000 = \mu\text{g g}^{-1} \text{DW} \end{aligned} \quad (2)$$

Where ‘intPA’ is integrated peak area. The formula was carried out for each DRA peak in the sample and the $\mu\text{g g}^{-1}$ DW concentrations were added to give a total concentration of DRA per technical replicate; biological replicates were calculated from an average of two technical replicates.

Compounds were identified based on the comparison of retention times and mass spectra of the synthesized authentic standards and reference spectra from Adams (2007) and the National Institute of Standards and Technology MS Library searches (Hochmuth, 2007).

2.5.5. Statistical analysis of changes in DRA concentrations

DRA concentrations in whole apical bud and apical shoot samples were statistically analyzed over time points 12-31 (time points 1-11 could not be statistically analyzed due to a lack of material for biological replicates and pooling of samples) using univariate analysis of variance (ANOVA). Data met normality of residuals and homogeneity of variance when analyzed using Levene's test. Following significant *F*-tests, means were separated using the least significant difference (LSD) test ($\alpha=0.05$). All data were analyzed using IBM SPSS Statistics v. 20 (SPSS Inc., 2011). Data annotations with letters in figures and tables show significant differences based on *P* values from post-hoc pairwise comparisons. Letter annotations were deciphered manually based on scrutiny of the large data output files from the statistical testing.

Whole apical bud and apical shoot samples from time points 13, 15, 17, 19, 21, 23, and 25 were separated into 2 or 3 sample parts (as described in section 2.5.2). DRA concentrations in these sample parts were analyzed using two-way ANOVA to identify significant differences between sample parts over time. Exploratory analyses and Levene's test were used to evaluate normality of residuals and homogeneity of variance, and ultimately square-root transformations of DRA concentration values were used in all cases. Significant differences between time points within a specific sample part were also compared using univariate ANOVA. Following significant *F*-tests, means were separated using the LSD test ($\alpha=0.05$). All data were analyzed using IBM SPSS Statistics v. 20 (SPSS Inc., 2011). Letter annotations were added as in above paragraph.

2.5.6. Total RNA isolation

Total RNA was isolated from white spruce samples for use in qPCR analysis. Time points 1-11 were pooled consisting of 4 individual biological samples (pooled due to sample limitations), while time points 12-31 each consisted of four biological replicates. Total RNA isolation from white spruce was facilitated by use of the PureLink Plant RNA Reagent (Life Technologies). Samples were ground to a fine powder with mortar and pestle under liquid nitrogen. PureLink Plant RNA reagent (500 μ L) was mixed with 30-50 mg ground white spruce apical bud or apical shoot sample (including either needle, stem and new buds) and incubated at room temperature for 5 min. This solution was clarified through centrifugation at 12,000g for 2 min at 4°C. The clarified extract layer was removed from the resulting sample pellet and 100 μ L 5 M NaCl and 300 μ L chloroform were mixed with the clarified extract. The sample was again centrifuged as above resulting in a separation of phases. The upper aqueous phase was removed, mixed with an equal volume of isopropanol and allowed to stand at room temperature for 10 min. To obtain the precipitated total RNA, the sample was centrifuged at 12,000g for 10 min at 4°C and the resulting pellet was washed with 70% EtOH. The pellet was resuspended in 20-30 μ L diethylpyrocarbonate (DEPC)-treated ddH₂O and stored at -80°C until further use. All solutions were prepared with DEPC-treated ddH₂O in glassware baked at 200°C for at least 4 h. RNA concentration was quantified by use of an Agilent 2100 Bioanalyzer (Agilent Technologies) following manufacturer guidelines using RNA 6000 Nano chips (Agilent Technologies).

2.5.7. cDNA synthesis

cDNA was synthesized from total RNA using Superscript III reverse transcriptase (RT, Invitrogen). Total RNA (1 µg) was initially treated with 1 µL deoxyribonuclease I containing 1 U of activity (DNase I amplification grade, Invitrogen) and 1 µL DNase 10X buffer (200 mM Tris-HCl, pH 8.4, 20 mM MgCl₂, 500 mM KCl) and incubated for 15 min at room temperature. The DNase reaction was stopped by the addition of EDTA to a final concentration of 2.3 mM and heating for 10 min at 65°C. The DNase treated total RNA was then incubated with 50 ng random primers (Invitrogen) and dNTP mix at a final concentration of 0.77 mM (dNTP mix contains equal concentrations of dATP, dGTP, dCTP, dTTP; Invitrogen) for 5 min at 65°C. This mixture was then incubated with 1 µL RNaseOUT Recombinant RNase Inhibitor (containing 40 U, Invitrogen), 5 mM DTT and 1 µL Superscript III RT (containing 200 U) in 4 µL Superscript III 5X buffer (250 mM Tris-HCl, pH 8.3), 375 mM KCl, 15 mM MgCl₂, Invitrogen) in a PCR machine, with protocol as follows: 5 min at 25°C, 50 min at 50°C, and 15 min at 70°C. The resulting first strand synthesized cDNA was stored at -80°C until further use.

2.5.8. Quantitative real-time PCR (qPCR) analysis

Gene transcript levels of *PgCPS*, *PgKS*, *PgLAS*, *PgCYP701*, *PgCYP720B4*, *PgDXS1*, *PgDXS2A* and *PgDXS2B* were measured by qPCR with a BioRad CFX96 Real-Time Detection System and using BioRad Hard-Shell Low-Profile Thin-Wall 96-well Skirted PCR plates. The qPCR program was: initial denaturation at 95°C for 30 sec, 40 cycles at 95°C for 5 sec, then 57°C for 5 sec with plate read, followed by melting curve analysis starting at 65°C and increasing to 90°C in 0.5°C increments at 5 sec intervals. Selected qPCR products

for each primer pair were PCR purified (using Qiagen MinElute PCR purification kit) and sequenced to validate qPCR primer specificity; PCR products varied from 208-284 bp in length. The qPCR well plates were set up in a sample maximized fashion (Hellemans et al., 2007) with corresponding reference gene, elongation factor 1 α (eEF1 α), being run with identical sample cDNAs on each plate alongside the gene of interest. In this experiment four biological replicates and three technical replicates were employed; in addition, no template controls (NTC) for each primer pair were run on each qPCR plate. Each sample well contained 3.75 μ L of a 1.2 μ M mix of forward and reverse primers (Table 2.1; Table 2.2), 7.5 μ L SsoFast Evagreen Supermix (2X mix; Bio-Rad) and 3.75 μ L cDNA template (3 ng μ L⁻¹). NTC wells contained 3.75 μ L DEPC-treated dH₂O in place of cDNA. Quantification and normalization of qPCR data to eEF1 α was carried out using BioRad CFX Manager (v. 1.6) software, employing the delta-delta Ct algorithm (Livak and Schmittgen, 2001), coupled with analysis of data via Excel spreadsheet (Microsoft) for standard error calculations and visualization. Transcript abundance levels for each gene of interest are expressed relative to the expression of the reference gene eEF1 α (\pm SEM).

2.5.9. Statistical analysis of gene expression data

Relative transcript abundance of *PgCPS*, *PgKS*, *PgLAS*, *PgCYP701*, *PgCYP720B4*, *PgDXS1*, *PgDXS2A* and *PgDXS2B* from time points 1-11 could not be statistically analyzed due to a lack of material for biological replicates and pooling of samples; however, time points 12-31 were statistically analyzed. Relative transcript levels did not meet assumptions of normality and homogeneity of variance, and thus were analyzed using non-parametric methods. Overall effects were analyzed using the Kruskal-Wallis test, which is a rank-based

nonparametric test. Here data values are given ranks and the test statistic is expressed as H which is a representation of the variance of the ranks among groups. Also calculated was the P value which if it is equal to or smaller than the chosen significance level (α) indicates that the data are not consistent with the null hypothesis (which in the Kruskal-Wallis test is that the medians of all groups are equal and not significantly different). In addition, the Kruskal-Wallis test was used in post-hoc pairwise comparisons ($\alpha=0.05$). Statistical analysis results are presented as:

$$H(\text{degrees of freedom})= x, N= y, P= z$$

Where x , y , and z represent specific values, N is the number of data points and degrees of freedom is the number of groups minus 1. All data were analyzed using IBM SPSS Statistics v. 20 (SPSS Inc., 2011). Data annotations with letters in figures and tables show significant differences based on P values from post-hoc pairwise comparisons. Letter annotations were deciphered manually based on scrutiny of the large data output files from the statistical testing.

Whole apical bud or apical shoot samples from time points 13, 15, 17, 19, 21, 23, and 25 were separated into 2 or 3 sample parts (as described in section 2.5.2.) and relative transcript abundances of *PgCPS*, *PgKS*, *PgLAS*, *PgCYP701*, *PgCYP720B4*, *PgDXS1*, *PgDXS2A* and *PgDXS2B* were measured in each sample part. Data was statistically analyzed as described above, assessing the significant differences between sample parts over time.

2.6. Effects of methyl jasmonate treatment on diterpenoid production and gene expression over time

2.6.1. Experimental treatment of plant materials

White spruce (*Picea glauca*; clone Pg653) seedlings were obtained and grown as described in section 2.5.1 above. Trees were repotted from individual cone pots to 1-gallon pots using perennial soil mix from West Creek Farms (Fort Langley, BC). Each 1-gallon pot was fertilized with 13g Professional Horticulture 'ProHort' Premium 20-10-10 controlled release fertilizer (Direct Solutions, Delta, BC). Trees were 5 years old at the time that experiments began. Four weeks prior to MeJA treatment, on April 22, 2012, trees were moved inside the University of British Columbia horticulture greenhouse with a constant 16/8 h photoperiod and mean temperatures of 23°C/21°C (day/night), with daily watering. During this time period the trees underwent vegetative bud break/flush and development of new vegetative shoot tissues, signalling a complete break from dormancy. On May 22, 2012, after bud growth had ceased, individual trees were placed under large autoclave bags and each tree was treated by spraying with 20 mL 0.1% MeJA (95% w/w pure, Sigma-Aldrich) in 0.1% Tween-20 (v/v) using an atomizer. Control trees were sprayed with 20 mL 0.1% Tween-20 to account for solvent effects (as reported in Miller et al., 2005); bags were removed after spraying. Control and MeJA-treated trees were separated by at least 10 feet of bench space in the greenhouse. On day 0, four control trees were sampled, whereas at all other time points (days 2, 4, 6, 8, 16 and 30) four control and four MeJA-treated trees were harvested. During harvest, trees were dissected into distinct sample types, using pruning shears and razor blades. Bark/Phloem from the 1st interwhorl denotes all tissues outside the vascular cambium (including phloem, cortex, and periderm) that grew in the previous year;

wood/xylem from the 1st interwhorl denotes all xylem tissues and pith of a stem section that grew in the previous year (Figure 2.2). Young needles are exclusive to the current year's growth and were harvested in part in conjunction with young stems which constitute the developing bark/phloem and wood/xylem of a side branch originating on the 1st interwhorl (note: young stems were not harvested on day 0). Mature needles were harvested exclusively from the previous year's growth. After harvesting and dissection, samples were flash frozen in liquid nitrogen and stored at -80°C prior to analyses.

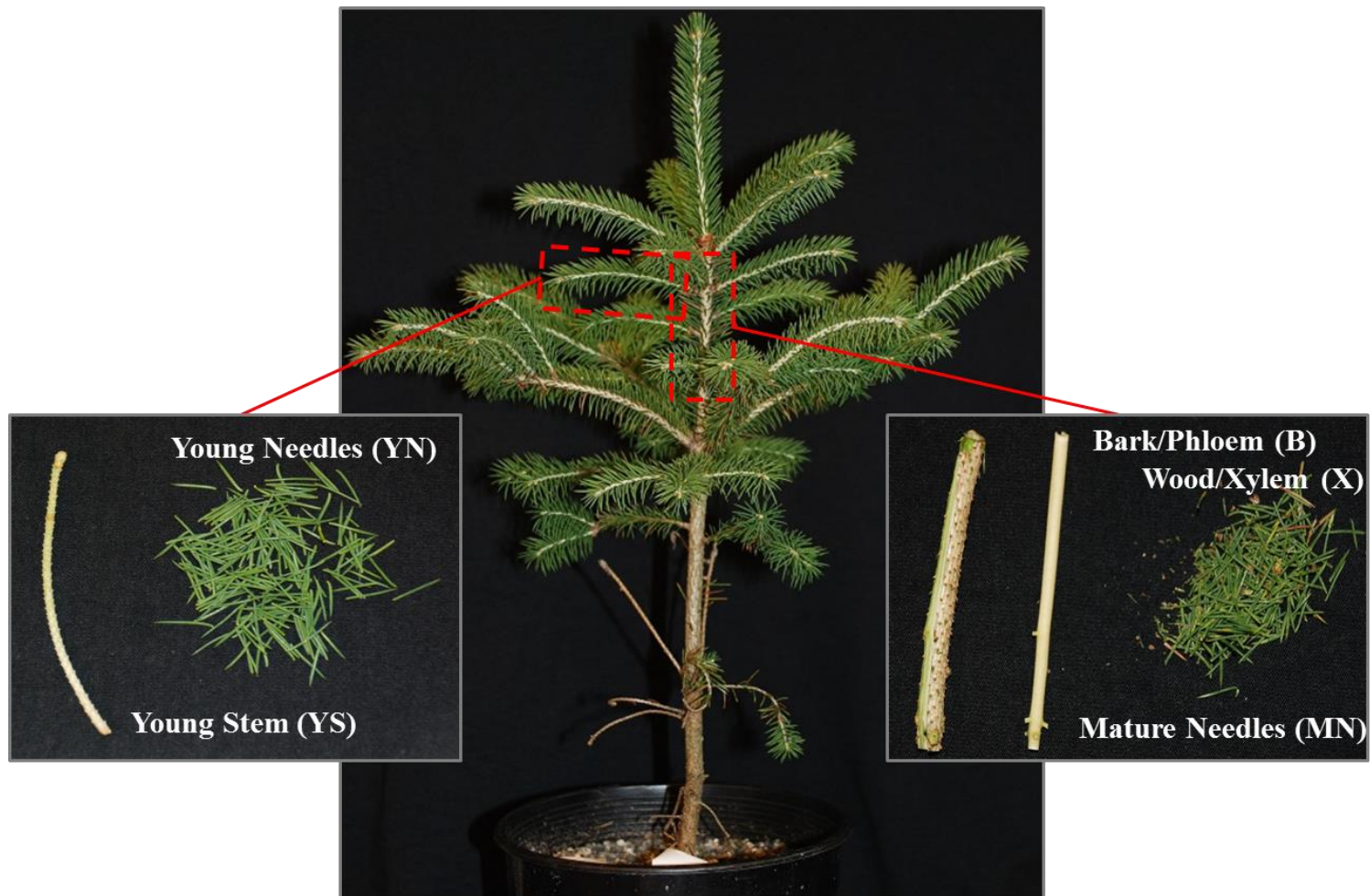


Figure 2.2. White spruce *Pg653* samples for transcript and metabolite analysis in the MeJA treatment experiment. Samples included: bark/phloem (B), and wood/xylem (X) originating from the 1st interwhorl; mature needles (MN) exclusively from the previous year's growth; young stem (YS) samples consisting of phloem and xylem of a side branch from the current year's growth; and young needles (YN) exclusively from the current year's growth.

2.6.2. Extraction of DRAs

Methods for the extraction and derivatization of diterpenoids and GC-MS analysis were adapted from Lewinsohn et al. (1993) and Hamberger et al. (2011) and performed with three technical replicates and three to four biological replicates for each time point and/or sample type. All steps were carried out in 2-mL amber vials (Agilent). Samples weighing 5-50 mg were ground to a fine powder with mortar and pestle under liquid nitrogen and extracted by shaking overnight in 750 μ L of tert-butyl methyl ether with 101.2 μ g mL⁻¹ 12,14-dichlorodehydroabietic acid as an internal standard. Remaining extraction and derivatization steps to prepare samples for GC-MS are as in section 2.5.3.

2.6.3. Analysis of DRA metabolites by GC-MS

Extracted DRAs from samples of the MeJA-treated time course were analyzed by GC-MS with an AT-1000 capillary column (24.5m x 250 μ m i.d., x 0.25 μ m film thickness; Alltech) in scan/SIM mode (scan, m/z 40-500; SIM, m/z 270, 272, 284, 286, 288, 307, 314, 316 [dwell time 35]) on an Agilent 6890N series GC-MS system, with an Agilent 7683B autosampler, coupled to an Agilent 5975 MSD system (Agilent Technologies). Samples of 0.1 μ L or 0.2 μ L were injected in pulsed splitless mode at 250°C with a column flow of 0.9mL helium min⁻¹ and 25 p.s.i. pulse pressure. The following GC temperature program was used: 150°C for 1 min, ramp at 1.65°C min⁻¹ to 200°C, ramp again at 25°C min⁻¹ to 240°C, hold for 12 min, for a run time of 44.9 min. Remaining data analysis and calculation steps were conducted as in section 2.5.4.

2.6.4. Statistical analysis of changes in DRA concentrations

DRA concentration data for the 5 white spruce sample types (YN, MN, B, X, YS) treated with 0.1% MeJA (or Tween control) and collected over a 30-day time course did not meet assumptions of normality and homogeneity of variance, even after several transformations of the data were attempted (square-root, log₁₀, ln(x), 1/square-root, etc.). Therefore, non-parametric methods were used to analyze the DRA data. Data were analyzed using the Kruskal-Wallis test to identify significant differences among treatment groups, time points and sample types (see Section 2.5.9). In addition, the Kruskal-Wallis test was used in post-hoc pairwise comparisons ($\alpha=0.05$) to separate sample and treatment interactions, sample and time interactions, and treatment and time interactions within each specific sample type. All data were analyzed using IBM SPSS Statistics v. 20 (SPSS Inc., 2011). Data annotations with letters in figures and tables show significant differences based on *P* values from post-hoc pairwise comparisons. Letter annotations were deciphered manually based on scrutiny of the data output files from the statistical testing.

2.6.5. Total RNA isolation and cDNA synthesis

Total RNA isolation was carried out with 30-100mg finely ground sample as described previously in section 2.5.6. and then cDNA was synthesized from total RNA using Maxima First Strand cDNA Synthesis Kit for RT-qPCR with double stranded DNase (dsDNase; Thermo Scientific). Total RNA (1 μ g) was incubated with 0.5 μ L dsDNase, 0.5 μ L 10X dsDNase buffer (Thermo Scientific), and ddH₂O to a final volume of 5 μ L for 2 min at 37°C. DNase treated total RNA was mixed with 1 μ L Maxima Enzyme Mix (containing Maxima Reverse Transcriptase and RiboLock RNase Inhibitor; Thermo Scientific), 2 μ L of

5x reaction mix [250 mM Tris-HCl, pH 8.3, 375 mM KCl, 15 mM MgCl₂, 50 mM DTT as well as dNTPs, oligo (dT)₁₈ and random hexamer primers (Thermo Scientific)], and 2 µL ddH₂O. This mixture was subjected to the following PCR program: 25°C for 10 min, 50°C for 15 min, and 85°C for 5 min to terminate the reaction. The resulting first strand synthesized cDNA was stored at -80°C until further use.

2.6.6. Quantitative real-time PCR analysis

Gene transcript levels of *PgCPS*, *PgKS*, *PgLAS*, *PgCYP701*, *PgCYP720B4*, *PgDXS1*, *PgDXS2A* and *PgDXS2B* were measured by qPCR with a BioRad CFX384 Touch Real-Time Detection System using BioRad Hard-Shell Thin-Wall 384-well Skirted PCR plates. The qPCR program was: initial denaturation at 95°C for 30 sec, 40 cycles at 95°C for 5 sec, then 57°C for 5 sec with plate read, followed by melting curve analysis starting at 65°C and increasing to 90°C in 0.5°C increments at 5 sec intervals. Selected qPCR products for each primer pair were PCR purified (using Qiagen MinElute PCR purification Kit) and sequenced to validate qPCR primer specificity; PCR products varied from 208-284 bp in length. The qPCR well plates were set up in a sample maximized fashion (Hellemans et al., 2007). Four biological replicates and two technical replicates were used for each data point; no template controls (NTC) for each primer pair were included on every plate. Each sample well contained 1 µL of a 3.6 µM mix of forward and reverse primers (Table 2.1; Table 2.2), 6 µL SsoFast Evagreen Supermix (2X mix; Bio-Rad) and 5 µL cDNA template 1.8 ng µL⁻¹; NTC wells contained 5 µL DEPC-treated dH₂O in place of cDNA.

Quantification of qPCR data was carried out using qbase plus software (v. 2.6.1; Biogazelle) coupled with analysis of data via Excel spreadsheet (Microsoft) for standard error calculations and visualization. The qbase plus software implements a modified delta-delta-Ct algorithm designed to take into account multiple reference genes as well as integrate an inter-run calibration algorithm to account for differences between plates and runs (Hellemans et al., 2007). Within the qbase plus program qPCR runs are translated into transcript abundances through first calculating the average sample Cq value (cycle quantification value, otherwise known as Ct, cycle threshold value) from the technical replicates of the same gene. The mean Cq values for each sample are then transformed into RQs (relative quantities; relative to other samples within the same run for the same gene) using the average Cq across all samples for that given gene as a reference point and a defined PCR amplification efficiency [here amplification efficiency (E) is assumed to be 100%, and is represented as a value of 2 in the calculations to reflect the exponential function of PCR)]. The RQ values are converted into normalized relative quantities (NRQs) by division of the RQ by a normalization factor (NF, the geometric mean of the RQs of the reference genes). Next the NRQs are calibrated to avoid plate-to-plate variation using inter-run calibrators (IRCs, identical qPCR samples run for every gene target/primer pair that appears on the multiple plates that are being compared). This is done by division of the NRQs by a calibration factor (CF, the geometric mean of the different IRCs' NRQs) to yield CNRQs (calibrated normalized relative quantities). Detailed equations can be found in Hellemans et al. (2007). The CNRQs can then be exported into Excel to determine standard error of the mean and visualize via graphing.

This experiment employed two IRCs composed of mixtures of 5 cDNA samples from individual biological samples spanning all 5 sample types used as well as a selection of time points. IRC1 contained equal volumes of $1.8 \text{ ng } \mu\text{L}^{-1}$ cDNA samples from: 1st interwhorl phloem control day 6, 1st interwhorl xylem control day 16, mature needles MeJA-treated day 8, young needles control day 0, and young stems MeJA-treated day 4. IRC2 contained equal volumes of $1.8 \text{ ng } \mu\text{L}^{-1}$ cDNA samples from: 1st interwhorl phloem control day 16, 1st interwhorl xylem MeJA-treated day 4, mature needles MeJA-treated day 4, young needles control day 0, and young stems control day 30). Using the qbase plus software, transcript abundance was normalized to translation initiation factor 4E (*eIF4E*) and core histone protein 3 (*H3*).

2.6.7. Reference gene stability testing

Reference gene stability testing was carried out using qbase plus software component GeNorm (Biogazelle; Vandesompele 2002) to find the most stable and suitable candidate reference genes for this experiment since it spans multiple sample types, time points, and two treatment types. A total of eight reference genes were tested (*Cdc2*, *RPL3*, *eIF4E*, *eIF5A*, *H3*, *UBE2*, *eEF1 α* , *ACT2*) using primers modified from Beaulieu et al. (2013) and Hamberger et al. (2011) (Table 2.4). Primer pairs for these putative reference genes were tested against all 5 sample types (young needle, mature needle, 1st interwhorl wood/xylem, 1st interwhorl bark/phloem, and young stems), both treatment types (Tween control versus MeJA-treated) and 4 time points (days 2, 6, 8, and 30). In each case, one biological replicate was chosen and primer pairs were tested in duplicated wells of each of the above sample types, using a

sample maximized well plate layout. All detailed equations can be found in Hellemans et al. (2007).

Table 2.4. Oligonucleotide primers used for reference gene stability testing.

Gene	Direction	Sequence (5'→ 3')	Putative Annotation
qPCR reference gene stability testing			
<i>PgACT2</i>	Forward Reverse	GTTTCCTGGTATGCTGACCGT ATGAGC TGGACGATGGAAGGACCAGA TTCA	Actin 2
<i>PgCdc2</i>	Forward Reverse	GGACACCAAATGAAGAAACA TGG CGAGAGAAGATCAATCCTGCT	Cell division cycle protein 2
<i>PgeEF1a</i>	Forward Reverse	GTTGCTGTAACAAGATGGATG C CCCTCAAAACCAGAGATAGG C	eukaryotic elongation factor 1 alpha
<i>PgeIF4E</i>	Forward Reverse	GTAGGGGAGTATGCGAGCTC TGGACCAGCAATTAGAACTA GG	eukaryotic translation initiation factor 4E
<i>PgeIF5A</i>	Forward Reverse	CATCCGCAAGAACGGCTAC GTAACATGAGGGACATCGCA G	eukaryotic translation initiation factor 5A
<i>PgH3</i>	Forward Reverse	ATCTTGTGGGTCTGTTTGAGG CATATCCCCTCCCATCAAAGT	Core histone 3
<i>PgRPL3</i>	Forward Reverse	GGTTACTTTGCGACAGTCATT G CCCATGTCCAAACTTAGAGGA TG	Ribosomal protein L3
<i>PgUBE2</i>	Forward Reverse	CTGAACAGAGGAATCAAGAA GTG CATACTTAAGCACCAATCGCA TA	Ubiquitin-conjugating enzyme E2

2.6.8. Statistical analysis of gene expression data

Relative transcript abundance of *PgCPS*, *PgKS*, *PgLAS*, *PgCYP701*, *PgCYP720B4*, *PgDXS1*, *PgDXS2A* and *PgDXS2B* in control or MeJA-treated samples over the 30-day time course were statistically analyzed using the Kruskal-Wallis test, as relative transcript levels did not meet assumptions of normality and homogeneity of variance (see Section 2.5.9). Overall effects of treatment types, time and sample types were analyzed within data of each gene; in addition the Kruskal-Wallis test was used in post-hoc pairwise comparisons ($\alpha=0.05$) to separate sample and treatment interactions, sample and time interactions, and treatment and time interactions within each specific sample type. All data were analyzed using IBM SPSS Statistics v. 20 (SPSS Inc., 2011). Data annotations with letters in figures and tables show significant differences based on *P* values from post-hoc pairwise comparisons. Letter annotations were deciphered manually based on scrutiny of the large data output files from the statistical testing.

Chapter 3: Functional characterization and comparison of expression of genes involved in gibberellin and diterpene resin acid biosynthesis in white spruce

3.1. Introduction

Although the GA and DRA pathways serve different functions in conifers, these two pathways are biochemically similar and appear to share common evolutionary ancestry. Despite the biochemical similarity between these pathways, studies with gymnosperms have yet to accomplish a comprehensive comparison of the diTPSs and CYP450s involved in GA and DRA metabolism within a single species. A major goal of this chapter was to elaborate on the knowledge base of the genes involved in GA and DRA biosynthesis in spruce, and provide a thorough comparison of how these similar pathways of general and specialized metabolism are organized within a conifer species. The present chapter investigates the corresponding diTPS and CYP450 genes from the GA and DRA pathways, representing growth and defense centric processes, respectively. The chapter compares and contrasts gene function and expression with respect to different sample types, treatments and times across the annual growing cycle of spruce.

Experiments to attain these goals were carried out with white spruce (*Picea glauca*), an economically valuable tree species used commercially for pulp and paper, and lumber products. White spruce and its hybrids are dominant across Canada. To tolerate northern winters, white spruce has developed a seasonal cycle that allows the tree to enter dormancy over the winter months and to resume growth once temperature and photoperiod conditions become favorable in the spring. Within a relatively short growing season, white spruce and

other conifers must deal with competing demands for resource allocation - on the one hand a need to maximize growth and on the other hand the need to defend the living tree against attack by pests and pathogens. Hence, the white spruce system offers a good model with which to compare the GA (growth) and DRA (defense) pathways.

In a determinate/overwintering species, such as *P. glauca*, vegetative buds contain preformed primordia of stem units, which generally constitute all of the next season's terminal shoot growth. These buds ensure regrowth once environmental conditions are again favorable, however uncontrolled growth or late bud development can have disastrous effects on the tree's fitness (Rohde et al., 2000; Kozlowski and Pallardy, 1997). The development of vegetative buds corresponds with growth cessation and dormancy acquisition and represents a concession within the plant between active growth and preparation for winter temperatures. The timing of this process is critical, since early bud set would shorten the growth phase and affect the biomass of the tree whereas late bud set would hamper the tree's growth potential in the next season (Howe et al., 2003, Horvath et al., 2003, Ruttink et al., 2007; Rohde and Bhalerao, 2007). The initiation of vegetative and apical bud set in determinate species is an autonomous process, but in order to complete development and enter into dormancy these buds must be subjected to shortened photoperiods and low temperature over several weeks or months (Howe et al., 2003; Kayal et al., 2011). Once dormancy is established, trees must be exposed to uninterrupted temperatures estimated to be between -5 to +1°C for a period of 4 to 8 weeks before growth will resume in the bud meristem (Heide, 1993; Nienstaedt, 1966).

In conifers, biologically active gibberellins include GA₁, GA₃, GA₄, GA₇ and GA₉ that promote shoot elongation as well as function in a variety of other areas such as cone bud differentiation and seed germination (Little and Macdonald, 2003; Moritz, 1995; Moritz et

al., 1990; Odén et al. 1995; Wang et al., 1996). Experimentally, the importance of GAs was demonstrated in hybrid aspen/poplar trees (*Populus tremula* x *P. alba*) where lowered levels of active GAs, due to overexpression of the catabolic enzyme GA 2-oxidase, led to early bud set and late bud burst (Zawaski et al. 2011). Reduced GA levels were associated with the down-regulation of gibberellin 3 β -hydroxylase and 20-oxidase genes, which act in the synthesis of bioactive gibberellins (Yamaguchi and Kamiya, 2000; Eriksson and Moritz, 2002; Cooke et al., 2012; Kayal et al., 2011). Studies in hybrid aspen/poplar (*Populus tremula* x *P. alba* and *Populus tremula* x *P. tremuloides*) and bay willow (*Salix pentandra*) also showed that decreased GA levels correlated with subsiding of subapical cell division and led to stem growth cessation under short day conditions (Olsen et al., 1995a, b; Olsen et al., 1997; Ruttink et al., 2007). A study by Kayal et al. (2011) that followed apical bud formation events in white spruce under short day conditions showed that after the active elongation phase of the current year's stem, GA levels were low or non-detectable throughout the subsequent 70 days of bud development.

The role of GAs in conifers can be linked to growth cessation, bud set and bud development. However the specific relationship between terpenoid biosynthetic pathways of general and specialized metabolism has not been directly addressed with respect to the bud developmental processes. The present chapter investigates this with a comprehensive analysis of the responses of genes involved in the GA and DRA pathways as they relate to the development of apical buds and apical shoots over a year-long time course. Over the course of a year, apical buds and shoots show a range of developmental processes including cessation of dormancy, initiation of new growth, and oleoresin accumulation. Apical bud growth shows identifiable phenology, allowing growth to be easily divided into defined

stages that are also commonly used as an index of plant development in forestry practices. To identify stages of the development of white spruce apical buds the phenological classification system of Alfaro et al. (2000), which describes the growth and budburst stages of Sitka spruce vegetative apical buds according to the level of bud swell, colour, and elongation, was adapted for this current study in white spruce (see Appendix 1). Apical bud and apical shoot samples were collected at 31 time points to cover a calendar year of growth, and samples taken during times of fast growth were also dissected into more specific parts to better understand the organization of the GA and DRA biosynthetic genes over time and space.

Another example of the potential interplay between growth and defense pathways is during pest attack. Conifers utilize an array of defenses against many kinds of potential pests. These defensive systems include chemicals, such as terpenoids and phenolics, as well as physical barriers, such as stone cells, resin ducts and resin blisters (Zulak and Bohlmann, 2010; Miller et al., 2005; Franceschi et al., 2005; Keeling and Bohlmann, 2006). The types of defence strategies used can be grouped into two basic categories - inducible defenses that can be generated *de novo* when a pest challenge is received and constitutive defenses that are continuously present.

Induction of defenses can be mimicked experimentally through fungal or pathogen application, mechanical wounding, or MeJA treatment (Martin et al., 2002; Miller et al., 2005; Franceschi et al., 2002). Previous studies have shown that gene expression of conifer TPSs and CYP450s involved in oleoresin and volatile defense production can be induced by MeJA or mechanical wounding (Fäldt et al., 2003; Miller et al., 2005; Hamberger et al., 2011), leading to increased enzyme activity, protein levels and changes in the tree's terpenoid metabolite profile (Zulak et al., 2009; Hall et al., 2011). However, the response of

specific GA pathway TPSs and CYP450s to MeJA treatment has not been investigated in conifers.

The second part of this chapter used a MeJA challenge to stimulate a defense response that was hypothesized to include induction of terpene biosynthetic genes of the DRA pathway. Analysis covered a variety of white spruce sample types representing both young, fast growing, and mature samples, collected over a time course. The results provide a better understanding of the coordination between the GA and DRA pathways under stress.

3.2. Results

3.2.1. Cloning and identification of spruce diTPSs: CPS, KS and LAS

Two monofunctional diterpene synthases, copalyl diphosphate synthase (*CPS*) and kaurene synthase (*KS*), from Sitka spruce and one bifunctional, levopimaradiene/abietadiene synthase (*LAS*), from white spruce were cloned based on previously isolated orthologs in other spruce species. *PgLAS* was cloned as N-terminally truncated sequence with 76 amino acids removed, which produces a more active protein than that of the native sequence (Keeling et al., 2011b). *PsCPS* and *PsKS* were previously cloned as a full-length cDNA and a pseudomature cDNA (lacking a putative transit peptide), respectively, described in Keeling et al. (2010). Amino acid sequence alignments (Figure 3.1; Figure 3.2) with previously characterized diTPSs from conifers and the angiosperm *Arabidopsis thaliana* (*At*) confirmed the presence of characteristic diTPS motifs, including: the DxDD motif found in active site-II that catalyzes the cyclization of GGPP to *ent*-CPP (Prisic et al., 2007), and the DDxxD and

NDxxTxxxE motifs found in active site-I which are required for the ionization of the substrate's diphosphate group (Christianson, 2006; Keeling et al., 2010; Zerbe et al., 2012).

Compared to previously characterized orthologs, *PgLAS* (784 amino acids) has 90.2% and 90.6% sequence identity to *PsLAS* and *PaLAS* respectively (Keeling et al., 2011b; Martin et al., 2004). Conserved motifs in active site-I and -II are seen in *PgLAS* (Figure 3.1). *PsCPS* (761 amino acids) has 99.7% sequence identity to spruce ortholog *PgCPS* (Keeling et al., 2010), but shares only 41.4% identity with *AtCPS* (Sun and Kamiya, 1994). The conserved motif DxDD in active site-II is observed in all aligned CPS sequences (Figure 3.1). *PsKS* (757 amino acids) shares 99.2% sequence identity with *PgKS* (Keeling et al., 2010) and 40.3% identity with *AtKS* (Yamaguchi et al., 1998). The class-I active site conserved motifs are seen in all aligned KS sequences (Figure 3.2).

[illegible]

[illegible]

Phylogenetic analysis of selected characterized diTPSs originating from GA and DRA pathways from angiosperms and gymnosperm, including those characterized as ‘like’ genes, (Figure 3.3) shows predicted monophyletic clades TPS-c, for CPS sequences, TPS-e, for KS, and TPS-d3, a gymnosperm specific clade containing bifunctional LAS and ISO sequences as well as some monofunctional diTPS (Hall et al., 2013), when rooted with moss *Physcomitrella patens* bifunctional CPS/KS. White spruce CPS, KS and LAS sequences group very closely with previously characterized gymnosperm orthologs in spruce species. Within clades for CPS and KS, are monophyletic groupings of sequences from monocot and dicot plants with gymnosperm groups sharing a common ancestor with angiosperm plant sequences.

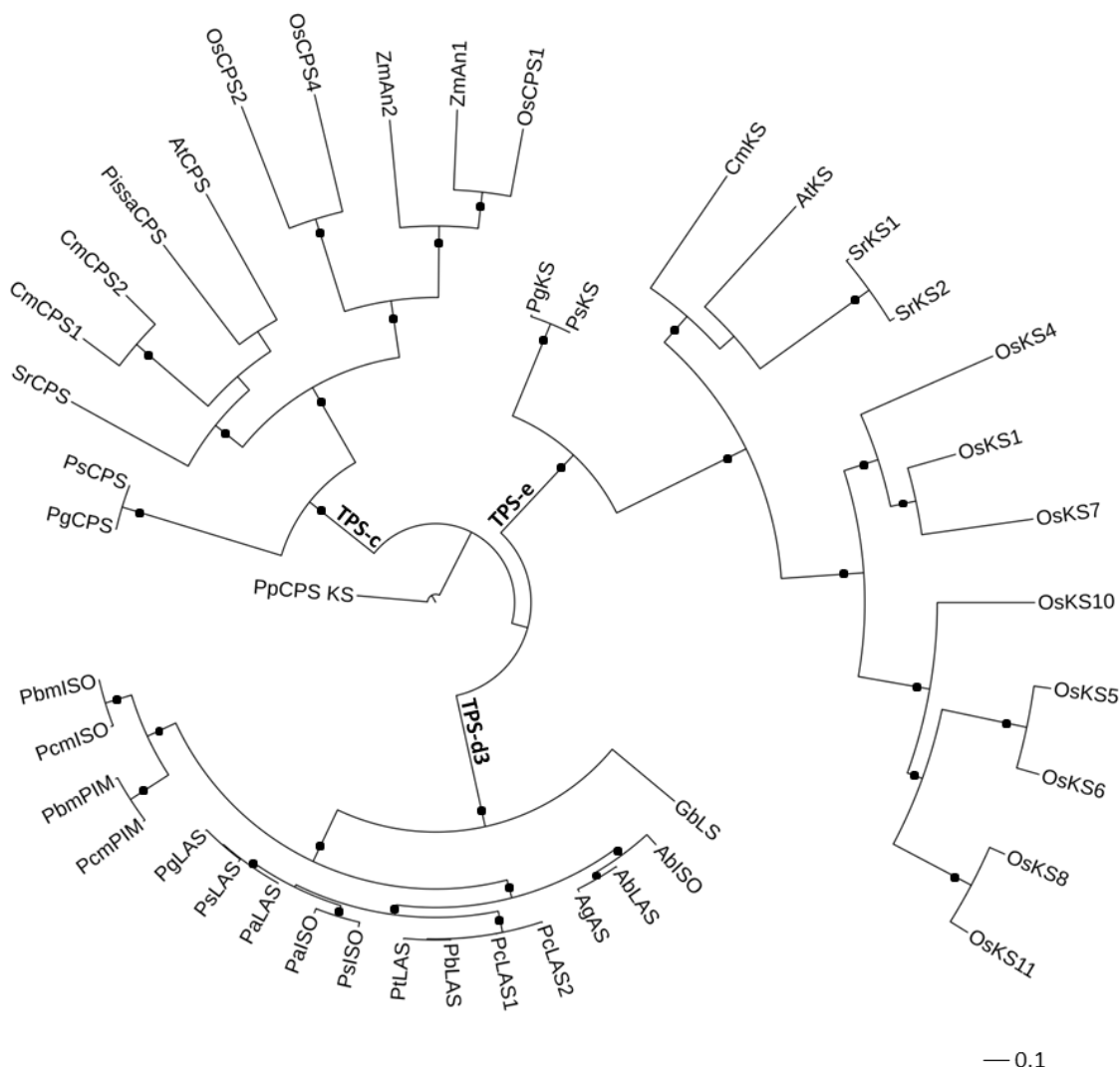


Figure 3.3. Phylogenetic maximum-likelihood tree of full-length amino acid diTPS sequences from angiosperms and gymnosperms characterized as or like CPS, KS or involved in the conifer specific TPS-d3 family. Outgroup used was the bifunctional *Physcomitrella patens* CPS/KS sequence (*PpCPS KS*; accession no. BAF61135). Legend bar indicates substitutions per site, black dots indicate branches with 80% or more bootstrap support (500 replications). Abbreviations and accession numbers are as follows: *AtCPS* (*Arabidopsis thaliana*; AAA53632), *AtKS* (AAC39443), *AbISO* (*Abies balsamea*; H8ZM71), *AbLAS* (H8ZM70), *AgAS* (*Abies grandis*; AAB05407), *CmCPS1* (*Cucurbita maxima*; AAD04292), *CmCPS2* (AAD04293), *CmKS* (AAB39482), *GbLS* (*Ginkgo biloba*; AAL09965), *OsCPS1* (*Oryza sativa*; BAD42449), *OsCPS2* (AAT11021), *OsCPS4* (syn-CPS; AAS98158), *OsKS1* (AAQ72559), *OsKS4* (syn-pimara-7,15-diene synthase; AAU05906), *OsKS5* (iso-KS; ABH10732), *OsKS6* (iso-KS; ABH10733), *OsKS7* (*ent*-cassadiene synthase; ABH10734), *OsKS8* (stemer-13-ene synthase; BAD34478), *OsKS10* (*ent*-sandaracopimaradiene synthase; ABH10735), *OsKS11* (stemodene synthase; AAZ76733), *PaISO* (*Picea abies*; AAS47690), *PaLAS* (AAS47691), *PbmISO* (*Pinus banksiana*; JQ240313), *PbLAS* (JQ240312), *PbmPIM* (JQ240316), *PcmISO* (*Pinus contorta*; JQ240314), *PcLAS1* (JQ240310), *PcLAS2* (JQ240311), *PcmPIM* (JQ240315), *PissaCPS* (*Pisum sativum*; AAB58822), *PgCPS* (ADB55707), *PgKS* (ADB55708), *PgLAS*, *PsCPS* (ADB55709), *PsKS* (ADB55710), *PsISO* (ADZ45512), *PsLAS* (ADZ45517), *PtLAS* (*Pinus taeda*; AY779541), *SrCPS* (*Stevia rebaudiana*; AAB87091), *SrKS1* (AAD34294), *SrKS2* (AAD34295), *ZmAn1* (*Zea mays* CPS1; AAA73960), *ZmAn2* (*ZmCPS2*; AAT70084).

3.2.2. Heterologous expression and functional characterization of spruce diTPSs: CPS, KS and LAS

PsCPS, *PsKS* and *PgLAS* were expressed in *E. coli* to conduct *in vitro* enzyme assays to test function. For protein purification, pET28b+ expression vector was used as it facilitates the addition of an N-terminal polyhistidine tag to each protein. SDS-PAGE and western blotting (with monoclonal anti-polyhistidine antibodies) were carried out to confirm expression and visualize purity of the proteins (Figure 3.4). While expressed at lower levels, *PsCPS* was present as shown by gel electrophoresis with some background *E. coli* proteins present. Western blotting confirmed a single enzyme band at 87.79 kD with no obvious degradation. *PsKS* protein was also visualized by gel electrophoresis with some background protein contamination. Subsequent western blotting confirmed a single band at 87.28 kD. Of the three diTPSs, *PgLAS* was most highly expressed; frequently, purified *PgLAS* protein concentrations would be more than twice that of *PsCPS* or *PsKS*. *PgLAS* could be visualized as a single protein band at 90.5 kD by gel electrophoresis with little to no background *E. coli* protein contamination.

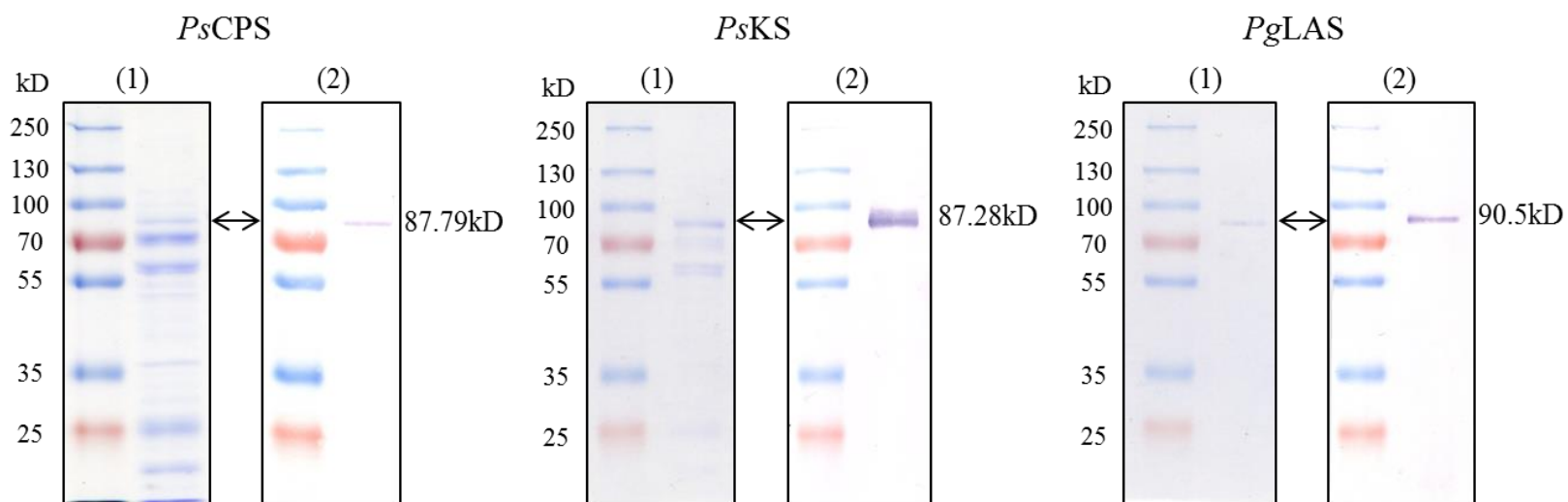


Figure 3.4. Polyacrylamide gel electrophoresis and corresponding Western blots showing the expression of three His-tag purified recombinant proteins from expression of recombinant Sitka and white spruce diTPS genes in *E. coli*: *PsCPS*, *PsKS*, and *PgLAS*. For each pair of gel images, the SDS-PAGE gel on the left (1) shows total protein stained with Coomassie blue dye and the gel image on the right (2) shows the immunoreactive band using monoclonal anti-polyHistidine-alkaline phosphatase antibodies. On each gel, molecular weight standards are shown in the left lane and sample protein in the right. The 2-headed arrow shows the position of the recombinant, 6x His-tagged protein. Molecular weight markers are Thermo Scientific, PageRuler Plus prestained protein ladder. Protein weights shown are calculated using average atomic masses of amino acids.

In vitro enzyme assays for *PsCPS* and *PsKS* were conducted with either protein alone or in conjunction with the other to produce *ent*-kaurene that could be observed by GC-MS. *PsCPS* protein was incubated with GGPP substrate and when performed as a single step enzyme assay produced *ent*-copalyl diphosphate, which after enzymatic dephosphorylation could be observed via GC-MS (Figure 3.5). A synthetic standard was not available, so *PsCPS* enzymatic product was compared to that of previously characterized *Zea mays* CPS (*ZmAn2*; Harris et al., 2005). The results showed that both *PsCPS* and *ZmAn2* produced *ent*-copalyl diphosphate, based on identical retention times (product had a retention time of approximately 12.7 minutes in the experiment shown in Figure 3.5) and mass spectra.

When *PsCPS* and *PsKS* proteins were coupled in a reaction with GGPP substrate (Figure 3.6), *ent*-kaurene was produced as shown by identical retention times with synthetic *ent*-kaurene standard as well as comparable mass spectra showing characteristic ions 272, 257 and 229 of diTPSs. When incubated with GGPP alone, *PsKS* did not produce *ent*-copalyl diphosphate or *ent*-kaurene, solidifying previous knowledge in white spruce (Keeling et al., 2010) that both *PsCPS* and *PsKS* are monofunctional diTPSs.

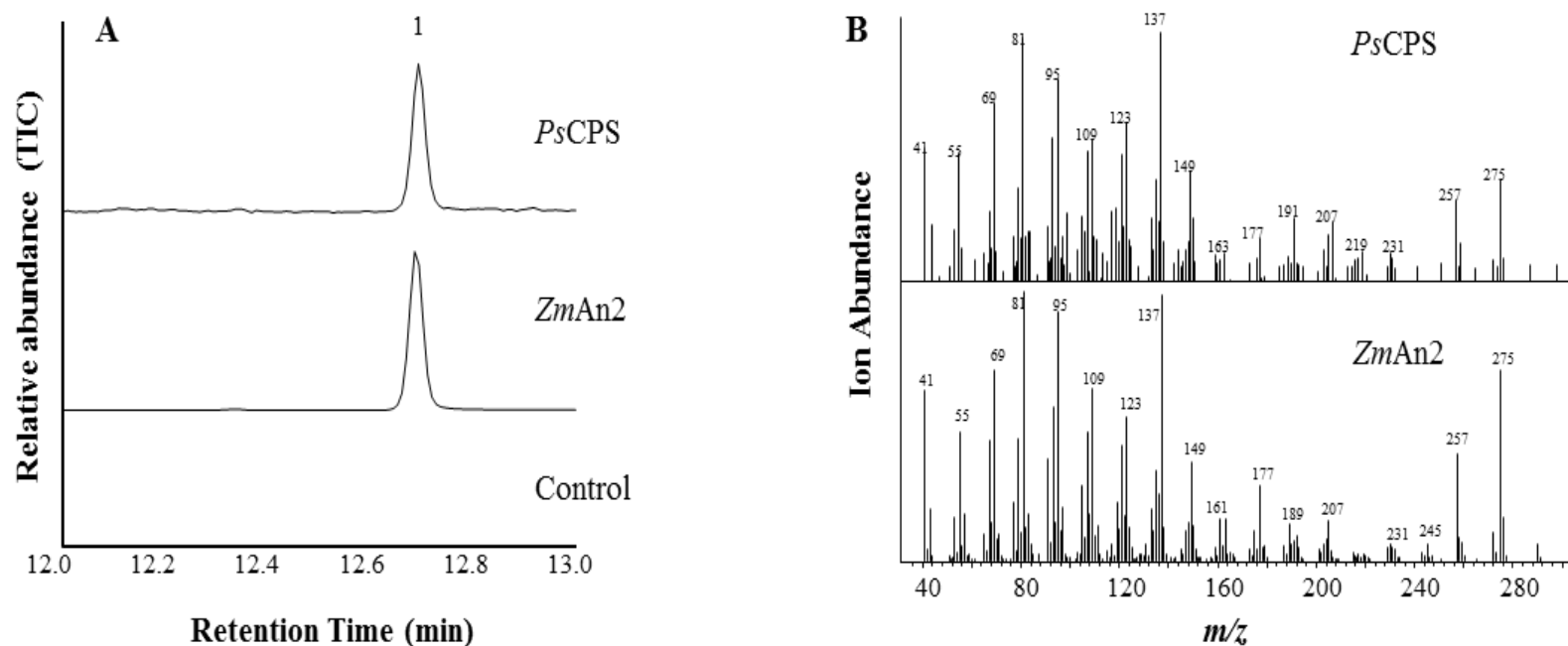


Figure 3.5. GC-MS analysis of *in vitro* assays with purified recombinant CPS proteins. (A) Assays were performed with either 50 μ g *PsCPS* or *ZmAn2* (*ent*-CPP synthase from *Zea mays*), incubated with GGPP, and analyzed on a SolGel-WAX column. Assay products were enzymatically dephosphorylated to produce *ent*-copalol (peak 1). Control consisted of *PsCPS* protein, heat denatured and incubated with GGPP. Assays are presented as individually scaled TIC (total ion current) chromatograms. (B) Mass spectrum of *PsCPS* assay product verified by comparison to mass spectrum from characterized *ZmAn2* assay product. m/z , Mass-to-charge ratio.

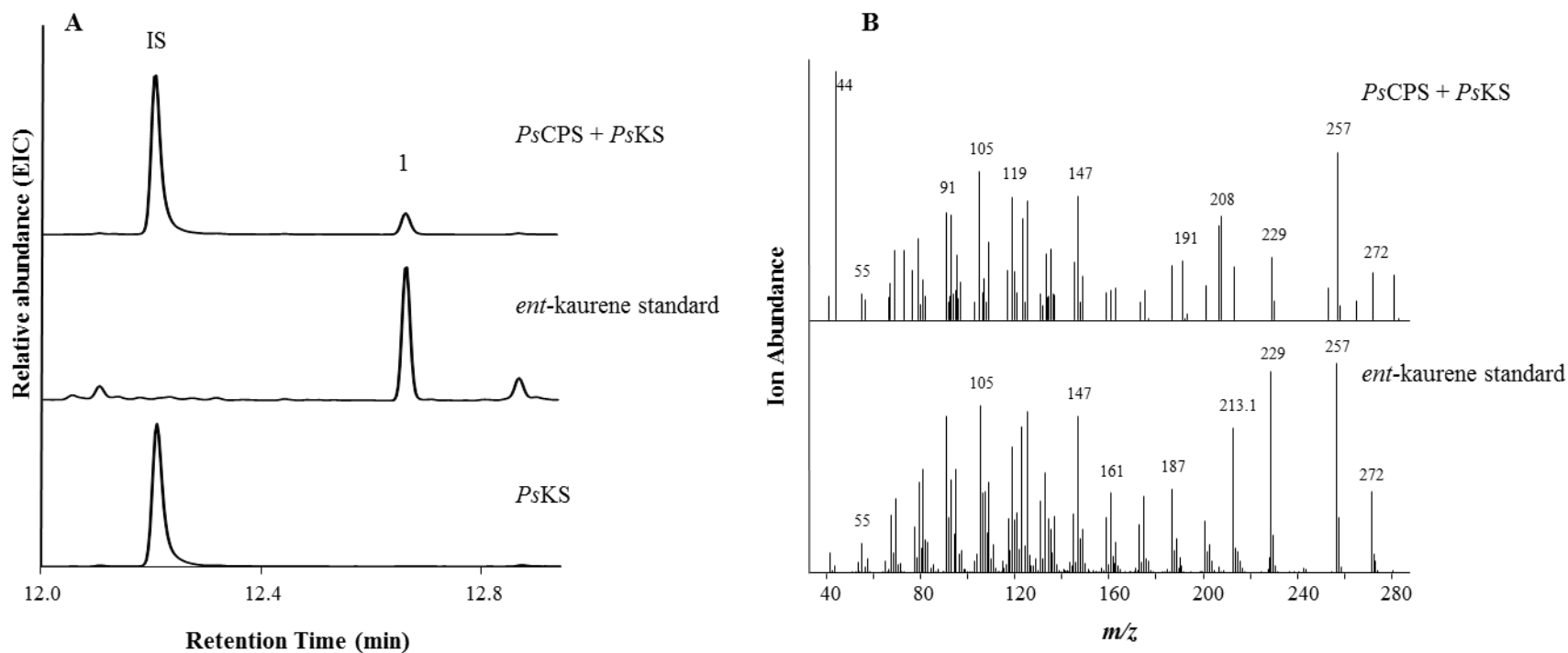


Figure 3.6. GC-MS analysis of the reaction product of recombinant *PsKS* protein. (A) Coupled *PsCPS* and *PsKS* *in vitro* assays were incubated with GGPP and analyzed on an HP-5 column (83, 272 m/z extracted-ion chromatogram). Predicted coupled *in vitro* assay product peak 1, *ent*-kaurene, was compared to authentic standard and single enzyme assay with *PsKS* (which did not produce any detectable products). (B) Mass spectrum of the *PsCPS* and *PsKS* assay product verified by comparison to authentic *ent*-kaurene standard. m/z , Mass-to-charge ratio. Internal standard, IS, is 1-eicosene.

In vitro enzyme assays to test function of *PgLAS* were performed as single enzyme assays incubated with GGPP as substrate. LAS functionality has been previously characterized in several conifer species including *Picea abies* (Martin et al., 2004) and *Picea sitchensis* (Keeling et al., 2011b), therefore enzyme assays of *PgLAS* were performed in parallel to *PaLAS* to confirm LAS olefin production (Figure 3.7). Both enzyme assays when analyzed by GC-MS showed the predicted olefin products: palustradiene, levopimaradiene, abietadiene and neoabietadiene. Further confirmation of assay products was done by LC-MS based on previous work by Keeling et al. (2011a) which suggests that *PaLAS* produces epimeric thermally unstable allylic tertiary alcohols, 13-hydroxy-8(14)-abietene as an initial product which is dehydrated under high temperature GC-MS conditions to the apparent LAS olefin products abietadiene, levopimaradiene, neoabietadiene and palustradiene. Enzyme assay products from *PgLAS* and *PaLAS* analyzed by LC-APCI-MS in positive ion mode showed a compound more polar than the diterpene abietadiene (Figure 3.8), consistent with the elution pattern of 13-hydroxy-8(14)-abietene. Mass spectra analysis showed characteristic ion 273, similar to m/z 272 of abietadiene, which is proposed to be due to dehydration of the allylic diterpenol during LC and subsequent ionization due to proton transfer at the APCI-MS interface (Keeling et al., 2011a).

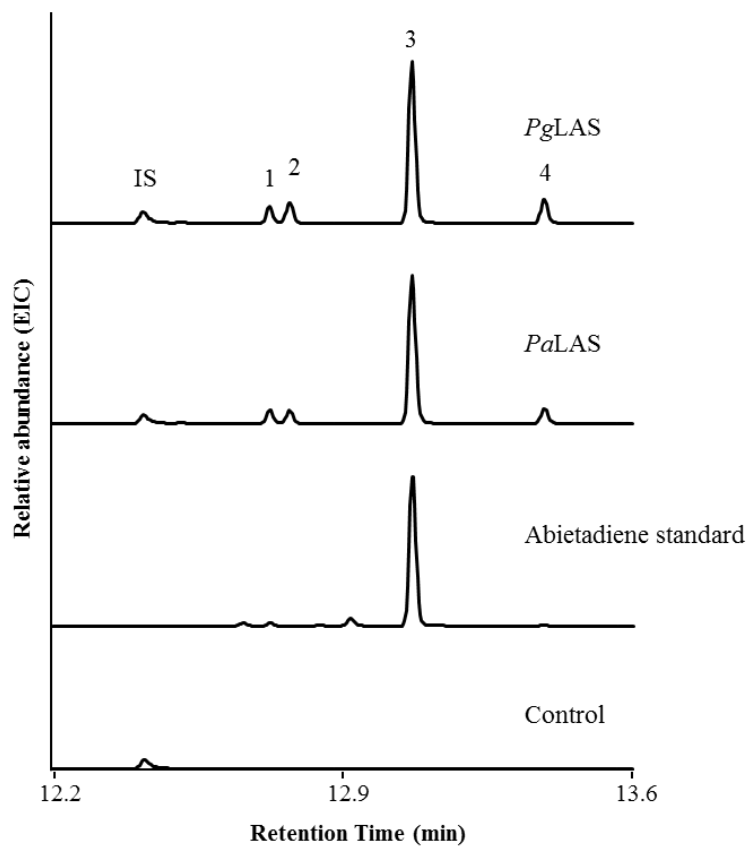


Figure 3.7. GC-MS analysis of the reaction products of recombinant LAS proteins. *In vitro* assays with purified LAS recombinant proteins were incubated with GGPP, and analyzed on an HP-5 column (83, 272 m/z extracted-ion chromatogram). Both *PgLAS* and *PaLAS* produced the predicted products: peak 1, palustradiene, peak 2, levopimaradiene; peak 3, abietadiene; peak 4 neoabietadiene with identical mass spectra and elution characteristics. Control consisted of *PgLAS* protein, heat denatured and incubated with GGPP, with internal standard (IS) 1-eicosene.

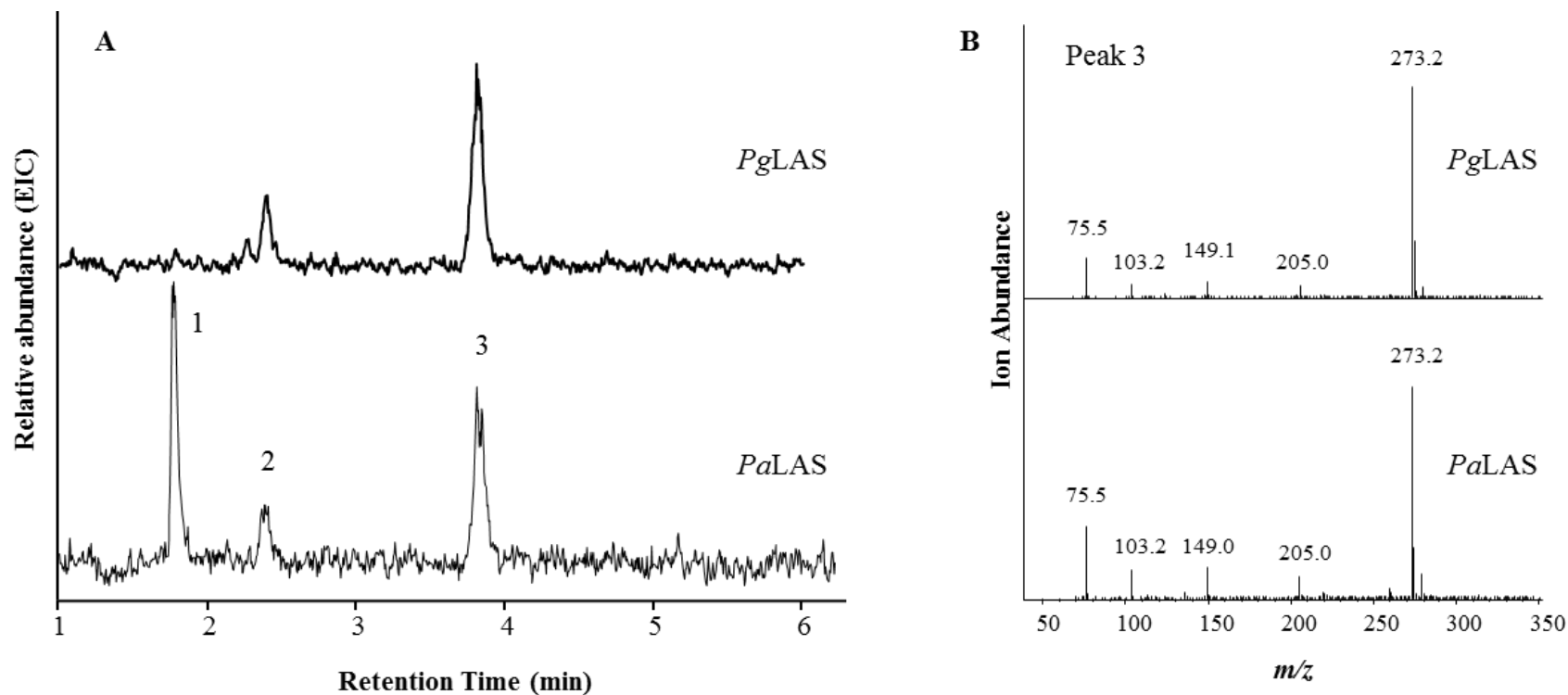


Figure 3.8. LC-MS analysis of assay products from *PgLAS* and *PaLAS*. (A) Chromatogram of *PgLAS* and *PaLAS* assay products for comparison (273 m/z extracted-ion chromatogram). Peaks are as follows: peak 1, abietadiene; peak 2, *in vitro* assay degradation product; peak 3, 13-hydroxy-8(14)-abietene. (B) Mass spectra of peak 3 of *PgLAS* and *PaLAS* assays. m/z , Mass-to-charge ratio.

3.2.3. Cloning and identification of white spruce CYP450s: CYP701 and CYP720B4

Cytochromes P450 monooxygenases *ent*-kaurene oxidase (*PgCYP701*) and *PgCYP720B4* were cloned from white spruce as full-length cDNAs. Cloning of *PgCYP701* was facilitated through the use of available bacterial artificial chromosome libraries (Hamberger et al., 2009) and sequences from databases of the white spruce genome project (Birol et al., 2013; Warren et al., 2015). *PgCYP720B4* was cloned using primers designed based on the previously published sequence of ortholog *PsCYP720B4* (Hamberger et al., 2011).

Amino acid sequence alignments (Figure 3.9; Figure 3.10) with previously characterized CYP450s from conifers and some angiosperms confirmed the presence of commonly found CYP450 motifs, including: the proline-rich region and the oxygen binding motif (A/G-G-X-D/E-T-T/S) (Durst and Nelson, 1995; Danielson, 2002). As well, the universally conserved motifs which interact with the heme iron center: the E-X-X-R motif which is thought to help stabilize the core structure and heme binding motif F-X-X-G-X-R-X-C-G where the conserved cysteine residue forms a thiolate ligand that essentially tethers the heme iron to the P450 (Werck-Reichhart and Feyereisen, 2000; Graham and Peterson, 1999).

Sequence identity between P450s can often be quite low, sometimes even falling below 20% identity; the two CYP450s in this study are proof of this as their identity is only 17.6%. Nomenclature guidelines state that CYP450s need 40% identity or more to fall within the same families (Nelson, 2006; Werck-Reichhart and Feyereisen, 2000). *PgCYP701* (512 amino acids), when compared to previously characterized orthologs in Figure 3.9, shared 52.6% identity with *Pisum sativum* (pea, *Pissa*) CYP701A10 (Davidson et al., 2004), 47.7%

identity with *AtCYP701A3* (Helliwell et al., 1999) and 51.0% identity with *Stevia rebaudiana* (*Stevia*, *Sr*) *CYP701A5* (Humphrey et al., 2006). All *CYP701* sequences examined contained the three conserved motifs that are characteristic of *CYP450s*, the fourth motif (the oxygen binding motif) did not clearly fit the consensus sequences and was annotated by aligning these *CYP701* sequences with previously annotated cytochrome P450s (*Mus musculus* [mouse] *CYP2A5*, Gotoh, 1992; *AtCYP73A5* and *AtCYP84A1*, Rupasinghe et al., 2003; *Santalum album* [sandalwood] *CYP76F37v1*, Diaz-Chavez et al., 2013).

PgCYP720B4 (483 amino acids) was aligned with previously characterized ortholog *PsCYP720B4* and a homologous member of the *CYP720B* subfamily from *Pinus taeda* (loblolly pine), *PtCYP720B1*, which was shown to have overlapping substrate specificity to *720B4* (Ro et al., 2005; Hamberger and Bohlmann, 2006). Compared to *PgCYP720B4*, *PsCYP720B4* and *PtCYP720B1* shared 99.2% and 85.5% identity respectively. The *CYP720B* subfamily is conifer specific, however looking more broadly at the *CYP720* family, an *A. thaliana* *CYP720A1* has been identified (AEE35445.1; Theologis et al., 2000). Comparing this putative *AtCYP720A1* to *PgCYP720B4* (data not shown) results in a 40.7% identity which is closer to the levels of identity seen within the *CYP701* family reported above.

PgCYP701	MEDVEAMLRV	FLMAAAAI	ICIGRL	LLW----	-----	--SRRPSKKY	P--PVVPGWP	IVGNLLQLRE	KKPHHTFTKW	ARNYGP	IYSI	72		
PissaCYP701	M---DTL---	-----	TLSLGF	-LSLFLFL	FLLKR----	--STHKHSKL	SHVPVVPGLP	VIGNLLQLKE	KKPHKTFTKM	AQKYGP	IFSI	70		
AtCYP701	MAFFSMI---	-----	SILLGF	VISSFIFI	FFFFKLLFS	RKNMSEVSTL	PSVPVVPVPGF	VIGNLLQLKE	KKPHKTFTTRW	SEIYGP	PIYSI	81		
SrCYP701	MDAFTGLLTV	---PATAIT	I	GGTAAVALA	VLIFWYLKSYT	SARRSQSNHL	<u>PRVPEVPGVP</u>	<u>LVGNLLQLKE</u>	KKPYMTFTTRW	AATYGPI	IYSI	87		
PgCYP701	RDVATPMVVV	NSSQLAKEAM	VTKFTA	ISSRKL	PNALRI	LTKT	REKTMVAMSD	YGDYHRMAKK	MVLTNL	LGA	AQKRNN	SHFL	162	
PissaCYP701	KAGSSKII	IVLNTAHLAKEAM	VTRYSS	ISKRL	STALT	ILTSD	KCMVAMSD	YDNDFHKMVKK	HILASV	LGAN	AQKRLR	HF--	158	
AtCYP701	KMGSSSL	IVLNSTETAKEAM	VTRFSS	ISTRK	LSNAL	TVLTC	DKSMVATSD	YDDFHKLVKR	CLNLGL	LGAN	AQKRKR	HH--	169	
SrCYP701	KTGATSMVVV	SSNEIAKEAL	VTRFQS	ISTRN	LSKALK	VLTK	ADKTMVAMSD	YDDYHKTVKR	HILTA	VLGN	AQKKHR	HH--	175	
PgCYP701	NIHSQSVST-	--EGVNL	RQIF	FINEL	FPFAL	KSVIG	RDIES	LYVEE	IGSTL					
PissaCYP701	KFNEHVKTLS	-DSAVDF	RKI	FVSELF	GLAL	KQALGS	RDIES	IYVEGL	TATL					
AtCYP701	KLHAHARDHP	-QEPVN	FRAI	FEHEL	FGVAL	KQAFG	KDVES	IYVKEL	GVTL					
SrCYP701	QLHEFVKNNP	EQEEVD	LRKI	FQSELF	GLAM	RQALG	KDVES	LYVED	LKITM					
PgCYP701	MKRMDRRRRA	VLRTL	IEEQK	RLLDS	GKEPN	CYLD	ILLKEA	PQLTE	KQLEM					
PissaCYP701	IRRVDRQRKI	IMKAL	INEQK	KRLTS	GKLED	CYDYL	VMSEA	KEVTEE	QMIM					
AtCYP701	IQQKHKKRRLA	VMNAL	IQDRL	KQNGS	ESDDD	CYLN	NFLMSEA	KTLTKE	QIAI					
SrCYP701	IQQMYIRREA	VMKSL	IKENK	KRIAS	GKELN	SYIDY	LLSEA	QTLTD	QQLLM					
PgCYP701	VSGDKDVTDE	YLPKL	PYLSA	VFQET	LRKH	PVP	IPLR	YV	HEDV	ELGGF	VPAGS	QIAIN	429	
PissaCYP701	VCGHEKVTE	ELSKL	PYLSA	VFHET	LRKHS	PVP	IPLR	YV	DEDTE	ELGGY	IPAGSE	IAIN	425	
AtCYP701	VCGGEKFKEE	QLSQV	PYLN	G	VFHET	LRKYS	PAPLV	PIRYA	HEDT	QIGGYH	VPAGSE	IAIN	437	
SrCYP701	VCGSEKITEE	HLSQL	PYITA	IFHET	LRHS	PVPI	IPLRHV	HEDT	VLGGYH	VPAGTE	LAVN	IYGCN	MDKNV	442
PgCYP701	VLDVKRTMAF	GAGK	RACAGT	LQATL	IACTA	IARFV	QRFNW	ELAAGE	EEDST	GTVTL	TTHKL	HPLKA	IVTPR	512
PissaCYP701	QADLYKTMAF	GGGKR	VCAGS	LQAML	IACTA	IGRLV	QEFEW	ELHG	GEEN	VTMGL	TTHRL	HPLQV	KLKPR	499
AtCYP701	TSDLHKTMAF	GAGKR	VCAGA	LQASL	MAGIA	IGRLV	QEFEW	KLRD	GEEN	VTYGL	TSQKL	YPLMA	IINPR	509
SrCYP701	TIDFQKTMAF	GGGKR	VCAGS	LQALL	TASIG	IGRMV	QEFEW	KLKDM	TQEEV	NTIGL	TQML	RPLRA	IIPKR	513

Figure 3.9. Comparison of the amino acid sequence of *PgCYP701* with characterized orthologs from *Pisum sativum* (Pissa), *Arabidopsis thaliana* (At) and *Stevia rebaudiana* (Sr). Highly conserved cytochrome P450 specific motifs are underlined: the proline-rich region (solid black line), oxygen binding motif A/G-G-X-D/E-T-T/S (black dashed line), E-X-X-R motif (solid red line) and heme binding motif F-X-X-G-X-R-X-C-G (red dashed line). Full gene names and accession numbers are: *PissaCYP701* (CYP701A10; AAP69988), *AtCYP701* (CYP701A3; AAC39505), *SrCYP701* (CYP701A5; AAY42951.1).

PgCYP720B4	MAPMADQISL	LLVVFTVAVA	LLHLIHRWWN	IQRGPKMS - -	- -NKEVHLPP	GSTGWPLIGE	TFSYYRSMTS	66
PsCYP720B4	MAPMADQISL	LLVVFTVAVA	LLHLIHRWWN	IQRGPKMS - -	- -NKEVHLPP	GSTGWPLIGE	TFSYYRSMTS	66
PtCYP720B1	MA - - DQISL	LLVVFTAAVA	LLHLIYRWWN	AQRGQKRTSN	EKNQELHLPP	<u>GSTGWPLIGE</u>	<u>TYSYYRSMTS</u>	67
PgCYP720B4	NHPRKFIDDR	EKRYDSDIFI	SHLFGGRTVV	SADPQFNKFV	LQNEGRFFQA	QYPKALKALI	GNYGLLSVHG	136
PsCYP720B4	NHPRKFIDDR	EKRYDSDIFI	SHLFGGRTVV	SADPQFNKFV	LQNEGRFFQA	QYPKALKALI	GNYGLLSVHG	136
PtCYP720B1	NRPRQFIDDR	EKRYDSDVFF	SHLFGSQAVI	SSDPQFNKYV	LQNEGRFFQA	HYPKALKALI	GDYGLLSVHG	137
PgCYP720B4	DLQRKLHGIA	VNLLRFERLK	VDFMEEIQNL	VHSTLDRWAD	MKEISLQNEC	HQMVLNLMAK	QLLDLSPSKE	206
PsCYP720B4	DLQRKLHGIA	VNLLRFERLK	VDFMEEIQNL	VHSTLDRWAD	MKEISLQNEC	HQMVLNLMAK	QLLDLSPSKE	206
PtCYP720B1	DLQRKLHGIA	VNLLRFERLK	FDFMEEIQNL	VHSTLDRWVD	KKEIALQNEC	HQMVLNLMAK	QLLDLSPSKE	207
PgCYP720B4	TSEICELFVD	YTNAVIAIPI	KIPGSTYAKG	LKARELLIKK	ISEMIKERRN	HPEVVHNDLL	TKLVEEGLIS	276
PsCYP720B4	TSDICELFVD	YTNAVIAIPI	KIPGSTYAKG	LKARELLIKK	ISEMIKERRN	HPEVVHNDLL	TKLVEEGLIS	276
PtCYP720B1	TNEICELFVD	YTNAVIAIPI	KIPGSTYAKG	LKARELLIRK	ISNMIKERRD	HPHIVHKDLL	TKLLEEDSIS	277
PgCYP720B4	DEIICDFILF	LLFAGHETSS	RAMTFAIKFL	TFCPKALKQM	KEEHDAILKS	KGGHKKLDWD	DYKSMAFTQC	346
PsCYP720B4	DEIICDFILF	LLFAGHETSS	RAMTFAIKFL	TYCPKALKQM	KEEHDAILKS	KGGHKKLNWD	DYKSMAFTQC	346
PtCYP720B1	DEIICDFILF	<u>LLFAGHETSS</u>	RAMTFAIKFL	TTCPKALTQM	KEEHDAILKA	KGGHKKLEWD	DYKSMKFTQC	347
PgCYP720B4	VINETLRLGN	FGPGVFREAK	EDTKVKDCLI	PKGWWVFAFL	TATHLHEKFH	NEALTFPNWR	WQLDKDVPDD	416
PsCYP720B4	VINETLRLGN	FGPGVFREAK	EDTKVKDCLI	PKGWWVFAFL	TATHLHEKFH	NEALTFPNWR	WQLDKDVPDD	416
PtCYP720B1	VINET <u>LR</u> RLGN	FGPGVFRET	EDTKVKDCLI	PKGWWVFAFL	TATHLDEKFH	NEALTFPNWR	WELDQDVSNN	417
PgCYP720B4	SLFSPFGGGA	RLCPGSHLAK	LELSLFLHIF	ITRFSWEARA	DDRTSYFPLP	YLTKGFPI SL	HGRVENE	483
PsCYP720B4	SLFSPFGGGA	RLCPGSHLAK	LELSLFLHIF	ITRFSWEARA	DDRTSYFPLP	YLTKGFPI SL	HGRVENE	483
PtCYP720B1	HLFSPFGGGA	<u>RLCPGSHLAR</u>	LELALFLHIF	ITRFRWEALA	DEHPSYFPLP	YLAKGFPML	YNR - - E	481

Figure 3.10. Comparison of the amino acid sequence of *PgCYP720B4* with characterized ortholog *PsCYP720B4* and closely related *PtCYP720B1*.

Highly conserved cytochrome P450 specific motifs are underlined: the proline-rich region (solid black line), oxygen binding motif A/G-G-X-D/E-T-T/S (black dashed line), E-X-X-R motif (solid red line) and heme binding motif F-X-X-G-X-R-X-C-G (red dashed line). Accession numbers are: *PsCYP720B4* (ADR78276.1), *PtCYP720B1* (AY779537.1).

Phylogenetic analysis of selected CYP701 and CYP720 sequences relating to GA and DRA pathways from angiosperms and gymnosperm (Figure 3.11) shows separate clades of CYP701 and CYP720 family members, when rooted with moss *P. patens* CYP701. Newly characterized *Pg*CYP701 shares a common ancestor to angiosperm CYP701 sequences. White spruce CYP720B4 groups most closely with previously characterized gymnosperm CYP720B family members (Hamberger et al., 2011; Ro et al. 2005).

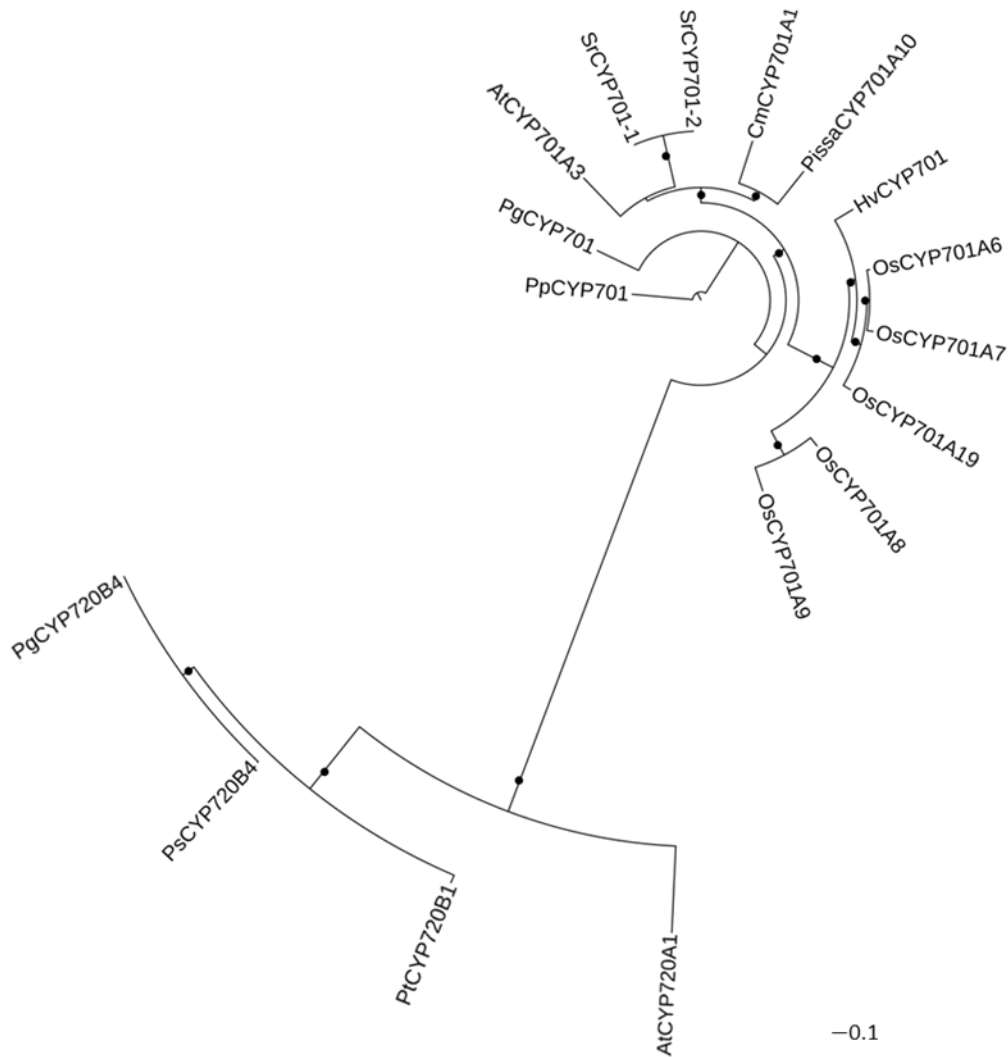


Figure 3.11. Phylogenetic maximum-likelihood tree of full-length amino acid CYP450 sequences from angiosperms and gymnosperms characterized as CYP701 and CYP720. Outgroup used was *Physcomitrella patens* CYP701 (*PpCYP701B1*; accession no. BAK19917). Legend bar indicates substitutions per site, black dots indicate branches with 80% or more bootstrap support (500 replications). Abbreviations and accession numbers are as follows: *AtCYP701A3* (*Arabidopsis thaliana*);, *CmCYP701A1* (*Cucurbita maxima*; AAG41776), *OsCYP701A6* (*Oryza sativa*; AAT81230), *OsCYP701A7* (BAF19826), *OsCYP701A8* (AAT46567), *OsCYP701A9* (AAT81229), *OsCYP701A19* (AAT91065), *HvCYP701* (*Hordeum vulgare*; BAK05490), *PissaCYP701A10* (*Pisum sativum*; AAP69988), *PgCYP701*, *PgCYP720B4*, *PsCYP720B4* (ADR78276), *PtCYP720B1* (*Pinus taeda*; Q50EK6), *SrCYP701-1* (*Stevia rebaudiana* CYP701A5; AAQ63464), *SrCYP701-2* (KO2; AAY42951).

3.2.4. Heterologous expression and functional characterization of white spruce CYP701 and CYP720B4

For functional characterization, *PgCYP701* and *PgCYP720B4* were heterologously expressed as recombinant enzymes in yeast. *PgCYP701* was cloned into yeast expression vector pYeDP60 for use in *in vitro* enzyme assay; initial attempts at *in vivo* enzyme assays with yeast co-expressing upstream pathway genes *ScGGPPS*, *PgCPS* and *PgKS* failed, most likely due to the complexity of the pathway being reconstructed as well as documented low expression rates of conifer CPS and KS enzymes which could have led to an inadequate amount of *ent*-kaurene precursor being produced (data not shown). *PgCYP701* protein was purified from the transformed yeast cells in the form of microsomes. To test for enzyme activity and proper P450 folding, CO difference spectrum assays were carried out. When CO is bound to the reduced iron in the CYP450, it yields a difference spectrum with a maximum at 450 nm if the enzyme has been properly folded (in the proper conformation) during expression. *PgCYP701* CO difference assays showed a classic peak at 450 nm, with a much smaller peak at 420 nm which indicates some denaturation of the CYP450 (Figure 3.12). Microsomes from yeast expressing *PgCYP701* were purified and used in combination with *ZmAn2* (*ZmCPS*) and *PgKS* (recombinantly expressed and purified from *E. coli*) and diTPS precursor GGPP. Diterpenoid acid products were derivatized and analyzed by GC-MS. This triple-enzyme *in vitro* assay system (Figure 3.13) was shown to produce *ent*-kaurene (excess diTPS product) as well as the predicted *ent*-kaurenoic acid. Products were confirmed by analysis of their mass spectra against authentic standards; *ent*-kaurenoic acid produced from *PgCYP701* matched the authentic standard exhibiting the major predicted ion of 374, as well as the retention time of the enzymatically produced *ent*-kaurenoic acid was identical to that of the standard (at approximately 12.3 min in the results shown in Figure 3.13).

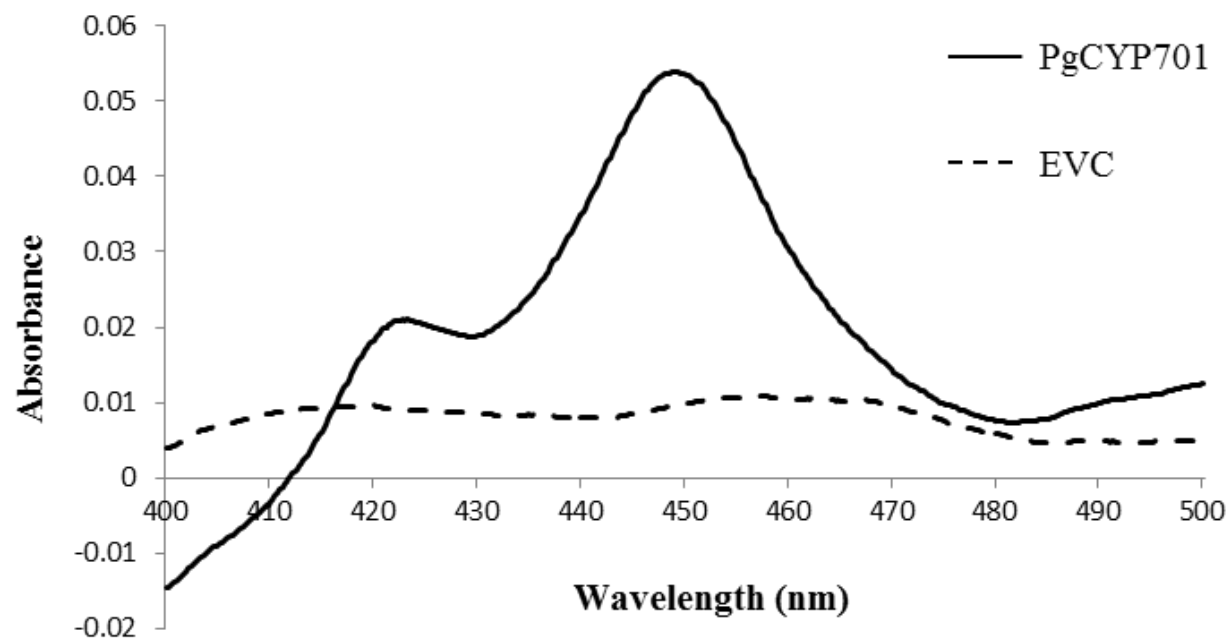


Figure 3.12. CO-difference spectra. Isolated yeast microsomes heterologously expressing *PgCYP701* or pYeDP60 (empty vector control [EVC]) are used to produce a CO-difference spectra.

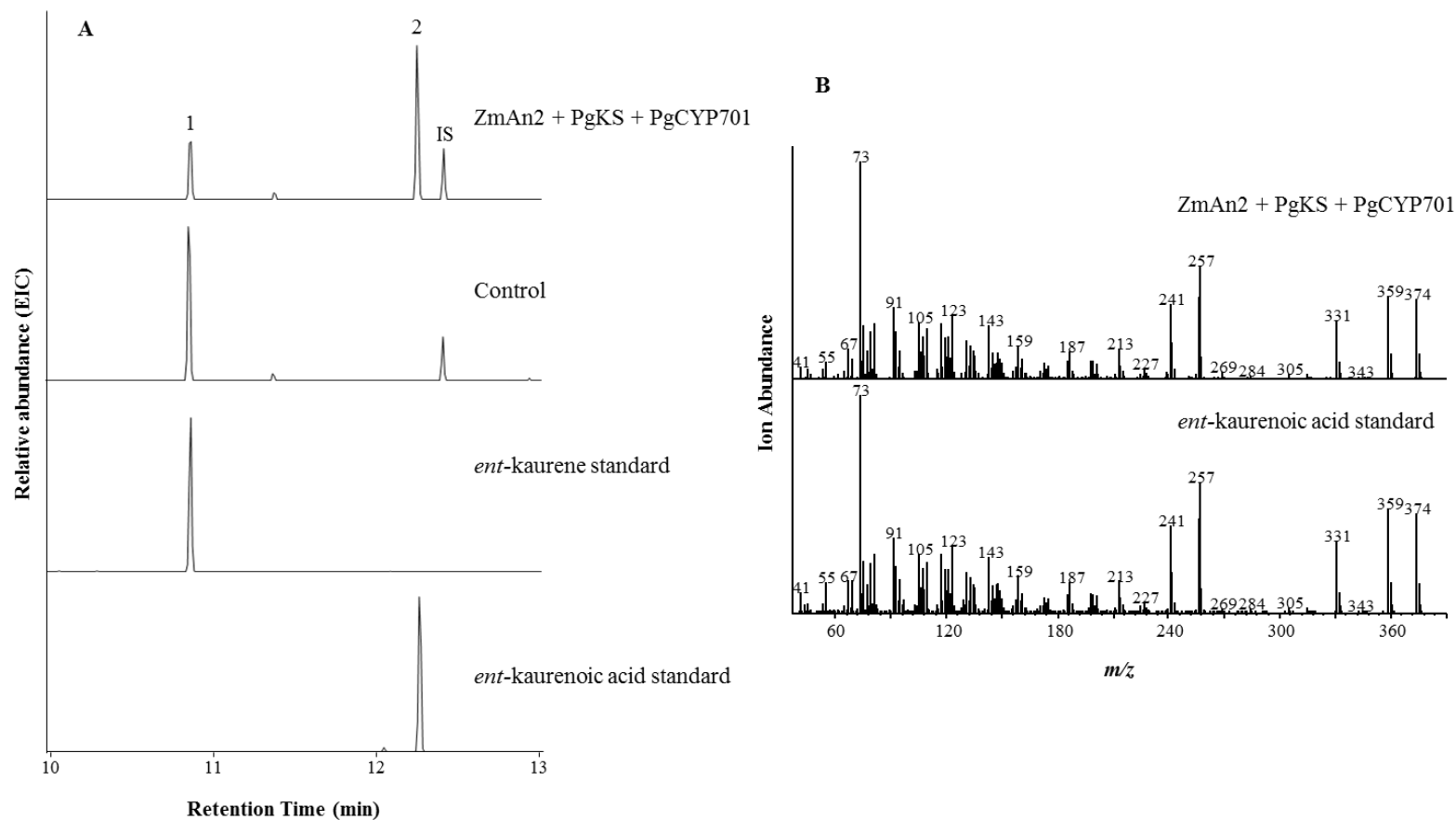


Figure 3.13. GC-MS analysis of the reaction product of recombinant *PgCYP701* protein. (A) *In vitro* assays with purified recombinant microsomal fractions expressing *PgCYP701* were assayed in the presence of *ZmAn2*, *PgKS*, and GGPP for production of the predicted product *ent*-kaurenoic acid (peak 2). Control was produced with microsomal fractions expressing empty pYedP60 expression vector, with *ZmAn2*, *PgKS* enzymes for production of *ent*-kaurene substrate (peak 1). Assays were derivatized with BSTFA and analyzed on an HP-5 column (272, 374 m/z extracted-ion chromatogram). Internal standard, IS, is dichlorodehydroabietic acid. (B) Mass spectrum of *PgCYP701* assay product, peak 2, verified by comparison to authentic *ent*-kaurenoic acid standard. m/z , Mass-to-charge ratio.

The function of *PgCYP720B4* was confirmed using an *in vivo* assay system in yeast. *PgCYP720B4* was cloned into expression vector pESC-Leu and co-expressed with a second construct containing *ScGGPPS* and *PaLAS* in yeast cells carrying a chromosomally integrated *PcCPR*. After expression, possible diterpenoid acid products were derivatized and analysed by GC-MS. Figure 3.14 shows the successful production of three predicted acid peaks: palustic acid, levopimaric acid and abietic acid. From previous work in the Bohlmann lab it is known that *PsCYP720B4* is active with 24 different diterpenoid products (Hamberger et al., 2011). Such extensive testing was not carried out on the *Pg* ortholog as it can be assumed that based on very high sequence identity (99.2% to *PsCYP720B4*) as well as predicted function with abietadiene substrate that this enzyme has been properly functionally characterized as *PgCYP720B4*.

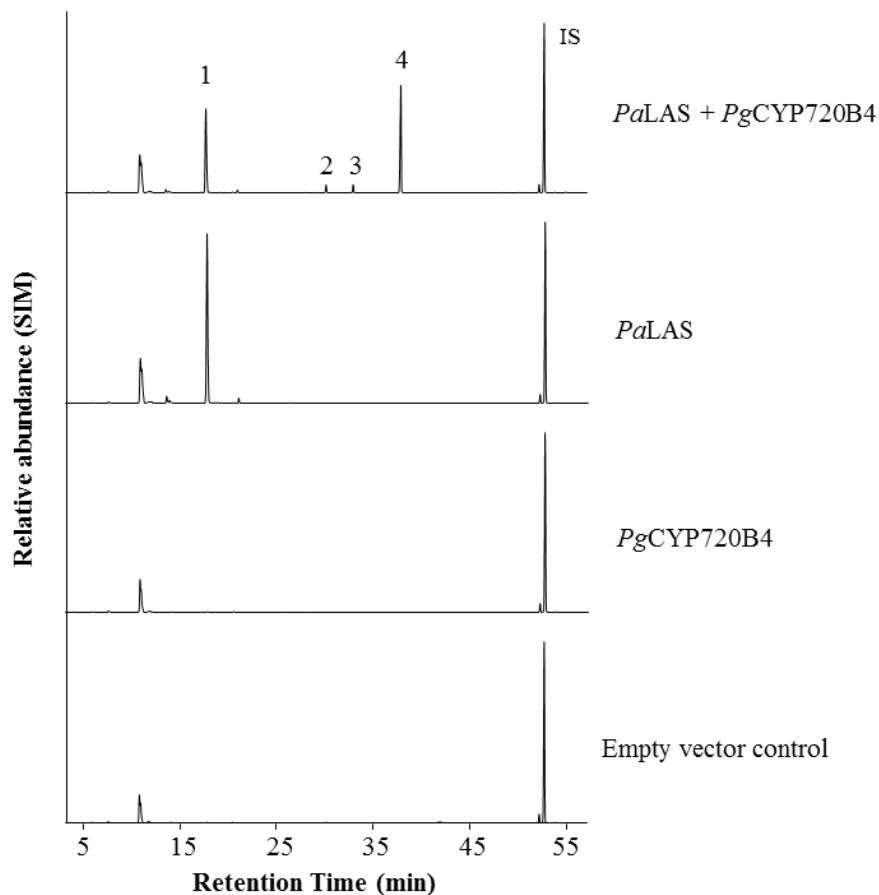


Figure 3.14. GC-MS analysis of *in vivo* enzyme assays of recombinant *PgCYP720B4* expressed in a yeast recombinant system. Yeast strains expressed a chromosomally integrated *PcCPR*, as well as combinations of *SsGGPPS*, *PaLAS*, and *PgCYP720B4*; assays were extracted and run on a HP-5 column (272, 374 *m/z*, selected ion monitoring [SIM]). Retention times and mass spectra match those of compounds abietadiene (peak 1), palustric acid (peak 2), levopimaric acid (peak 3), and abietic acid (peak 4). Control was produced using a yeast strain expressing empty pESC-LEU and pESC-HIS expression vectors. Assays were derivatized with TMS-diazomethane. Internal standard (IS) is dichlorodehydroabietic acid.

3.2.5. DRA concentrations in white spruce apical bud and developing apical shoots over time

In this experiment whole spruce vegetative apical buds and developing apical shoots were sampled at 31 time points over a one-year time course from January to December (Figure 2.1; Table 2.3). At eight of these time points (11, 13, 15, 17, 19, 21, 23, and 25) samples were further dissected into three parts (needles, stem, and new buds) and these three different parts of each sample were independently analyzed. For the aforementioned eight time points the dissection was completed before freezing, and thus “whole” apical bud and apical shoot samples refers to a biologically proportional recreation of the entire sample by combining finely ground tissues from stem, needles and new buds (where applicable). For all other time points, “whole” apical bud and apical shoot samples refers to a sample that was collected without further dissection.

DRA concentrations in whole apical bud and apical shoot samples changed significantly over time ($F_{19,78} = 1.904$; $P=0.031$) (Figure 3.15). Whole samples from time point 22 had the highest levels of DRA ($16.14 \pm 1.15 \text{ mg g}^{-1} \text{ DW}$) while time points 12 and 13 contained the lowest levels ($9.04 \pm 1.21 \text{ mg g}^{-1} \text{ DW}$, and $8.68 \pm 0.41 \text{ mg g}^{-1} \text{ DW}$, respectively). Samples from all other time points showed intermediate DRA levels. Of particular note, DRA concentrations rose very rapidly between time points 13 and 14, the change being over 1.6-fold during this one week period.

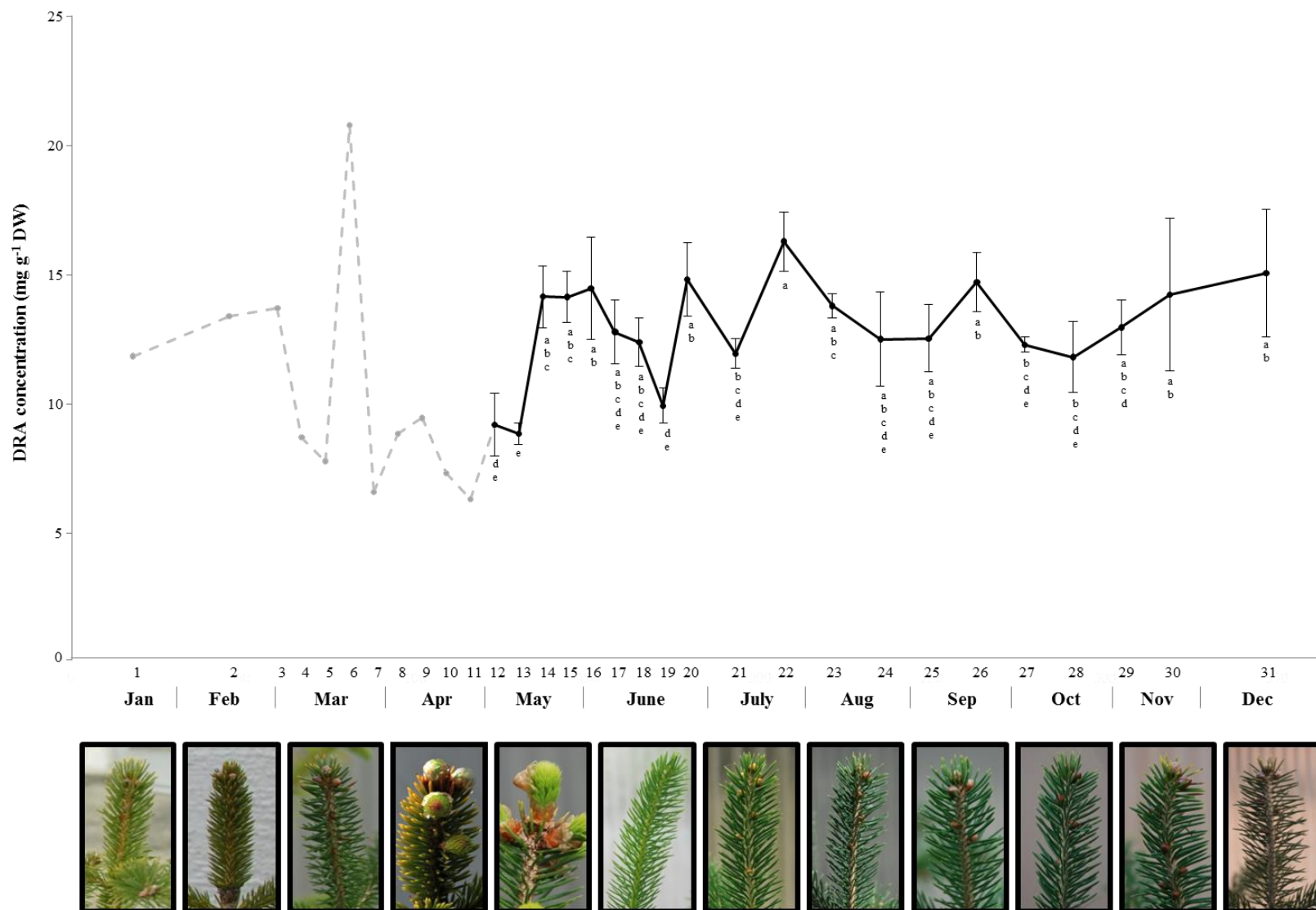


Figure 3.15. Total DRA concentration (mg g^{-1} DW) in white spruce vegetative apical bud and apical shoot samples over a year-long time course. Time points were spaced 1-4 weeks apart depending on growth season and were chosen based on previous knowledge of the documented phenotypic growth stages that spruce progresses through during vegetative apical bud flushing and growth. Representative images of apical buds and shoots collected during each month are also shown. Light gray dotted line (time points 1-11) represents values for pooled samples consisting of 4 individual biological replicates; samples were pooled due to limitation. Heavy black line (time points 12-31) shows data for 4 biological replicates, mean (\pm SEM). DRA concentrations were found to differ significantly over time, $P = 0.031$, letters signify means separated by the post hoc LSD (least significant difference) test ($\alpha = 0.05$).

3.2.6. DRA concentrations in dissected apical buds and shoots from selected times during apical bud development

Developing vegetative apical buds and apical shoots were dissected into three parts: stem, needle and new buds at selected time points (time points 11, 13, 15, 17, 19, 21, 23, and 25) and DRA concentrations were measured. Analyses of these data showed that concentrations of DRA differed significantly across the different parts of the apical bud or apical shoot ($F_{2,72} = 216.467$; $P < 0.0001$) and over time ($F_{6,72} = 8.257$; $P < 0.0001$); in addition, the interaction between sample part and time was significant ($F_{10,72} = 5.708$; $P < 0.0001$) (Figure 3.16). Among the three different parts, DRA concentrations varied significantly across time in stem ($F_{6,26} = 7.092$; $P < 0.0001$), needle ($F_{6,27} = 5.912$; $P = 0.001$), and new buds ($F_{4,17} = 4.934$; $P = 0.012$). In needles, DRA concentrations rose quickly during April-May, approximately 1.9-fold, and were highest at time point 15 ($12.09 \pm 0.63 \text{ mg g}^{-1} \text{ DW}$) before declining somewhat to a near constant level over the remaining sampling times. In stems, DRA levels rose over 2-fold from April until mid-July, reaching a peak at time point 21 ($33.34 \pm 2.79 \text{ mg g}^{-1} \text{ DW}$) and remained high through September. In new buds DRA levels rose continuously from early June and reached a maximum in mid-August at time point 23 ($27.32 \pm 3.40 \text{ mg g}^{-1} \text{ DW}$), this translates into a 1.8-fold increase, DRA levels remained consistently high into September.

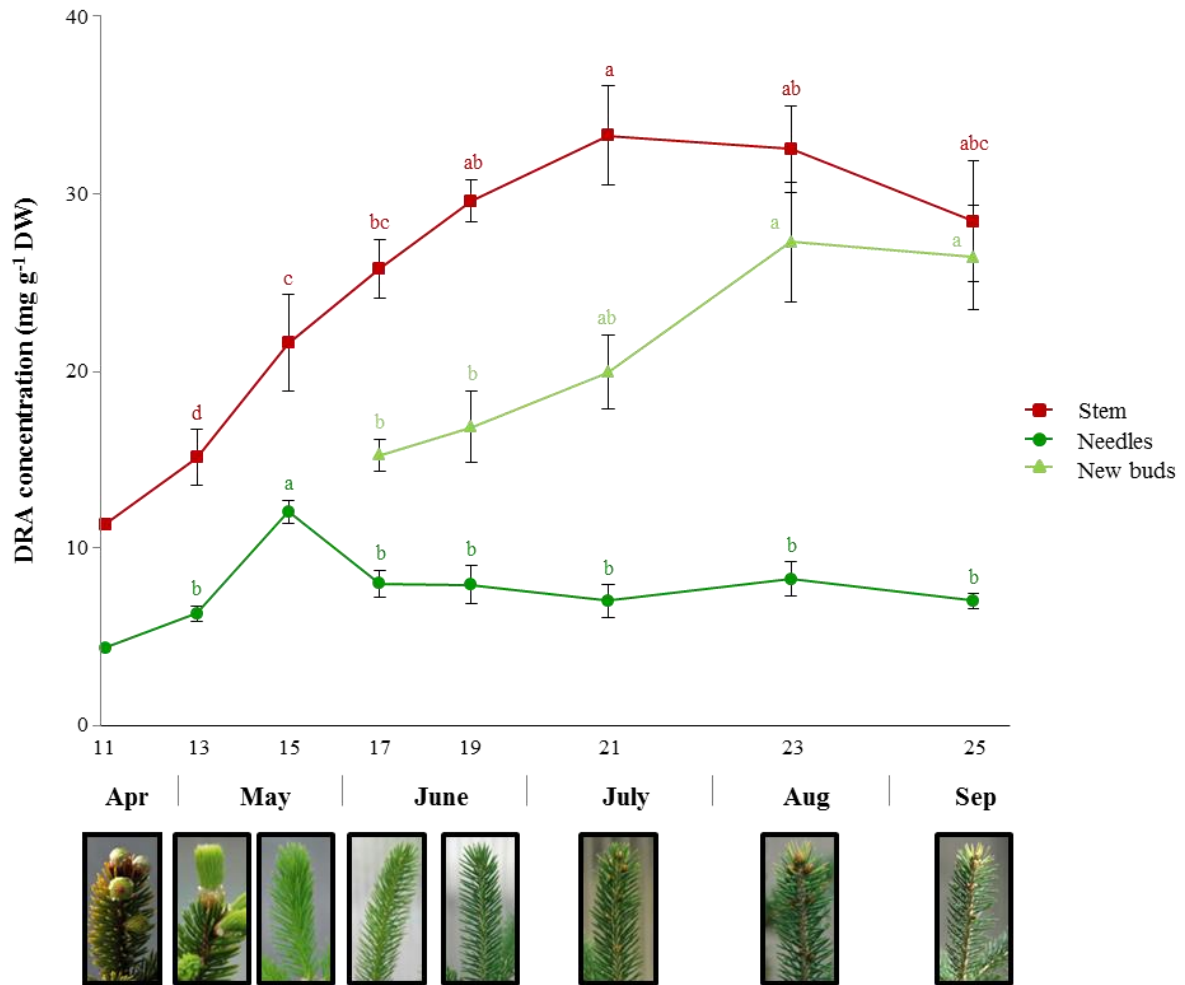


Figure 3.16. Total DRA concentration (mg g⁻¹ DW) in white spruce vegetative apical buds and apical shoots over a time course, focusing on biological time points that correspond with shoot development and new bud set. Samples were separated into 2 or 3 parts (needles, stem, new buds) based on developmental stage; new buds first appeared (as observed by eye) at time point 17. The images below the graph are representative of apical buds and shoots collected at each time point to best describe the major phenotype seen. Over time and between sample parts, DRA concentrations differed significantly ($P < 0.0001$ and $P < 0.0001$, respectively); an interaction between sample part and time was also significant ($P < 0.0001$). Data represent the mean (\pm SEM) of 4 biological replicates except for time point 11 that is a pooled sample of all 4 individual biological replicates (due to limitation). DRA concentrations differed significantly over the time course within each part of the apical sample: stem ($P < 0.0001$), needle ($P = 0.001$), and new buds ($P = 0.012$); letters signify significantly different means separated, within each part of the developing apical bud or apical shoot, by the post hoc LSD (least significant difference) test ($\alpha = 0.05$).

When data averages from the three different sample parts of the developing apical bud or apical shoot, at each time point, were combined, DRA concentrations differed significantly over time ($P<0.0001$) (Figure 3.17A). Overall, mean DRA levels increased steadily, rising over 3-fold between time points 13 and 23. Time points 23 and 25 showed the highest overall DRA concentrations followed by time point 21 (68.17 ± 7.37 , 61.99 ± 6.83 , and 60.36 ± 7.59 mg g⁻¹ DW, respectively). Time points 15, 17, and 19 showed intermediate mean concentrations of DRA (33.71 ± 4.77 , 49.10 ± 5.16 and 54.47 ± 6.29 mg g⁻¹ DW, respectively) which were significantly different from the two highest time points. Time point 13 contained the lowest overall DRA concentration (21.49 ± 4.39 mg g⁻¹ DW).

DRA concentrations also differed significantly between the different sample parts of the apical bud or shoot ($P<0.0001$) (Figure 3.17B). Mean concentrations of DRAs were highest in stems (186.57 ± 2.44 mg g⁻¹ DW) and were significantly different from new buds which showed intermediate levels (105.93 ± 2.45 mg g⁻¹ DW), and needles (56.79 ± 0.711 mg g⁻¹ DW) which were the lowest.

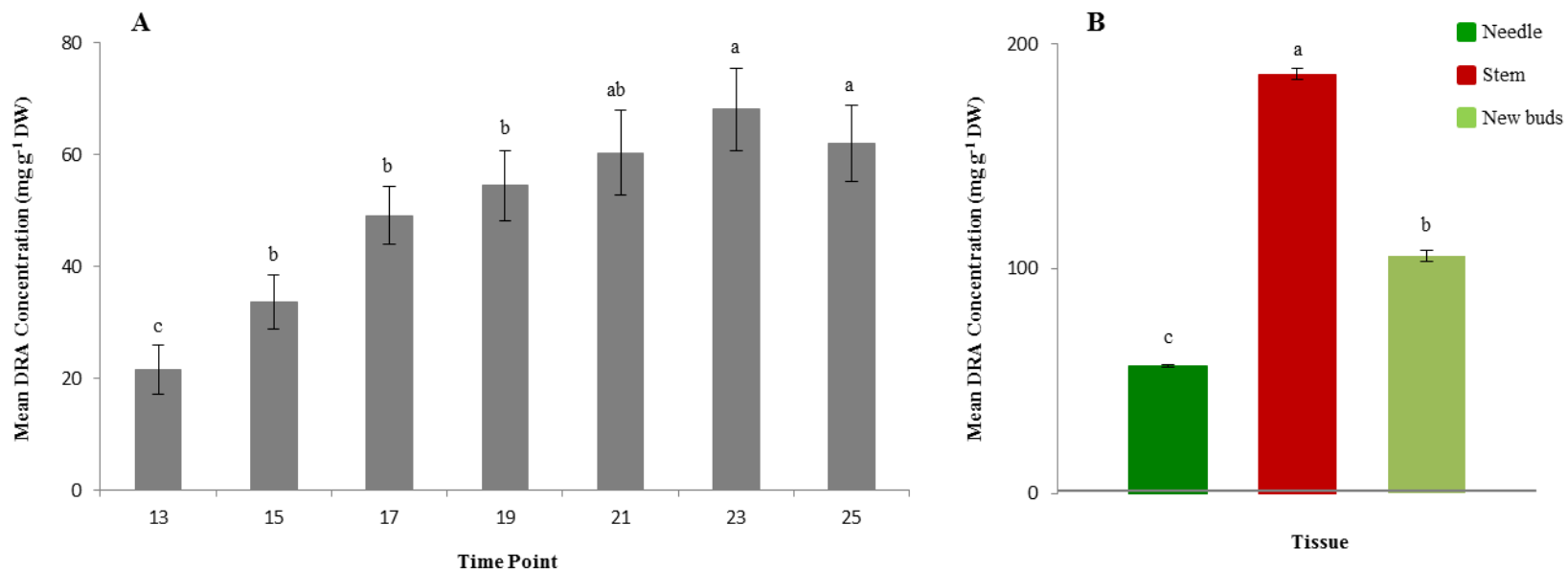


Figure 3.17. Mean concentrations of DRA (mg g⁻¹ DW) in white spruce over a vegetative apical bud developmental time course separated by time point and sample part. Over time DRA concentrations differed significantly ($P<0.0001$) (A); mean concentrations reflect all sample parts per time point. Between sample parts, DRA mean concentrations differed significantly ($P<0.0001$) (B); mean concentrations represent all time points per sample part, and differences between time points are not considered. Error bars represent the standard error of the mean and different letters indicate significantly different means separated by LSD post-hoc comparisons ($\alpha=0.05$).

3.2.7. Relative expression of GA and DRA biosynthetic genes in whole samples of developing spruce apical buds and shoots

Quantitative PCR (qPCR) was used to measure transcript abundance of 5 genes related to GA and DRA biosynthesis, *PgCPS*, *PgKS*, *PgLAS*, *PgCYP701*, and *PgCYP720B4*, over a one-year apical bud and apical shoot development time course, from January to December (Figure 2.1; Table 2.3) containing 31 time points. Transcript levels are expressed relative to the transcript abundance of reference gene *eEF1 α* (\pm SEM). All genes analyzed showed significant changes in transcript abundance over the time course (Figure 3.18).

PgCPS transcript levels (Figure 3.18A) were significantly affected by time ($H(19)=53.113$, $N=74$, $P<0.0005$). The highest relative transcript levels were seen in June at time points 16, 17 and 18 (relative abundance values of 5.207 ± 1.362 , 4.068 ± 0.594 and 4.194 ± 0.971 , respectively) with transcript levels falling quickly to their lowest levels in July-September at time points 22 and 26 (0.348 ± 0.044 and 0.296 ± 0.121 , respectively) (Table 3.1). Time points 13, 14, 15, 19 and 31 were not significantly different from the time points with the highest transcript levels. The remaining time points, and time point 31, from the end of June to December remained at a low and relatively constant level; they were not significantly different from the lowest transcript levels. All other time points were not significantly different from the time points with the lowest transcript abundances.

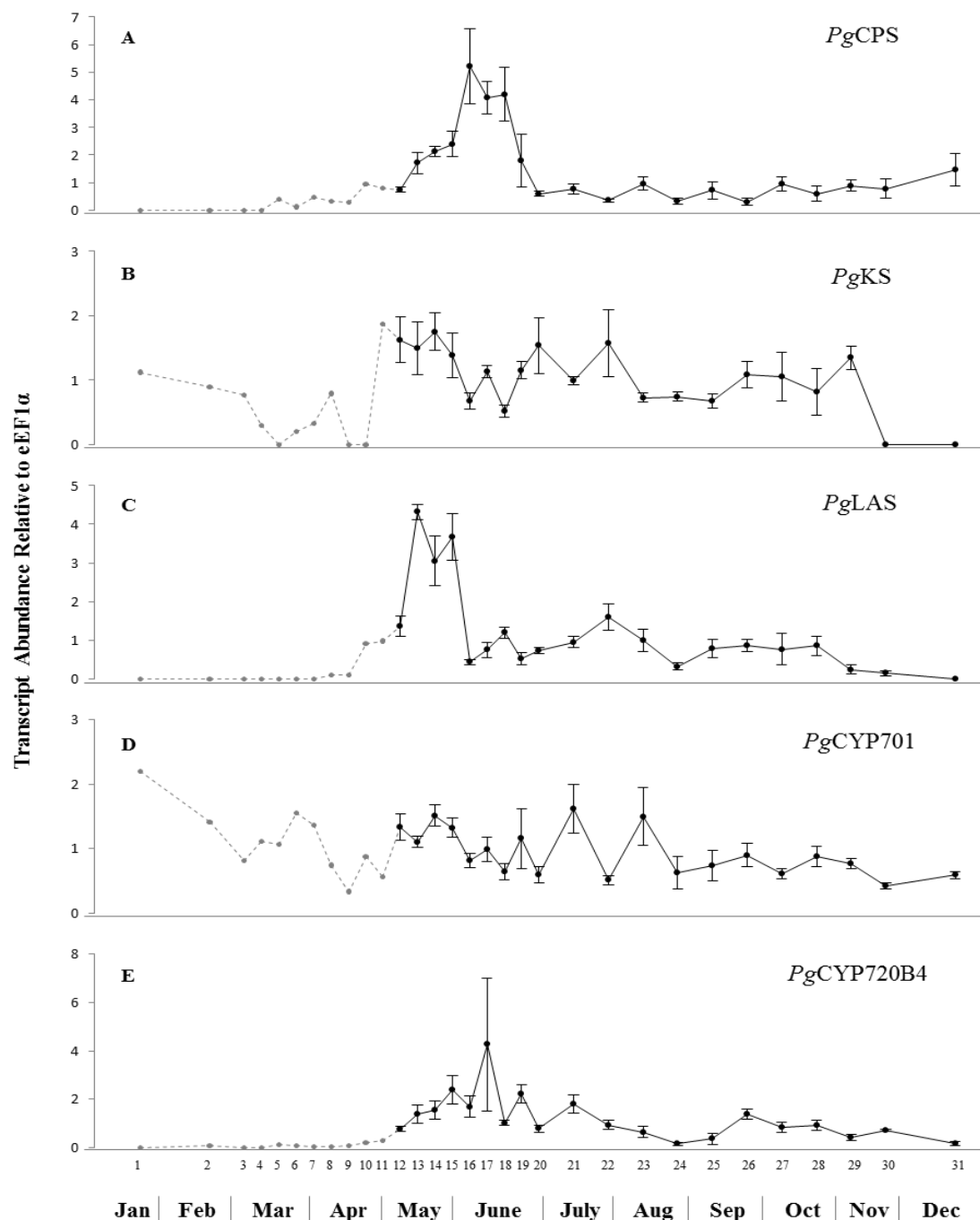


Figure 3.18. Relative transcript abundance of diTPS and CYP450 genes in white spruce developing apical buds and shoots over a one-year time course. Transcript abundance was measured by real-time qPCR and expressed as relative to the reference gene *eEF1a*. Light gray dotted line (time points 1-11) represents values for pooled samples consisting of 4 individual biological replicates; samples were pooled due to limitations. Heavy black line (time points 12-31) shows data for 4 biological replicates, mean (\pm SEM). Transcript abundance for each gene was found to differ significantly over time ((A) *PgCPS*, $P < 0.0005$; (B) *PgKS*, $P = 0.001$; (C) *PgLAS*, $P < 0.0005$; (D) *PgCYP701*, $P = 0.002$; (E) *PgCYP720B4*, $P < 0.0005$). Data was statistically analyzed and means were separated using Kruskal-Wallis test statistic ($\alpha = 0.05$), see Table 3.1.

Table 3.1. Relative transcript abundance of diTPS and CYP450 genes related to DRA and GA biosynthesis in white spruce developing apical buds and shoots over a one-year time course. Data are expressed as relative transcript abundance to expression of reference gene *eEF1a* (\pm SEM). Different letters within each gene indicate significantly different means separated by the Kruskal-Wallis test statistic ($\alpha=0.05$).

Gene of Interest	Time Point	Relative Transcript Abundance	
<i>PgCPS</i> ($P>0.0005$)	12	0.743 ± 0.085	<i>bcde</i>
	13	1.706 ± 0.381	<i>abc</i>
	14	2.121 ± 0.178	<i>ab</i>
	15	2.394 ± 0.452	<i>ab</i>
	16	5.207 ± 1.362	<i>a</i>
	17	4.068 ± 0.594	<i>a</i>
	18	4.194 ± 0.971	<i>a</i>
	19	1.779 ± 0.958	<i>abcd</i>
	20	0.596 ± 0.103	<i>cde</i>
	21	0.765 ± 0.186	<i>bcde</i>
	22	0.348 ± 0.044	<i>e</i>
	23	0.963 ± 0.245	<i>bcde</i>
	24	0.328 ± 0.105	<i>de</i>
	25	0.722 ± 0.315	<i>cde</i>
	26	0.296 ± 0.121	<i>e</i>
	27	0.956 ± 0.268	<i>bcde</i>
	28	0.597 ± 0.260	<i>cde</i>
	29	0.891 ± 0.213	<i>bcde</i>
	30	0.783 ± 0.340	<i>bcde</i>
	31	1.451 ± 0.592	<i>abcde</i>
<i>PgKS</i> ($P=0.001$)	12	1.625 ± 0.357	<i>ab</i>
	13	1.493 ± 0.414	<i>abc</i>
	14	1.750 ± 0.290	<i>a</i>
	15	1.382 ± 0.346	<i>abc</i>
	16	0.675 ± 0.122	<i>cde</i>
	17	1.128 ± 0.095	<i>abcd</i>
	18	0.517 ± 0.090	<i>de</i>
	19	1.151 ± 0.132	<i>abcd</i>
	20	1.534 ± 0.435	<i>abc</i>
	21	0.989 ± 0.058	<i>abcd</i>
	22	1.572 ± 0.524	<i>abc</i>
	23	0.725 ± 0.068	<i>cde</i>
	24	0.743 ± 0.071	<i>bcde</i>
	25	0.671 ± 0.106	<i>cde</i>
	26	1.084 ± 0.202	<i>abcd</i>
	27	1.051 ± 0.379	<i>abcd</i>
	28	0.816 ± 0.364	<i>abcd</i>
	29	1.347 ± 0.185	<i>abc</i>
	30	0.000 ± 0.000	<i>e</i>
	31	0.000 ± 0.000	<i>e</i>

Gene of Interest	Time Point	Relative Transcript Abundance	
<i>PgLAS</i> ($P>0.0005$)	12	1.357 ± 0.256	<i>ab</i>
	13	4.320 ± 0.203	<i>a</i>
	14	3.054 ± 0.650	<i>a</i>
	15	3.677 ± 0.611	<i>a</i>
	16	0.432 ± 0.061	<i>bcde</i>
	17	0.746 ± 0.196	<i>bcd</i>
	18	1.193 ± 0.147	<i>ab</i>
	19	0.514 ± 0.157	<i>bcde</i>
	20	0.734 ± 0.080	<i>bcd</i>
	21	0.951 ± 0.152	<i>abc</i>
	22	1.599 ± 0.333	<i>ab</i>
	23	0.998 ± 0.292	<i>abc</i>
	24	0.317 ± 0.098	<i>cde</i>
	25	0.780 ± 0.237	<i>bcd</i>
	26	0.853 ± 0.154	<i>bcd</i>
	27	0.767 ± 0.404	<i>bcde</i>
	28	0.855 ± 0.253	<i>bcd</i>
	29	0.241 ± 0.117	<i>cde</i>
	30	0.144 ± 0.063	<i>de</i>
	31	0.000 ± 0.000	<i>e</i>
<i>PgCYP70I</i> ($P=0.002$)	12	1.339 ± 0.205	<i>ab</i>
	13	1.107 ± 0.086	<i>abcd</i>
	14	1.515 ± 0.160	<i>a</i>
	15	1.324 ± 0.152	<i>ab</i>
	16	0.816 ± 0.118	<i>abcdef</i>
	17	0.989 ± 0.194	<i>abcde</i>
	18	0.647 ± 0.125	<i>cdef</i>
	19	1.156 ± 0.463	<i>abcde</i>
	20	0.599 ± 0.121	<i>ef</i>
	21	1.620 ± 0.378	<i>ab</i>
	22	0.510 ± 0.074	<i>ef</i>
	23	1.499 ± 0.449	<i>abc</i>
	24	0.625 ± 0.251	<i>ef</i>
	25	0.743 ± 0.238	<i>bcdef</i>
	26	0.903 ± 0.178	<i>abcde</i>
	27	0.607 ± 0.079	<i>cdef</i>
	28	0.876 ± 0.153	<i>abcdef</i>
	29	0.768 ± 0.084	<i>abcdef</i>
	30	0.418 ± 0.048	<i>f</i>
	31	0.589 ± 0.053	<i>def</i>
<i>PgCYP720B4</i> ($P>0.0005$)	12	0.761 ± 0.102	<i>cdef</i>
	13	1.385 ± 0.372	<i>abcd</i>
	14	1.553 ± 0.370	<i>abcd</i>
	15	2.386 ± 0.578	<i>a</i>
	16	1.676 ± 0.441	<i>abcd</i>
	17	4.264 ± 2.739	<i>abcd</i>
	18	1.008 ± 0.099	<i>abcde</i>
	19	2.228 ± 0.389	<i>ab</i>
	20	0.784 ± 0.144	<i>cdef</i>
	21	1.799 ± 0.397	<i>abc</i>
	22	0.932 ± 0.187	<i>abcde</i>
	23	0.629 ± 0.229	<i>def</i>
	24	0.146 ± 0.058	<i>f</i>
	25	0.349 ± 0.214	<i>ef</i>
	26	1.382 ± 0.208	<i>abcd</i>
	27	0.830 ± 0.216	<i>bcdef</i>
	28	0.902 ± 0.212	<i>abcdef</i>
	29	0.411 ± 0.140	<i>ef</i>
	30	0.697 ± 0.032	<i>def</i>
	31	0.163 ± 0.097	<i>f</i>

PgKS transcript levels (Figure 3.18B) were also significantly affected by time ($H(19)=43.582$, $N=74$, $P=0.001$). The highest relative transcript level was seen in late May at time point 14 (1.750 ± 0.290) with the lowest levels at the end of the year, at points 30 and 31 (both of which were effectively zero, i.e. below the limit of detection). Time points 12, 13, 15, 17, 19, 20, 21, 22, 26, 27, 28 and 29 were not significantly different from time point 14 (with the highest transcript levels). All other time points are not significantly different from the time points with the lowest transcript abundances. With the exception of the time points with lowest and highest transcript levels, *PgKS* relative transcript abundance showed little fluctuation over the time course, with the highest overall change being 1.75-fold (Table 3.1).

PgLAS expression was also significantly affected by time ($H(19)=57.867$, $N=76$, $P<0.0005$) (Figure 3.18C). The highest relative transcript levels were seen in late May (late spring) at time points 13, 14 and 15 (relative abundances of 4.320 ± 0.203 , 3.054 ± 0.650 and 3.677 ± 0.611 , respectively) and levels declined significantly by over 8-fold by time point 16 (Table 3.1). Two minor peaks in *PgLAS* transcript abundance were seen at time points 18 and 22 but between time points 24 and 31 (i.e. from mid-August onwards), transcript levels remained consistently low. *PgLAS* transcript abundance reached its lowest level with a value that was effectively zero (below detection limit) at time point 31.

PgCYP701 transcript levels (Figure 3.18D) were significantly affected by time ($H(19)=41.900$, $N=77$, $P=0.002$). The highest relative transcript level was seen in late May at time point 14 (1.515 ± 0.160) and the lowest levels were late in the year, in December, at time point 30 (0.418 ± 0.048). Time points 12, 13, 15, 16, 17, 19, 21, 23, 26, 28 and 29 were not significantly different from time point 14 (with the highest transcript levels), however all

of these, except time points 16, 28 and 29 were significantly different from time point 30 (with the lowest transcript level). All other time points were not significantly different from time point 30 (Table 3.1). Overall, with the exception of the time points with lowest and highest transcript levels, *PgCYP701* relative transcript abundance did not fluctuate greatly over the time course.

PgCYP720B4 transcript levels were significantly affected by time ($H(19)=52.674$, $N=80$, $P<0.0005$) (Figure 3.18E). The highest relative transcript level was seen in late May at time point 15 (2.386 ± 0.578); and the lowest levels at time points 24 and 31 (0.146 ± 0.058 and 0.163 ± 0.097 respectively). Time points 13, 14, 16, 17, 18, 19, 21, 22, 26, and 28 (ranging from May to October) were not significantly different from time point 15 (with the highest transcript levels), and all except time point 28 were significantly different from the time points with the lowest transcript (Table 3.1).

3.2.8. Expression of genes involved in GA and DRA biosynthesis in stems, needles and new buds in spruce during apical bud and shoot development

Analysis of relative transcript abundance of 5 genes related to GA and DRA biosynthesis (*PgCPS*, *PgKS*, *PgLAS*, *PgCYP701* and *PgCYP720B4*) was assessed in 2 or 3 sample parts (N, needles; S, stem; NB, new buds) over 8 time points (time points 11, 13, 15, 17, 19, 21, 23 and 25) focused on the spring/summer portion of the year-long time course of apical bud and shoot development in white spruce. Transcript abundance levels were expressed as relative to the expression of reference gene *eEF1 α* (\pm SEM) (Figure 3.19). Within the data for each gene, statistical analyses were run to determine the effect of this

experiment's main factors: time and sample part, as well as the interactions between these factors.

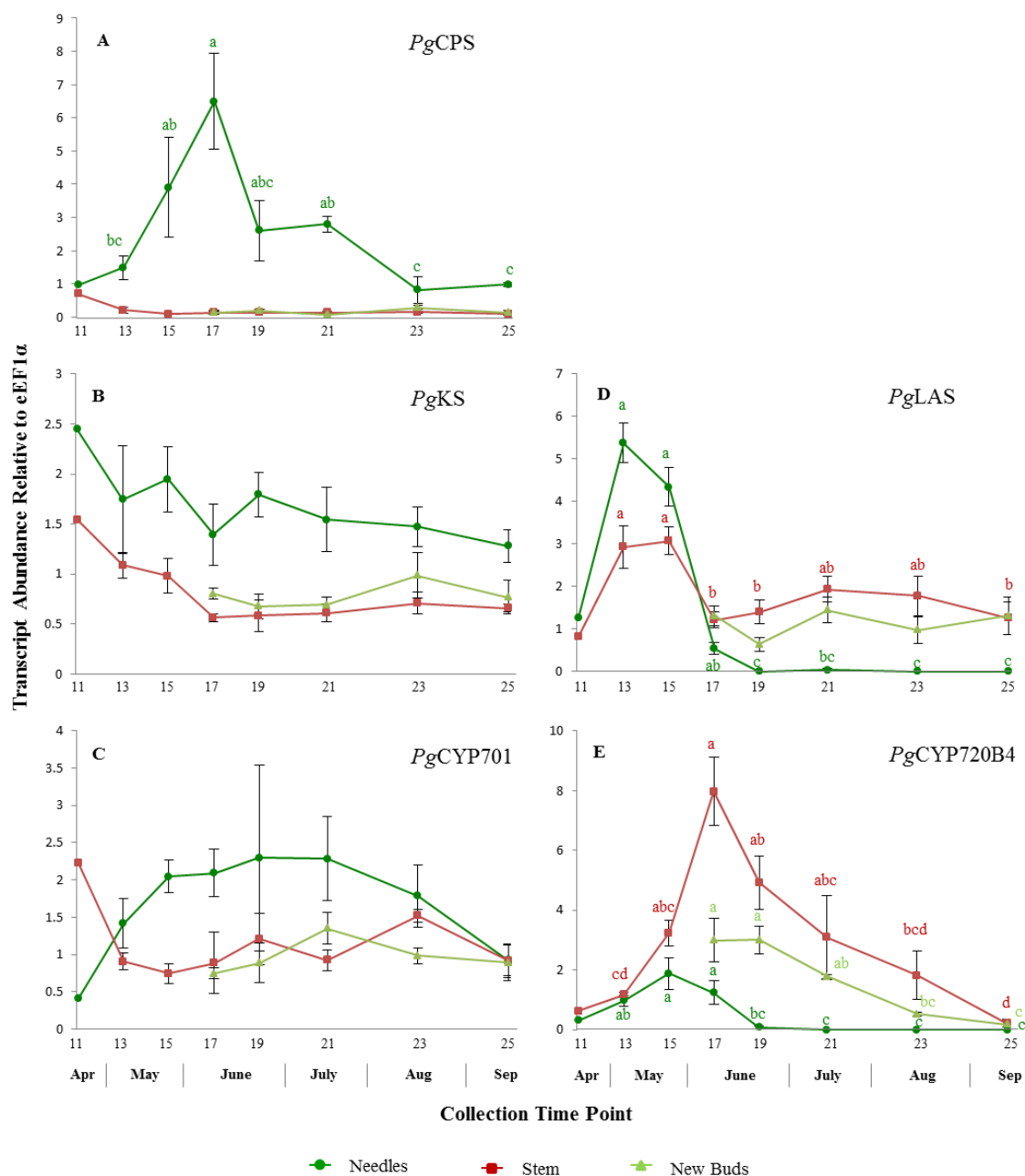


Figure 3.19. Relative transcript abundance of diTPS and CYPs related to DRA and GA biosynthesis in different parts of white spruce developing vegetative apical buds and apical shoots. Apical bud or apical shoot samples were separated into 2 or 3 sample parts (needles, stem, new buds) based on developmental stage; new buds appeared (as observed by eye) at time point 17. Transcript abundance was measured by real-time qPCR and expressed as relative to the reference gene *eEF1α*. Data represent the mean (\pm SEM) of 4 biological replicates except for point 11 that is a pooled sample of the 4 replicates (due to limitations). Transcript abundance levels of *PgCYP720B4* were found to differ significantly over time in all sample parts (needles, $P=0.001$; stem, $P=0.002$; new buds, $P=0.005$), levels of *PgLAS* differed in two sample parts (needles, $P<0.0005$; stem, $P=0.014$), and *PgCPS* levels differed in needles ($P=0.034$). Letters signify means separated by the Kruskal-Wallis test statistic ($\alpha=0.05$).

Combining relative transcript data for all time points and sample parts, *PgCPS* mean transcript levels were significantly affected by sample part ($P<0.0005$) (Figure 3.20F; Table 3.2); with the mean transcript abundance of needles being the highest (2.650 ± 0.450) and both stem and new buds having significantly lower mean relative abundances (0.137 ± 0.016 and 0.169 ± 0.025 , respectively). Indeed, *PgCPS* mean transcript levels were 16- to 19-fold higher in needles than in stem and new buds. *PgCPS* transcript levels were also significantly affected by the interaction between sample part and time ($P<0.0005$) (Figure 3.19A). Within sample part, only needles showed a significant difference in relative transcript abundance over time ($P=0.034$), Table 3.2. In needles, *PgCPS* transcript levels rose steeply over the spring weeks to peak at time point 17 (relative abundance 6.490 ± 1.450) before declining again at later time points. The lowest *PgCPS* transcript levels occurred in early fall, at time points 23 and 25 (0.816 ± 0.392 and 0.990 ± 0.060 , respectively) (Table 3.3).

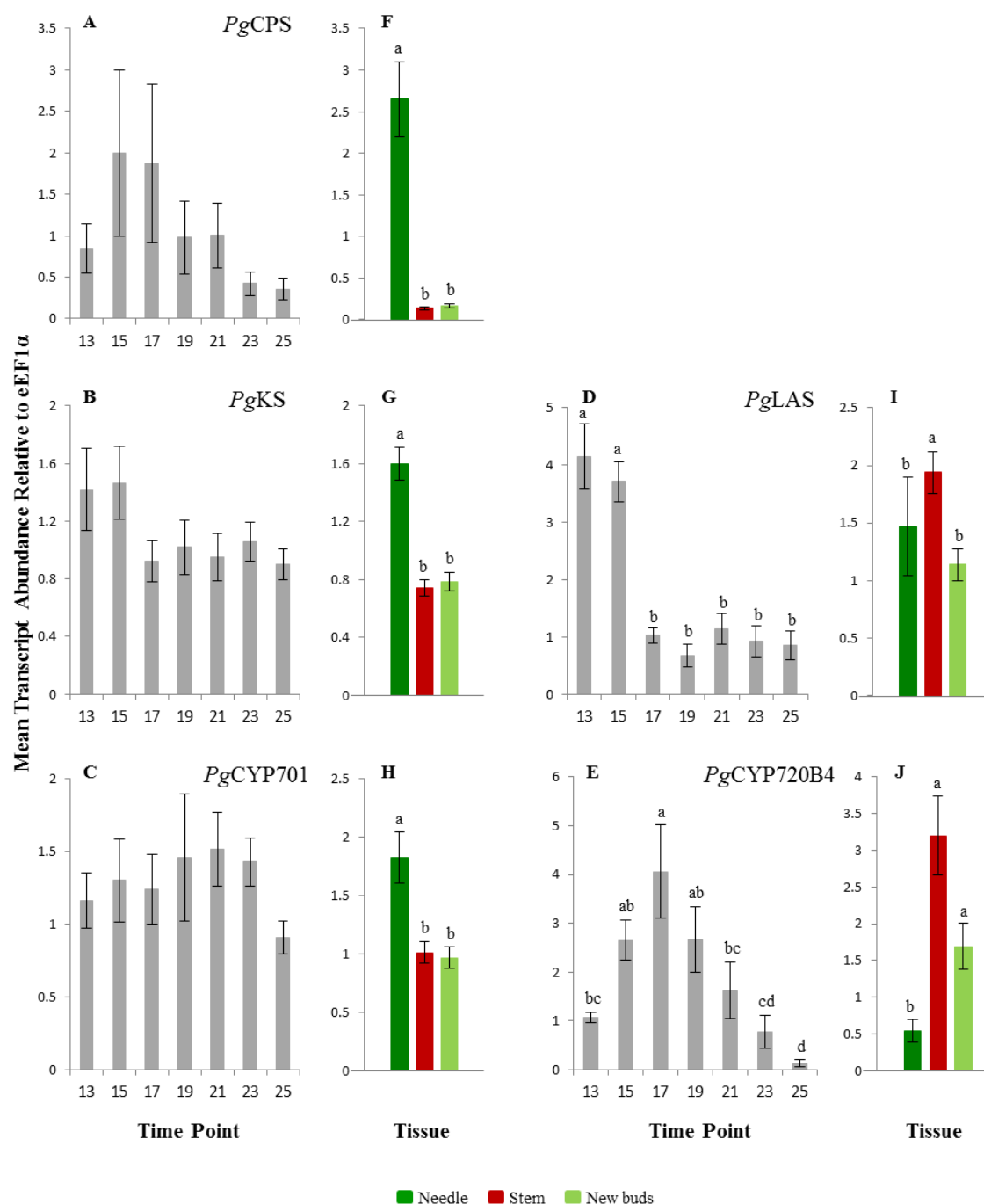


Figure 3.20. Mean relative transcript abundance diTPS and CYP450 genes in a white spruce developing vegetative apical buds and apical shoots over a time course separated by time point and sample part. Transcript abundance was measured by real-time qPCR and expressed as relative to the reference gene *eEF1α*. Over time significant differences in transcript levels were only seen for *PgLAS* ($P < 0.0005$) and *PgCYP720B4* ($P < 0.0005$) (D and E respectively); mean transcript abundances reflect all sample parts per time point. Between sample parts significant differences in transcript levels were found for *PgCPS* ($P < 0.0005$), *PgKS* ($P < 0.0005$), *PgLAS* ($P = 0.002$), *PgCYP701* ($P = 0.001$) and *PgCYP720B4* ($P < 0.0005$) (F, G, H, I, J respectively); mean abundances represent all time points per sample part, and differences between time points are not considered. Error bars represent the standard error of the mean and different letters indicate significantly different means separated by the Kruskal-Wallis test statistic ($\alpha = 0.05$).

Table 3.2. Statistical results based on analysis of relative transcript abundance of diTPS and CYP450 genes related to DRA and GA biosynthesis in white spruce developing apical buds and apical shoots over a year-long time course. Statistical data obtained by analysis with Kruskal-Wallis test statistic ($\alpha=0.05$); light grey text shows statistical results that are not significant for ease of interpretation. These results pertain to Figure 3.19 and Figure 3.20.

Gene of Interest	Factor or Interaction	
<i>PgCPS</i>	Sample part	H(2)=35.980, N=74, $P<0.0005$
	Time	H(6)=2.759, N=74, $P=0.838$
	Sample part x Time	H(18)=45.559, N=74, $P<0.0005$
	Needle Time	H(6)=13.628, N=26, $P=0.034$
	Stem Time	H(6)=4.095, N=28, $P=0.664$
	New Buds Time	H(4)=6.194, N=20, $P=0.185$
<i>PgKS</i>	Sample part	H(2)=38.757, N=76, $P<0.0005$
	Time	H(6)=9.236, N=76, $P=0.161$
	Sample part x Time	H(18)=49.196, N=76, $P<0.0005$
	Needle Time	H(6)=3.601, N=28, $P=0.730$
	Stem Time	H(6)=11.865, N=28, $P=0.065$
	New Buds Time	H(4)=2.729, N=20, $P=0.604$
<i>PgLAS</i>	Sample part	H(2)=12.360, N=76, $P=0.002$
	Time	H(6)=37.028, N=76, $P<0.0005$
	Sample part x Time	H(18)=64.309, N=76, $P<0.0005$
	Needle Time	H(6)=25.560, N=28, $P<0.0005$
	Stem Time	H(6)=15.876, N=28, $P=0.014$
	New Buds Time	H(4)=4.357, N=20, $P=0.360$
<i>PgCYP701</i>	Sample part	H(2)=13.194, N=75, $P=0.001$
	Time	H(6)=6.079, N=75, $P=0.414$
	Sample part x Time	H(18)=49.196, N=76, $P<0.0005$
	Needle Time	H(6)=6.862, N=27, $P=0.334$
	Stem Time	H(6)=8.202, N=28, $P=0.224$
	New Buds Time	H(4)=5.786, N=20, $P=0.216$
<i>PgCYP720B4</i>	Sample part	H(2)=23.051, N=75, $P<0.0005$
	Time	H(6)=31.986, N=75, $P<0.0005$
	Sample part x Time	H(18)=65.697, N=75, $P<0.0005$
	Needle Time	H(6)=23.171, N=27, $P=0.001$
	Stem Time	H(6)=21.287, N=28, $P=0.002$
	New Buds Time	H(4)=14.954, N=20, $P=0.005$

Table 3.3. Relative transcript abundance of diTPS and CYP450 genes related to DRA and GA biosynthesis in white spruce developing apical buds and shoots over a year-long time course. Data are expressed as relative transcript abundance to reference gene *eEF1 α* (\pm SEM). Different letters within each gene indicate significantly different means separated by the Kruskal-Wallis test statistic ($\alpha=0.05$). This data pertains to Figure 3.19.

Gene of Interest	Sample Part	Time Point	Relative Transcript Abundance	
<i>PgCPS</i>	Needles	13	1.491 \pm 0.364	<i>bc</i>
		15	3.909 \pm 1.503	<i>ab</i>
		17	6.490 \pm 1.450	<i>a</i>
		19	2.603 \pm 0.907	<i>abc</i>
		21	2.796 \pm 0.233	<i>ab</i>
		23	0.816 \pm 0.392	<i>c</i>
		25	0.990 \pm 0.060	<i>c</i>
<i>PgLAS</i>	Needles	13	5.376 \pm 0.464	<i>a</i>
		15	4.345 \pm 0.456	<i>a</i>
		17	0.542 \pm 0.132	<i>ab</i>
		19	0.000 \pm 0.000	<i>c</i>
		21	0.040 \pm 0.040	<i>bc</i>
		23	0.000 \pm 0.000	<i>c</i>
		25	0.000 \pm 0.000	<i>c</i>
	Stem	13	2.929 \pm 0.501	<i>a</i>
		15	3.074 \pm 0.325	<i>a</i>
		17	1.217 \pm 0.186	<i>b</i>
		19	1.398 \pm 0.275	<i>b</i>
		21	1.934 \pm 0.308	<i>ab</i>
		23	1.777 \pm 0.455	<i>ab</i>
		25	1.256 \pm 0.382	<i>b</i>
<i>PgCYP720B4</i>	Needles	13	0.967 \pm 0.182	<i>ab</i>
		15	1.878 \pm 0.527	<i>a</i>
		17	1.236 \pm 0.391	<i>a</i>
		19	0.076 \pm 0.045	<i>bc</i>
		21	0.000 \pm 0.000	<i>c</i>
		23	0.000 \pm 0.000	<i>c</i>
		25	0.000 \pm 0.000	<i>c</i>
	Stem	13	1.165 \pm 0.091	<i>cd</i>
		15	3.232 \pm 0.419	<i>abc</i>
		17	7.971 \pm 1.148	<i>a</i>
		19	4.920 \pm 0.897	<i>ab</i>
		21	3.093 \pm 1.409	<i>abc</i>
		23	1.822 \pm 0.795	<i>bcd</i>
		25	0.213 \pm 0.125	<i>d</i>
	New buds	17	2.983 \pm 0.729	<i>a</i>
		19	3.003 \pm 0.454	<i>a</i>
		21	1.776 \pm 0.079	<i>ab</i>
		23	0.520 \pm 0.070	<i>bc</i>
		25	0.174 \pm 0.157	<i>c</i>

PgKS mean relative transcript levels were significantly affected by sample part ($P<0.0005$) (Figure 3.20G; Table 3.2). The mean transcript levels of *PgKS* were highest in needles (1.599 ± 0.114), with both stem and new buds being significantly lower by approximately 50% (0.743 ± 0.054 and 0.785 ± 0.063 , respectively). Mean relative transcript levels were also significantly affected by the interaction between sample part and time factors ($P<0.0005$) (Table 3.2). However, analysis within any one individual sample part did not show significant changes in *PgKS* transcript levels over time (Figure 3.19B), indicating that transcript levels held relatively constant over the time course.

PgLAS mean transcript levels were significantly affected by sample part ($P=0.002$) (Figure 3.20I; Table 3.2), with the mean transcript abundance of stem being the highest (1.941 ± 0.183) and both needles and new buds having lower mean relative abundances (1.472 ± 0.426 and 1.139 ± 0.140 , respectively). As well, mean transcript levels were significantly affected by time ($P<0.0005$) (Figure 3.20D); time points 13 and 15 having the highest mean transcript levels (4.153 ± 0.560 and 3.710 ± 0.354 , respectively) and time points 17-25 all having significantly lower mean transcript levels that were not different from each other (1.025 ± 0.142 , 0.679 ± 0.198 , 1.140 ± 0.275 , 0.918 ± 0.276 and 0.858 ± 0.255 , respectively). *PgLAS* transcript levels were also significantly affected by the interaction between sample part and time ($P<0.0005$) (Figure 3.19D). Within sample parts, both needles and stems showed significant differences in relative transcript abundance over time ($P<0.0005$ and $P=0.014$, respectively), Table 3.2. *PgLAS* transcript levels rose sharply in needles in the spring with the highest relative transcript abundances at time points 13 and 15 (5.376 ± 0.464 and 4.345 ± 0.456 , respectively), Table 3.3. Subsequently, *PgLAS* expression in needles rapidly declined and was undetectable at time points 19, 23 and 25 (all were

effectively zero, i.e. below the limit of detection); transcript levels at time point 21 were not significantly different from the lowest time points. In stems, time points 13 and 15 also had the highest transcript abundances (2.929 ± 0.501 and 3.074 ± 0.325 , respectively) and again, expression was reduced at later times. Time points 17, 19 and 25 had the lowest (1.217 ± 0.186 , 1.398 ± 0.275 and 1.256 ± 0.382 , respectively) which were significantly different from the peak levels.

PgCYP701 mean relative transcript levels were significantly affected by sample part ($P=0.001$) (Figure 3.20H; Table 3.2). The mean transcript levels were highest in needles (1.826 ± 0.220), with both stem and new buds being significantly lower (1.015 ± 0.092 and 0.970 ± 0.090 , respectively). Mean relative transcript levels were not affected by time but were significantly affected by the interaction between sample part and time ($P<0.0005$) (Figure 3.19C). However, when analyzed separately, no sample part showed significantly different transcript levels of *PgCYP701* over time.

The mean transcript levels of *PgCYP720B4* were significantly affected by sample part ($P<0.0005$) (Figure 3.20J; Table 3.2), with the mean relative transcript abundance of stems and new buds being the highest (3.202 ± 0.542 and 1.691 ± 0.314 , respectively) and needles having significantly lower mean relative abundance (0.546 ± 0.152), just 17% of the value in stems. Mean *PgCYP720B4* transcript levels were also significantly affected by time ($P<0.0005$), with transcript levels rising over the spring weeks to peak at time point 17 (relative mean transcript level 4.064 ± 0.960) (Figure 3.20E). Subsequently, levels declined steadily over time with time point 25 showing the lowest mean transcript level (0.129 ± 0.067). Time points 15 and 19 were not significantly different than the highest time point, time points 13 and 21 had intermediary levels and time point 23 had low transcript levels that

were not significantly different from time point 25. Mean transcript levels were also significantly affected by the interaction between sample part and time ($P<0.0005$).

PgCYP720B4 relative transcript abundance changed significantly over time in all three sample parts (stem: $P=0.002$, needle: $P=0.001$, and new buds: $P=0.005$) (Figure 3.19E; Table 3.2). Within stem, time point 17 had the highest relative transcript levels (7.971 ± 1.148) and time point 25 had the lowest (0.213 ± 0.125), representing an over 37-fold transcript level decrease, (Table 3.3). Time points 15, 19 and 21 had intermediate levels that were not significantly different from the highest time point, and the remaining time points (13, and 23) had transcript levels that were not different from the time point with the lowest value. Within needle, time points 15 and 17 had the highest relative transcript abundances (1.878 ± 0.527 and 1.236 ± 0.391 , respectively), whereas transcripts were below the detection limits at time points 21, 23 and 25. Transcript levels at time point 13 were not significantly different from the highest time points, and levels at time point 19 were not significantly different from the lowest time points. Within new bud, time points 17 and 19 had the highest transcript levels (2.983 ± 0.729 and 3.003 ± 0.454 , respectively) with values declining steadily thereafter to time point 25 which had the lowest levels (0.174 ± 0.157). Time point 21 had transcript levels that were not significantly different from time points 17 and 19 that had the highest levels, and transcript levels at time point 23 were not significantly different from the lowest time point.

3.2.9. Effect of MeJA treatment and time on DRA concentration in specific samples of white spruce

DRA profiling was performed to determine the presence and total concentration of eight DRAs (pimaric acid, sandaracopimaric acid, levopimaric acid, palustric acid, isopimaric acid, abietic acid, dehydroabietic acid, neoabietic acid) in response to MeJA treatment (or Tween control) in 5 different white spruce sample types over a 30-day time course. The samples were: bark/phloem (B), wood/xylem (X), young needles (YN), mature needles (MN), young stems (YS).

When data averages for all 5 sample types were combined, DRA metabolite concentrations were found to differ significantly by factors of sample type ($P<0.0005$) and treatment ($P=0.017$), whereas time did not have a significant effect ($P=0.515$) (Table 3.4). Several interactions were found to have a significant effect on DRA concentrations: sample x treatment ($P<0.0005$), sample x time ($P<0.0005$) and sample x treatment x time ($P<0.0005$). By contrast, there was no interaction observed between treatment and time ($P=0.328$) (Table 3.4).

The interaction of sample type and time was found to have a significant effect on DRA concentration ($P<0.0005$) (Figure 3.21). Here treatment type was not taken into account. To further elucidate the interaction of sample type and time, data was separated into two categories: comparisons within a sample type, and comparison within a time point. Within sample pairwise comparison of time points were not significant (YN ($P=0.263$); MN ($P=0.062$); B ($P=0.485$); X ($P=0.128$); YS ($P=0.209$)). Within each time point, pairwise comparisons between sample types (Figure 3.21) were all significant: day 2 ($P<0.0005$), day 4 ($P<0.0005$), day 6 ($P<0.0005$), day 8 ($P<0.0005$), day 16 ($P<0.0005$), day 30 ($P<0.0005$)

(Table 3.5). At all time points, bark/phloem had the highest mean DRA concentration, and mature needles had the lowest. The mean DRA concentration of young stems at all time points was consistently higher than that of young needles, both of which had intermediate concentrations. Wood/xylem was the only sample type that changed its position in relation to the other sample types, starting from second lowest mean DRA concentration and moving to second highest over the time course (Figure 3.21; Table 3.5).

Table 3.4. Statistical results based on analysis of DRA abundance in control or MeJA-treated samples from white spruce over a time course. Statistical data obtained by analysis with Kruskal-Wallis test statistic ($\alpha=0.05$); for ease of interpretation light grey text shows statistical results that are not significant. These results pertain to Figure 3.21, 3.22, and 3.23.

Sample	Factor or Interaction	
DRA	Sample	H(4)=156.348, N=229, $P<0.0005$
	Treatment	H(1)=5.743, N=229, $P=0.017$
	Time	H(5)=4.242, N=229, $P=0.515$
	Sample x Treatment	H(9)=170.766, N=229, $P<0.0005$
	Sample x Time	H(29)=170.048, N=229, $P<0.0005$
	Treatment x Time	H(11)=12.487, N=229, $P=0.328$
	Sample x Treatment x Time	H(59)=196.784, N=229, $P<0.0005$
Young Needles	Treatment x Time	H(12)=16.238, N=49, $P=0.181$
Mature Needles	Treatment x Time	H(12)=15.395, N=46, $P=0.221$
Bark/Phloem	Treatment x Time	H(12)=10.626, N=48, $P=0.561$
Wood/Xylem	Treatment x Time	H(12)=27.714, N=52, $P=0.006$
Young Stems	Treatment x Time	H(11)=26.034, N=45, $P=0.006$

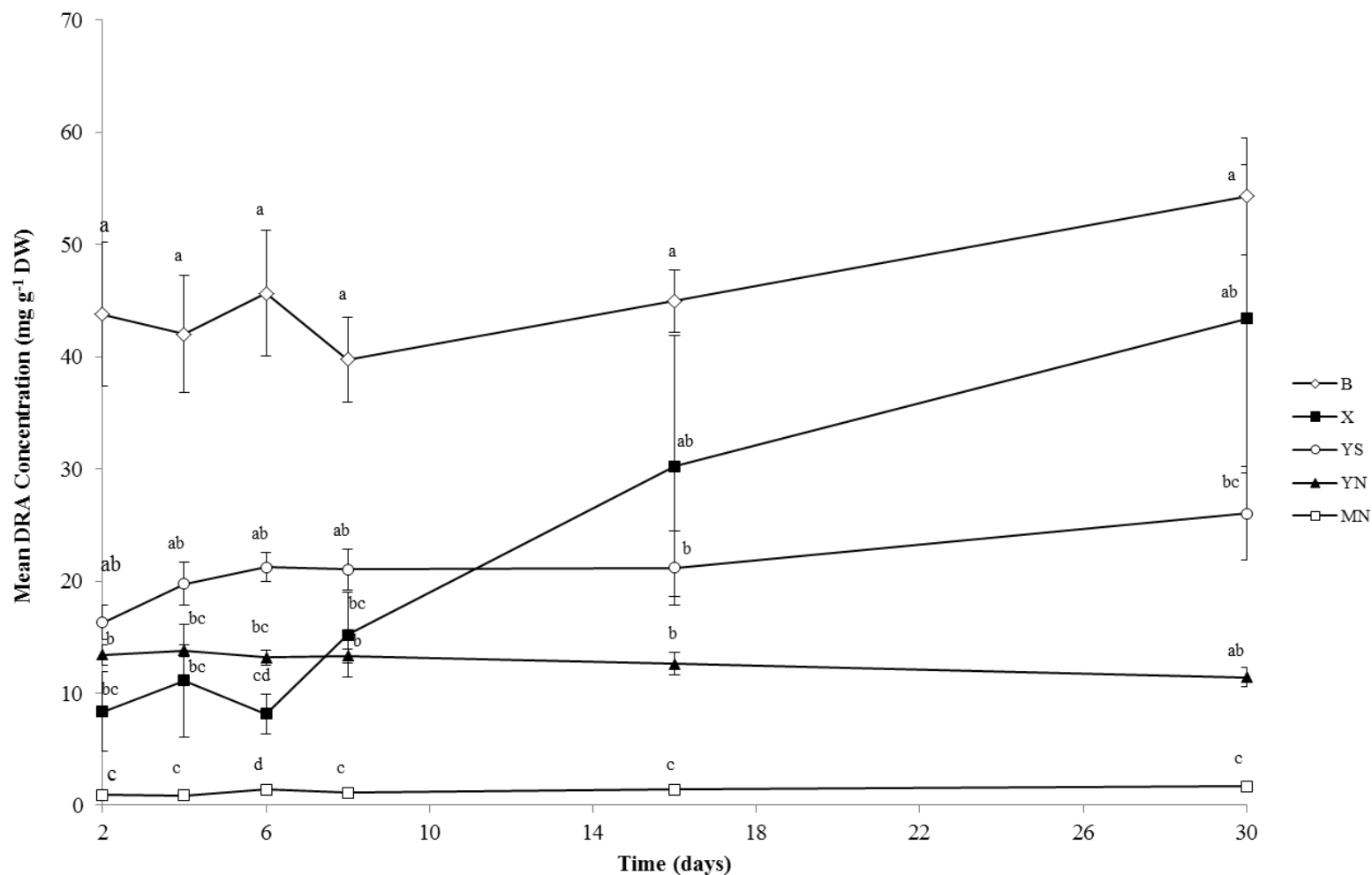


Figure 3.21. Mean concentration of DRA (mg g⁻¹ DW) over sample type and time point in white spruce. The interaction between sample type and time factors was shown to have a significant effect ($P < 0.0005$). Differences between treatment types are not considered, DRA mean concentrations reflect all data from both treatment types per sample and time point. Error bars represent the standard error of the mean and different letters indicate significantly different means between sample types, at each time point, separated by the Kruskal-Wallis test statistic ($\alpha = 0.05$). Differences within a sample type over time were not significantly different. Sample types are as follows: bark/phloem (B), wood/xylem (X), young needles (YN), mature needles (MN), young stems (YS).

Table 3.5. Mean DRA concentrations and statistical results in different samples from white spruce over time. The interaction of time and sample type factors was found to have a significant effect on DRA concentration ($P<0.0005$). Here treatment type is not taken into account. Contents are expressed as mean DRA concentrations ($\text{mg g}^{-1} \text{DW}$) \pm SEM. Letters indicate significantly different means between sample types, at each time point, separated by the Kruskal-Wallis test statistic ($\alpha=0.05$). Sample types: bark/phloem (B), wood/xylem (X), young needles (YN), mature needles (MN), young stems (YS). These results pertain to Figure 3.21.

Day/ Time Point	Sample	DRA ($\text{mg g}^{-1} \text{DW}$)	
2	B	43.80 ± 6.39	<i>a</i>
	YS	16.31 ± 1.53	<i>ab</i>
	YN	13.40 ± 0.90	<i>b</i>
	X	8.37 ± 3.55	<i>bc</i>
	MN	0.92 ± 0.15	<i>c</i>
H(4)=27.844, N=38, $P<0.0005$			
4	B	42.01 ± 5.21	<i>a</i>
	YS	19.76 ± 1.94	<i>ab</i>
	YN	13.79 ± 0.57	<i>bc</i>
	X	11.14 ± 5.02	<i>bc</i>
	MN	0.89 ± 0.17	<i>c</i>
H(4)=25.273, N=38, $P<0.0005$			
6	B	45.66 ± 5.60	<i>a</i>
	YS	21.22 ± 1.29	<i>ab</i>
	YN	$13.17 \pm .71$	<i>bc</i>
	X	8.14 ± 1.77	<i>cd</i>
	MN	1.43 ± 0.13	<i>d</i>
H(4)=31.380, N=36, $P<0.0005$			
8	B	39.78 ± 3.78	<i>a</i>
	YS	21.02 ± 1.85	<i>ab</i>
	X	15.18 ± 3.78	<i>bc</i>
	YN	13.31 ± 0.60	<i>b</i>
	MN	1.12 ± 0.16	<i>c</i>
H(4)=29.774, N=39, $P<0.0005$			
16	B	44.97 ± 2.78	<i>a</i>
	X	30.24 ± 11.64	<i>ab</i>
	YS	21.17 ± 3.31	<i>b</i>
	YN	12.63 ± 1.01	<i>b</i>
	MN	1.43 ± 0.14	<i>c</i>
H(4)=26.127, N=40, $P<0.0005$			
30	B	54.33 ± 5.22	<i>a</i>
	X	43.39 ± 13.76	<i>ab</i>
	YS	26.02 ± 4.16	<i>bc</i>
	YN	11.42 ± 0.85	<i>ab</i>
	MN	1.69 ± 0.34	<i>c</i>
H(4)=25.033, N=38, $P<0.0005$			

Mean DRA concentrations were also found to differ significantly due to the interaction between sample type and treatment factors ($P < 0.0005$) (Figure 3.22; Table 3.4). In this analysis the difference between time points was not considered. Bark/Phloem (B) treated with MeJA had the highest DRA concentration ($48.80 \pm 3.14 \text{ mg g}^{-1} \text{ DW}$) although this was not significantly different from the DRA concentration in control B ($41.57 \pm 2.45 \text{ mg g}^{-1} \text{ DW}$). The lowest overall DRA concentration was in control mature needles (MN) ($1.11 \pm 0.08 \text{ mg g}^{-1} \text{ DW}$) which again was not significantly different from its MeJA-treated counterpart ($1.36 \pm 0.15 \text{ mg g}^{-1} \text{ DW}$). Within the MeJA treatment, wood/xylem (X), young stems (YS) and young needles (YN) displayed intermediate DRA concentrations (31.01 ± 6.25 , 25.67 ± 1.81 and $13.30 \pm 0.46 \text{ mg g}^{-1} \text{ DW}$, respectively) whereas comparable values for controls were 7.80 ± 1.64 , 16.99 ± 0.64 , $12.58 \pm 0.46 \text{ mg g}^{-1} \text{ DW}$, respectively). Comparing all 5 sample types, wood/xylem was the only sample which exhibited a significant change in DRA concentrations between MeJA and control treatments (Table 3.6).

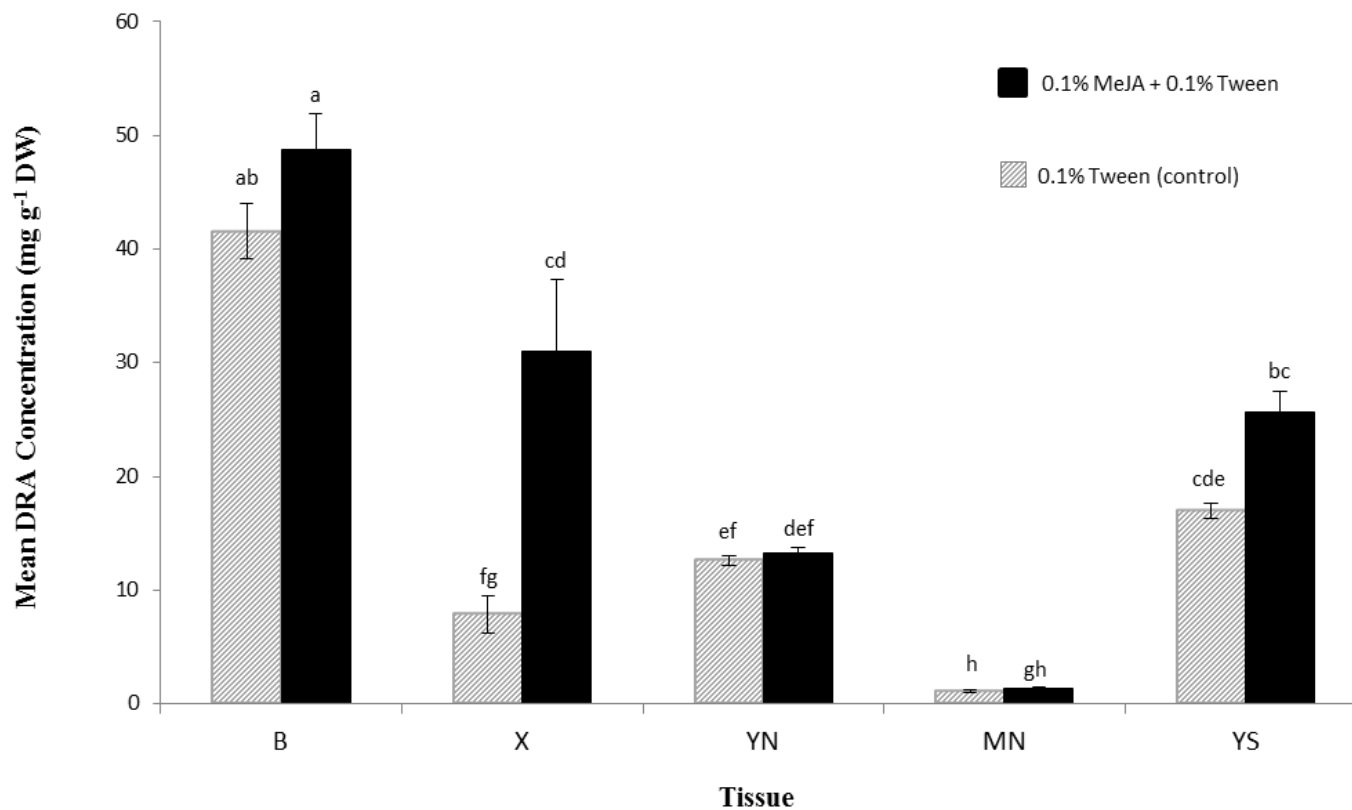


Figure 3.22. Mean concentrations of DRA (mg g⁻¹ DW) over MeJA treatment and sample type in white spruce. The interaction between sample and treatment factors was shown to be significant ($P < 0.0005$). Differences between time points are not considered, DRA mean concentrations reflect all time points per sample and treatment type; error bars represent the standard error of the mean and different letters indicate significantly different means separated by the Kruskal-Wallis test statistic ($\alpha=0.05$). Sample types are as follows: bark/phloem (B), wood/xylem (X), young needles (YN), mature needles (MN), young stems (YS).

Table 3.6. Mean DRA concentrations in control and MeJA-treated samples from white spruce. The interaction of sample type and treatment factors was found to have a significant effect on DRA concentration ($P < 0.0005$). Here time points are not taken into account. Contents are expressed as mean DRA concentrations ($\text{mg g}^{-1} \text{DW}$) ($\pm \text{SEM}$). Letters indicate significantly different means separated by the Kruskal-Wallis test statistic ($\alpha=0.05$). This data pertains to Figure 3.22.

Sample	Control		MeJA	
	$(\text{mg g}^{-1} \text{DW})$		$(\text{mg g}^{-1} \text{DW})$	
Bark/Phloem	41.57 ± 2.45	<i>ab</i>	48.80 ± 3.14	<i>a</i>
Wood/Xylem	7.80 ± 1.64	<i>fg</i>	31.01 ± 6.25	<i>cd</i>
Young Stems	16.99 ± 0.64	<i>cde</i>	25.67 ± 1.81	<i>bc</i>
Young Needles	12.58 ± 0.46	<i>ef</i>	13.30 ± 0.46	<i>def</i>
Mature Needles	1.11 ± 0.08	<i>h</i>	1.36 ± 0.15	<i>gh</i>

DRA concentrations were also found to differ significantly with the interaction of sample, treatment and time ($P < 0.0005$). To further elucidate these interactions data were separated into sample types and significance was analyzed between the interaction of treatment and time within each sample type (Figure 3.23). No significant difference was observed in the interaction between treatment type and time for bark/phloem ($P = 0.561$), young needles ($P = 0.181$), or mature needles ($P = 0.221$). However, significant differences were observed due to the interactions of treatment and time for wood/xylem ($P = 0.006$) and young stems ($P = 0.006$) (Table 3.4).

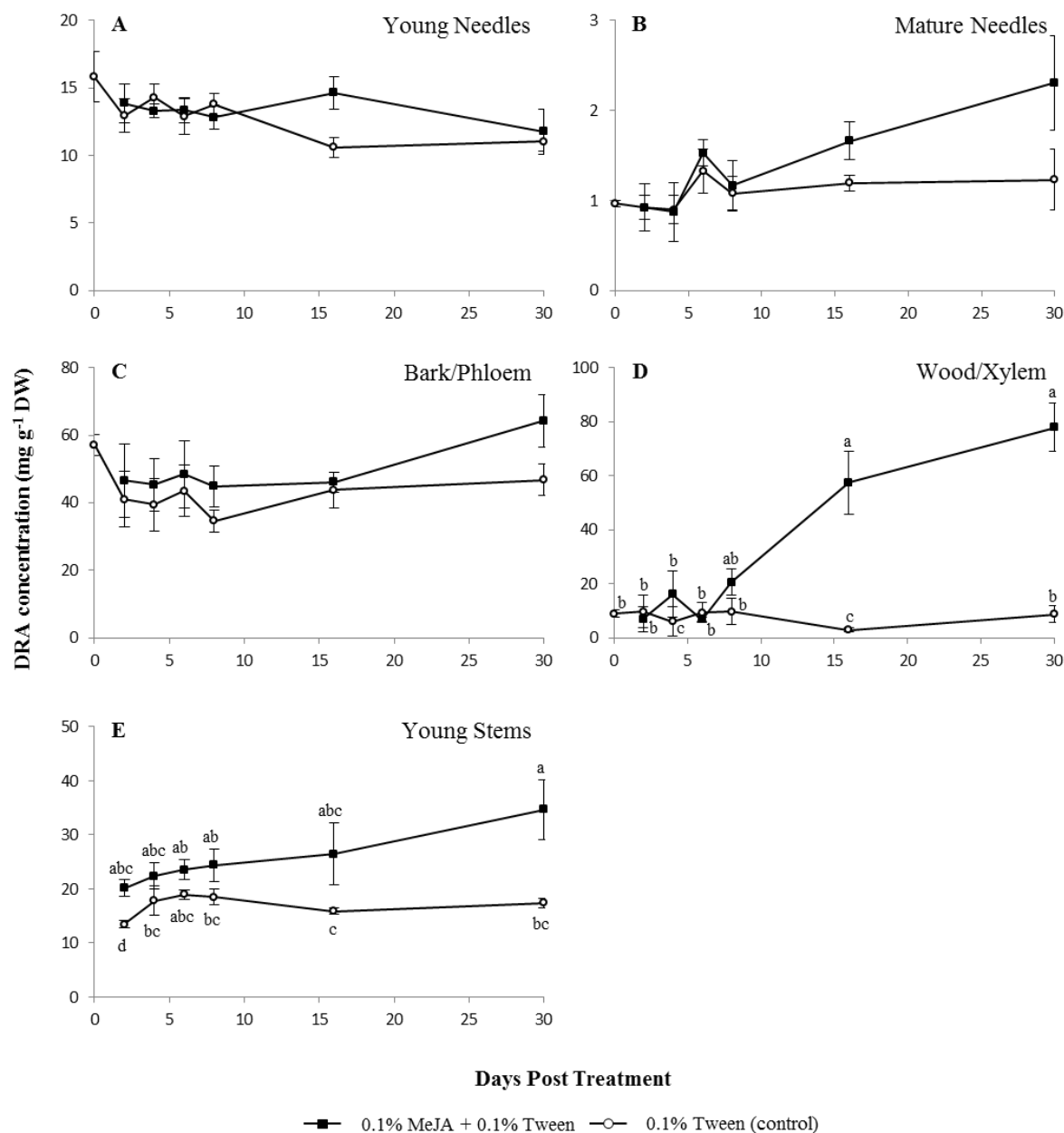


Figure 3.23. Total DRA concentration in MeJA-treated white spruce samples over a time course. DRA metabolites were found to differ significantly by sample type ($P<0.0005$) and treatment ($P=0.017$). A significant interaction between sample type, treatment, and time factors was also found ($P<0.0005$). Within sample types, differences between DRA in xylem ($P=0.006$) and young stems ($P=0.006$) were found to be significant. Data represent the mean (\pm SEM) of 3-4 biological replicates. Graph (A) shows young needles, (B) mature needles, (C) bark/phloem, (D) wood/xylem, and (E) young stems. Letters indicate means separated, within a sample type, by the Kruskal-Wallis test statistic ($\alpha=0.05$).

Within the wood/xylem sample type (Figure 3.23D) the highest concentrations of DRA were reached on days 16 and 30 of MeJA treatment (57.51 ± 11.67 and 77.95 ± 8.84 , mg g^{-1} DW respectively). By contrast, control DRA values were lowest on days 4 and 16 (6.11 ± 5.45 and 2.97 ± 0.78 mg g^{-1} DW respectively). The remaining control DRA values were low and were not significantly different from each other; in general, control DRA values were relatively unchanged over the time course. MeJA-treated wood/xylem on days 2, 4 and 6 showed no significant difference from their respective control values, however on day 8 DRA values increased to intermediary levels (between earlier time points and days 16 and 30), suggesting that it was at about this time that enhanced accumulation of DRA was beginning to occur in this MeJA-treated sample (Table 3.7). Overall, DRA levels in MeJA-treated wood/xylem rose approximately 9-fold over the 30-day time course.

For young stems (YS) (Figure 3.23E) the highest concentration of DRA was found in MeJA-treated trees sampled after 30 days (34.65 ± 5.51 mg g^{-1} DW) whereas control trees sampled after 2 days showed the lowest overall concentration of DRA (13.44 ± 0.69 mg g^{-1} DW). Although there was a clear rising trend of DRA concentration in MeJA-treated YS samples over time, due to substantial variation in DRA levels, there were no significant differences in DRA levels over the time course of MeJA treatment. However, at day 30, there was a significant difference between the MeJA-treated and control value, an approximately 2-fold greater amount in the MeJA-treated YS samples (Table 3.7).

Table 3.7. DRA concentrations in control and MeJA-treated samples from white spruce. The interaction of sample type, treatment and time factors was found to have a significant effect on DRA concentration ($P < 0.0005$). Data were separated into sample types and significance was analyzed. Shown are sample types in which there was a significant difference of DRA concentrations, p-values indicate significance of interaction between time and treatment at each sample type. Contents are expressed as mean DRA concentrations (mg g^{-1} DW) \pm SEM. Letters indicate significantly different means between sample types, at each time point, separated by the Kruskal-Wallis test statistic ($\alpha=0.05$). This data pertains to Figure 3.23.

Sample	Day	Control (mg g^{-1} DW)	MeJA (mg g^{-1} DW)
Wood/Xylem ($P=0.006$)	0	8.99 ± 1.42 <i>b</i>	
	2	9.76 ± 5.97 <i>b</i>	6.97 ± 4.69 <i>b</i>
	4	6.11 ± 5.45 <i>c</i>	16.17 ± 8.45 <i>b</i>
	6	9.42 ± 3.59 <i>b</i>	6.86 ± 0.81 <i>b</i>
	8	9.74 ± 4.84 <i>b</i>	20.62 ± 4.83 <i>ab</i>
	16	2.97 ± 0.78 <i>c</i>	57.51 ± 11.67 <i>a</i>
	30	8.82 ± 3.04 <i>b</i>	77.95 ± 8.84 <i>a</i>
Young Stems ($P=0.006$)	2	13.44 ± 0.69 <i>d</i>	20.14 ± 1.61 <i>abc</i>
	4	17.79 ± 2.70 <i>bc</i>	22.38 ± 2.40 <i>abc</i>
	6	18.93 ± 0.92 <i>abc</i>	23.50 ± 1.84 <i>ab</i>
	8	18.52 ± 1.53 <i>bc</i>	24.35 ± 3.08 <i>ab</i>
	16	15.87 ± 0.64 <i>c</i>	26.47 ± 5.65 <i>abc</i>
	30	17.39 ± 0.84 <i>bc</i>	34.65 ± 5.51 <i>a</i>

3.2.10. Effect of MeJA treatment and time on transcript abundance of DRA and GA biosynthetic genes in specific sample types of white spruce

Real-time quantitative PCR was used to quantify transcript abundance of 5 genes related to GA and DRA biosynthesis, diterpene synthases *PgCPS*, *PgKS* and *PgLAS* and cytochrome P450s *PgCYP701* and *PgCYP720B4*. The objective was to measure the response to MeJA treatment (or Tween control) in 5 sample types of white spruce over a 30-day time course. Samples were as follows: bark/phloem (B), wood/xylem (X), young needles (YN), mature needles (MN), young stems (YS). Transcript abundance levels were expressed as relative to normalizing genes *eIF4E* and *H3* (\pm SEM). Within the data for each gene, statistical analyses were run to determine the effect of this experiment's main factors: time, sample type, and treatment type; as well as the interactions between these factors.

PgCPS

Combining data for all 5 sample types, transcript abundance levels of *PgCPS* were found to differ significantly by factors of sample type (Kruskal-Wallis, $P < 0.0005$), treatment type ($P < 0.0005$), and time ($P = 0.001$). Interactions between all factors were found to have a significant effect on *PgCPS* transcript levels: sample x treatment ($P < 0.0005$), sample x time ($P < 0.0005$), treatment x time ($P < 0.0005$) and sample x treatment x time ($P < 0.0005$), see Table 3.8 for detailed statistical analysis results.

PgCPS transcript levels were found to differ significantly due to the interaction between sample type and treatment factors ($P < 0.0005$) (Figure 3.24A). In this analysis the difference between time points was not considered. Bark/Phloem (B) control, treated with

Tween-20, and control mature needles (MN) had the highest mean transcript abundances (4.173 ± 0.884 , 3.825 ± 0.772 , respectively), both means being significantly higher than their MeJA-treated counterparts (0.556 ± 0.209 , 0.969 ± 0.313 , respectively). The only other sample type which had a significant difference between the means of its treatment types was young needles (YN) with control samples having a higher transcript abundance than MeJA-treated (1.168 ± 0.215 and 0.337 ± 0.071 respectively). Control wood/xylem (X) had the lowest mean (0.026 ± 0.020) which was not significantly different from its MeJA-treated mean, and young stems (YS) also showed no difference between treatment types.

Table 3.8. Statistical results based on analysis of relative transcript abundance of diTPS and CYP450 genes related to DRA and GA biosynthesis in control or MeJA-treated samples from white spruce.

Statistical data obtained by analysis with Kruskal-Wallis test statistic ($\alpha=0.05$); for ease of interpretation light grey text shows statistical results that are not significant. These results pertain to Figures 3.24, 3.25, 3.26, 3.27, 3.28, and 3.29.

Gene of Interest	Factor or Interaction	
<i>PgCPS</i>	Sample	H(4)=64.052, N=243, $P<0.0005$
	Treatment	H(1)=22.181, N=243, $P<0.0005$
	Time	H(6)=23.125, N=243, $P=0.001$
	Sample x Treatment	H(9)=110.551, N=243, $P<0.0005$
	Sample x Time	H(33)=104.735, N=243, $P<0.0005$
	Treatment x Time	H(12)=55.409, N=243, $P<0.0005$
	Sample x Treatment x Time	H(63)=178.567, N=243, $P<0.0005$
Young Needles	Treatment x Time	H(12)=18.565, N=49, $P=0.100$
Mature Needles	Treatment x Time	H(12)=33.709, N=47, $P=0.001$
Bark/Phloem	Treatment x Time	H(12)=40.540, N=51, $P<0.0005$
Wood/Xylem	Treatment x Time	H(12)=15.040, N=48, $P=0.239$
Young Stems	Treatment x Time	H(11)=25.028, N=48, $P=0.009$
<i>PgKS</i>	Sample	H(4)=15.072, N=248, $P=0.005$
	Treatment	H(1)=159.679, N=248, $P<0.0005$
	Time	H(6)=25.617, N=248, $P<0.0005$
	Sample x Treatment	H(9)=178.702, N=248, $P<0.0005$
	Sample x Time	H(33)=50.135, N=248, $P=0.028$
	Treatment x Time	H(12)=170.378, N=248, $P<0.0005$
	Sample x Treatment x Time	H(63)=210.428, N=248, $P<0.0005$
Young Needles	Treatment x Time	H(12)=41.845, N=51, $P<0.0005$
Mature Needles	Treatment x Time	H(12)=35.503, N=51, $P<0.0005$
Bark/Phloem	Treatment x Time	H(12)=40.914, N=51, $P<0.0005$
Wood/Xylem	Treatment x Time	H(12)=41.922, N=48, $P<0.0005$
Young Stems	Treatment x Time	H(11)=36.298, N=47, $P<0.0005$
<i>PgLAS</i>	Sample	H(4)=141.312, N=249, $P<0.0005$
	Treatment	H(1)=42.994, N=249, $P<0.0005$
	Time	H(6)=12.260, N=249, $P=0.056$
	Sample x Treatment	H(9)=198.952, N=249, $P<0.0005$
	Sample x Time	H(33)=173.386, N=249, $P<0.0005$
	Treatment x Time	H(12)=48.815, N=249, $P<0.0005$
	Sample x Treatment x Time	H(63)=226.219, N=249, $P<0.0005$
Young Needles	Treatment x Time	H(12)=41.485, N=52, $P<0.0005$
Mature Needles	Treatment x Time	H(12)=22.855, N=51, $P=0.029$
Bark/Phloem	Treatment x Time	H(12)=38.882, N=51, $P<0.0005$
Wood/Xylem	Treatment x Time	H(12)=42.785, N=48, $P<0.0005$
Young Stems	Treatment x Time	H(11)=29.344, N=47, $P=0.002$
<i>PgCYP70I</i>	Sample	H(4)=69.831, N=245, $P<0.0005$
	Treatment	H(1)=13.682, N=245, $P<0.0005$
	Time	H(6)=16.251, N=245, $P=0.012$
	Sample x Treatment	H(9)=106.535, N=245, $P<0.0005$
	Sample x Time	H(33)=113.063, N=245, $P<0.0005$
	Treatment x Time	H(12)=44.984, N=245, $P<0.0005$
	Sample x Treatment x Time	H(63)=177.829, N=245, $P<0.0005$
Young Needles	Treatment x Time	H(12)=28.535, N=50, $P=0.005$
Mature Needles	Treatment x Time	H(12)=39.764, N=51, $P<0.0005$
Bark/Phloem	Treatment x Time	H(12)=22.118, N=51, $P=0.036$
Wood/Xylem	Treatment x Time	H(12)=30.212, N=48, $P=0.003$
Young Stems	Treatment x Time	H(11)=24.768, N=45, $P=0.010$

Gene of Interest	Factor or Interaction	
<i>PgCYP720B4</i>	Sample	H(4)=148.586, N=250, $P<0.0005$
	Treatment	H(1)=19.787, N=250, $P<0.0005$
	Time	H(6)=9.666, N=250, $P=0.139$
	Sample x Treatment	H(9)=174.254, N=250, $P<0.0005$
	Sample x Time	H(33)=196.139, N=250, $P<0.0005$
	Treatment x Time	H(12)=27.271, N=250, $P=0.007$
	Sample x Treatment x Time	H(63)=225.183, N=250, $P<0.0005$
Young Needles	Treatment x Time	H(12)=41.822, N=52, $P<0.0005$
Mature Needles	Treatment x Time	H(12)=25.580, N=51, $P=0.012$
Bark/Phloem	Treatment x Time	H(12)=19.756, N=51, $P=0.072$
Wood/Xylem	Treatment x Time	H(12)=39.734, N=48, $P<0.0005$
Young Stems	Treatment x Time	H(11)=32.551, N=48, $P=0.001$

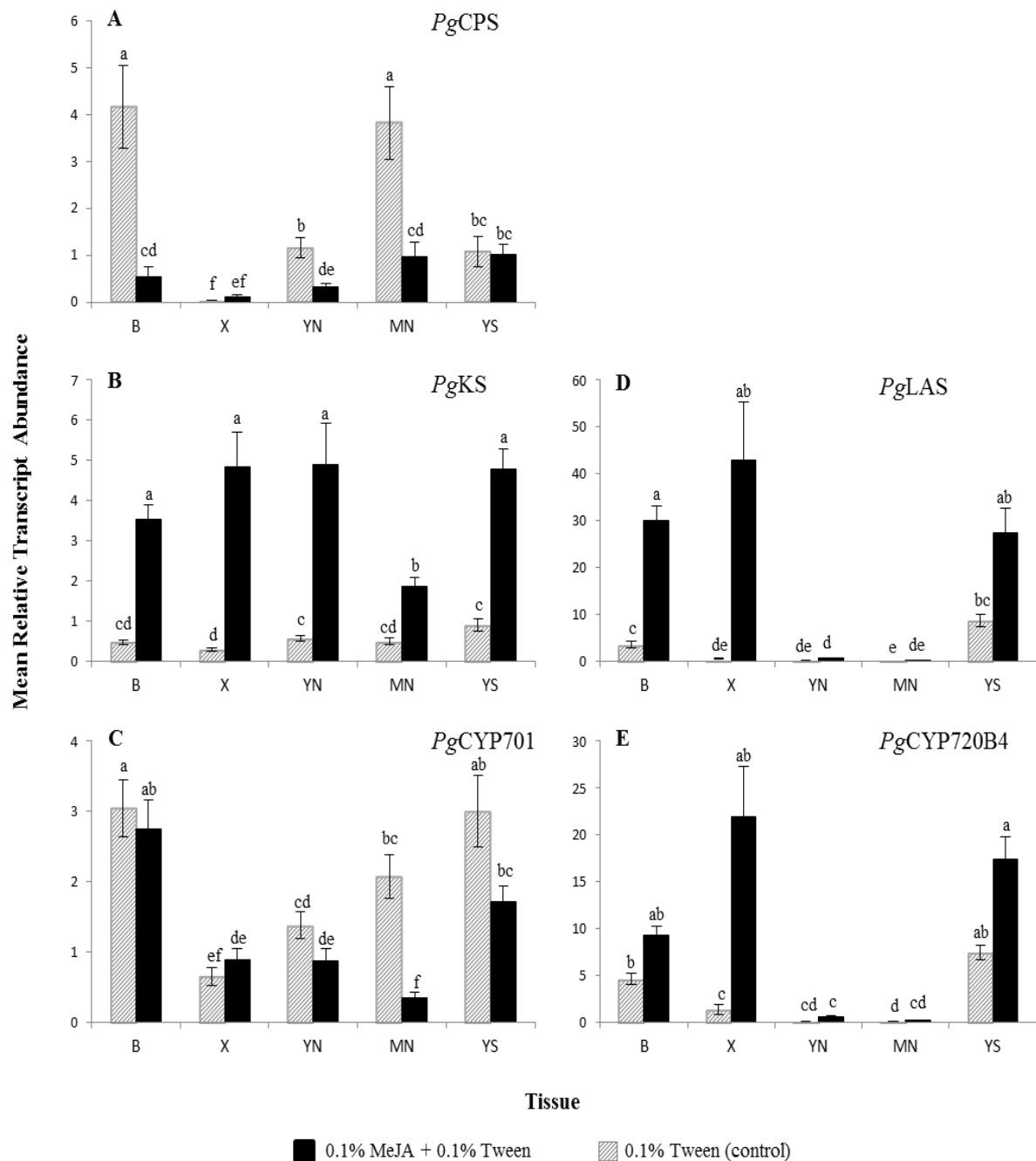


Figure 3.24. Mean relative transcript abundance over MeJA treatment and sample type in white spruce. The interaction between sample and treatment factors was shown to have a significant effect on the expression profile of *PgCPS* (A, $P < 0.0005$), *PgKS* (B, $P < 0.0005$), *PgLAS* (D, $P < 0.0005$), *PgCYP701* (C, $P < 0.0005$), and *PgCYP720B4* (E, $P < 0.0005$). Differences between time points are not considered, mean transcript abundances reflect all time points per sample and treatment type. Error bars represent the standard error of the mean and different letters indicate significantly different means separated by the Kruskal-Wallis test statistic ($\alpha = 0.05$). Sample types are as follows: bark/phloem (B), wood/xylem (X), young needles (YN), mature needles (MN), young stems (YS). Transcript abundance was measured by real-time qPCR, normalized to reference genes *eIF4E* and *H3*.

PgCPS transcript levels were found to differ significantly with the interaction of sample, treatment and time ($P < 0.0005$). To further elucidate these interactions data was separated into sample types and significance was analyzed between the interaction of treatment and time within each sample type (Figure 3.25). No significant difference was observed in the interaction between treatment type and time in YN ($P = 0.100$) and X ($P = 0.239$) samples. Significant differences were observed from the interactions of treatment and time in MN ($P = 0.001$), B ($P < 0.0005$) and YS ($P = 0.009$) samples (Table 3.8).

Within the MN sample type, *PgCPS* transcript levels in control (Tween-treated) were significantly higher than in MeJA from days 2 to 8 but values for days 16 and 30 were not statistically different between treatment types (Figure 3.25B; Table 3.9). *PgCPS* transcripts for MeJA-treated trees rose significantly over the time course by approximately 4-fold to a peak at day 16. Although the figure suggests differently, *PgCPS* transcript levels, in control treatment, did not show a significant change over the time course.

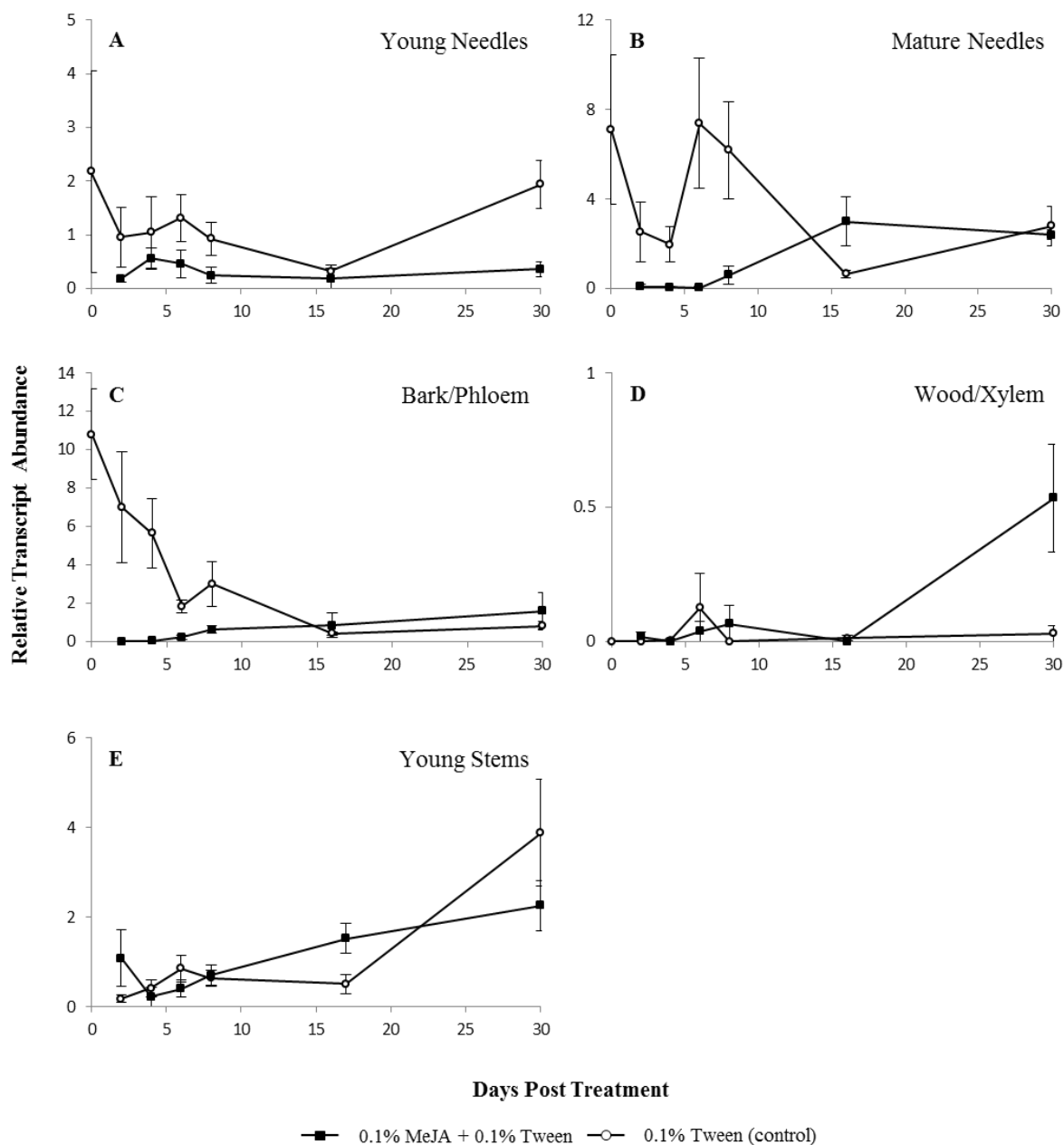


Figure 3.25. Relative transcript abundance of *PgCPS* in white spruce samples in response to MeJA treatment over a time course. Transcript abundance was measured by real-time qPCR, normalized to reference genes *eIF4E* and *H3*. Samples analyzed were: (A) young needles, (B) mature needles, (C) bark/phloem, (D) wood/xylem, (E) young stems. Data are means of 3-4 biological replicates at each time point; error bars represent standard error of the mean. Data was statistically analyzed and means were separated using Kruskal-Wallis test statistic ($\alpha=0.05$), see Table 3.9.

Table 3.9. Relative transcript abundance of *PgCPS* in control or MeJA-treated samples from white spruce. Contents are expressed as relative transcript abundance to reference genes *eIF4E* and *H3* (\pm SEM). Different letters within control and MeJA columns indicate significantly different means separated by the Kruskal-Wallis test statistic ($\alpha=0.05$); p-values indicate significance of interaction between time and treatment at each sample type.

Gene of Interest	Sample	Day	Control	MeJA
<i>PgCPS</i>	Young Needles ($P=0.100$)	0	2.184 \pm 1.879	
		2	0.959 \pm 0.559	0.178 \pm 0.062
		4	1.044 \pm 0.670	0.561 \pm 0.195
		6	1.312 \pm 0.439	0.458 \pm 0.264
		8	0.924 \pm 0.306	0.240 \pm 0.147
		16	0.319 \pm 0.127	0.184 \pm 0.184
		30	1.940 \pm 0.442	0.362 \pm 0.143
	Mature Needles ($P=0.001$)	0	7.096 \pm 3.351 <i>a</i>	
		2	2.536 \pm 1.329 <i>ab</i>	0.085 \pm 0.085 <i>cd</i>
		4	1.962 \pm 0.785 <i>abc</i>	0.053 \pm 0.053 <i>d</i>
		6	7.382 \pm 2.912 <i>a</i>	0.038 \pm 0.038 <i>d</i>
		8	6.176 \pm 2.178 <i>a</i>	0.597 \pm 0.395 <i>bcd</i>
		16	0.660 \pm 0.171 <i>abcd</i>	3.000 \pm 1.088 <i>ab</i>
		30	2.792 \pm 0.869 <i>ab</i>	2.402 \pm 0.220 <i>ab</i>
	Bark/Phloem ($P<0.0005$)	0	10.811 \pm 2.371 <i>a</i>	
		2	7.017 \pm 2.877 <i>ab</i>	0.000 \pm 0.000 <i>f</i>
		4	5.651 \pm 1.813 <i>ab</i>	0.028 \pm 0.028 <i>ef</i>
		6	1.849 \pm 0.355 <i>abcd</i>	0.222 \pm 0.088 <i>def</i>
		8	3.009 \pm 1.154 <i>abc</i>	0.636 \pm 0.195 <i>bcdef</i>
		16	0.416 \pm 0.101 <i>cdef</i>	0.847 \pm 0.651 <i>cdef</i>
		30	0.824 \pm 0.219 <i>bcde</i>	1.600 \pm 0.959 <i>abcd</i>
	Wood/Xylem ($P=0.239$)	0	0.000 \pm 0.000	
		2	0.000 \pm 0.000	0.019 \pm 0.019
		4	0.005 \pm 0.005	0.000 \pm 0.000
		6	0.126 \pm 0.126	0.038 \pm 0.038
		8	0.000 \pm 0.000	0.067 \pm 0.067
		16	0.013 \pm 0.009	0.000 \pm 0.000
		30	0.030 \pm 0.030	0.536 \pm 0.201
	Young Stems ($P=0.009$)	2	0.176 \pm 0.082 <i>c</i>	1.083 \pm 0.627 <i>abc</i>
		4	0.405 \pm 0.188 <i>c</i>	0.217 \pm 0.217 <i>c</i>
		6	0.847 \pm 0.288 <i>abc</i>	0.400 \pm 0.189 <i>c</i>
		8	0.640 \pm 0.159 <i>abc</i>	0.698 \pm 0.236 <i>abc</i>
		16	0.503 \pm 0.213 <i>bc</i>	1.524 \pm 0.335 <i>ab</i>
		30	3.880 \pm 1.195 <i>a</i>	2.253 \pm 0.569 <i>a</i>

In the B sample type, *PgCPS* transcript levels were highest at day 0 in the control treatment, after which transcript levels fell significantly by over 10-fold by day 30 (Figure 3.25C; Table 3.9). Transcript levels in the MeJA treatment remained relatively constant at very low levels over time, only rising significantly at day 30. Times where controls were significantly higher than in the MeJA treatment were days 2 and 4; while the later days (6, 8, 16 and 30) showed no difference between control and MeJA treatment.

In YS, *PgCPS* transcript levels remained relatively low in both control and MeJA samples over time (Figure 3.25E). Transcripts in both treatment types, however, rose significantly to their highest levels by day 30 in YS (Table 3.9). Comparing between treatment types, there were no specific days that showed a significant difference between control and MeJA treatments.

PgKS

Combining data for all 5 sample types, transcript abundance levels of *PgKS* were found to differ significantly by factors of sample type (Kruskal-Wallis, $P=0.005$), treatment type ($P<0.0005$), and time ($P<0.0005$). Interactions between all factors were found to have a significant effect on *PgKS* transcript levels: sample x treatment ($P<0.0005$), sample x time ($P=0.028$), treatment x time ($P<0.0005$) and sample x treatment x time ($P<0.0005$) (Table 3.8).

PgKS transcript levels were found to differ significantly due to the interaction between sample and treatment factors ($P<0.0005$) (Figure 3.24B). In this analysis the difference between time points was not considered. MeJA treatment in YN, X, YS and B had

the highest mean transcript abundances (4.904 ± 1.022 , 4.851 ± 0.853 , 4.788 ± 0.487 and 3.525 ± 0.364 , respectively); all of the means were significantly higher than their control counterparts (0.572 ± 0.063 , 0.292 ± 0.036 , 0.897 ± 0.161 , 0.476 ± 0.053 , respectively). The MN sample type also had a significant difference between the means of its treatment types, with MeJA treatment having higher transcript abundance than control (1.854 ± 0.238 and 0.490 ± 0.079 , respectively). In general all MeJA-treated sample had significantly higher mean *PgKS* transcript abundances than any control sample.

PgKS transcript levels were found to differ significantly with the interaction of sample, treatment and time ($P < 0.0005$). To further elucidate these interactions data was separated into sample types and significance was analyzed between the interaction of treatment and time within each sample type (Figure 3.26). In all samples, significant differences were observed from the interactions of treatment and time in YN ($P < 0.0005$), MN ($P < 0.0005$), B ($P < 0.0005$), X ($P < 0.0005$), YS ($P < 0.0005$) (Table 3.8).

In the YN sample type, *PgKS* transcripts showed a significant difference over time and treatment type ($P < 0.0005$) (Figure 3.26A). Transcript levels in the MeJA treatment were, for the most part, significantly higher than those in control (Table 3.10). A peak in MeJA treatment transcript levels was reached at day 6 with transcript levels 14-fold higher than the control counterpart. However, due to wide variation at selected sampling points, *PgKS* transcript levels in MeJA-treated YN were not significantly different over the entire time course. *PgKS* transcript levels in the control treatment remained relatively constant at low levels over the time course.

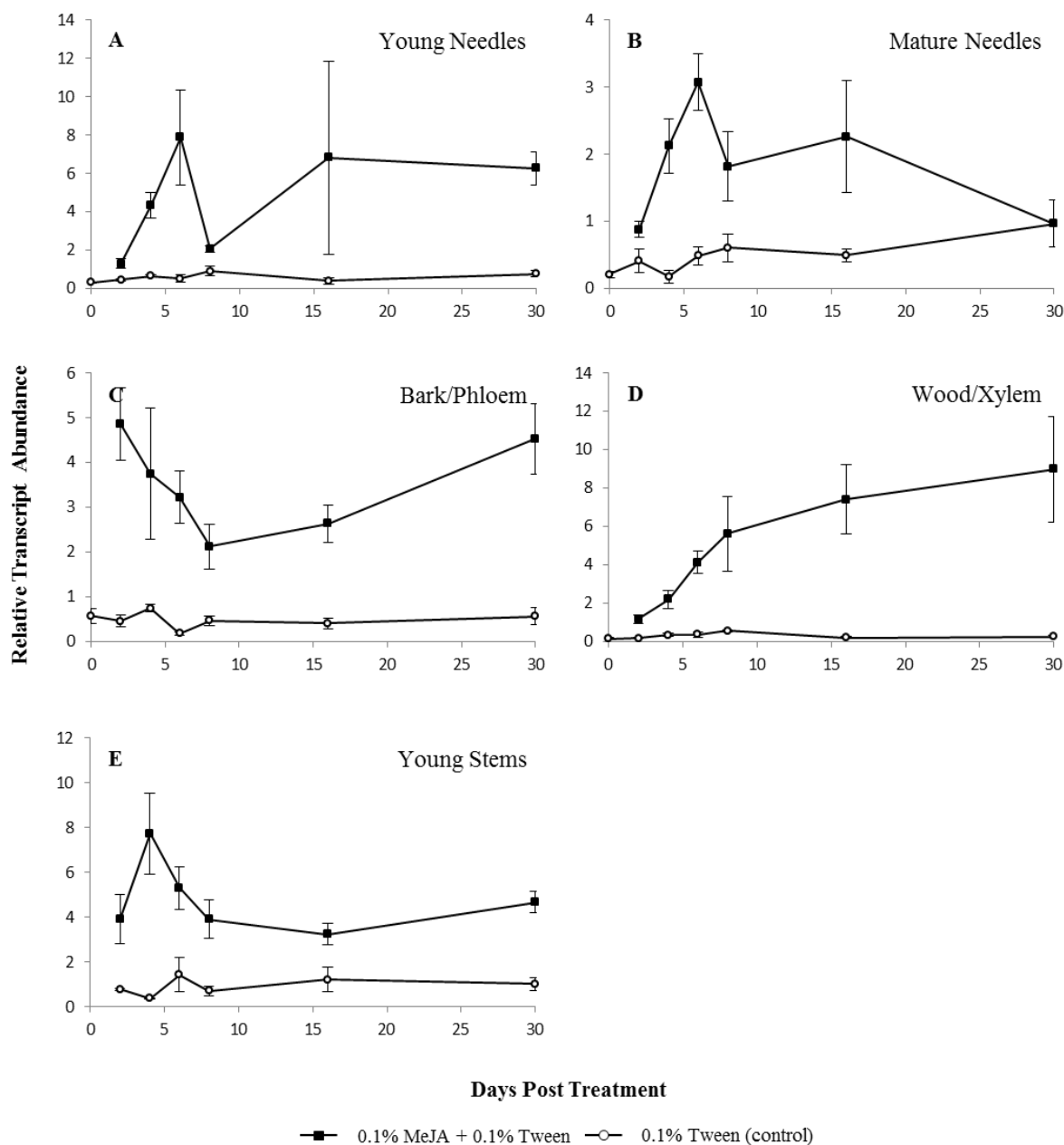


Figure 3.26. Relative transcript abundance of *PgKS* in white spruce samples in response to MeJA treatment over a time course. Transcript abundance was measured by real-time qPCR, normalized to reference genes *eIF4E* and *H3*. Samples analyzed were: (A) young needles, (B) mature needles, (C) bark/phloem, (D) wood/xylem, (E) young stems. Data are means of 3-4 biological replicates at each time point; error bars represent standard error of the mean. Data was statistically analyzed and means were separated using Kruskal-Wallis test statistic ($\alpha=0.05$), see Table 3.10.

Table 3.10. Relative transcript abundance of *PgKS* in control or MeJA-treated samples from white spruce. Contents are expressed as relative transcript abundance to reference genes *eIF4E* and *H3* (\pm SEM). Different letters within control and MeJA columns indicate significantly different means separated by the Kruskal-Wallis test statistic ($\alpha=0.05$); p-values indicate significance of interaction between time and treatment at each sample type.

Gene of Interest	Sample	Day	Control	MeJA
<i>PgKS</i>	Young Needles ($P<0.0005$)	0	0.305 \pm 0.045 <i>f</i>	
		2	0.448 \pm 0.073 <i>ef</i>	1.300 \pm 0.254 <i>abcde</i>
		4	0.663 \pm 0.080 <i>cdef</i>	4.363 \pm 0.667 <i>ab</i>
		6	0.524 \pm 0.176 <i>def</i>	7.886 \pm 2.490 <i>a</i>
		8	0.914 \pm 0.227 <i>bcdef</i>	2.075 \pm 0.172 <i>abcd</i>
		16	0.387 \pm 0.193 <i>ef</i>	6.822 \pm 5.029 <i>abc</i>
		30	0.769 \pm 0.149 <i>bcdef</i>	6.274 \pm 0.861 <i>a</i>
	Mature Needles ($P<0.0005$)	0	0.213 \pm 0.048 <i>de</i>	
		2	0.411 \pm 0.179 <i>cde</i>	0.879 \pm 0.120 <i>abc</i>
		4	0.178 \pm 0.094 <i>e</i>	2.124 \pm 0.411 <i>a</i>
		6	0.489 \pm 0.134 <i>bcde</i>	3.075 \pm 0.426 <i>a</i>
		8	0.605 \pm 0.211 <i>bcde</i>	1.818 \pm 0.511 <i>ab</i>
		16	0.492 \pm 0.092 <i>bcde</i>	2.262 \pm 0.832 <i>a</i>
		30	0.964 \pm 0.348 <i>abcd</i>	0.964 \pm 0.348 <i>abcd</i>
	Bark/Phloem ($P<0.0005$)	0	0.572 \pm 0.169 <i>bc</i>	
		2	0.462 \pm 0.133 <i>bc</i>	4.860 \pm 0.816 <i>a</i>
		4	0.749 \pm 0.075 <i>abc</i>	3.754 \pm 1.474 <i>a</i>
		6	0.181 \pm 0.039 <i>c</i>	3.227 \pm 0.586 <i>a</i>
		8	0.465 \pm 0.103 <i>bc</i>	2.128 \pm 0.506 <i>ab</i>
		16	0.405 \pm 0.116 <i>bc</i>	2.634 \pm 0.409 <i>a</i>
		30	0.568 \pm 0.186 <i>bc</i>	4.536 \pm 0.783 <i>a</i>
	Wood/Xylem ($P<0.0005$)	0	0.146 \pm 0.054 <i>c</i>	
		2	0.186 \pm 0.036 <i>c</i>	1.172 \pm 0.219 <i>ab</i>
		4	0.347 \pm 0.095 <i>bc</i>	2.213 \pm 0.470 <i>ab</i>
		6	0.379 \pm 0.133 <i>bc</i>	4.134 \pm 0.587 <i>a</i>
		8	0.554 \pm 0.064 <i>abc</i>	5.628 \pm 1.961 <i>a</i>
		16	0.215 \pm 0.074 <i>c</i>	7.420 \pm 1.794 <i>a</i>
		30	0.274 \pm 0.031 <i>bc</i>	9.005 \pm 2.755 <i>a</i>
	Young Stems ($P<0.0005$)	2	0.767 \pm 0.050 <i>bc</i>	3.897 \pm 1.109 <i>ab</i>
		4	0.356 \pm 0.042 <i>c</i>	7.727 \pm 1.822 <i>a</i>
		6	1.426 \pm 0.745 <i>bc</i>	5.293 \pm 0.939 <i>a</i>
		8	0.699 \pm 0.222 <i>c</i>	3.908 \pm 0.842 <i>ab</i>
		16	1.198 \pm 0.555 <i>bc</i>	3.233 \pm 0.480 <i>ab</i>
		30	1.012 \pm 0.292 <i>bc</i>	4.668 \pm 0.476 <i>a</i>

Within the MN sample type, *PgKS* transcript levels in the MeJA treatment were significantly higher than those in the control treatment over three time points (Figure 3.26B; Table 3.10); on these days (4, 6 and 16) transcript levels in the MeJA treatment were 12-fold, 6-fold and 4.5-fold higher, respectively, than controls. *PgKS* transcript levels in the control treatment remained stable over the time course, with only a statistically significant difference between days 4 and 30.

In B sample type, *PgKS* transcript levels in MeJA-treated samples were, for the majority, significantly higher than those in the control; only day 8 was not significantly different from its control counterpart (Figure 3.26C; Table 3.10). Over the time course, MeJA-treated transcript levels were between 5- and over 15-fold higher than controls. *PgKS* transcript levels in the controls remained constant at relatively low levels over the time course, with no statistical difference over time.

Over time, within the X sample type, *PgKS* transcript levels were significantly higher in MeJA-treated samples than control (Figure 3.26D; Table 3.10). Transcript levels in control samples remained constant over the time course at low levels, as was also seen in other sample types. MeJA treatment showed an over 8-fold increase in transcript levels from days 2 to 30; although these levels were significantly higher than controls they did not indicate a significant increase within the MeJA treatment.

In YS for the majority of time points, *PgKS* transcript levels were higher in MeJA-treated samples than control samples (Figure 3.26E). Transcript levels in the control treatment remained relatively constant at low levels. *PgKS* transcript abundance in MeJA-treated samples peaked at day 4, representing a 20-fold increase over control, however

overall there was no statistical difference in transcript levels between MeJA-treated time points.

PgLAS

Combining data for all 5 sample types, transcript abundance levels of *PgLAS* were found to differ significantly by factors of sample type (Kruskal-Wallis, $P<0.0005$), treatment type ($P<0.0005$), but not time ($P=0.056$). Interactions between all factors were found to have a significant effect on *PgLAS* transcript levels: sample x treatment ($P<0.0005$), sample x time ($P<0.0005$), treatment x time ($P<0.0005$) and sample x treatment x time ($P<0.0005$) (Table 3.8).

PgLAS transcript levels were found to differ significantly due to the interaction between sample and treatment factors ($P<0.0005$) (Figure 3.24D). In this analysis the difference between time points was not considered. MeJA-treated samples of X, B and YS had the highest mean transcript abundances (43.016 ± 12.308 , 30.091 ± 3.038 , 27.408 ± 5.215 , respectively), however only X and B samples had mean transcript abundances that were significantly higher than their control counterparts (0.634 ± 0.167 , 3.529 ± 0.672 respectively). MN, YN and control X samples had the lowest mean transcript abundances overall, with the means of control and MeJA treatment in MN and YN being at near zero levels (near the detection limit).

PgLAS transcript levels were found to differ significantly with the interaction of sample, treatment and time ($P<0.0005$). To further elucidate these interactions data was separated into sample types and significance was analyzed between the interaction of

treatment and time within each sample type (Figure 3.27). In all sample types, the interaction between treatment type and time caused a significant difference in *PgLAS* transcript abundance, YN ($P<0.0005$), MN ($P=0.029$), B ($P<0.0005$), X ($P<0.0005$), YS ($P=0.002$) (Table 3.8).

In the YN sample type, *PgLAS* transcripts in the MeJA treatment declined significantly by over 15-fold from a peak at day 4 to near zero levels at days 16 and 30 (Figure 3.27A; Table 3.11). Transcript levels in the MeJA treatment group were significantly higher than the control treatment at their peak at day 4. *PgLAS* transcripts in control samples were consistently low over time, with only day 2 being statistically different than the lowest transcript levels at days 16 and 30.

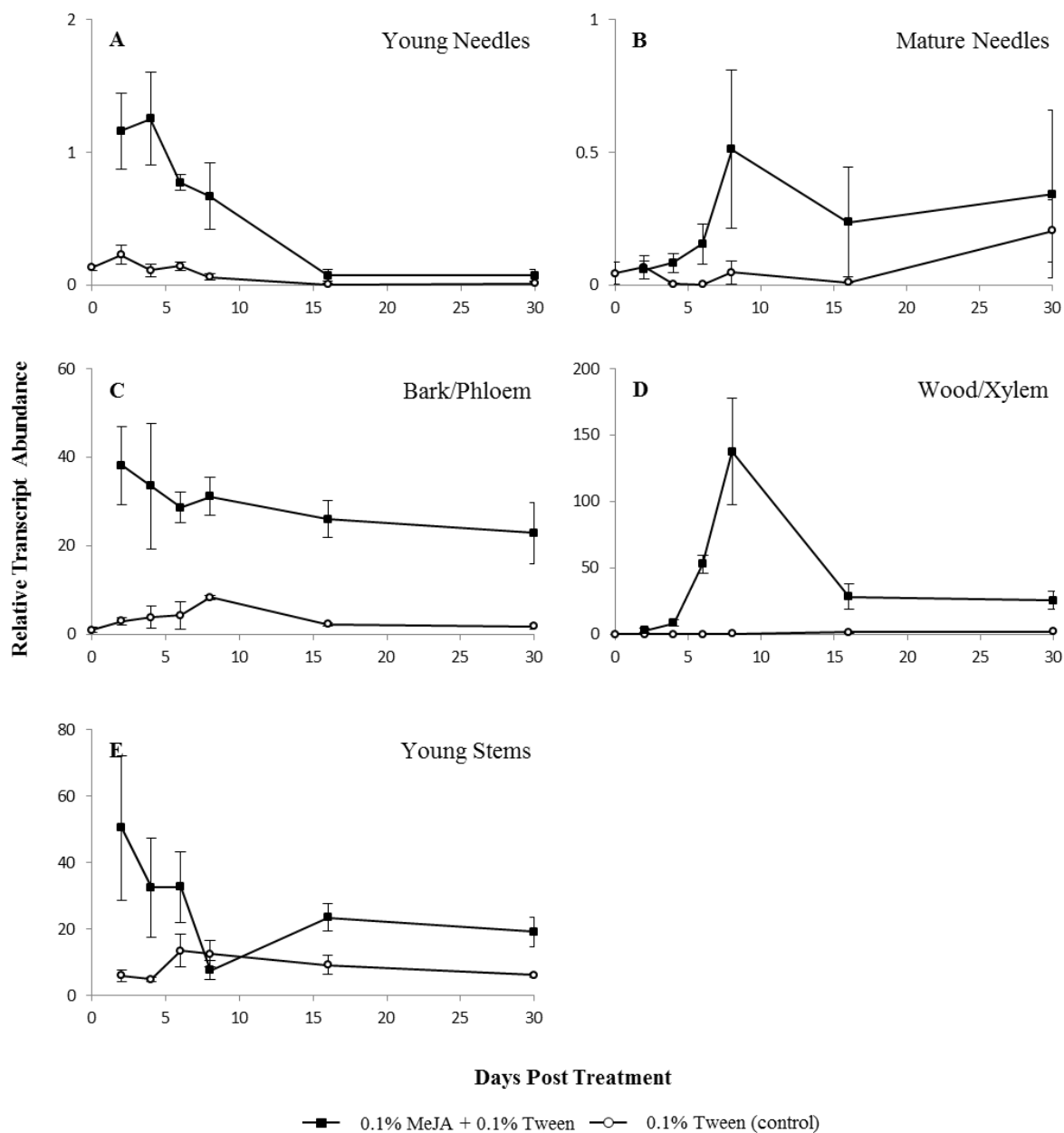


Figure 3.27. Relative transcript abundance of *PgLAS* in white spruce samples in response to MeJA treatment over a time course. Transcript abundance was measured by real-time qPCR, normalized to reference genes *eIF4E* and *H3*. Samples analyzed were: (A) young needles, (B) mature needles, (C) bark/phloem, (D) wood/xylem, (E) young stems. Data are means of 3-4 biological replicates at each time point; error bars represent standard error of the mean. Data was statistically analyzed and means were separated using Kruskal-Wallis test statistic ($\alpha=0.05$), see Table 3.11.

Table 3.11. Relative transcript abundance of *PgLAS* in control or MeJA-treated samples from white spruce. Contents are expressed as relative transcript abundance to reference genes *eIF4E* and *H3* (\pm SEM). Different letters within control and MeJA columns indicate significantly different means separated by the Kruskal-Wallis test statistic ($\alpha=0.05$); p-values indicate significance of interaction between time and treatment at each sample type.

Gene of Interest	Sample	Day	Control	MeJA
<i>PgLAS</i>	Young Needles ($P<0.0005$)	0	0.131 \pm 0.021 <i>cde</i>	
		2	0.228 \pm 0.071 <i>abcd</i>	1.161 \pm 0.286 <i>ab</i>
		4	0.112 \pm 0.051 <i>cde</i>	1.254 \pm 0.352 <i>a</i>
		6	0.144 \pm 0.030 <i>bcde</i>	0.774 \pm 0.058 <i>ab</i>
		8	0.061 \pm 0.023 <i>de</i>	0.669 \pm 0.249 <i>abc</i>
		16	0.006 \pm 0.006 <i>e</i>	0.074 \pm 0.047 <i>de</i>
		30	0.012 \pm 0.011 <i>e</i>	0.074 \pm 0.043 <i>de</i>
	Mature Needles ($P=0.029$)	0	0.045 \pm 0.043 <i>bcd</i>	
		2	0.068 \pm 0.045 <i>abcd</i>	0.058 \pm 0.034 <i>abc</i>
		4	0.005 \pm 0.002 <i>cd</i>	0.084 \pm 0.037 <i>ab</i>
		6	0.003 \pm 0.002 <i>d</i>	0.155 \pm 0.076 <i>ab</i>
		8	0.049 \pm 0.044 <i>bcd</i>	0.511 \pm 0.298 <i>a</i>
		16	0.010 \pm 0.002 <i>bcd</i>	0.238 \pm 0.208 <i>abc</i>
		30	0.205 \pm 0.118 <i>ab</i>	0.343 \pm 0.317 <i>abc</i>
	Bark/Phloem ($P<0.0005$)	0	1.055 \pm 0.556 <i>c</i>	
		2	3.027 \pm 0.892 <i>bc</i>	38.183 \pm 8.774 <i>a</i>
		4	3.810 \pm 2.511 <i>bc</i>	33.535 \pm 14.188 <i>a</i>
		6	4.378 \pm 3.095 <i>bc</i>	28.677 \pm 3.524 <i>a</i>
		8	8.444 \pm 0.480 <i>abc</i>	31.205 \pm 4.212 <i>a</i>
		16	2.292 \pm 0.351 <i>bc</i>	26.047 \pm 4.160 <i>a</i>
		30	1.776 \pm 0.497 <i>c</i>	22.894 \pm 7.021 <i>ab</i>
	Wood/Xylem ($P<0.0005$)	0	0.028 \pm 0.027 <i>d</i>	
		2	0.209 \pm 0.206 <i>d</i>	3.117 \pm 1.278 <i>bcd</i>
		4	0.188 \pm 0.140 <i>d</i>	8.654 \pm 2.369 <i>abc</i>
		6	0.306 \pm 0.243 <i>d</i>	53.086 \pm 6.630 <i>ab</i>
		8	0.544 \pm 0.341 <i>cd</i>	137.885 \pm 40.136 <i>a</i>
		16	1.550 \pm 0.473 <i>bcd</i>	28.477 \pm 9.450 <i>ab</i>
		30	1.987 \pm 0.398 <i>bcd</i>	25.766 \pm 6.794 <i>ab</i>
	Young Stems ($P=0.002$)	2	5.869 \pm 1.596 <i>c</i>	50.425 \pm 21.671 <i>a</i>
		4	4.831 \pm 0.702 <i>c</i>	32.478 \pm 14.942 <i>ab</i>
		6	13.487 \pm 4.846 <i>abc</i>	32.613 \pm 10.765 <i>ab</i>
		8	12.432 \pm 3.974 <i>abc</i>	7.559 \pm 2.817 <i>c</i>
		16	9.175 \pm 2.862 <i>bc</i>	23.462 \pm 4.168 <i>ab</i>
		30	6.029 \pm 0.533 <i>c</i>	19.211 \pm 4.441 <i>ab</i>

Within the MN sample type, *PgLAS* transcript levels in the MeJA treatment, for the majority, were significantly higher than those in the control treatment (Figure 3.27B; Table 3.11). Transcript abundance in MeJA samples reached a peak at day 8, while in control, transcripts reached their peak later in the time course, at day 30.

In B, *PgLAS* transcript levels were, for the majority, significantly higher in the MeJA treatment than in control (Figure 3.27C; Table 3.11). MeJA-treated sample transcript levels did not change significantly over time; they were consistently high throughout the entire time course. *PgLAS* transcript abundance in control treatment was low over the time course. While transcript levels peaked at day 8, this did not amount to a significant change. Comparing between treatment types, over the time course MeJA-treated *PgLAS* transcripts were between approximately 7- to 13-fold higher than that of control, with the exception of day 8 where control sample transcripts levels were no longer significantly different than MeJA.

In the X sample type, treatment with MeJA resulted in *PgLAS* transcript levels that were significantly higher than that of control from day 4 onwards (Figure 3.27D; Table 3.11). Transcript levels reached a peak at day 8 in MeJA-treated samples, which was an over 40-fold increase from day 2. Control transcript levels were low and did not change significantly over the time course.

In YS, *PgLAS* transcript levels were found to differ significantly over time and between treatment type ($P=0.002$) (Figure 3.27E; Table 3.11). In MeJA-treated YS, transcript levels were at their peak at the beginning of the time course, day 2, after which levels dropped significantly by approximately 6-fold by day 8; from this drop to the end of

the time course, transcript abundance rose approximately 2.5-fold and returned to a steady level by day 16 to 30. Control transcript levels remained constant over time; a slight rise was indicated at days 6 and 8 but this was not a significant change. Comparison between control and MeJA-treated transcript levels showed significant differences at days 2, 4, and 30. At the early time points MeJA-treated transcript levels were between approximately 7-fold to 9-fold higher than those in control and similarly at the end of the time course MeJA-treated transcript levels had rebounded to be over 3-fold higher than their control counterpart.

PgCYP701

Combining data for all 5 sample types, transcript abundance levels of *PgCYP701* were found to differ significantly by factors of sample type (Kruskal-Wallis, $P<0.0005$) treatment type ($P<0.0005$), and time ($P=0.012$). Interactions between all factors were found to have a significant effect on *PgCYP701* transcript levels: sample x treatment ($P<0.0005$), sample x time ($P<0.0005$), treatment x time ($P<0.0005$) and sample x treatment x time ($P<0.0005$) (Table 3.8).

PgCYP701 transcript levels were found to differ significantly due to the interaction between sample and treatment factors ($P<0.0005$) (Figure 3.24C). In this analysis the difference between time points was not considered. Control B sample had the highest mean transcript abundance (3.046 ± 0.406), while MeJA-treated MN had the lowest mean transcript abundance (0.343 ± 0.080). Only one sample type, MN, showed a significant difference between treatment types, the mean relative transcript abundance in the control treatment here is 6-fold higher than MeJA.

PgCYP701 transcript levels were found to differ significantly with the interaction of sample, treatment and time ($P < 0.0005$). To further elucidate these interactions data was separated into sample types and significance was analyzed between the interaction of treatment and time within each sample type (Figure 3.28). In all sample types, the interaction between treatment type and time caused a significant difference in *PgCYP701* transcript abundance, YN ($P = 0.005$), MN ($P < 0.0005$), B ($P = 0.036$), X ($P = 0.003$), YS ($P = 0.010$) (Table 3.8).

In the YN sample type, day 30 of the MeJA treatment had the highest *PgCYP701* transcript abundance (control transcript value at this time point was not significantly different), while days 2, 4 and 8 of MeJA-treated sample and time point 16 of control sample had the lowest (Figure 3.28A; Table 3.12). Comparing the control and MeJA-treated time points, transcript levels in the MeJA treatment were significantly lower at day 4 only. Over the time course within the control treatment there was no significant difference between the majority of sampled time points, with the notable exception of the dip down at day 16. Transcript levels in MeJA-treated YN samples rose significantly over the time course, again with exception of day 16 which mirrors that of control.

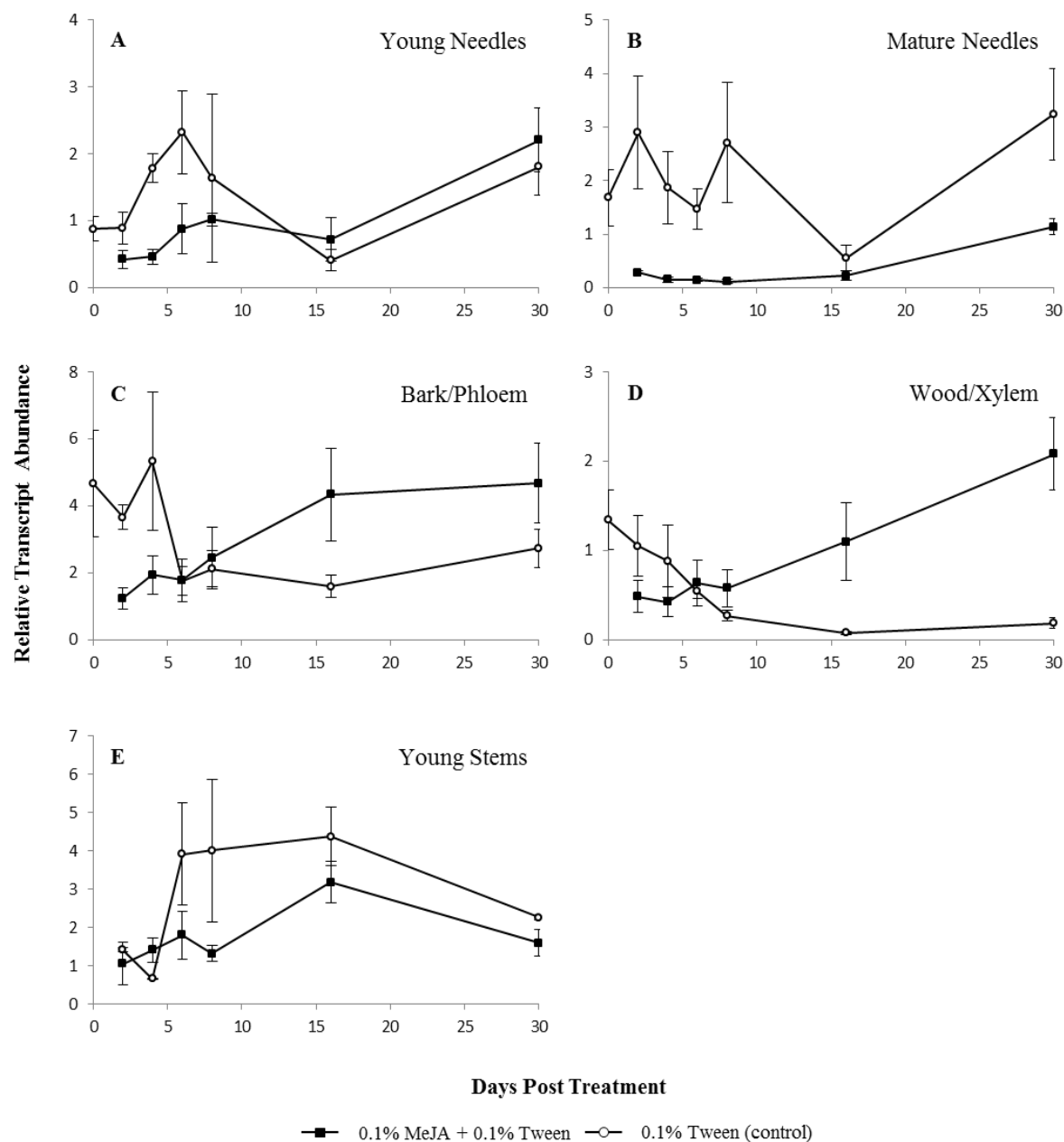


Figure 3.28. Relative transcript abundance of *PgCYP701* in white spruce samples in response to MeJA treatment over a time course. Transcript abundance was measured by real-time qPCR, normalized to reference genes *eIF4E* and *H3*. Samples analyzed were: (A) young needles, (B) mature needles, (C) bark/phloem, (D) wood/xylem, (E) young stems. Data are means of 3-4 biological replicates at each time point; error bars represent standard error of the mean. Data was statistically analyzed and means were separated using Kruskal-Wallis test statistic ($\alpha=0.05$), see Table 3.12.

Table 3.12. Relative transcript abundance of *PgCYP701* in control or MeJA-treated samples from white spruce. Contents are expressed as relative transcript abundance to reference genes *eIF4E* and *H3* (\pm SEM). Different letters within control and MeJA columns indicate significantly different means separated by the Kruskal-Wallis test statistic ($\alpha=0.05$); p-values indicate significance of interaction between time and treatment at each sample type.

Gene of Interest	Sample	Day	Control	MeJA
<i>PgCYP701</i>	Young Needles ($P=0.005$)	0	0.880 \pm 0.183 <i>abc</i>	
		2	0.894 \pm 0.235 <i>abc</i>	0.422 \pm 0.131 <i>c</i>
		4	1.784 \pm 0.212 <i>ab</i>	0.466 \pm 0.113 <i>c</i>
		6	2.325 \pm 0.623 <i>ab</i>	0.881 \pm 0.377 <i>abc</i>
		8	1.637 \pm 1.258 <i>abc</i>	1.018 \pm 0.098 <i>c</i>
		16	0.407 \pm 0.158 <i>c</i>	0.722 \pm 0.321 <i>bc</i>
		30	1.807 \pm 0.429 <i>ab</i>	2.205 \pm 0.475 <i>a</i>
	Mature Needles ($P<0.0005$)	0	1.685 \pm 0.525 <i>abc</i>	
		2	2.900 \pm 1.050 <i>ab</i>	0.287 \pm 0.023 <i>cd</i>
		4	1.870 \pm 0.676 <i>abc</i>	0.149 \pm 0.052 <i>d</i>
		6	1.465 \pm 0.380 <i>abc</i>	0.140 \pm 0.031 <i>d</i>
		8	2.704 \pm 1.123 <i>abc</i>	0.118 \pm 0.031 <i>d</i>
		16	0.548 \pm 0.240 <i>bcd</i>	0.225 \pm 0.088 <i>d</i>
		30	3.243 \pm 0.857 <i>a</i>	1.135 \pm 0.150 <i>abc</i>
	Bark/Phloem ($P=0.036$)	0	4.679 \pm 1.591 <i>ab</i>	
		2	3.659 \pm 0.362 <i>ab</i>	1.240 \pm 0.325 <i>c</i>
		4	5.336 \pm 2.073 <i>a</i>	1.942 \pm 0.563 <i>bc</i>
		6	1.768 \pm 0.437 <i>abc</i>	1.791 \pm 0.634 <i>abc</i>
		8	2.125 \pm 0.551 <i>abc</i>	2.450 \pm 0.909 <i>abc</i>
		16	1.595 \pm 0.337 <i>c</i>	4.351 \pm 1.382 <i>ab</i>
		30	2.734 \pm 0.563 <i>abc</i>	4.682 \pm 1.193 <i>a</i>
	Wood/Xylem ($P=0.003$)	0	1.342 \pm 0.333 <i>ab</i>	
		2	1.054 \pm 0.339 <i>abc</i>	0.485 \pm 0.181 <i>bcde</i>
		4	0.883 \pm 0.408 <i>abcd</i>	0.426 \pm 0.168 <i>cde</i>
		6	0.546 \pm 0.083 <i>abcd</i>	0.640 \pm 0.257 <i>abcd</i>
		8	0.271 \pm 0.059 <i>cde</i>	0.581 \pm 0.210 <i>bcd</i>
		16	0.079 \pm 0.018 <i>e</i>	1.101 \pm 0.439 <i>abc</i>
		30	0.186 \pm 0.059 <i>de</i>	2.085 \pm 0.407 <i>a</i>
	Young Stems ($P=0.010$)	2	1.410 \pm 0.055 <i>bcd</i>	1.052 \pm 0.553 <i>cd</i>
		4	0.654 \pm 0.015 <i>d</i>	1.405 \pm 0.312 <i>bcd</i>
		6	3.916 \pm 1.332 <i>ab</i>	1.794 \pm 0.634 <i>bcd</i>
		8	4.007 \pm 1.866 <i>ab</i>	1.320 \pm 0.206 <i>bcd</i>
		16	4.380 \pm 0.759 <i>a</i>	3.183 \pm 0.534 <i>ab</i>
		30	2.255 \pm 0.052 <i>abc</i>	1.590 \pm 0.348 <i>bcd</i>

In the MN sample type, *PgCYP701* transcripts showed a significant difference over time and treatment type ($P<0.0005$) (Figure 3.28B). *PgCYP701* transcript levels in both control and MeJA-treated samples remained relatively stable over the time course (although with greater variability in control), with transcript levels in the control treatment being significantly higher than MeJA until days 16 and 30 where transcript levels were no longer significantly different between treatment types (Table 3.12).

In the B sample type, *PgCYP701* transcript levels showed a significant difference over time and treatment type ($P=0.036$) (Figure 3.28C). Transcript levels in control did not change significantly over the time course, with the notable exception of a drop at day 16, which was significantly different from levels at days 0, 2 and 4. Transcript levels in MeJA samples showed a steady increase over the time course with day 2 having the lowest levels and 30 having the highest, however MeJA-treated transcript levels at day 30 were not different from those in control samples. Overall, days 2 and 4 of the control treatment were significantly higher than their MeJA counterparts, while these levels were reversed at day 16 where MeJA transcript levels were higher than those in control samples (Table 3.12).

In X, *PgCYP701* transcript levels in control and MeJA-treated samples showed a significant difference over time ($P=0.003$) and relatively opposite trends in transcript abundance over time (Figure 3.28D). *PgCYP701* transcript levels rose significantly over 4-fold in the MeJA treatment from day 2 to day 30, while transcript levels in control declined over 7-fold during the same period. The highest transcript levels in both control and MeJA samples were not significantly different from each other, as is the case with the lowest transcript levels of both treatments. Between control and MeJA samples at specific times, only days 16 and 30 were significantly different from each other (Table 3.12).

Within the YS sample type, *PgCYP701* transcript levels were significantly different over time and treatment type ($P=0.010$) (Figure 3.28E). Over the time course, transcript levels in both control and MeJA-treated YS samples reached a peak at day 16, representing a rise of over 3-fold, however they were not significantly different from each other. In both treatment types, transcript levels at day 16 were only significantly different from those at day 2, with levels in control also being different from day 4. After their peak at day 16, transcript levels in both treatment types fell by almost 2-fold by day 30 (Table 3.12).

PgCYP720B4

Combining data for all 5 sample types, transcript abundance levels of *PgCYP720B4* were found to differ significantly by factors of sample type ($P<0.0005$) and treatment type ($P<0.0005$), but not time ($P=0.139$). Interactions between all factors were found to have a significant effect on *PgCYP701* transcript levels: sample x treatment ($P<0.0005$), sample x time ($P<0.0005$), treatment x time ($P=0.007$) and sample x treatment x time ($P<0.0005$) (Table 3.8).

PgCYP720B4 transcript levels were found to differ significantly due to the interaction between sample and treatment factors ($P<0.0005$) (Figure 3.24E). In this analysis the difference between time points was not considered. MeJA-treated X samples had the highest mean transcript abundance (21.907 ± 5.345), which was statistically different from transcript levels in the control treatment (1.374 ± 0.492). *PgCYP720B4* transcript levels of MeJA-treated X samples were not different from levels in MeJA-treated B samples (9.296 ± 0.993) and MeJA and control YS samples (17.450 ± 2.398 and 7.473 ± 0.788 , respectively). The

lowest *PgCYP720B4* transcript levels were in control MN sample (0.045 ± 0.016), which were not statistically different from MN MeJA-treated sample (0.187 ± 0.087) and control YN sample (0.130 ± 0.021). Overall, only X showed a significant difference in *PgCYP720B4* transcript levels between treatment types.

PgCYP720B4 transcript levels were found to differ significantly with the interaction of sample, treatment and time ($P < 0.0005$). To further elucidate these interactions data was separated into sample types and significance was analyzed between the interaction of treatment and time within each sample type (Figure 3.29). In four sample types the interaction between treatment type and time caused a significant difference in *PgCYP720B4* transcript abundance, YN ($P < 0.0005$), MN ($P = 0.012$), X ($P < 0.0005$), YS ($P = 0.001$), B sample type showed no significant difference ($P = 0.072$); see Table 3.8 for detailed statistical analysis results.

In the YN sample type, *PgCYP720B4* transcript levels in both treatment types fell to near zero values (near detection limit) at days 16 and 30 (Figure 3.29A; Table 3.13). Similar trends were seen within both the MeJA and control transcript levels, where in both treatments values peaked at day 4 and fell significantly at the end of the time course (days 16 and 30), translating to an approximate 16-fold and 30-fold drop in transcript levels in control and MeJA samples, respectively. However, when comparing between the control and MeJA treatments, there were no time points where *PgCYP720B4* transcript levels were significantly different from one another.

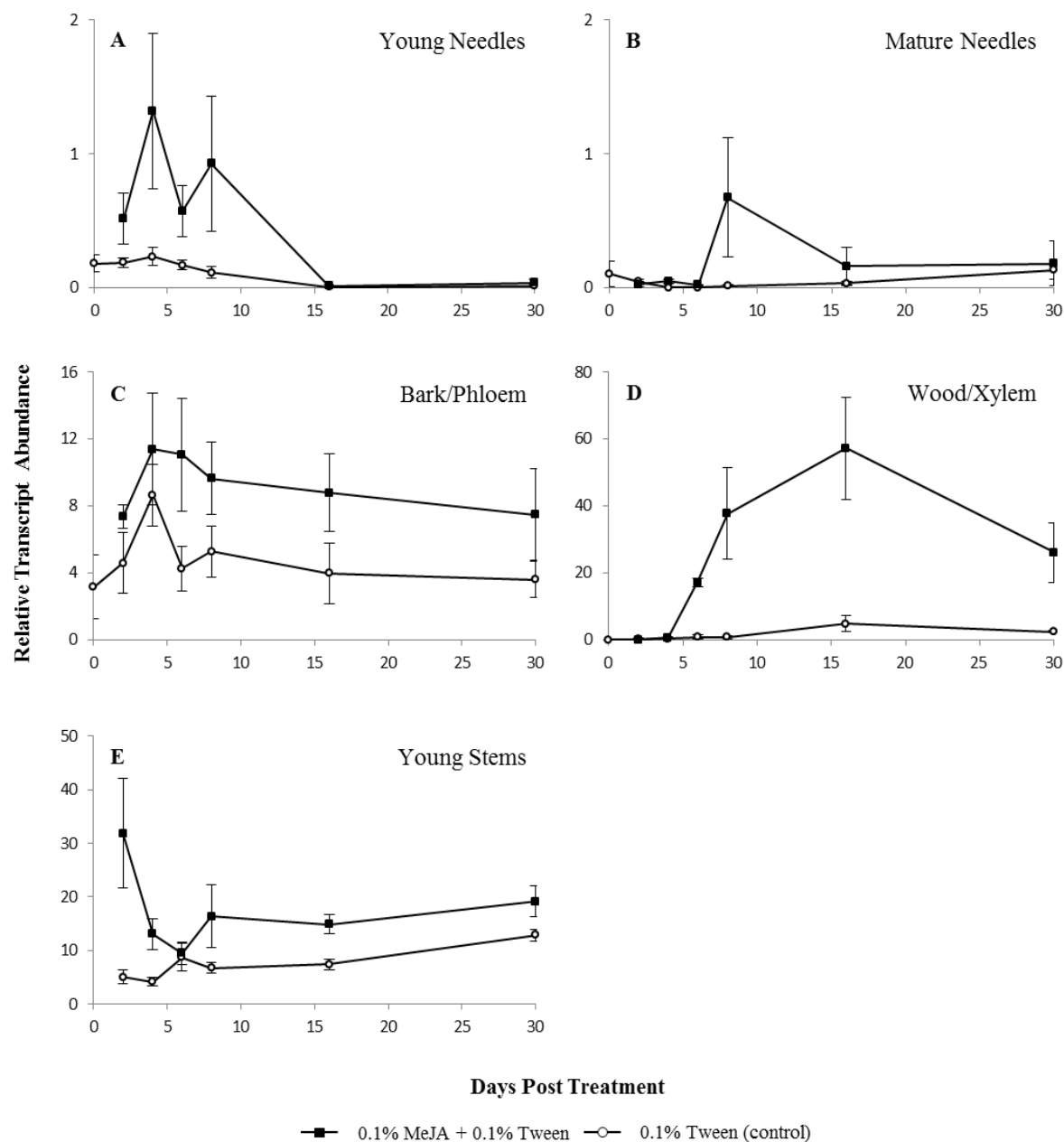


Figure 3.29. Relative transcript abundance of *PgCYP720B4* in white spruce samples in response to MeJA treatment over a time course. Transcript abundance was measured by real-time qPCR, normalized to reference genes *eIF4E* and *H3*. Samples analyzed were: (A) young needles, (B) mature needles, (C) bark/phloem, (D) wood/xylem, (E) young stems. Data are means of 3-4 biological replicates at each time point; error bars represent standard error of the mean. Data was statistically analyzed and means were separated using Kruskal-Wallis test statistic ($\alpha=0.05$), see Table 3.13.

Table 3.13. Relative transcript abundance of *PgCYP720B4* in control or MeJA-treated samples from white spruce. Contents are expressed as relative transcript abundance to reference genes *eIF4E* and *H3* (\pm SEM). Different letters within control and MeJA columns indicate significantly different means separated by the Kruskal-Wallis test statistic ($\alpha=0.05$); p-values indicate significance of interaction between time and treatment at each sample type.

Gene of Interest	Sample	Day	Control	MeJA
<i>PgCYP720B4</i>	Young Needles ($P<0.0005$)	0	0.182 \pm 0.064	<i>abcde</i>
		2	0.187 \pm 0.035	<i>abcd</i>
		4	0.231 \pm 0.067	<i>abc</i>
		6	0.170 \pm 0.033	<i>abcd</i>
		8	0.114 \pm 0.041	<i>bcde</i>
		16	0.006 \pm 0.005	<i>e</i>
		30	0.014 \pm 0.011	<i>de</i>
	Mature Needles ($P=0.012$)	0	0.104 \pm 0.098	<i>abc</i>
		2	0.045 \pm 0.020	<i>ab</i>
		4	0.000 \pm 0.000	<i>c</i>
		6	0.000 \pm 0.000	<i>c</i>
		8	0.013 \pm 0.013	<i>bc</i>
		16	0.032 \pm 0.012	<i>ab</i>
		30	0.134 \pm 0.070	<i>ab</i>
	Bark/Phloem ($P=0.072$)	0	3.167 \pm 1.893	
		2	4.602 \pm 1.813	7.365 \pm 0.687
		4	8.655 \pm 1.848	11.385 \pm 3.342
		6	4.284 \pm 1.331	11.069 \pm 3.354
		8	5.276 \pm 1.557	9.652 \pm 2.146
		16	3.974 \pm 1.828	8.801 \pm 2.311
		30	3.610 \pm 1.087	7.502 \pm 2.751
	Wood/Xylem ($P<0.0005$)	0	0.074 \pm 0.071	<i>f</i>
		2	0.257 \pm 0.254	<i>ef</i>
		4	0.324 \pm 0.246	<i>def</i>
		6	0.892 \pm 0.705	<i>cdef</i>
		8	0.864 \pm 0.435	<i>bcdef</i>
		16	4.902 \pm 2.535	<i>abcd</i>
		30	2.449 \pm 0.256	<i>abcde</i>
	Young Stems ($P=0.001$)	2	5.044 \pm 1.260	<i>d</i>
		4	4.121 \pm 0.778	<i>d</i>
		6	8.726 \pm 2.632	<i>bcd</i>
		8	6.733 \pm 1.062	<i>cd</i>
		16	7.358 \pm 1.046	<i>bcd</i>
		30	12.857 \pm 1.084	<i>abc</i>

In the MN sample type, *PgCYP720B4* transcripts remained at near zero levels in both the control and MeJA treatment (Figure 3.29B; Table 3.13). A significant difference in transcript levels between treatment types was seen as a peak at day 8, where MeJA-treated transcript levels were higher than their control counterparts.

In X samples, *PgCYP720B4* transcript levels in the control and MeJA treatment showed similar trends in transcript abundance over time, although on widely different scales (Figure 3.29D). *PgCYP720B4* transcript levels in MeJA-treated samples rose significantly over time; from days 2 to 16, transcript levels increased by over 400-fold. In control, transcript levels rose approximately 20-fold during the same time period. When comparing between treatments, a significant difference is seen at day 8, where transcript levels in MeJA-treated samples were over 40-fold higher than transcript levels in control samples.

Within the YS sample type, *PgCYP720B4* transcript levels were significantly different over time and treatment type ($P=0.001$) (Figure 3.29E). Over the time course, transcript levels in the MeJA treatment remained relatively stable, with a single significant drop at day 6. *PgCYP720B4* transcript levels in control rose over 2.5-fold over the length of the time course. Comparing between treatment types, only days 2 and 4 were significantly different from each other, where transcript levels in MeJA-treated samples were approximately 6-fold and 3-fold higher, respectively, than control; at later time points, transcript levels were no longer significantly different between treatments.

3.3. Discussion

This chapter provides an analysis of the white spruce diTPSs and CYP450s involved in GA and DRA biosynthesis, representing growth and defense centric pathways, respectively. The work compares and contrasts gene function and expression with respect to different sample types, treatments and times across the seasonal cycle of spruce development.

Two diTPSs, *PsCPS* and *PsKS*, were cloned and characterized from Sitka spruce (*Picea sitchensis*); this work was important to fill a knowledge gap in this species. *PsCPS* and *PsKS* showed a conserved functionality with previously characterized white spruce orthologs (Keeling et al., 2010) and *Arabidopsis thaliana* orthologs (Sun and Kamiya, 1994; Yamaguchi et al., 1998). This thesis also reports the cloning and functional characterization of two central genes of DRA biosynthesis in white spruce (*PgLAS* and *PgCYP720B4*), as well as *PgCYP701*, the first GA related CYP450 characterized in a gymnosperm species. The spruce diTPSs showed conserved motifs specific to active sites I and/or II and fit the proposed evolutionary scheme of diTPS in plants, arising from a bifunctional ancestor (Figure 3.3) (Bohlmann et al., 1998; Trapp and Croteau, 2001; Keeling et al., 2010), and also showed the same product profile as their previously characterized orthologs (Figure 3.5-3.8) (Keeling et al., 2010; Keeling et al., 2011b). The CYP450s characterized contained conserved key motifs and grouped with previously characterized angiosperm and gymnosperm orthologs (Figure 3.11); they also showed conserved functional product profiles with previously characterized orthologs when combined in *in vitro* or *in vivo* enzyme assays with diTPSs producing substrates (Figure 3.13, 3.14).

DiTPSs and CYP450s of GA and DRA biosynthesis in spruce show specific changes of transcript abundance through vegetative apical bud and apical shoot development

Mapping transcription changes of diTPSs and CYP450s involved in GA and DRA metabolism was conducted on developing apical buds and apical shoots, a part of the plant which undergoes major developmental changes, relating to both growth and defense. A year-long time course of white spruce apical bud and apical shoot development provided ample opportunities to monitor and compare transcript levels of GA and DRA related genes. Analysis of DRA pathway genes is also of particular interest in newly developing apical buds and shoots since they are susceptible to pests and require de novo synthesis of defensive chemicals. Therefore, because developing apical buds and shoots are both growing and synthesizing defensive chemicals at the same time, this system is a good platform to compare that spatial separation between the GA and DRA pathways.

Developing apical buds and apical shoots (Figure 3.18), including needles, stem and eventually young buds, showed general trends with respect to transcript levels of all studied genes with expression peaking in late spring/summer when bud flush occurs and apical shoots undergo fast growth (Figure 2.1; Table S1). Clear statistically significant patterns were seen in *PgLAS* and *PgCPS*, with both showing prolonged elevated transcript levels for approximately 2 weeks in May or June. Transcript levels of *PgKS* and *PgCYP701* as well as *PgLAS* and *PgCYP720B4* showed suppression in the last two months of the year, which is consistent with a period of dormancy of the tree during the winter months. The examination of transcript levels at the beginning of the year (January-April), although represented by pooled tissues only due to the very small amounts of sample material available, suggested that GA related genes are up-regulated sooner than those of DRA pathway genes as

illustrated by both *PgLAS* and *PgCYP720B4* transcript levels that remained nearly undetectable until mid-April. Overall, this analysis provided valuable information to show that differential expression of GA and DRA pathway genes does occur over the seasonal timeframe and correlates well with known times of growth vs dormancy or with times when pest challenge would be high. The information from this time course then set the stage to shift focus to a spatially more specific analysis of transcript expression in needles, stems and emerging buds of the developing apical shoot. For this goal, the time frame was narrowed to the spring and summer portions of the year where growth processes are most prominent and vegetative apical buds and shoots are undergoing major phenotypic changes (Figure 3.19).

An analysis of developing apical bud and shoot sample part-specific expression of the GA related genes revealed the following patterns. The greatest increase in transcript levels of *PgCPS* (Figure 3.19A) occurred during the period of fast growth of vegetative buds and was localized almost exclusively to needle samples. Expression of *PgKS* and *PgCYP701* (Figure 3.19B) was also highest in needles but substantial expression also occurred in stem and new buds. However, unlike the expression of *PgCPS*, transcript levels of these two genes changed little over time in all sample parts. As the first committed step in the GA biosynthetic pathway, strong up-regulation of *PgCPS* during peak growth season, where it competes directly with LAS and other diTPSs of specialized metabolism, strongly suggests that CPS may be a rate-limiting or gatekeeper step in GA biosynthesis in spruce. Indeed, in angiosperms, several studies have indicated that CPS is a regulatory point controlling the flow of GGPP into the GA biosynthetic pathway (Silverstone et al., 1997; Smith et al., 1998; Prsic and Peters, 2007). This is backed by overexpression studies in *Arabidopsis thaliana* showing that *AtCPS* was the limiting factor to *ent*-kaurene biosynthesis (Fleet et al., 2003).

In *Arabidopsis thaliana* and rice, expression of *CPS* was localized mainly to vascular tissues, and strongly associated with tissues undergoing rapid growth such as shoot apices, developing anthers and root tips (Silverstone et al., 1997; Yamaguchi et al., 2001; Toyomasu et al., 2015). The present data for white spruce indicate a similar function and pattern of expression of *CPS* in conifers.

DRA pathway genes were differently expressed than their GA counterparts. In stem sample from the apical shoot, transcript levels of *PgLAS* were at their peak a few weeks before maximum expression levels of *PgCYP720B4* occurred (Figure 3.19D,E). High expression of DRA genes in the stem are consistent with the presence of constitutive and induced resin ducts (Martin et al., 2002; Miller et al., 2005; Zulak and Bohlmann, 2010) which fill with DRAs during apical shoot development. Up-regulation of these genes is also consistent with previous studies showing localization of Sitka spruce *LAS* to cortical resin duct epithelial cells in stem tissue (Zulak et al., 2010) and transcript expression mapping of *CYP720B4* in Sitka spruce bark and phloem (Hamberger et al., 2011). Approaching autumn months, stem and new buds shared relatively constant *PgLAS* expression; in contrast, *PgCYP720B4* expression levels in all sample parts dropped dramatically in the autumn. Interestingly, *PgCYP720B4* expression in needles peaked in the month of May, at the same time as *PgLAS* transcripts (Figure 3.19D,E) and expression of both these genes in needles dropped to near zero in June, perhaps indicative of a very short time period of DRA synthesis and accumulation occurring in early spring in needles. The observation that *PgCYP720B4* in apical shoot stem peaked prominently at a later time might suggest that this enzyme may function more broadly in this sample, beyond its link with *PgLAS*. In fact this agrees with the assessment of the relative activity of *PsCYP720B4* shown by Hamberger et

al. (2011), where this CYP450 was shown to be active with 24 different diterpenoid substrates, derived from 8 olefins, only 4 of which are primary products of LAS.

In a previous study, Martin et al. (2003) were unable to detect endogenous enzyme activity of diTPSs in cell-free extracts of Norway spruce needles but found constitutive levels of diterpenes in mature needles. This suggested that diTPSs might have been active in young needles and their diterpene products were accumulated and stored in resin ducts as the needles matured. The highest transcript levels of *PgLAS* and *PgCYP720B4* in white spruce needles correspond to an early phenological stage of development of the needles - time points 13 and 15 (mid to late May) that correspond with the apical shoot transitioning from bud flush to rapid shoot elongation and growth (Table S1), a time when needles are not yet mature. However, transcript levels of *PgLAS* and *PgCYP720B4* were virtually undetectable in white spruce needles from mid-June onwards (Figure 3.19). Taken together with the results from Martin et al. (2003) this indicates that DRA products are synthesized over a short time frame in young needles and gene expression and enzyme activity of the pathway enzymes is subsequently down-regulated when needles mature. Thus, DRA pathway genes in expanding apical buds and developing shoots are apparently up-regulated before seasonal insect attack and subsequently transcript levels decline to near zero well before dormancy, which is earlier than GA associated genes. This suggests that DRA metabolites are produced, and sequestered, and are not catabolized during dormancy, whereas GA metabolites may undergo breakdown and may require fine-tuned biosynthesis for their role in regulation of growth and development. Indeed, a study by Kong et al. (2008) in Douglas-fir (*Pseudotsuga menziesii*) showed that stem injected bioactive GA mixtures fell below detectable limits at around 5 weeks post treatment, even when injected with much higher than physiological GA

concentrations. As phytohormones, gibberellins must be quickly responsive to changing stimuli (e.g. developmental, nutritional, environmental). Hence, GA pathway gene expression and protein levels should be present constitutively but also still have the capacity to respond to selected stimuli. For example, the peak in expression of *PgCPS* (the purported gatekeeper enzyme of the pathway) at time point 17 (early June) in needles is suggestive of the importance of gibberellin-stimulated growth processes at this time.

Transcript levels of the GA related genes studied here are significantly higher in needles than stem or new bud samples of the apical shoot (Figure 3.20), suggesting that in white spruce, needles are possibly the main site of production. Being photosynthetically active, it is possible that needles are the first site to use the resulting bioactive GAs for growth; subsequently GAs could then be transported elsewhere throughout the plant, to serve fast growing tissues or reproductive organs. For example, in Norway spruce, Odén et al. (1995) injected tritiated and deuterated gibberellin A₄ (GA₄, one of the bioactive forms) into the xylem tissue of an elongating shoot and found that the majority was first transported to needles and then ultimately to the stem with a small amount in the lateral buds.

DRA accumulation through vegetative apical bud and apical shoot development and relationships to diTPSs and CYP450s gene expression of GA and DRA metabolism

Measuring transcript levels is important to understand the fine regulation and localization of GA and DRA associated gene expression with respect to seasonal time and treatment, but changes in transcript levels are not necessarily definitive in predicting corresponding changes to protein/enzyme activity or metabolite production. For this reason,

changes in transcript levels were compared with DRA metabolite data which provided a measure of pathway function and end point metabolite production.

Over the time course in developing apical buds and shoots (Figure 3.15) DRA concentrations were largely stable throughout the year. A significant DRA increase specifically stood out in mid-May (time points 13-14) where during the final stages of vegetative bud flush, over the course of one week, DRA concentrations increased 1.6-fold. This could be linked to the growing apical shoot rapidly sequestering resin while new stem tissue is being rapidly produced in this fast growing stage (Table S1). As well, considering needles constitute a large proportion of the entire apical bud or shoot by weight, the rise in DRA concentration in needles, seen in Figure 3.16, could very well be influencing this increase. When inspecting this rise in DRA levels we see that *PgLAS* transcript levels in the apical shoot were at their highest over these same time points (Figure 3.18); *PgCYP720B4* levels were high at this point in time as well.

Looking at DRA concentrations over the shortened time course of different sample parts of the fast growing apical buds and shoots (Figure 3.16), needles showed the first peak in DRA levels in May. Comparing resin accumulation to transcript levels (Figure 3.19), *PgLAS* and *PgCYP720B4* were both up-regulated rapidly in needles during the month of May with *PgLAS* levels rising to their peak 2 weeks before *PgCYP720B4*. DRA levels in needles then returned to stable levels for the remainder of the time course. This reinforces the notion of a very short period of DRA synthesis in needles in early spring followed by long lasting persistence of DRAs in the tissue even as transcript levels of *PgLAS* and *PgCYP720B4* fall to near zero levels. DRA accumulation in apical shoot stem samples began in May, as it did in needles, followed by a steep rise in DRA concentration in stem over time

as shoots expand and elongate. Stem DRA levels peaked about 1 month after *PgLAS* and *PgCYP720B4* transcript levels were highest, indicating a build-up of resin in stem samples over time as pathway genes are up-regulated. New buds developed in June (Table S1) and they quickly accumulated DRAs. Soon after new bud development, resin concentration in the stem reached a plateau which could possibly allude to substrate allocation, the favorable transfer of precursors to new buds during rapid growth rather than to other tissues. DRA levels in new buds peaked in August-September when they had reached maturity (Table S1) for the year.

Although represented by pooled samples only (Figure 3.15), DRA concentrations in apical buds at the beginning of the year (Jan-Feb) were similar to those present after apical buds had flushed and shoots elongated (June onwards). Hence, DRAs must be sequestered in apical bud tissue and remain over winter months and the ensuing dormancy stage.

Spatially, where DRA levels were the lowest, in needles, the GA pathway gene transcript levels were highest over time. Specifically, *PgCPS* transcript levels peaked just 2 weeks after the highest DRA concentrations were observed in needles. In this case, then, GA and DRA pathways are primarily spatially separated but also show some temporal separation in needles.

DiTPSs and CYP450s of GA and DRA biosynthesis show different patterns of transcriptional changes with MeJA treatment

Treatment with MeJA simulates the effect of insect attack on spruce, with effects including increased accumulation of DRAs and diTPS transcripts in the bark and phloem

(Miller et al., 2005). MeJA induces oleoresin defenses, and mimics insect infestation at the level of traumatic resin duct formation, terpenoid accumulation and terpene synthase gene expression (Franceschi et al., 2002; Martin et al., 2002; Fäldt et al., 2003; Miller et al., 2005). The present study examined the responses of diTPSs and CYP450s of the GA and DRA biosynthesis pathways in different sample types of white spruce when exposed to MeJA treatment. With MeJA as an elicitor, the aim was to uncover if there were novel responses of the GA pathway enzymes in spruce and allow a spatial and temporal comparison to the changes in the DRA pathway under the same conditions.

For this study the focus was narrowed to five distinct sample types that represented both developed as well as growing samples, comparing sample types that are known to hold large volumes of resin, like wood/xylem, versus those that are fast growing and possible sites of changes in GAs. Age specific differences were also considered by analyzing young versus mature needles as well as bark/phloem and wood/xylem from a year-old internode compared with young stems from new growth (representing growing phloem and xylem tissue). Spatially and temporally this experiment offered insights into the comparison between pathways related to growth versus defense.

Notably, transcript levels of *PgCPS* of the GA pathway increased significantly over time in the young stems (Figure 3.25) under both MeJA and control treatments. Thus, expression was apparently unaffected by MeJA treatment; instead, the rise of *PgCPS* transcripts over time appeared to be a phenomenon of this fast growing young sample, affected either by internal or other external factors. Strong and increasing expression of *PgCPS* in growing samples agrees with indicators found in the study of developing apical

buds and shoots that implicated CPS as most likely the rate-limiting step controlling the flow of GGPP into the GA pathway.

In other sample types, *PgCPS* was down-regulated with MeJA treatment, and significant differences between treatments were seen in bark and mature needles. In both of these sample types, *PgCPS* transcript levels dropped substantially within 2 days after treatment with MeJA, and remained suppressed until day 16. *PgCPS* transcript levels in Tween-treated bark and mature needles dropped to a low at day 16 as well, which was contrary to possible predictions that *CPS* levels should remain relatively stable since these samples were not undergoing rapid growth over this short time frame. This might suggest that the Tween/control treatment was also having an effect on *PgCPS* expression levels.

Opposite to the response of the first diTPS of the GA biosynthetic pathway, *PgKS* was up-regulated under MeJA treatment in all sample types (Figure 3.26); however, trends of activity differed between them. For instance in green, photosynthetically active sample types (needles and young stems) transcript levels of *PgKS* peaked around days 4 or 6, and only in the mature needles did transcript levels fall to control levels at the end of the time course. In wood/xylem, *PgKS* transcript levels climbed steadily from 2 days post treatment onwards, whereas in bark, *PgKS* levels were consistently high in the MeJA treatment and showed the fastest response to MeJA, rising over 10-fold in 2 days. Throughout the study, *PgKS* transcript levels in all Tween-treated sample types were detectable but stayed low. Previously this response of up-regulation of a kaurene synthase due to MeJA treatment seemed to occur only for *KS-like* genes that were redirected to specialized metabolism pathways through neofunctionalization; for example in *Salvia miltiorrhiza* (red sage) the *KS-like* gene dedicated to the tanshinone biosynthesis pathway was significantly up-

regulated by MeJA treatment (Hao et al., 2014). Hence, the results described here for *PgKS* of the GA pathway were unexpected.

In response to MeJA treatment, *PgCYP701* was the only gene explored in this pathway that showed a markedly different response based on sample type. In the MeJA treatment, *PgCYP701* transcript levels from both wood/xylem and bark were elevated, rising above control levels from day 8 onwards (Figure 3.28). However, in both young and mature needles, *PgCYP701* transcripts were down-regulated by MeJA treatment, which was similar to the responses seen for *PgCPS*, with expression returning to near control levels by day 16. Furthermore in young stems, treatment with MeJA had no statistically significant effect on *PgCYP701* transcript levels (again similar to the *PgCPS* response). Previous work on *CYP701* response to MeJA treatment appears to be limited to analysis of whole *Arabidopsis thaliana* seedlings where transcript levels were not affected by the phytohormone (Winter et al., 2007; part of the AtGenExpress project, funded by RIKEN). However, the pattern observed here suggests that *PgCYP701* and *PgCPS* have generally parallel responses in some sample types to both MeJA and control treatments suggesting a coordination of the gene expression of these two GA pathway enzymes. Such coordination is not unexpected for the regulation of a metabolic pathway.

When treated with MeJA, both *PgLAS* and *PgCYP720B4* of the DRA pathway showed similar expression responses (Figure 3.27, 3.29). Wood/xylem treated with MeJA showed the most dramatic induction of *PgLAS* and *PgCYP720B4* transcripts; MeJA-treated transcript levels rose steeply beginning at day 6 and by day 8 expression of *PgLAS* had peaked at over 100-fold higher than control, whereas *PgCYP720B4* expression was over 40-fold higher than control. In bark, MeJA-treated *PgLAS* transcript levels were significantly

higher than those of controls across the entire time course and *PgCYP720B4* transcript levels showed a similar trend although not significantly different from controls in bark. Zulak et al. (2010) visualized this phenomenon by localizing LAS by immunofluorescence in Sitka spruce stems to epithelial cells surrounding constitutive resin ducts (found in bark) at 2 days post MeJA treatment and in epithelial cells of traumatic resin ducts (TRDs, found in xylem) at day 8; this agrees with the time course of current *PgLAS* expression results for both wood and bark. The wood/xylem response occurs several days after that of bark due to the fact that TRDs are formed *de novo* at the cambial zone in response to wounding, MeJA or pest inoculation. In Norway spruce, TRDs could be visualized as early as 6-9 days post MeJA treatment (Martin et al., 2002). The timing of the expression of these gene transcripts also concurs with results for Sitka spruce reported by Hamberger et al. (2011) who found that both *PsCYP720B4* and *PsLAS* were significantly up-regulated by day 8 in response to MeJA treatment in bark and phloem.

In growing sample types, young needles and young stems, treatment with MeJA prompted a quick response, elevating transcript levels of both DRA pathway genes (*PgLAS* and *PgCYP720B4*) as early as 2 days post treatment. In mature needles, MeJA treatment induced a delayed response of *PgLAS* and *PgCYP720B4* transcripts, both peaking at day 8, similar to the trend seen in wood/xylem, possibly pointing to the formation of induced ducts here as well. However, when scaled to other sample types, transcript levels in needles are so low that the changes seen overall were not considerable. In fact, in Sitka spruce, Hamberger et al. (2011) also reported that *PsCYP720B4* transcripts levels were very low in young and mature needles, which also coincides with data from Miller et al. (2005) which showed no significant increase in diterpenoids 20 days after MeJA treatment in Sitka spruce needles.

Comparing general patterns of differences in the response to MeJA between the genes in this study is easily apparent from the results shown in Figure 3.24, where transcript levels are averaged across all time points. Despite losing the dimension of temporal changes, a clear spatial separation in the DRA associated gene expression data can be seen. When treated with MeJA, *PgLAS* and *PgCYP720B4* were highly up-regulated in bark, wood/xylem and young stems, with levels near zero in needles. Control treatment showed highest relative expression of *PgLAS* and *PgCYP720B4* in bark and young stems, albeit at a much lower level than during MeJA treatment. While the patterns seen in DRA related genes follow those of previous studies, the genes relating to the GA pathway show different expression patterns than what could be expected from a phytohormone pathway. Figure 3.24 shows that the spatial distribution of *PgCPS*, *PgKS* and *PgCYP701* expression is more uniform than that of the DRA related genes studied, clearly pointing to the functionality of the GA pathway proceeding in both young and well established sample types. A novelty, given its role in the GA biosynthetic pathway, is the up-regulation of *PgKS* in response to MeJA treatment. Indeed in many sample types, MeJA-treated *PgKS* transcript levels remained significantly up-regulated until the end of the time course. This confuses the question of spatial allocation of resources between the DRA and GA pathways at a time of pest attack (simulated by MeJA); it is difficult to imagine why *PgKS* of the GA pathway would be up-regulated when spruce defense pathways are needed.

DRA accumulation in MeJA-treated spruce samples and relationships to diTPSs and CYP450s of GA and DRA metabolism

DRA levels were measured as part of the study of MeJA treatment effects in order to determine if there was a correlation between changes in the transcript abundances of the diTPS and CYP450s and the levels of DRA pathway end-point metabolites. Comparing DRAs to gene expression allows a greater understanding of the effects of MeJA treatment on white spruce sample types and the organization of GA and DRA metabolic pathways.

DRA concentrations significantly increased with MeJA treatment in wood/xylem and in young stems of white spruce (Figure 3.23). In both of these sample types, DRA levels began to rise approximately 8 days post treatment and reached the highest detected levels at the end of the time course. Young stems represent both bark and wood/xylem of the current year's growth; thus, the increase seen over time in DRA concentrations in this sample type (Figure 3.23E) roughly corresponds to what would be seen if the data for the more mature bark/phloem and wood/xylem samples were combined (Figure 3.23C, D). Overall, then, it appears from these experiments that the pattern of DRA accumulation as the result of MeJA treatment does not change markedly between younger and older stems. When comparing gene expression timing and DRA accumulation it can be noted that both *PgLAS* and *PgCYP720B4* transcript levels in MeJA-treated wood/xylem began to increase around day 6, which correlates with the advent of DRA accumulation in that sample type (Figure 3.27, 3.29). In young stems, transcript levels of both *PgLAS* and *PgCYP720B4* were quickly up-regulated by MeJA, eventually reaching a steady state later in the time course; this loosely correlated with the slow and steady increase in DRA levels observed over time.

By far the lowest levels of DRA accumulation were seen in mature and young needles, and DRA levels in neither sample type were significantly affected by MeJA treatment. A previous study by Martin et al. (2003) found no significant change in total diterpenoid content in Norway spruce needles 20 days after MeJA treatment, as well Miller et al. (2005) found no increase in diterpenoid accumulation 20 days after MeJA treatment in either young or mature Sitka spruce needles. These previous studies agree with the current study in the lack of response of needles to MeJA treatment in white spruce. A novel result of the present study shows that between the two needle types, young needles of white spruce have DRA concentrations over 10-fold higher than in their mature counterparts (Figure 3.22; Table 3.6); this occurred despite just marginally higher transcript abundances of the DRA associated genes (*PgLAS* and *PgCYP720B4*) in young compared with mature needles (Figure 3.27, 3.29).

When comparing DRA concentrations to expression of genes in the biosynthesis pathway it is perhaps easier to see general patterns by comparing mean DRA levels averaged over the entire time course (Figure 3.22) to the equivalent mean transcript levels (Figure 3.24). This comparison illustrates the strong correlation between DRA abundance and *PgLAS* and *PgCYP720B4* expression in terms of spatial organization. Thus, DRAs have high mean concentrations in wood/xylem, bark and young stems, which are the tissues where DRA associated genes are most highly expressed in response to treatment with MeJA. Furthermore, sample types such as wood/xylem that respond robustly to stress with DRA synthesis show low overall expression levels of genes encoding the GA pathway enzymes, *PgCPS* and *PgCYP701*. This indicates that resource allocation in wood/xylem strongly favours defense mechanisms with a high capacity for redirection of resources into the DRA

pathway. A potential overlap can be seen with high transcript levels of *PgKS* and *PgCYP701* in the MeJA-treated bark and young stem tissue, however it is unclear whether expression of GA related genes could actually translate into a reallocation of biosynthetic resources away from the DRA pathway and towards the GA pathway in this case.

Chapter 4: Functional characterization and comparison of expression of *DXS* genes involved in gibberellin and diterpene resin acid biosynthesis in white spruce

4.1. Introduction

Building on the knowledge obtained about the genes of GA and DRA metabolism and their responses to growth and stress in multiple samples in white spruce (Chapter 3), it became important to extend this work to investigate the MEP pathway to evaluate possible differential expression of the genes involved in the biosynthesis of the isoprenoid precursors for both the GA and DRA pathways. Within the MEP pathway, 1-deoxy-D-xylulose 5-phosphate synthase (DXS) is recognised as the first rate-limiting step (Estévez et al., 2001; Lois et al., 2000; Cordoba et al., 2009). The *DXS* gene family can be divided in three different functionally specialized clades, type I, type II and type III (Walter et al., 2002; Cordoba et al., 2011). These clades are based on phylogenetic analysis and differences in gene expression patterns in both angiosperms and gymnosperms (Kim et al., 2005; Kim et al., 2006; Phillips et al., 2007). *DXS* type I genes are usually constitutively expressed in growing and photosynthetic tissues and are involved in general metabolic pathways whereas *DXS* type II enzymes are typically involved in specialized metabolic pathways.

Because *DXS* enzymes catalyze a rate-limiting step in the biosynthesis of isoprenoid precursors for diterpenoids, it can be reasoned that changes in the expression of *DXS* gene transcripts could affect or have a relationship with the downstream pathways of GA and DRA biosynthesis, among others, potentially affecting the output of the metabolites produced from these pathways. Indeed, studies spanning a diverse set of plant species have

shown that DXS enzymes play a crucial role in the biosynthesis of isoprenoid precursors as well as modulate the flux of precursors through the MEP pathway itself (Wright et al., 2014; Boronat, 2010). In *Arabidopsis thaliana*, transgenic lines overexpressing *DXS* showed increased levels of multiple isoprenoid metabolites including carotenoids, abscisic acid and gibberellins, and the reverse was true of antisense *DXS* lines that showed reduced levels of isoprenoid products (Estévez et al., 2001). Overexpression of bacterial *DXS* genes in tomato (Enfissi et al., 2005) and potato tubers (Morris et al., 2006) also led to significant increases of 1.6-fold and 2-fold, respectively, in the accumulation of carotenoids. Insertion of a constitutively expressed *Arabidopsis thaliana* *DXS* cDNA into spike lavender, *Lavandula latifolia*, revealed that these transgenic plants contained over 3-fold more essential oils when compared to controls, the major constituent of these oils being monoterpenoids originating from the MEP pathway (Muñoz-Bertomeu et al., 2006). As well, a positive correlation between the expression levels of an endogenous *DXS* and the synthesis of isoprenoid products has been shown in *Ginkgo biloba* with ginkgolide b accumulation paralleling the increase in *GbDXS* transcript levels (Gong et al., 2006). *DXS* type II genes have been shown to be inducible by elicitors or pests and also show positive correlations with isoprenoid product accumulation in response to these stresses. In *Medicago truncatula*, maize, and rice *DXS* type II genes showed up-regulated transcript levels upon colonization by mycorrhizal fungi which was mirrored by increases in carotenoid and apocarotenoid accumulation (Walter et al., 2002; Walter et al., 2000).

The study described in this chapter aimed to evaluate *DXS* gene expression in white spruce by characterizing seasonal, sample-specific and stress-specific responses, monitored over the time courses of apical bud and shoot development as well as in response to

induction by the elicitor MeJA (as in experiments described in chapter 3). Transcript levels of *PgDXSs* were also evaluated in relation to DRA metabolite accumulation because, as part of the pathway producing precursors to DRA biosynthesis, it is warranted to hypothesize that DXS gene expression could have a direct influence on the downstream DRA metabolite levels.

4.2. Results

4.2.1. Cloning and identification of spruce *DXS* genes

Three *DXS* genes, *PgDXS1*, *PgDXS2A* and *PgDXS2B*, from white spruce were cloned. Putative transit peptides, predicted by ChloroP and TargetP servers (Emanuelsson et al., 1999, 2000), were truncated before activity assays were performed (*PgDXS1*, 54 aa removed; *PgDXS2A*, 48 aa removed; *PgDXS2B*, 18 aa removed). Amino acid sequence alignment (Figure 4.1.) with previously characterized DXS sequences from Norway spruce (*Picea abies*) and the angiosperm *Zea mays* (*Zm*) confirmed the presence in the *P. glauca* sequences of the characteristic transketolase-like thiamine pyrophosphatase (TPP) binding domain (GDGX₂₅₋₃₀N), and conserved amino acids of the DXS active site (Hawkins et al., 1989, Xiang et al., 2007) (Figure 4.1).

Compared to previously characterized orthologs, *PgDXS1* (717 aa) has 98.9% identity to *PaDXS1* (Phillips et al., 2007) and between 77-78% identity to angiosperm counterparts, for example: *AtDXS1* 77.39%, *ZmDXS1* 77.58%, and *CrDXS1* 78.15% (Estévez et al., 2000, Cordoba et al., 2011, Han et al., 2013). *PgDXS2A* (740 aa) shares 99.7% identity to *PaDXS2A*, but less with angiosperm orthologs: 71.3% identity to

ZmDXS2 and 73.4% identity to *CrDXS2A* (Cordoba et al., 2011, Chahed et al., 2000).

PgDXS2B (746 aa) is 99.5% identical to ortholog *PaDXS2B*, but only 70.9% to *ZmDXS2* and 70% to *CrDXS2B* (Cordoba et al., 2011, Chahed et al., 2000). Comparing DXS proteins characterized in white spruce, the percent identity between types is 67.2% for *PgDXS1* versus *PgDXS2A* and 68.3% to *PgDXS2B* whereas within DXS type II genes *PgDXS2A* and *PgDXS2B* share 73.1% identity.

Phylogenetic analysis of selected DXSs from angiosperms and gymnosperms, including those characterized as *DXS-like* genes (Figure 4.2) shows the predicted distinction of DXS type I and DXS type II clades, when rooted with moss *Physcomitrella patens* DXS (*PpDXS*). The white spruce DXSs group very closely with gymnosperm orthologs and within the DXS type I clade, gymnosperm DXSs form a monophyletic clade. Within DXS clades are monophyletic groupings of sequences from monocot and dicot plants. In the DXS type II clade two separate duplication events potentially occurred in some dicot and gymnosperm species, resulting in spruce (*Pg* and *Pa*, as well as *Picea sitchensis*; data not shown) sequences marked A and B with similar distinctions in dicot plants *Populus trichocarpa* (*Ptc*) and *Catharanthus roseus* (*Cr*), in this phylogeny. Along with sequence alignments, this phylogenetic analysis confirms that *PgDXS1* belongs to the DXS type I clade and *PgDXS2A* and *PgDXS2B* are classified separately in the DXS type II clade.

PgDXS1	MAT----	TMA	MAAHAVIQSN	ANQLTSMPSA	LSSRSLRYQN	KHTKLEFEKL	G----	RRVG-	-----	-----	-----	KV	HAAALSDQ--	GEYYSEKPPT	71
PaDXS1	MAT----	TMA	MASPAVIQSN	ANQLTSMPSA	LSSRSLRYQI	KHTKLEFEKL	G----	RRFG-	-----	-----	-----	KV	HAAALSDQ--	GEYYSEKPPT	71
ZmDXS1	MAL----	STF	SVP-----	RG	FLGVP AQDSH	FASAVELHVN	KLLQA--	RP I	NLKP RRRA-	-----	-----	CV	-SASLSSERE	AEYYSQRPT	69
PgDXS2A	MAITSR--	-G	AAPVLQVDCH	LTHFHSI-TE	LGSRRNSAMFO	SAI PCTFQQI	SAATKRRCR I	LF AKLNNSDG	-EKM--	-KNV	RAAVEIAPKK	-DFS AEKPPT	92		
PaDXS2A	MAITSR--	-G	AAPVLQVDCH	LTHFHSI-TE	LGSRRNSAMFO	SAI PCTFQQI	SAATKRRCR I	LF AKLNNSDG	-EKM--	-KNV	RAAVEIAPKK	-DFS AEKPPT	92		
PgDXS2B	MASLGVASMG	SSPFMV INGS	NISQPS--	TA	LWSRGFK I F P	KQNI STLQWI	PL--	KSKHGT	VCAI SSDADG	DESI--	-KG I	SNTGKDGPLM	IKCSGEKPPT	93	
PaDXS2B	MASLGVASMG	SSPFMV INGS	NISQPS--	TA	LWSRGFK I F P	KQNI STLQWI	PL--	KSKHGT	VCAI SSDADG	NESI--	-KG I	SNTGKDGPLM	IKCSGEKPPT	93	
ZmDXS2	M-----	-	SPIMALQAS	SSPSAF-RA	VPATANASCR	RQFQVRAQVA	GGSSSSS I G-	-----	ADG	GKMMVSKEPA	AAATSSGPWK	IDFSGEKPPT	81		
PgDXS1	PLLD TINYP I	HMKNLS IREL	KQLSNELRSD	T I FEVARTGG	HLGSSSLGVVE	LTVALHYVFD	APEDK I LWDV	GHQAYPHK I L	TGRRDKMPTL	*RQTNGLSGFT	171				
PaDXS1	PLLD TINYP I	HMKNLS IREL	KQLSNELRSD	T I FEVARTGG	HLGSSSLGVVE	LTVALHYVFD	APEDK I LWDV	GHQAYPHK I L	TGRRDKMPTL	RQTNGLSGFT	170				
ZmDXS1	PLLD TINYP V	HMKNLSVKEL	RQLADELRSD	V I FHVSKTGG	HLGSSSLGVVE	LTVALHYVFN	APQDR I LWDV	GHQSYPHK I L	TGRRDKMPTM	RQTNGLAGFT	169				
PgDXS2A	PLLD TINYP V	HLKNLSVQDL	EQLATE IRAE	LVFGVSKTGG	HLGSSSLGVVD	LTVALHHVFD	SPEDR I IWDV	GHQSYPHK I L	TGRRSKMHT I	RQTSGLAGFP	192				
PaDXS2A	PLLD TINYP V	HLKNLSVQDL	EQLATE IRAE	LVFGVSKTGG	HLGSSSLGVVD	LTVALHHVFD	SPEDR I IWDV	GHQSYPHK I L	TGRRSKMHT I	RQTSGLAGFP	192				
PgDXS2B	PLLD TINYP I	HMKNFN I K E L	RQLAKELREE	I I FSV AETGG	HL SASLGVVD	LTVALHYVFN	TPHDKV VWDV	GHQSYPHK I L	TGRRSKMGTM	RQTSGLAGFP	193				
PaDXS2B	PLLD TINYP I	HMKNFN I K E L	RQLAKELREE	I I FSV AETGG	HL SASLGVVD	LTVALHYVFN	TPHDKV VWDV	GHQSYPHK I L	TGRRSKMGTM	RQTSGLAGFP	193				
ZmDXS2	PLLD TVNYPL	HMKNLS I L E L	EQLAAELRAE	VVHTVSKTGG	HLSSSLGVVE	LSVALHHVFD	TPEDK I IWDV	GHQAYPHK I L	TGRRSRMHT I	RQTSGLAGFP	181				
PgDXS1	KRSESEYDC F	GAGHSST S I S	AGLGM AVGRD	LKGRNNH V I S	V I GDGAMTAG	QAF EAMNNAG	YLD SNM I V I L	NDNKQVSLPT	ANLDGMP PPV	GALSSALSKL	271				
PaDXS1	KRSESEYDC F	GAGHSST S I S	AGLGM AVGRD	LKGRNNH V I S	V I GDGAMTAG	QAF EAMNNAG	YLD SNM I V I L	NDNKQVSLPT	ANLDGMP PPV	GALSSALSKL	270				
ZmDXS1	KRAESEYDS F	GTGHSST T I S	AALGM AVGRD	LKGGKNNVVA	V I GDGAMTAG	QAY EAMNNAG	YLDSDM I V I L	NDNKQVSLPT	ATLDGPV PPV	GALSSALSKL	269				
PgDXS2A	KRDESKYDA F	GAGHSST S I S	AGLGM AVGRD	LLRKSNNH V I A	V I GDGAMTAG	QAY EAMNNAG	YLD SNM I V I L	NDNKQVSLPT	ATLDGAAPPV	GALTRALTKL	292				
PaDXS2A	KRDESKYDA F	GAGHSST S I S	AGLGM AVGRD	LLRKSNNH V I A	V I GDGAMTAG	QAY EAMNNAG	YLD SNM I V I L	NDNKQVSLPT	ATLDGAAPPV	GALTRALTKL	292				
PgDXS2B	RRVESEHDA F	GVGHSST S I S	AA IGM AVGRD	LLGKNNH V I A	V I GDGAMTAG	QAY EALNNAG	F L DSNM I I I L	NDNKQVSLPT	AT I DGPAPPV	GALSGALCRL	293				
PaDXS2B	RRVESEHDA F	GVGHSST S I S	AA IGM AVGRD	LLGKNNH V I A	V I GDGAMTAG	QAY EALNNAG	F L DSNM I I I L	NDNKQVSLPT	AT I DGPAPPV	GALSGALCRL	293				
ZmDXS2	KRDESAHDA F	GVGHSST S I S	AALGM AVARD	LLGKNNH V I S	V I GDGAMTAG	QAY EAMNNAG	YLD SNM I V I L	NDNKQVSLPT	ATLDGP SKPV	GALSRALTKL	281				
PgDXS1	QSSKPLREL R	EVAKGVT KQL	GAPMHELA AK	VDEYARGM I S	GS RSTLFEEL	GLYY IGPVDG	HN I DDL L T I L	QDV KATH T T G	PVL I HVVTEK	GRGYPPAERA	371				
PaDXS1	QSSKPLREL R	EVAKGVT KQL	GAPMHELA AK	VDEYARGM I S	GS RSTLFEEL	GLYY IGPVDG	HN I DDL L T I L	QDV KATH T T G	PVL I HVVTEK	GRGYPPA-RA	369				
ZmDXS1	QSSRPLREL R	EVAKGVT KQ I	GGSVHELA AK	VDEYARGM I S	GP GSSLFEEL	GLYY IGPVDG	HN I DDL L T I L	NDV KST K T T G	PVL I HVVTEK	GRGYPPAERA	369				
PgDXS2A	QSSKKLRKL R	EAAKGLTKQ I	GGQTHEMA SK	V D K Y T R G I I N	PAASSLFEEL	GLYY IGPVDG	HN I E D M V T I L	E K I K S M P D S G	PVL I H L V T E K	GKGYPPAEAA	392				
PaDXS2A	QSSKKLRKL R	EAAKGLTKQ I	GGQTHEMA SK	V D K Y T R G I I N	PAASSLFEEL	GLYY IGPVDG	HN I E D M V T I L	E K I K S M P D S G	PVL I H L V T E K	GKGYPPAEAA	392				
PgDXS2B	QASKKFRQL R	EVAKD I THQ I	GGATHQLA AK	V D D Y A R G M F S	APGSALFEEL	GLYY IGPVDG	HN I Q D L V A I L	EN V K S M P T P G	PVL I H V V T E K	GKGYPPAEKA	393				
PaDXS2B	QASKKFRQL R	EVAKD I THQ I	GGATHQLA AK	V D D Y A R G M F S	APGSALFEEL	GLYY IGPVDG	HN I Q D L V A I L	EN V K S M P T P G	PVL I H V V T E K	GKGYPPAEKA	393				
ZmDXS2	QSSTKFRRL R	EAAKSVTKQ I	GGPTHEVA AK	VDEYARGM I S	ASGSLLFEEL	GLYY IGPVDG	HCVEDLVT I F	EKVKSMPAPG	PVL I H I V T E K	GKGYPPAEAA	381				
PgDXS1	ADKYHGVAK F	DPATGKQFKG	KAPTQTYT T Y	FAEAL I SEAD	IDNNVVA I HA	AMGGGTGLNM	FSKRFP SRCF	DVG I AEQH AV	TFAAGLACEG	LKPFCA I YSS	471				
PaDXS1	ADKYHGVAK F	DPATGKQFKG	KAPTQTYTAY	FAEAL I SEAD	IDN-VVA I HA	AMGGGTGLNM	FSKRFP SRCF	DVG I AEQH AV	TFAAGLACEG	LKPFCA I YSS	468				
ZmDXS1	ADKYHGVAK F	DPATGKQFKS	PAKTL SYTNY	FAEAL I AEAE	QDSK I V A I HA	AMGGGTGLNY	FLRRFP SRCF	DVG I AEQH AV	TFAAGLACEG	LKPFCA I YSS	469				
PgDXS2A	ADKLHG VVK F	DPATGKQFKS	KSSVLSYTQY	FAESL I AEAE	VDSK I V A I HA	AMGGGTGLNY	FQKKFP ER CF	DVG I AEQH AV	TFAAGLACEG	LKPFCA I YST	492				
PaDXS2A	ADKLHG VVK F	DPATGKQFKS	KSSVLSYTQY	FAESL I AEAE	VDSK I V A I HA	AMGGGTGLNY	FQKKFP ER CF	DVG I AEQH AV	TFAAGLACEG	LKPFCA I YST	492				
PgDXS2B	ADKLHG VVK F	DPATGKQFKP	KSSTLSYTQY	FAEGLMAEAE	RDEK I V A I HA	AMGGGTGLNY	FQKRFP ER CF	DVG I AEQH AV	TFAAGLACEG	LKPLCA I YSS	493				
PaDXS2B	ADKLHG VVK F	DPATGKQFKP	KSSTLSYTQY	FAEGLMAEAE	RDEK I V A I HA	AMGGGTGLNY	FQKRFP ER CF	DVG I AEQH AV	TFAAGLACEG	LKPLCA I YSS	493				
ZmDXS2	ADRMHG VVK F	EPATGRQLKS	KSPTLSYTQY	FAESL I AEAE	SDEK VVA I HA	AMGGGTGLNY	FQKRFP ER CF	DVG I AEQH AV	TFAAGLAAEG	LKPFCA I YSS	481				
PgDXS1	FLQRAYDQV I	HDVDLQKL PV	RFAMDRAGLV	GADGPTHCGA	FDV TYLACL P	NMVMAPSDE	AEL FHMVATA	AA I D D R P S C F	RFPRGNGVGA	R-LPPGNKG V	570				
PaDXS1	FLQRAYDQV I	HDVDLQKL PV	RFAMDRAGLV	GADGPTHCGA	FDV TYLACL P	NMVMAPSDE	AEL FHMVATA	AA I D D R P S C F	RFPRGNGVGA	R-LPPGNKG V	567				
ZmDXS1	FLQRGYDQV V	HDVDLQKL PV	RFAMDRAGLV	GADGPTHCGA	FDVAYMACLP	NMVMAPSDE	AELCHMVATA	AA I D D R P S C F	RYPRGNGVGV	P-LPPNYKGT	568				
PgDXS2A	FLQRGYDQV V	HDVDLQKL PV	RFAMDRAGLV	GADGPTHCGS	FDVAYMACLP	NMVMAPSDE	VELMHMVATA	AA I D D R P S C F	RFPRGNGVGL	SNLPLNNKGL	592				
PaDXS2A	FLQRGYDQV V	HDVDLQKL PV	RFAMDRAGLV	GADGPTHCGS	FDVAYMACLP	NMVMAPSDE	VELMHMVATA	AA I D D R P S C F	RFPRGNGVGL	SNLPLNNKGL	592				
PgDXS2B	FLQRGYDQV V	HDVDLQKL PV	RFALDRAGLV	GADGPTHCGA	FDV TYMACLP	NMVMAPSDE	AELMHMVATS	AA I D D R P S C F	RFPRGNGVGV	P-LPPNNKGT	592				
PaDXS2B	FLQRGYDQV V	HDVDLQKL PV	RFALDRAGLV	GADGPTHCGA	FDV TYMACLP	NMVMAPSDE	AELMHMVATS	AA I D D R P S C F	RFPRGNGVGV	P-LPPNNKGT	592				
ZmDXS2	FLQRGYDQV V	HDVDLQRL PV	RFALDRAGLV	GADGPTHCGA	FDVAYMACLP	NMVMAPADE	AELMHMVATA	AA I D D R P S C F	RFPRGNGVGA	A-LPPGNKG V	580				
PgDXS1	PLEVGKGRIL	LEG-DRVALL	GYGTVVQNCL	AASALLEEQ-	GLSLTVADAR	FC KPLDRDL I	RLSAREHEV I	ITVEEGT IGG	FGSHVAHFLA	LDGFLDGK LK	668				
PaDXS1	PLEVGKGRIL	LEG-DRVALL	GYGTVVQNCL	AASALLEEQ-	GLSLTVADAR	FC KPLDRDL I	RLSAREHEV I	ITVEEGT IGG	FGSHVAHFLA	LDGFLDGK LK	665				
ZmDXS1	PLEVGKGRIL	LEG-DRVALL	GYGSVQYCL	TAASLVQRH-	GLKVTVADAR	FC KPLDHAL I	RLSAKSHEVL	ITVEEGS IGG	FGSH I AQFMA	LDGLLDGK LK	666				
PgDXS2A	P I E I GRGRIL	VEG-TRVAIL	GFGT I I QNCL	AAGKMLNEQA	G I S V T I ADAR	FC KPLDGD L I	KRLAKEHE I L	LTVEEGS IGG	FGSHVSHFLA	LNGLLDGK LK	691				
PaDXS2A	P I E I GRGRIL	VEG-TRVAIL	GFGT I I QNCL	AAGKMLNEQA	G I S V T I ADAR	FC KPLDGD L I	KRLAKEHE I L	LTVEEGS IGG	FGSHVSHFLA	LNGLLDGK LK	691				
PgDXS2B	PLK I GKGRIL	AEG-TRIA I L	GYGS I VQNCL	AAREMLAQQ-	G I S V T VADAR	FC KPLDGD L I	RRLVKEHE I L	VTVEEGS IGG	FGSHVSHFLA	LHGLFDGK LK	690				
PaDXS2B	PLK I GKGRIL	AEG-TRIA I L	GYGS I VQNCL	AAREMLAQQ-	G I S V T VADAR	FC KPLDGD L I	RRLVKEHE I L	VTVEEGS IGG	FGSHVSHFLA	LHGLFDGK LK	690				
ZmDXS2	ALEVGRGRVL	VGGGTRVAL	GYGAMVQACL	KAAEALKEH-	DVYVTVADAR	FC KPLD L T A I	RELAAEHEVL	ITAEEGS IGG	FGSHVAHYLS	LTGLLDGPLK	679				
PgDXS1	WRPMVL PDHY	IEHGAPNDQM	VEAGLTASH I	AASVLN I LGR	TREALQVMS-	-----	717								
PaDXS1	WRPMVL PDHY	IEHGAPNDQM	VEAGLTASH I	AASVLN I LGR	TREALQVMS-	-----	714								
ZmDXS1	WRPLVL PDRY	IDHGSPADQL	AEAGLTPSH I	AASVFN I LGQ	NREALA I MAV	PNA--	719								
PgDXS2A	WRAMVL PDRY	IDHGAPKQDI	EEAGLSPKH I	AAT I MSLLGK	PHDAL----	L	KHR--	740							
PaDXS2A	WRAMVL PDRY	IDHGAPKQDI	EEAGLSPKH I	AAT I MSLLGK	PHDAL----	L	KHR--	740							
PgDXS2B	WRPMVL PDRY	IDHGSPKQDI	EEAGLSSRH I	AATVMSL I GK	PQNALQAPV I	EYSSL I	746								
PaDXS2B	WRPMVL PDRY	IDHGSPKQDI	EEAGLSSRH I	AATVMSL I GK	PQNALQAPV I	EYSSL I	746								
ZmDXS2	LRSFML PDRY	IDHGAPQDQ I	EEAGLTPRH I	AATVLSLLGR	PLEAMQ----	----	LK	727							

Figure 4.1. Comparison of the amino acid sequences of *PgDXS1*, *PgDXS2A* and *PgDXS2B* with characterized orthologs from *Picea abies* and *Zea mays*. Catalytically relevant residues of the active site are marked with an asterisks above (*) and the transketolase-like thiamine binding domain is underlined in red (dashed line). Truncated putative transit peptide sequences of *Pg* proteins are underlined in black (solid line) with the resultant protein being used for enzyme assays.

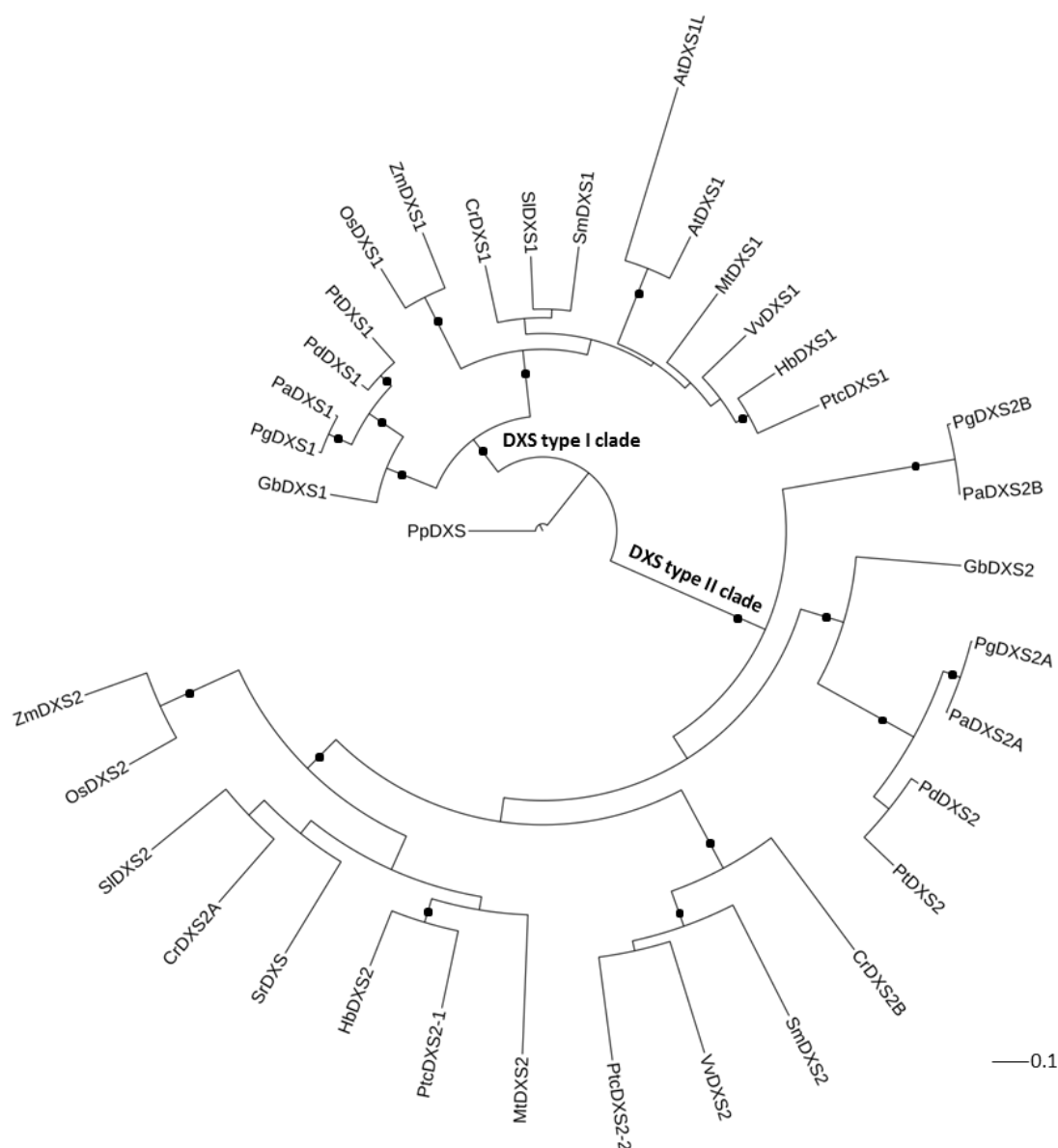


Figure 4.2. Phylogenetic maximum-likelihood tree of full-length amino acid DXS sequences from angiosperms and gymnosperms. Outgroup used was the *Physcomitrella patens* DXS sequence (*PpDXS*; accession no. XP_001756357). Legend bar indicates substitutions per site, black dots indicate branches with 80% or more bootstrap support (500 replications). Abbreviations and accession numbers are as follows: *AtDXS1* (*Arabidopsis thaliana* CLA1; AAC49368), *AtDXS1L* (DXS2; ACI49774), *CrDXS1* (*Catharanthus roseus*; AGL40532), *CrDXS2A* (AJ011840), *CrDXS2B* (ABI35993), *GbDXS1* (*Ginkgo biloba*; AAS89341), *GbDXS2* (AAR95699), *HbDXS1* (*Hevea brasiliensis*; AAS94123), *HbDXS2* (ABF18929), *MtDXS1* (*Medicago truncatula*; CAD22530), *MtDXS2* (CAD22531), *OsDXS1* (*Oryza sativa*; O22567), *OsDXS2* (Q6YU51), *PaDXS1* (*Picea abies*; ABS50518), *PaDXS2A* (ABS50519), *PaDXS2B* (ABS50520), *PdDXS1* (*Pinus densiflora*; ACC54557), *PdDXS2* (ACC54554), *PgDXS1*, *PgDXS2A*, *PgDXS2B*, *PtcDXS1* (*Populus trichocarpa*; XP_002312717), *PtcDXS2-1* (XP_006380580), *PtcDXS2-2* (XP_006381844), *PtDXS1* (*Pinus taeda*; ACJ67021), *PtDXS2* (ACJ67020), *SlDXS1* (*Solanum lycopersicum*; CAZ66648), *SlDXS2* (CAZ66649), *SmDXS1* (*Salvia miltiorrhiza*; ACF21004), *SmDXS2* (ACQ66107), *SrDXS* (*Stevia rebaudiana*; CAD22155), *VvDXS1* (*Vitis vinifera*; XP_002277919), *VvDXS2* (XP_002271585), *ZmDXS1* (*Zea mays*; AFW77975), *ZmDXS2* (DAA59892).

4.2.2. Heterologous expression and functional characterization of spruce *DXS* genes

PgDXS1, *PgDXS2A* and *PgDXS2B* were individually expressed in *E.coli* to conduct *in vitro* enzyme assays to test function. To facilitate purification, the pET28b+ expression vector was used which facilitates the addition of an N-terminal polyhistidine tag onto each protein. SDS-PAGE and western blotting (with monoclonal anti-polyhistidine antibodies) were carried out to confirm expression and visualize the purity of the proteins (Figure 4.3). *PgDXS1* was expressed in *E. coli* at high levels and could be visualized via gel electrophoresis and western blotting as a single protein band. The monomeric molecular weight was calculated to be 71.4 kD. Both *PgDXS2A* and *PgDXS2B*, with monomer weights calculated to be 74.5 kD and 78.3 kD, respectively, were expressed at lower levels and could be visualized with some background *E. coli* protein. Western blotting confirmed a single enzyme band for both *PgDXS2A* and *PgDXS2B*.

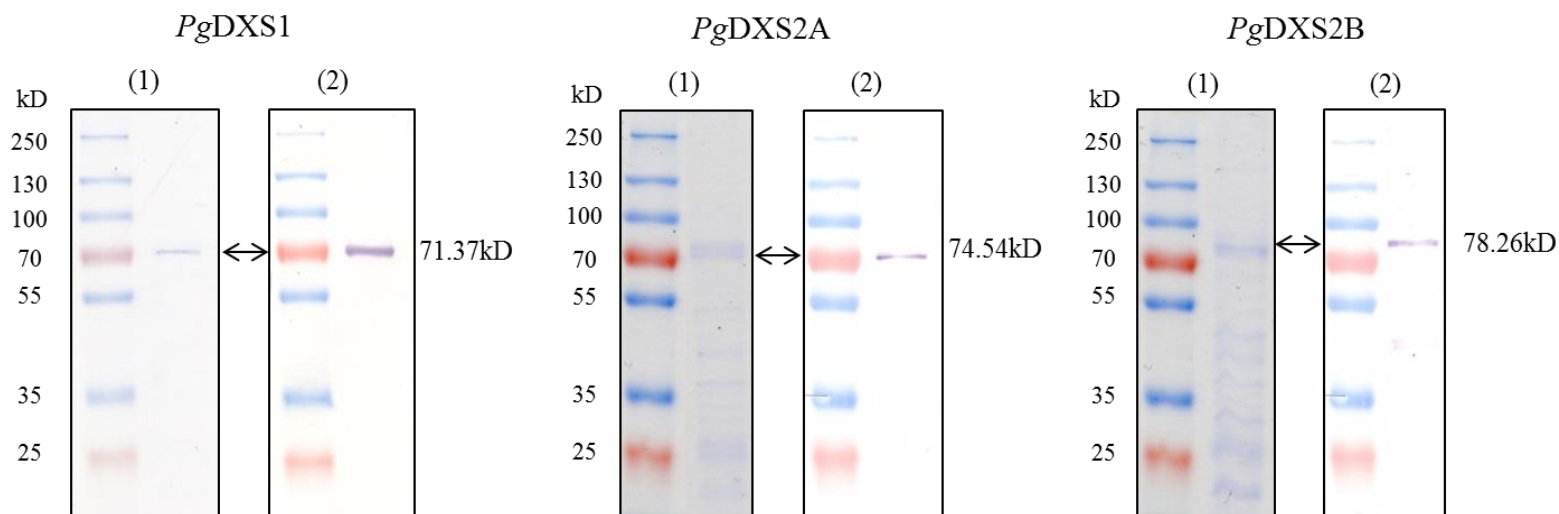


Figure 4.3. Polyacrylamide gel electrophoresis and corresponding Western blots showing the expression of three His-tag purified recombinant proteins from expression of recombinant white spruce DXS genes in *E. coli*: *PgDXS1*, *PgDXS2A*, and *PgDXS2B*. For each pair of gel images, the SDS-PAGE gel on the left (1) shows total protein stained with Coomassie blue dye and the gel image on the right (2) shows the immunoreactive band using monoclonal anti-polyHistidine-alkaline phosphatase antibodies. On each gel, molecular weight standards are shown in the left lane and sample protein in the right. The 2-headed arrow shows the position of the recombinant, 6x His-tagged protein. Molecular weight markers are Thermo Scientific, PageRuler Plus prestained protein ladder. Protein weights shown are calculated using average atomic masses of amino acids.

In vitro enzyme assays to confirm the function of *PgDXS1*, *PgDXS2A* and *PgDXS2B* enzymes were conducted individually and the predicted product, 1-deoxy-D-xylulose 5-phosphate (DXP), was observed by LC-MS. Each enzyme was incubated with its substrates, sodium pyruvate and glyceraldehyde 3-phosphate, and the cofactor thiamine pyrophosphate. Products of each enzyme assay were compared to a synthetic standard (Figure 4.4) and analyzed further by examining the corresponding mass spectra of the product peak. The results showed in all cases that the product produced in each assay was DXP, confirmed by the presence of characteristic ions 213, 139 and 97 also present in the synthetic standard. In addition, the retention times of the DXS products were identical to the standard at approximately 1.9 minutes (in the experiment shown in Figure 4.4) with the exception of *PgDXS2B* which produced a lower amount of DXP product than the other two spruce DXSs and thus the retention time was shifted slightly.

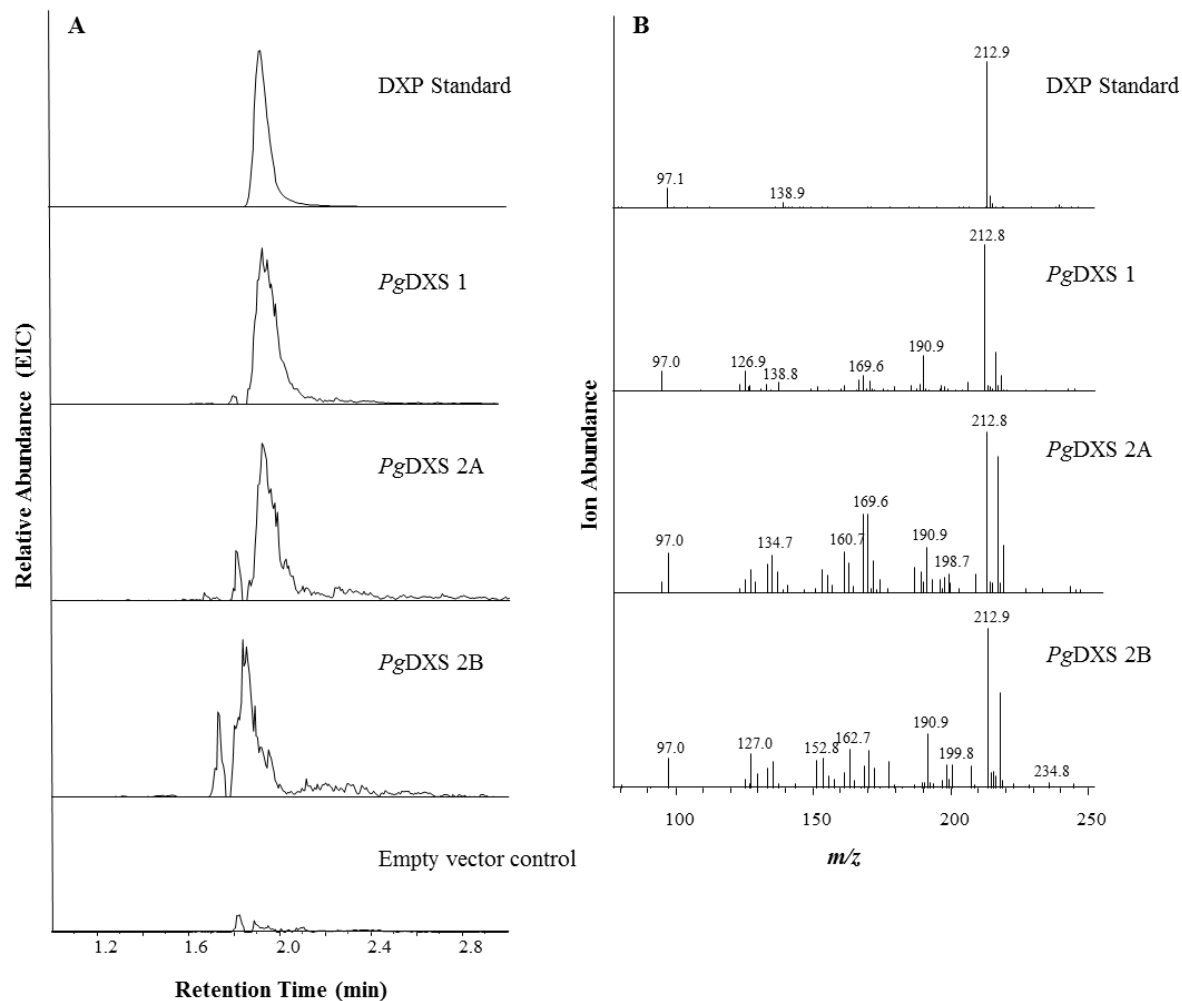


Figure 4.4. LC-MS analysis of *in vitro* assays with purified recombinant DXS proteins. (A) White spruce DXS enzymes (*PgDXS1*, *PgDXS2A* and *PgDXS2B*) were incubated with DL-glyceraldehyde 3-phosphate and thiamine pyrophosphate and analyzed on a Zorbax SB-C18 column (negative ESI mode, 213 m/z extracted-ion chromatograms). All white spruce DXS enzymes produced the predicted product DXP (1-deoxy D-xylulose 5-phosphate) which shared the same retention time as an authentic DXP standard (Sigma). (B) Mass spectrum of DXS enzyme assay product peaks compared to standard. m/z , Mass-to-charge ratio.

4.2.3. Relative expression of general and specialized related *DXS* genes in whole samples of developing spruce apical buds and shoots

Quantitative PCR was used to quantify transcript abundance of the three white spruce *DXS* genes, *PgDXS1*, *PgDXS2A*, *PgDXS2B*, over a one-year apical bud and apical shoot development time course, from January to December (Figure 2.1; Table 2.3). Transcript abundance levels are expressed relative to the expression of reference gene *eEF1 α* (\pm SEM). All genes analyzed showed significant changes in transcript abundance over the time course (Figure 4.5).

PgDXS1 transcript levels (Figure 4.5A) were significantly affected by time ($H(19)=57.533$, $N=79$, $P<0.0005$). Relative transcript levels of *PgDXS1* peaked in June at time point 14 and 15 (3.588 ± 0.689 and 3.981 ± 0.790 , respectively) but quickly fell by roughly half in the later part of June and early July. By the end of the year, transcripts fell significantly to their lowest levels at time point 23 in August and time point 29 in November (0.487 ± 0.043 and 0.352 ± 0.073 , respectively). Interestingly, transcript levels of *PgDXS1* exhibited a second increase as the trees entered autumn in late August (time points 24 and 25), before falling to a low and relatively constant level for the remainder of the year (Table 4.1).

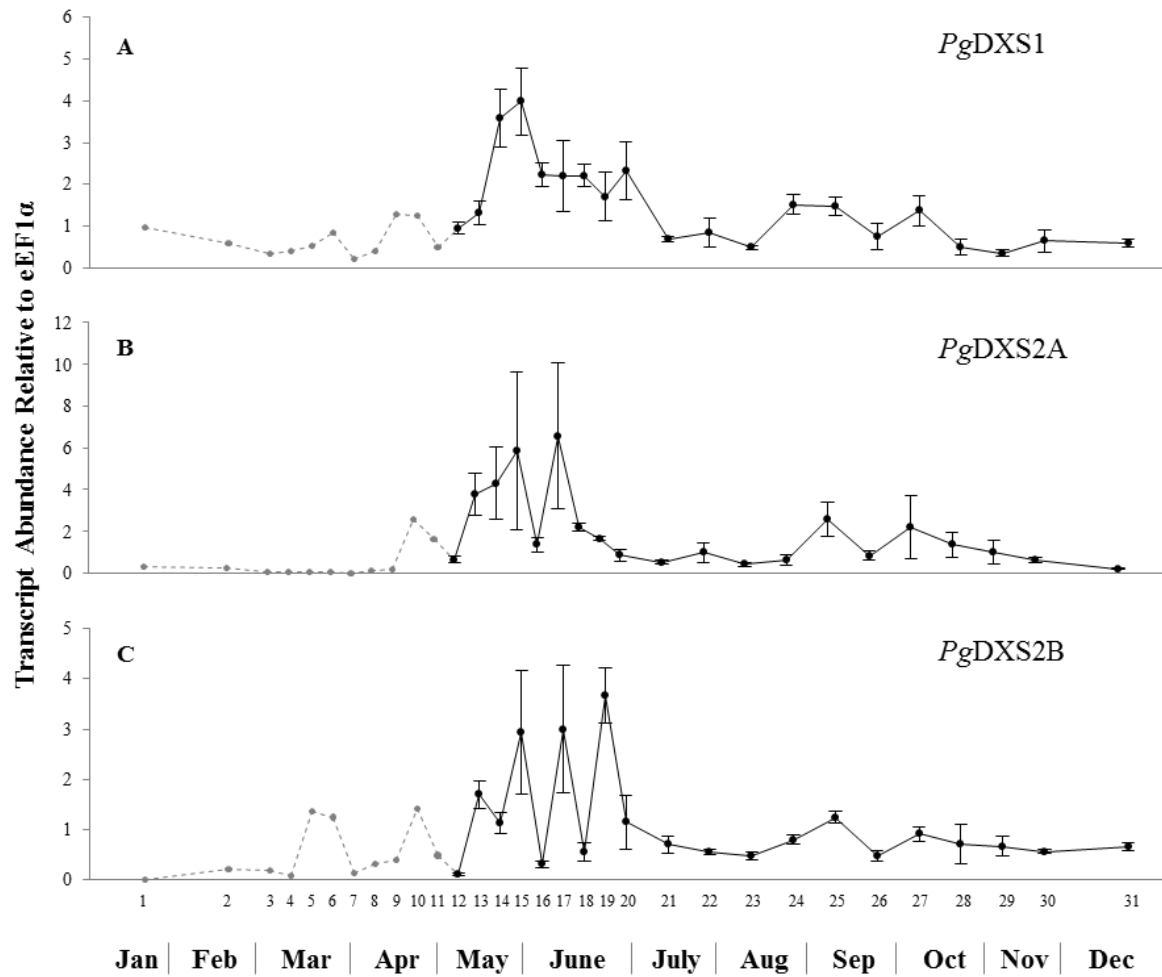


Figure 4.5. Relative transcript abundance of *DXS* genes in white spruce developing apical buds and shoots over a one-year time course. Transcript abundance was measured by real-time qPCR and expressed as relative to the reference gene *eEF1α*. Light gray dotted line (time points 1-11) represents values for pooled samples consisting of 4 individual biological replicates; samples were pooled due to limitations. Heavy black line (time points 12-31) shows data for 4 biological replicates, mean (\pm SEM). Transcript abundances of each gene were found to differ significantly over time, *PgDXS1* ($P < 0.0005$), *PgDXS2A* ($P < 0.0005$), and *PgDXS2B* ($P < 0.0005$). Data was statistically analyzed and means were separated using Kruskal-Wallis test statistic ($\alpha = 0.05$), see Table 4.1.

Gene of Interest	Time Point	Relative Transcript Abundance	
<i>PgDXS1</i> (<i>P</i> >0.0005)	12	0.953 ± 0.141	<i>bcdef</i>
	13	1.317 ± 0.281	<i>abcdef</i>
	14	3.588 ± 0.689	<i>a</i>
	15	3.981 ± 0.790	<i>a</i>
	16	2.231 ± 0.276	<i>ab</i>
	17	2.195 ± 0.845	<i>abc</i>
	18	2.204 ± 0.272	<i>ab</i>
	19	1.707 ± 0.593	<i>abcd</i>
	20	2.322 ± 0.704	<i>ab</i>
	21	0.688 ± 0.059	<i>ef</i>
	22	0.843 ± 0.355	<i>cdef</i>
	23	0.487 ± 0.043	<i>f</i>
	24	1.520 ± 0.247	<i>abcd</i>
	25	1.471 ± 0.230	<i>abcde</i>
	26	0.735 ± 0.315	<i>cdef</i>
	27	1.371 ± 0.356	<i>abcdef</i>
	28	0.510 ± 0.189	<i>def</i>
	29	0.352 ± 0.073	<i>f</i>
	30	0.641 ± 0.259	<i>cdef</i>
	31	0.587 ± 0.093	<i>cdef</i>
<i>PgDXS2A</i> (<i>P</i> >0.0005)	12	0.641 ± 0.169	<i>def</i>
	13	3.739 ± 1.009	<i>a</i>
	14	4.299 ± 1.746	<i>a</i>
	15	5.851 ± 3.754	<i>ab</i>
	16	1.346 ± 0.370	<i>abcde</i>
	17	6.574 ± 3.499	<i>a</i>
	18	2.206 ± 0.175	<i>abc</i>
	19	1.638 ± 0.097	<i>abcd</i>
	20	0.853 ± 0.287	<i>cdef</i>
	21	0.519 ± 0.114	<i>def</i>
	22	0.982 ± 0.468	<i>bcdef</i>
	23	0.409 ± 0.111	<i>ef</i>
	24	0.612 ± 0.245	<i>def</i>
	25	2.568 ± 0.801	<i>abc</i>
	26	0.829 ± 0.208	<i>bcdef</i>
	27	2.204 ± 1.519	<i>abcd</i>
	28	1.368 ± 0.596	<i>abcdef</i>
	29	0.980 ± 0.560	<i>cdef</i>
	30	0.628 ± 0.107	<i>cdef</i>
	31	0.200 ± 0.026	<i>f</i>
<i>PgDXS2B</i> (<i>P</i> >0.0005)	12	0.090 ± 0.026	<i>g</i>
	13	1.693 ± 0.276	<i>abc</i>
	14	1.118 ± 0.213	<i>abcde</i>
	15	2.938 ± 1.234	<i>abc</i>
	16	0.301 ± 0.071	<i>fg</i>
	17	2.997 ± 1.270	<i>ab</i>
	18	0.557 ± 0.184	<i>efg</i>
	19	3.665 ± 0.548	<i>a</i>
	20	1.140 ± 0.541	<i>abcde</i>
	21	0.695 ± 0.170	<i>cdefg</i>
	22	0.547 ± 0.050	<i>defg</i>
	23	0.475 ± 0.081	<i>efg</i>
	24	0.796 ± 0.102	<i>abcde</i>
	25	1.234 ± 0.118	<i>abcd</i>
	26	0.471 ± 0.104	<i>efg</i>
	27	0.908 ± 0.143	<i>abcde</i>
	28	0.705 ± 0.389	<i>defg</i>
	29	0.663 ± 0.195	<i>bcdefg</i>
	30	0.554 ± 0.039	<i>defg</i>
	31	0.664 ± 0.079	<i>bcdef</i>

Table 4.1. Relative transcript abundance of DXS genes related to DRA and GA biosynthesis in white spruce developing apical buds and shoots over a year-long time course. Data are expressed as relative transcript abundance to reference gene *eEF1a* (± SEM). Different letters within each gene indicate significantly different means separated by the Kruskal-Wallis test statistic ($\alpha=0.05$).

PgDXS2A transcript levels (Figure 4.5B) were also significantly affected by time over the course of apical bud and shoot development ($H(19)=49.559$, $N=73$, $P<0.0005$). Relative transcript levels rose steeply from near zero levels in the first four months of the year to reach a general peak in June at time points 15 and 17 (5.851 ± 3.754 and 6.574 ± 3.499 , respectively). After this, transcript abundances fell significantly for the remainder of the summer months. In September, transcript levels rose to a second peak (2.568 ± 0.801 at time point 25), before descending again to near zero levels in December (0.200 ± 0.026) (Table 4.1).

PgDXS2B expression was also significantly affected by time ($H(19)=53.750$, $N=75$, $P<0.0005$) (Figure 4.5C). The highest relative transcript levels were seen in late June at time point 19 (3.665 ± 0.548), however transcript levels at time points 15 and 17 were not significantly different from this peak (3.665 ± 0.548 and 2.997 ± 1.270 , respectively). During the month of June, transcript levels fluctuated dramatically from the highest levels to low levels; e.g. at time point 16 and 18 values were just 0.301 ± 0.071 and 0.557 ± 0.184 , respectively, values that were not significantly different from those in the winter months. As with other *PgDXS*s, transcript levels of *PgDXS2B* showed a second peak of expression at time point 25 (1.234 ± 0.118), before descending to low levels in the fall and winter months (October-December) (Table 4.1).

4.2.4. Expression of *DXS* genes in white spruce stems, needles and new buds during apical bud and shoot development

The relative transcript abundance of the three white spruce *DXS* genes (*PgDXS1*, *PgDXS2A* and *PgDXS2B*) was assessed in different sample parts (N, needles; S, stem; NB,

new buds) over 8 time points (time points 11, 13, 15, 17, 19, 21, 23 and 25) that focused on the spring/summer portion of the year-long time course of apical bud and shoot development. Transcript abundance was expressed relative to the reference gene *eEF1 α* (\pm SEM) (Figure 4.6). Within the data for each gene, statistical analyses were run to determine the effects of this experiment's main factors (time and sample part), as well as the interactions between the factors.

PgDXS1 mean transcript levels, calculated by including relative transcript data for all time points and sample parts, were significantly affected by time ($P<0.0005$) (Figure 4.7A; Table 4.2), with time point 15 showing the highest mean transcript abundance (4.613 ± 2.194). *PgDXS1* mean transcript levels were also affected by sample part ($P<0.0005$) (Figure 4.7D). The mean transcript abundance was highest in needles (2.889 ± 0.683), which was more than double that of stem (1.011 ± 0.138) and over seven-fold higher than mean transcript levels in new buds (0.393 ± 0.072). *PgDXS1* relative transcript abundances were also significantly affected by the interaction between sample part and time ($P<0.0005$) (Figure 4.6A). All three sample parts showed significant differences in relative transcript abundance over time (N: $P=0.016$, S: $P=0.001$ and NB: $P=0.002$) (Table 4.2). *PgDXS1* transcripts in needles rose to a peak at time point 19 in June (3.765 ± 1.009), declined quickly to a low at time point 23 (1.425 ± 0.142) but rebounded again at point 25 (2.893 ± 0.220), this value being not significantly different from the peak transcript abundance (Table 4.3). Transcript levels in stem reached a peak at time point 15 in May (2.350 ± 0.430) which was earlier than in needles. *PgDXS1* levels then fell to a relatively constant level in stem from June to September. New young bud transcript levels of *PgDXS1* were the lowest overall and remained at a relatively constant level throughout.

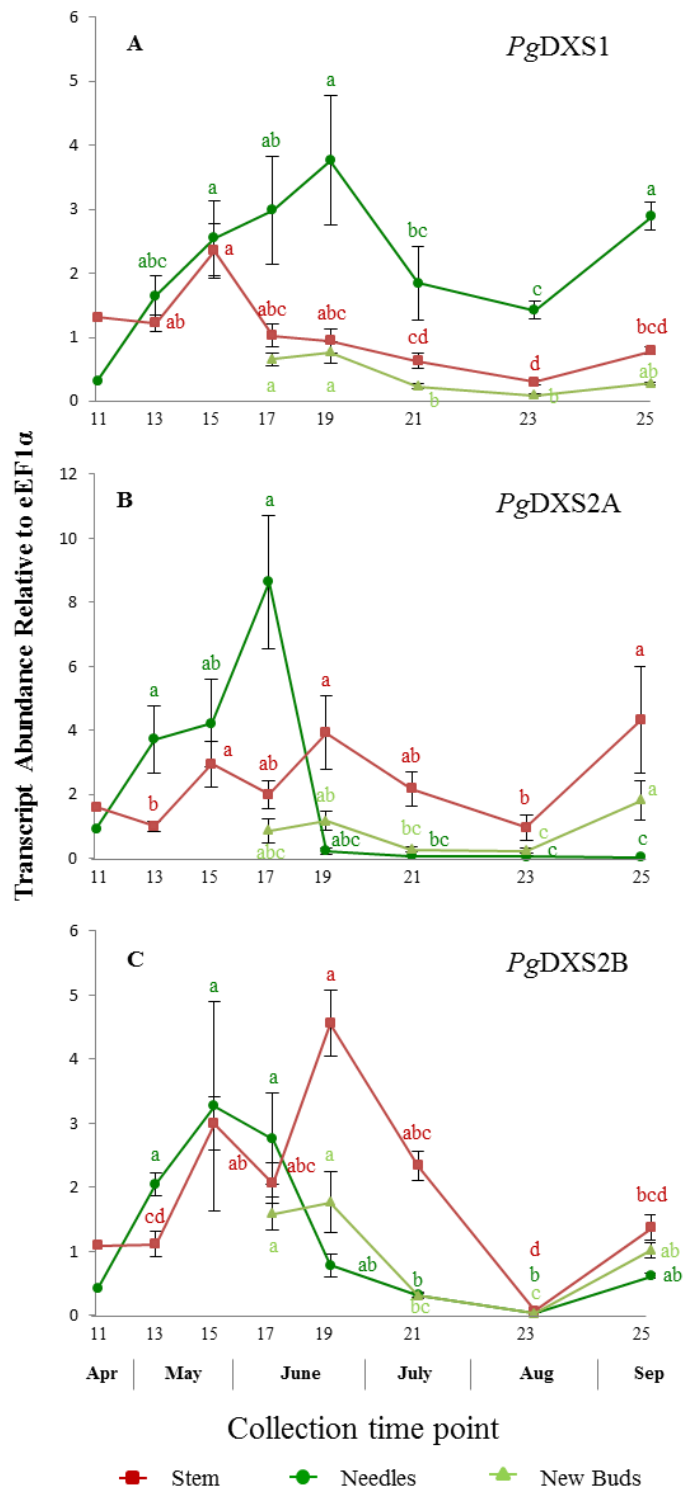


Figure 4.6. Relative transcript abundance of *PgDXS* in different parts of white spruce developing apical buds and apical shoots. Apical bud or apical shoot samples were separated into 2 or 3 sample parts (needles, stem, new buds) based on developmental stage; new buds appeared (as observed by eye) at time point 17. Transcript abundance was measured by real-time qPCR and expressed as relative to the reference gene *eEF1a*. Data represent the mean (\pm SEM) of 4 biological replicates except for point 11 that is a pooled sample of the 4 replicates (due to limitations). Transcript abundance levels of *PgDXS1* were found to differ significantly over time in all sample parts (needles, $P=0.001$; stem, $P=0.002$; new buds, $P=0.016$), as did transcript levels of *PgDXS2A* (needles, $P=0.048$; stem, $P=0.025$; new buds, $P=0.001$), and transcript levels of *PgDXS2B* (needles, $P=0.001$; stem, $P=0.003$; new buds, $P=0.001$). Letters signify means separated by the Kruskal-Wallis test statistic ($\alpha=0.05$).

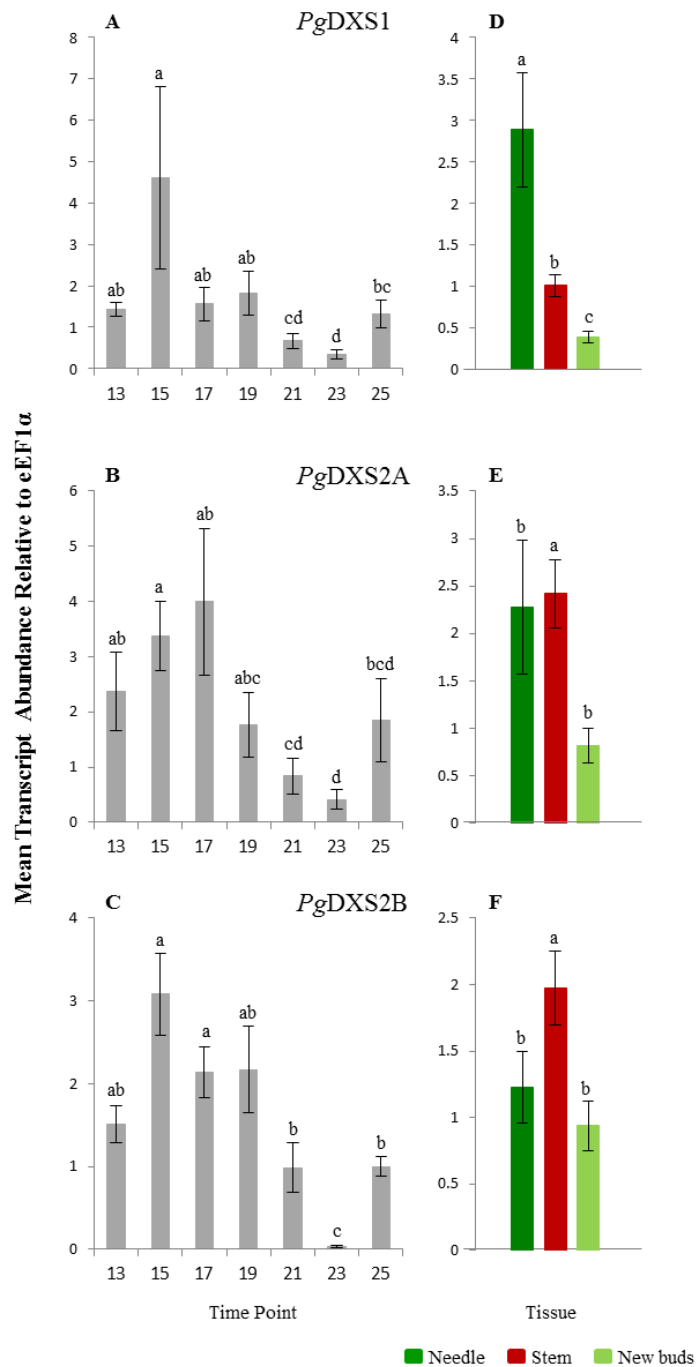


Figure 4.7. Mean relative transcript abundance of *PgDXS* genes in a white spruce developing apical buds and apical shoots over a time course separated by time point and sample part. Transcript abundance was measured by real-time qPCR and expressed as relative to the reference gene *eEF1α*. Over time significant differences of transcript levels were seen in *PgDXS1* ($P<0.0005$), *PgDXS2A* ($P=0.001$), and *PgDXS2B* ($P<0.0005$) (A,B,C); mean transcript abundances reflect all sample parts per time point. Between sample parts, significant differences of transcript levels were reported for *PgDXS1* ($P<0.0005$), *PgDXS2A* ($P=0.003$), and *PgDXS2B* ($P=0.016$) (D,E,F); mean abundances represent all time points per sample part, and differences between time points are not considered. Error bars represent the standard error of the mean and different letters indicate significantly different means separated by the Kruskal-Wallis test statistic ($\alpha=0.05$).

Table 4.2. Statistical results based on analysis of relative transcript abundance of *DXS* genes in white spruce developing apical buds and apical shoots over a year-long time course. Statistical data obtained by analysis with Kruskal-Wallis test statistic ($\alpha=0.05$). These results pertain to Figure 4.6 and Figure 4.7.

Gene of Interest	Factor or Interaction	
<i>PgDXS1</i>	Sample part	H(2)=34.990, N=76, $P<0.0005$
	Time	H(6)=32.761, N=76, $P<0.0005$
	Sample part x Time	H(18)=63.368, N=76, $P<0.0005$
	Needle Time	H(6)=15.562, N=28, $P=0.016$
	Stem Time	H(6)=21.724, N=28, $P=0.001$
	New Buds Time	H(4)=16.471, N=20, $P=0.002$
<i>PgDXS2A</i>	Sample part	H(2)=11.739, N=71, $P=0.003$
	Time	H(6)=22.526, N=71, $P=0.001$
	Sample part x Time	H(18)=60.389, N=71, $P<0.0005$
	Needle Time	H(6)=21.675, N=26, $P=0.001$
	Stem Time	H(6)=12.695, N=26, $P=0.048$
	New Buds Time	H(4)=11.150, N=19, $P=0.025$
<i>PgDXS2B</i>	Sample part	H(2)=8.254, N=71, $P=0.016$
	Time	H(6)=42.966, N=71, $P<0.0005$
	Sample part x Time	H(18)=62.845, N=71, $P<0.0005$
	Needle Time	H(6)=21.982, N=25, $P=0.001$
	Stem Time	H(6)=22.091, N=26, $P=0.001$
	New Buds Time	H(4)=15.726, N=20, $P=0.003$

Gene of Interest	Sample Part	Time point	Relative Transcript Abundance	
<i>PgDXS1</i>	Needles	13	1.653 ± 0.303	abc
		15	2.552 ± 0.589	a
		17	2.991 ± 0.844	ab
		19	3.765 ± 1.009	a
		21	1.847 ± 0.576	bc
		23	1.425 ± 0.142	c
		25	2.893 ± 0.220	a
	Stem	13	1.228 ± 0.128	ab
		15	2.350 ± 0.430	a
		17	1.030 ± 0.176	abc
		19	0.943 ± 0.181	abc
		21	0.630 ± 0.116	cd
		23	0.300 ± 0.037	d
		25	0.787 ± 0.057	bcd
	New buds	17	0.659 ± 0.096	a
		19	0.766 ± 0.166	a
		21	0.237 ± 0.045	b
		23	0.098 ± 0.020	b
		25	0.281 ± 0.020	ab
<i>PgDXS2A</i>	Needles	13	3.719 ± 1.048	a
		15	4.220 ± 1.373	ab
		17	8.630 ± 2.079	a
		19	0.230 ± 0.101	abc
		21	0.061 ± 0.004	bc
		23	0.047 ± 0.028	c
		25	0.021 ± 0.014	c
	Stem	13	1.006 ± 0.154	b
		15	2.939 ± 0.700	a
		17	1.987 ± 0.421	ab
		19	3.911 ± 1.149	a
		21	2.171 ± 0.540	ab
		23	0.963 ± 0.404	b
		25	4.324 ± 1.678	a
	New buds	17	0.857 ± 0.388	abc
		19	1.159 ± 0.299	ab
		21	0.273 ± 0.076	bc
		23	0.226 ± 0.086	c
		25	1.812 ± 0.602	a
<i>PgDXS2B</i>	Needles	13	2.043 ± 0.180	a
		15	3.263 ± 1.629	a
		17	2.755 ± 0.717	a
		19	0.778 ± 0.181	ab
		21	0.315 ± 0.032	b
		23	0.023 ± 0.023	b
		25	0.613 ± 0.032	ab
	Stem	13	1.108 ± 0.197	cd
		15	2.990 ± 0.411	ab
		17	2.057 ± 0.317	abc
		19	4.559 ± 0.512	a
		21	2.340 ± 0.228	abc
		23	0.062 ± 0.023	d
		25	1.367 ± 0.203	bcd
	New buds	17	1.585 ± 0.260	a
		19	1.763 ± 0.470	a
		21	0.299 ± 0.046	bc
		23	0.021 ± 0.014	c
		25	1.013 ± 0.119	ab

Table 4.3. Relative transcript abundance of *DXS* genes in white spruce developing apical buds and shoots over a year-long time course. Data are expressed as relative transcript abundance to reference gene *eEF1α* (± SEM). Different letters within each gene indicate significantly different means separated by the Kruskal-Wallis test statistic ($\alpha=0.05$). This data pertains to Figure 4.6.

Mean relative transcript levels of *PgDXS2A* were significantly affected by time ($P=0.001$) (Figure 4.7B; Table 4.2), with mean transcript levels being highest at time points 15 and 17 (3.366 ± 0.628 and 3.992 ± 1.322 , respectively) with the lowest values at points 21 and 23 (0.835 ± 0.329 and 0.412 ± 0.173 , respectively). *PgDXS2A* mean transcript levels were also significantly affected by sample part ($P=0.003$) (Figure 4.7E); the mean transcript abundance in stem and needles were each nearly triple that of new buds. As well, mean transcript levels were significantly affected by the interaction between sample part and time ($P<0.0005$) (Figure 4.6B). Within sample parts, transcript levels of *PgDXS2A* showed the largest changes in needle samples over time ($P=0.001$), rising to a peak at time point 17 in June (8.630 ± 2.079) but falling sharply by over 35-fold by the next time point to remain at a constant low level (Table 4.3). *PgDXS2A* transcripts in stem were also affected over the time course ($P=0.048$); transcripts fluctuated slightly reaching defined peaks at time points 19 and 25 (3.911 ± 1.149 and 4.324 ± 1.678 , respectively). Transcript abundance in new buds was lowest overall, however changes over time were significant ($P=0.025$), levels mirrored those of stem samples showing peaks at time points 19 and 25 (1.159 ± 0.299 and 1.812 ± 0.602 , respectively) (Table 4.3).

PgDXS2B mean relative transcript levels were significantly affected by time ($P<0.0005$) (Figure 4.7C; Table 4.2), with mean transcript levels being highest at time point 15 (3.081 ± 0.498). Levels fell significantly lower by time point 21 and were lowest at time point 23 (0.035 ± 0.012). Mean *PgDXS2B* transcript levels were also significantly affected by sample part ($P=0.016$), with the mean abundances being highest in stem samples (1.974 ± 0.276) and both needle and new buds having significantly lower mean relative abundances (1.223 ± 0.268 and 0.936 ± 0.186 , respectively). Mean relative transcript levels were also

significantly affected by the interaction between sample part and time ($P < 0.0005$) (Figure 4.6C). Within sample parts, needles, stem and new buds all showed significant differences in relative transcript abundance over time ($P = 0.001$, $P = 0.001$ and $P = 0.003$, respectively) (Table 4.2). Needle transcript levels peaked over time points 13, 15 and 17 (2.043 ± 0.180 , 3.263 ± 1.629 , 2.755 ± 0.717 , respectively) which roughly corresponds to early summer (Figure 4.6C). *PgDXS2B* transcript levels fell significantly to near zero by time point 23 (0.023 ± 0.023) in late summer, later showing a slight uptick in abundance by time point 25, representing approximately 18% of the highest value at time point 15. In stem, transcript levels rose steadily to a peak abundance at time point 19 (4.559 ± 0.512) in late June. Several weeks later at time point 23 transcript levels of *PgDXS2B* had fallen steadily to near zero levels (0.062 ± 0.023) but, as in the needle sample part, there was a slight uptick in transcript abundance at time point 25, representing approximately 30% of maximum value at time point 19 (Table 4.3). *PgDXS2B* transcript abundance in new buds showed the least variation over the time course, but abundance levels were highest at the initial two sampling points 17 and 19 (1.585 ± 0.260 and 1.763 ± 0.470 , respectively) when new buds emerged. Transcript abundance fell by time point 23 (0.021 ± 0.014) in mid-August but showed an uptick at time point 25 to a value over 50% of the initial peak.

4.2.5. Effect of MeJA treatment and time on transcript abundance of *DXS* genes in different sample types of white spruce

Real-time quantitative PCR was used to measure transcript abundance of the three white spruce *DXS* genes, *PgDXS1*, *PgDXS2A*, *PgDXS2B*, in response to MeJA treatment (or Tween control) in 5 sample types over a 30-day time course. Samples were as follows:

bark/phloem (B), wood/xylem (X), young needles (YN), mature needles (MN), young stems (YS). Transcript abundance levels were expressed relative to the transcript levels of the normalizing genes *eIF4E* and *H3* (\pm SEM). Within the data for each gene, statistical analyses were run to determine the effects of this experiment's main factors: time, sample type, and treatment type, as well as the interactions between these factors.

PgDXS1

Combining data for all 5 sample types, *PgDXS1* transcript levels were found to differ significantly by factors of sample type ($P < 0.0005$), treatment type ($P = 0.008$) and time ($P = 0.021$). Interactions between all factors were found to have a significant effect on *PgDXS1* transcript levels: sample x treatment ($P < 0.0005$), sample x time ($P < 0.0005$), treatment x time ($P = 0.019$) and sample x treatment x time ($P < 0.0005$), see Table 4.4 for detailed statistical analysis results.

In this experiment, *PgDXS1* transcript abundances were found to differ significantly due to the interaction of sample type and treatment type factors ($P < 0.0005$) (Figure 4.8A). In this analysis of means, the differences between time points were not considered. The highest mean transcript abundance was found in MeJA-treated YS (3.570 ± 0.920), however in this sample type there was no significant difference between mean transcript levels in control versus MeJA treatment. Three sample types showed significant differences in the mean transcript abundance of *PgDXS1* between MeJA and control treatments, these being B, X and MN, with the largest difference in the B sample type where MeJA mean transcript levels

were over 5-fold higher than control. Mean transcript abundance in the control treatment was higher than MeJA only in the MN sample, being 1.6-fold higher.

Table 4.4. Statistical results based on analysis of relative transcript abundance of *DXS* genes in control or MeJA-treated samples from white spruce. Statistical data obtained by analysis with Kruskal-Wallis test statistic ($\alpha=0.05$); for ease of interpretation light grey text shows statistical results that are not significant. These results pertain to Figures 4.8, 4.9, 4.10, and 4.11.

Gene of Interest	Factor or Interaction	
<i>PgDXS1</i>	Sample	H(4)=87.326, N=250, $P<0.0005$
	Treatment	H(1)=7.064, N=250, $P=0.008$
	Time	H(6)=14.887, N=250, $P=0.021$
	Sample x Treatment	H(9)=114.159, N=250, $P<0.0005$
	Sample x Time	H(33)=125.861, N=250, $P<0.0005$
	Treatment x Time	H(12)=24.216, N=250, $P=0.019$
	Sample x Treatment x Time	H(63)=173.014, N=250, $P<0.0005$
	Young Needles Treatment x Time	H(12)=18.276, N=52, $P=0.108$
	Mature Needles Treatment x Time	H(12)=19.119, N=51, $P=0.086$
	Bark/Phloem Treatment x Time	H(12)=30.782, N=51, $P=0.002$
	Wood/Xylem Treatment x Time	H(12)=25.692, N=48, $P=0.012$
	Young Stems Treatment x Time	H(11)=24.635, N=48, $P=0.010$
<i>PgDXS2A</i>	Sample	H(4)=142.362, N=250, $P<0.0005$
	Treatment	H(1)=16.980, N=250, $P<0.0005$
	Time	H(6)=8.547, N=250, $P=0.201$
	Sample x Treatment	H(9)=180.161, N=250, $P<0.0005$
	Sample x Time	H(33)=188.538, N=250, $P<0.0005$
	Treatment x Time	H(12)=23.941, N=250, $P=0.021$
	Sample x Treatment x Time	H(63)=228.362, N=250, $P<0.0005$
	Young Needles Treatment x Time	H(12)=41.850, N=52, $P<0.0005$
	Mature Needles Treatment x Time	H(12)=9.495, N=51, $P=0.660$
	Bark/Phloem Treatment x Time	H(12)=38.451, N=51, $P<0.0005$
	Wood/Xylem Treatment x Time	H(12)=36.362, N=48, $P<0.0005$
	Young Stems Treatment x Time	H(11)=26.628, N=48, $P=0.005$
<i>PgDXS2B</i>	Sample	H(4)=87.546, N=248, $P<0.0005$
	Treatment	H(1)=39.125, N=248, $P<0.0005$
	Time	H(6)=23.280, N=248, $P=0.001$
	Sample x Treatment	H(9)=174.138, N=248, $P<0.0005$
	Sample x Time	H(33)=122.410, N=248, $P<0.0005$
	Treatment x Time	H(12)=56.960, N=248, $P<0.0005$
	Sample x Treatment x Time	H(63)=214.488, N=248, $P<0.0005$
	Young Needles Treatment x Time	H(12)=32.017, N=51, $P=0.001$
	Mature Needles Treatment x Time	H(12)=20.231, N=51, $P=0.063$
	Bark/Phloem Treatment x Time	H(12)=42.529, N=51, $P<0.0005$
	Wood/Xylem Treatment x Time	H(12)=40.256, N=48, $P<0.0005$
	Young Stems Treatment x Time	H(11)=15.994, N=47, $P=0.141$

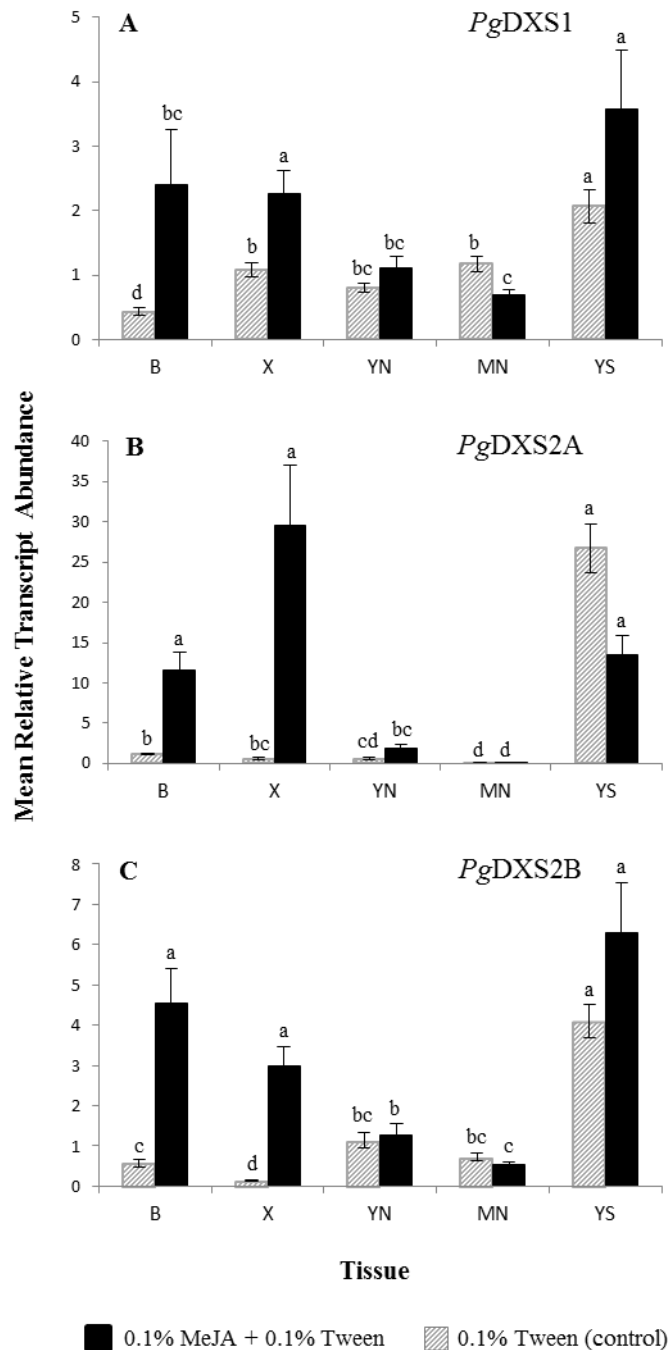


Figure 4.8. Mean relative transcript abundance over MeJA treatment and sample type in white spruce. The interaction between sample and treatment factors was shown to have a significant effect on the expression profile of *PgDXS1* (A, $P < 0.0005$), *PgDXS2A* (B, $P < 0.0005$), and *PgDXS2B* (C, $P < 0.0005$). Differences between time points are not considered, mean transcript abundances reflect all time points per sample and treatment type. Error bars represent the standard error of the mean and different letters indicate significantly different means separated by the Kruskal-Wallis test statistic. Sample types are as follows: bark/phloem (B), wood/xylem (X), young needles (YN), mature needles (MN), young stems (YS). Transcript abundance was measured by real-time qPCR, normalized to reference genes *eIF4E* and *H3*.

PgDXS1 transcript levels also differed significantly with the interaction of sample, treatment and time ($P < 0.0005$). To further elucidate these interactions data was separated into sample types and significance was analyzed between the interaction of treatment and time within each sample type (Figure 4.9). No significant difference was observed in the interaction between treatment type and time in YN ($P = 0.108$) and MN ($P = 0.086$) samples. Significant differences in transcript abundance due to the interaction of treatment and time were observed in sample types B ($P = 0.002$), X ($P = 0.012$), YS ($P = 0.010$) (Table 4.4).

For the B sample type, *PgDXS1* transcript abundance in the MeJA treatment was significantly higher (approximately 20-fold) than the control at day 2 (Figure 4.9C; Table 4.5). After this, transcript levels in MeJA-treated B sample fell to low levels by day 4, matching that of control. Transcript levels from both MeJA treatment and control remained very low and stable for the remainder of the time course.

In the X sample type, transcript levels of *PgDXS1* were affected by MeJA treatment, rising quickly to peak at day 8, essentially doubling levels from the previous sampling point (Figure 4.9D; Table 4.5). At their peak on day 8, transcript levels in MeJA-treated X sample were 3-fold higher than control and remained significantly higher than controls at day 16 (approximately 3.5-fold higher). Over the time course, transcript levels in the control treatment did not remain absolutely constant but showed a significant but small increase at day 4. Control transcript levels dropped again by day 16 to a value that was not significantly different from day 0.

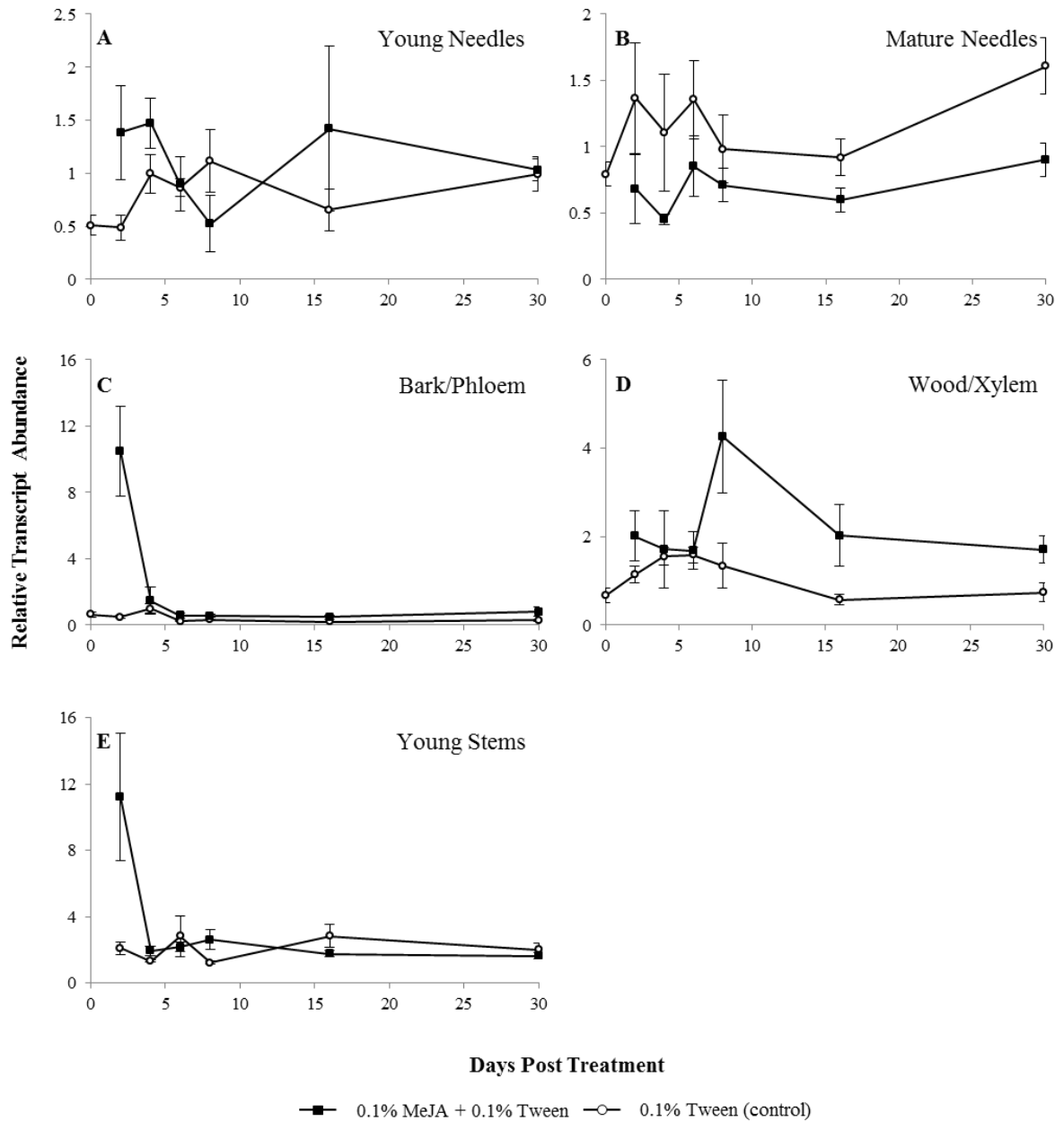


Figure 4.9. Relative transcript abundance of *PgDXSI* in white spruce samples in response to MeJA treatment over a time course. Transcript abundance was measured by real-time qPCR, normalized to transcript levels of reference genes *eIF4E* and *H3*. Samples analyzed were: (A) young needles, (B) mature needles, (C) bark/phloem, (D) wood/xylem, (E) young stems. Data are means of 3-4 biological replicates at each time point; error bars represent standard error of the mean. Data was statistically analyzed and means were separated using Kruskal-Wallis test statistic ($\alpha=0.05$), see Table 4.5.

Table 4.5. Relative transcript abundance of *PgDXS1* in control or MeJA-treated samples from white spruce. Contents are expressed as relative transcript abundance to reference genes *eIF4E* and *H3* (\pm SEM). Different letters within control and MeJA columns indicate significantly different means separated by the Kruskal-Wallis test statistic ($\alpha=0.05$); p-values indicate significance of interaction between time and treatment.

Gene of Interest	Sample	Day	Control	MeJA
<i>PgDXS1</i>	Young Needles (<i>P</i> =0.108)	0	0.511 ± 0.093	
		2	0.489 ± 0.117	1.385 ± 0.442
		4	0.995 ± 0.184	1.471 ± 0.236
		6	0.864 ± 0.081	0.897 ± 0.257
		8	1.114 ± 0.297	0.523 ± 0.265
		16	0.658 ± 0.196	1.421 ± 0.775
		30	0.992 ± 0.163	1.032 ± 0.106
	Mature Needles (<i>P</i> =0.086)	0	0.794 ± 0.092	
		2	1.366 ± 0.415	0.682 ± 0.258
		4	1.107 ± 0.441	0.452 ± 0.042
		6	1.354 ± 0.297	0.853 ± 0.228
		8	0.982 ± 0.255	0.711 ± 0.126
		16	0.920 ± 0.140	0.598 ± 0.090
		30	1.608 ± 0.212	0.903 ± 0.127
	Bark/Phloem (<i>P</i> =0.002)	0	0.631 ± 0.131	<i>abcd</i>
		2	0.490 ± 0.105	<i>bcde</i>
		4	0.983 ± 0.289	<i>ab</i>
		6	0.251 ± 0.044	<i>de</i>
		8	0.320 ± 0.032	<i>cde</i>
		16	0.189 ± 0.030	<i>e</i>
		30	0.300 ± 0.050	<i>cde</i>
	Wood/Xylem (<i>P</i> =0.012)	0	0.672 ± 0.164	<i>cd</i>
		2	1.143 ± 0.180	<i>bcd</i>
		4	1.555 ± 0.207	<i>ab</i>
		6	1.584 ± 0.176	<i>abc</i>
		8	1.345 ± 0.506	<i>bcd</i>
		16	0.578 ± 0.129	<i>d</i>
		30	0.742 ± 0.204	<i>bcd</i>
	Young Stems (<i>P</i> =0.010)	2	2.124 ± 0.390	<i>bc</i>
		4	1.333 ± 0.068	<i>cd</i>
		6	2.840 ± 1.225	<i>bcd</i>
		8	1.256 ± 0.099	<i>d</i>
		16	2.848 ± 0.705	<i>ab</i>
		30	2.029 ± 0.410	<i>bcd</i>

In YS, *PgDXS1* transcript abundance in the MeJA treatment peaked at day 2, which represented a 5-fold increase over controls (Figure 4.9E; Table 4.5). Transcript levels fell significantly by day 4 to a level not different from the control treatment and remained low until the end of the time course.

PgDXS2A

Combining data for all 5 sample types, transcript abundance levels of *PgDXS2A* were found to differ significantly by factors of sample type ($P < 0.0005$), treatment type ($P < 0.0005$) and time ($P = 0.201$). Interactions between all factors had a significant effect on *PgDXS2A* transcript levels: sample x treatment ($P < 0.0005$), sample x time ($P < 0.0005$), treatment x time ($P = 0.021$) and sample x treatment x time ($P < 0.0005$); see Table 4.4 for detailed statistical analysis results.

PgDXS2A transcript abundances were found to differ significantly due to the interaction of sample and treatment factors ($P < 0.0005$) (Figure 4.8B). In this analysis of means, the differences between time points were not considered. The highest mean transcript abundance was found in MeJA-treated X (29.640 ± 7.330), however this was not significantly different from the means of MeJA-treated B and both control and MeJA-treated YS. In the YS sample type there was no significant difference between mean transcript levels in control versus MeJA treatment (26.740 ± 3.067 and 13.433 ± 2.456 , respectively). Only two sample types showed significant differences in the mean transcript abundance of *PgDXS2A* between MeJA treatment and controls, these being B and X, with the largest difference being in the X sample type where MeJA mean transcript levels were

approximately 50-fold higher than control. In the B sample type, MeJA-treated mean transcript levels were almost 10-fold higher than controls. The lowest overall mean transcript values were found in MN samples where there was no significant difference between the control and MeJA treatment (0.093 ± 0.031 and 0.082 ± 0.027 , respectively).

Transcript levels of *PgDXS2A* were also found to differ significantly with the interaction of sample, treatment and time ($P < 0.0005$). To further elucidate these interactions data was separated into sample types and significance was analyzed between the interaction of treatment and time within each sample type (Figure 4.10). No significant difference was observed in the interaction between treatment type and time in the MN sample type ($P = 0.660$). However, significant differences in transcript abundance due to the interaction of treatment and time were observed in YN ($P < 0.0005$), B ($P < 0.0005$), X ($P < 0.0005$) and YS ($P = 0.005$) samples (Table 4.4).

In YN, *PgDXS2A* transcript levels in the MeJA treatment were significantly higher than control at day 6 (5.040 ± 1.489 and 0.946 ± 0.356 , respectively), an approximate 5-fold increase in abundance (Figure 4.10A). Although they dropped by more than half by day 8, transcript levels in MeJA-treated YN were still significantly higher than controls (Table 4.6). *PgDXS2A* transcript abundances from both treatment types fell to their lowest point, near zero, by days 16 and 30.

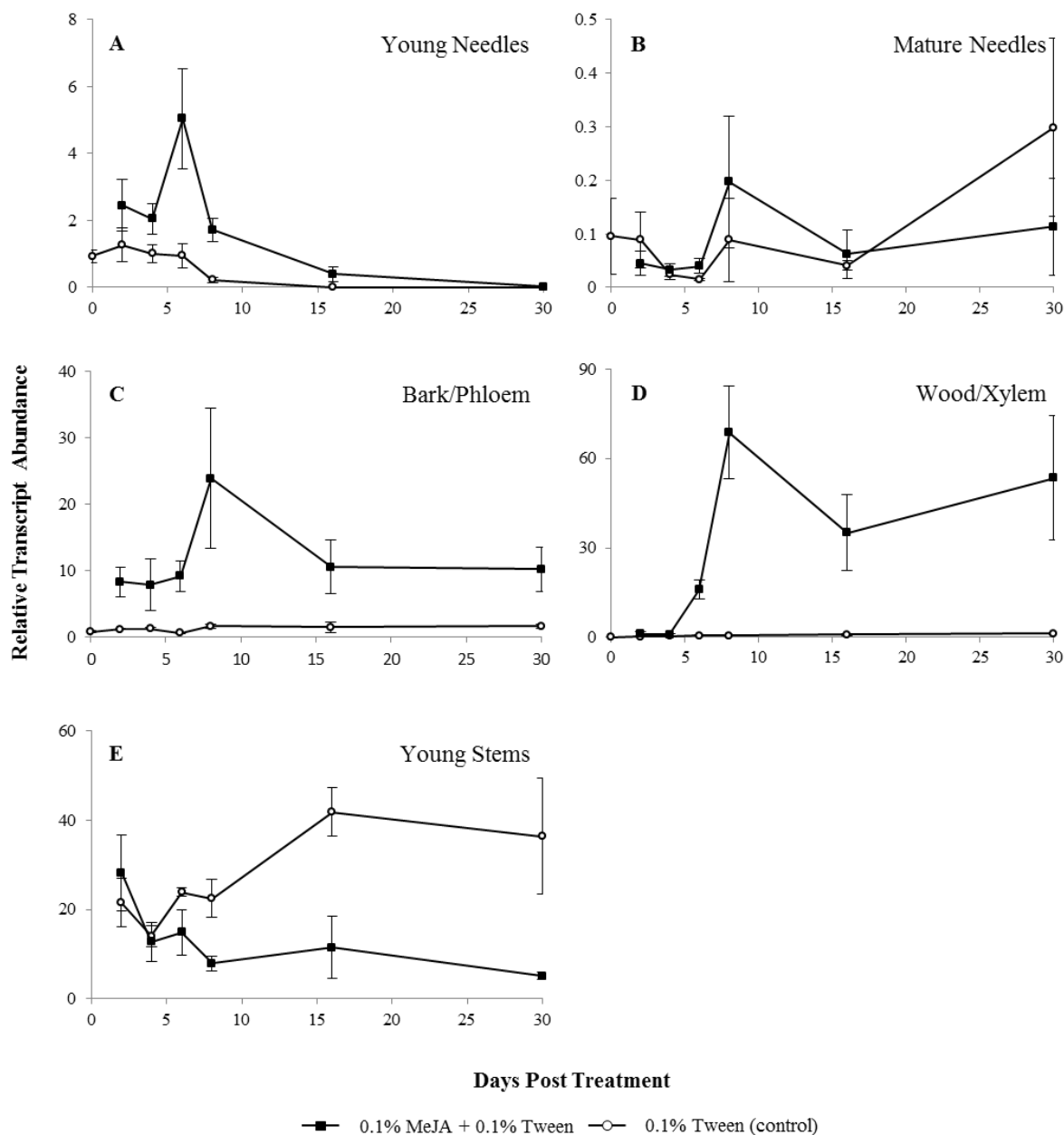


Figure 4.10. Relative transcript abundance of *PgDXS2A* in white spruce samples in response to MeJA treatment over a time course. Transcript abundance was measured by real-time qPCR, normalized to reference genes *eIF4E* and *H3*. Samples analyzed were: (A) young needles, (B) mature needles, (C) bark/phloem, (D) wood/xylem, (E) young stems. Data are means of 3-4 biological replicates at each time point; error bars represent standard error of the mean. Data was statistically analyzed and means were separated using Kruskal-Wallis test statistic ($\alpha=0.05$), see Table 4.6.

Table 4.6. Relative transcript abundance of *PgDXS2A* in control or MeJA-treated samples from white spruce. Contents are expressed as relative transcript abundance to reference genes *eIF4E* and *H3* (\pm SEM). Different letters within control and MeJA columns indicate significantly different means separated by the Kruskal-Wallis test statistic ($\alpha=0.05$); p-values indicate significance of interaction between time and treatment.

Gene of Interest	Sample	Day	Control	MeJA
<i>PgDXS2A</i>	Young Needles ($P<0.0005$)	0	0.935 \pm 0.193 <i>abc</i>	
		2	1.271 \pm 0.512 <i>abc</i>	2.451 \pm 0.765 <i>a</i>
		4	1.012 \pm 0.272 <i>abc</i>	2.056 \pm 0.452 <i>a</i>
		6	0.946 \pm 0.356 <i>bcd</i>	5.040 \pm 1.489 <i>a</i>
		8	0.231 \pm 0.074 <i>cde</i>	1.716 \pm 0.362 <i>ab</i>
		16	0.004 \pm 0.002 <i>e</i>	0.400 \pm 0.213 <i>bcde</i>
		30	0.004 \pm 0.001 <i>e</i>	0.022 \pm 0.011 <i>de</i>
	Mature Needles ($P=0.660$)	0	0.096 \pm 0.070	
		2	0.089 \pm 0.052	0.045 \pm 0.022
		4	0.024 \pm 0.010	0.032 \pm 0.012
		6	0.015 \pm 0.003	0.040 \pm 0.014
		8	0.089 \pm 0.077	0.197 \pm 0.124
		16	0.041 \pm 0.009	0.062 \pm 0.045
		30	0.299 \pm 0.167	0.113 \pm 0.091
	Bark/Phloem ($P<0.0005$)	0	0.753 \pm 0.202 <i>d</i>	
		2	1.105 \pm 0.079 <i>cd</i>	8.293 \pm 2.195 <i>ab</i>
		4	1.243 \pm 0.197 <i>bcd</i>	7.844 \pm 3.949 <i>abc</i>
		6	0.571 \pm 0.089 <i>d</i>	9.150 \pm 2.285 <i>ab</i>
		8	1.612 \pm 0.349 <i>bcd</i>	23.923 \pm 10.535 <i>a</i>
		16	1.421 \pm 0.787 <i>cd</i>	10.529 \pm 4.046 <i>ab</i>
		30	1.590 \pm 0.380 <i>bcd</i>	10.210 \pm 3.361 <i>ab</i>
	Wood/Xylem ($P<0.0005$)	0	0.075 \pm 0.043 <i>d</i>	
		2	0.311 \pm 0.250 <i>d</i>	1.078 \pm 0.921 <i>d</i>
		4	0.394 \pm 0.153 <i>cd</i>	0.998 \pm 0.304 <i>bcd</i>
		6	0.645 \pm 0.317 <i>cd</i>	16.076 \pm 3.059 <i>abc</i>
		8	0.585 \pm 0.273 <i>cd</i>	68.851 \pm 15.705 <i>a</i>
		16	1.044 \pm 0.361 <i>bcd</i>	35.175 \pm 12.673 <i>ab</i>
		30	1.320 \pm 0.433 <i>abcd</i>	53.655 \pm 20.786 <i>ab</i>
	Young Stems ($P=0.005$)	2	21.555 \pm 5.459 <i>abcd</i>	28.223 \pm 8.601 <i>abc</i>
		4	14.063 \pm 2.387 <i>bcde</i>	12.818 \pm 4.345 <i>bcde</i>
		6	23.934 \pm 1.019 <i>abcd</i>	14.945 \pm 5.094 <i>bcde</i>
		8	22.529 \pm 4.162 <i>abcd</i>	7.929 \pm 1.665 <i>de</i>
		16	41.886 \pm 5.390 <i>a</i>	11.537 \pm 6.885 <i>cde</i>
		30	36.473 \pm 13.063 <i>ab</i>	5.147 \pm 0.783 <i>e</i>

In the B sample type, *PgDXS2A* transcripts in MeJA-treated trees were higher than controls over the majority of the time course (Figure 4.10C). At day 2, transcript abundance in the MeJA treatment was over 7-fold higher than controls and rose sharply by day 8 where transcripts reached a peak (23.923 ± 10.535) almost 15-fold higher than controls (Table 4.6). After 16 days transcript levels were reduced again in the MeJA treatment but were still approximately 7-fold significantly higher than controls, and remained high to the end of the time course. *PgDXS2A* transcript levels in the B sample type of control trees remained relatively unchanged through the time course.

In X samples, transcript levels of *PgDXS2A* in both control and MeJA-treated trees were very low over the first 4 days of the time course (Figure 4.10D) and for controls, transcript levels remained low and constant over the whole time course. However, transcript levels in the MeJA treatment rose steeply from day 4 to 8, essentially increasing 70-fold at the peak value. On day 8, MeJA-treated transcripts were well over 100-fold higher than control (Table 4.6). From day 8 to 30 there were no significant changes in transcript levels in the MeJA treatment.

In the YS sample type (Figure 4.10E) transcript levels of *PgDXS2A* in both MeJA and control treatments began the time course at high levels (Table 4.6), and remained statistically unchanged and undifferentiated between treatments through to day 8. However, by day 16, transcript levels in controls had reached a peak that was almost 4-fold higher than in the MeJA treatment. Control transcript levels in YS remained high through to day 30, where they were approximately 7-fold higher than those in the MeJA treatment. By contrast, transcript levels in MeJA-treated samples fell progressively over the time course from day 2 onwards, a 5-fold reduction by day 30.

PgDXS2B

Combining data for all 5 sample types, *PgDXS2B* transcript levels were found to differ significantly by factors of sample type ($P<0.0005$), treatment type ($P<0.0005$) and time ($P=0.001$). Interactions between all factors were found to have a significant effect on *PgDXS2B* transcript levels: sample x treatment ($P<0.0005$), sample x time ($P<0.0005$), treatment x time ($P<0.0005$) and sample x treatment x time ($P<0.0005$) (Table 4.4).

PgDXS2B transcript abundances were found to differ significantly due to the interaction of sample and treatment factors ($P<0.0005$) (Figure 4.8C). In this analysis of means, the differences between time points were not considered. The highest mean transcript abundance was found in MeJA-treated YS samples (6.284 ± 1.241), however this was not significantly different from control (4.095 ± 0.410). Only two sample types, B and X, showed significant differences in the mean transcript abundance of *PgDXS2B* between MeJA and control treatments. The largest difference was in the X sample type where mean MeJA-treated transcript levels were over 20-fold higher than control; whereas in B, mean MeJA-treated transcript levels were approximately 8-fold higher than control. Both YN and MN sample types showed no significant difference in mean transcript abundance between their MeJA and control treatments, and these values were significantly lower than the peak values seen in YS, X and B samples.

Transcript levels of *PgDXS2B* also differed significantly with the interaction of sample, treatment and time ($P<0.0005$). To further elucidate these interactions data was separated into sample types and significance was analyzed between the interaction of treatment and time within each sample type (Figure 4.11). No significant difference was

observed in the interaction between treatment type and time in MN ($P=0.063$) or YS ($P=0.141$) samples. However, significant differences in transcript abundance due to the interaction of treatment and time were observed in sample types YN ($P=0.001$), B ($P<0.0005$) and X ($P<0.0005$) (Table 4.4).

In YN, *PgDXS2B* transcripts in both the MeJA and control treatments reached their highest levels between day 6 and 8, respectively (2.328 ± 1.311 and 2.240 ± 0.981), but were not significantly different from one another (Figure 4.11A; Table 4.7). The single time point that showed a significant difference between treatment types was day 2, where transcript abundance in the MeJA treatment was approximately 3-fold higher than control. Both control and MeJA-treated *PgDXS2B* transcript abundances fell to their lowest levels by the end of the time course.

In the B sample type, *PgDXS2B* transcript abundance in the MeJA treatment was significantly higher than control at two time points. On day 2 transcript levels were at their peak (11.583 ± 3.115) and were 35-fold higher than the corresponding control value, and at day 6 transcript levels were 15-fold higher than control (Figure 4.11C). Both control and MeJA-treated *PgDXS2B* transcript abundances fell to low levels by days 16 and 30 and were not significantly different from each other (Table 4.7).

In X, transcript levels of *PgDXS2B* were initially low in both control and MeJA-treated samples (Figure 4.11D; Table 4.7). While control transcript levels remained stable over the time course, MeJA-treated transcript abundances rose to a peak at day 8 (6.248 ± 1.166) which was almost 45-fold higher than control. For the majority of the time course, transcript levels in the MeJA-treated X sample type were significantly higher than

corresponding controls, with the exception of day 4. Transcript levels in MeJA-treated samples at days 16 and 30 were 29-fold and 19-fold higher, respectively, than their control counterparts (Table 4.7).

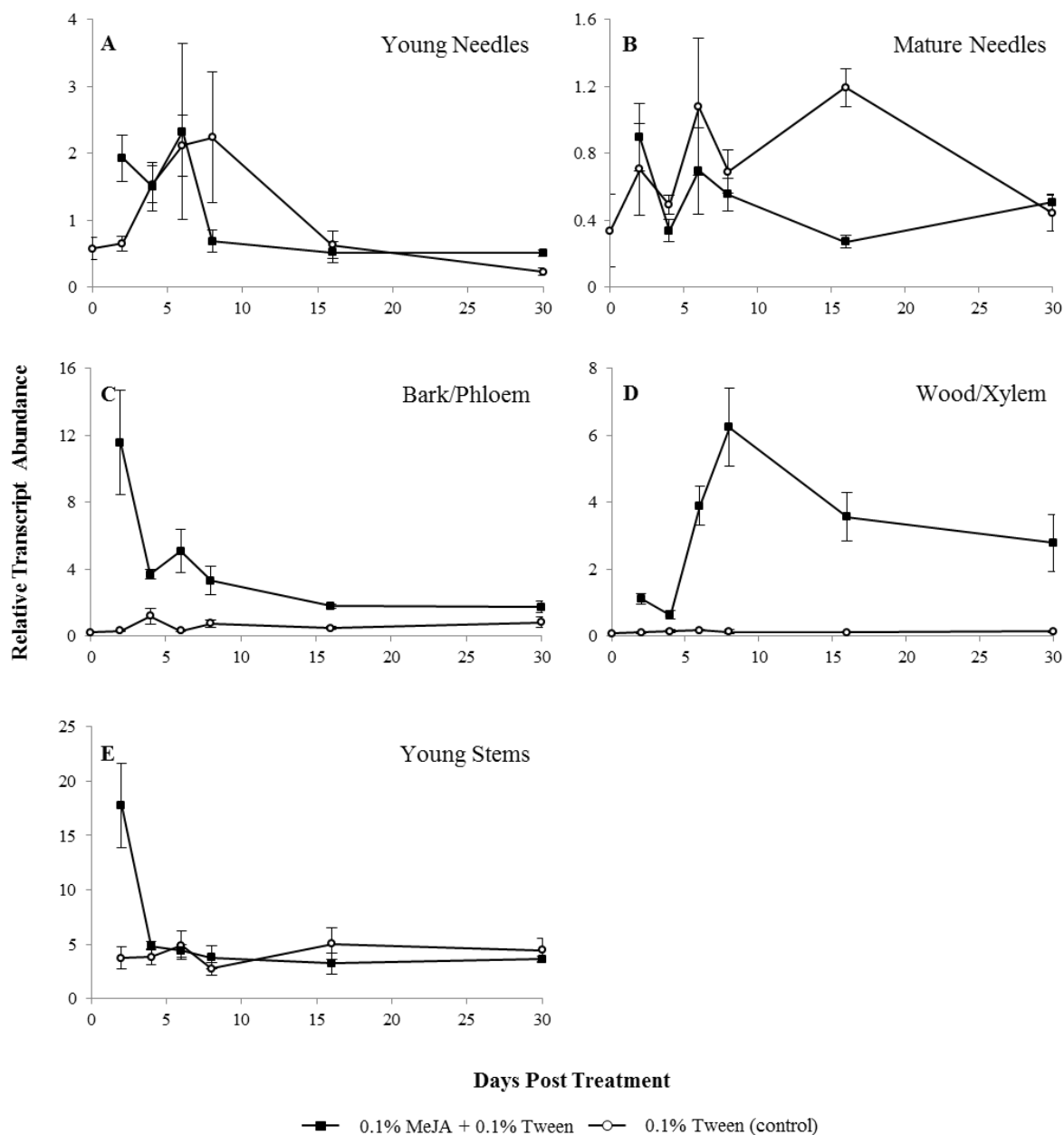


Figure 4.11. Relative transcript abundance of *PgDXS2B* in white spruce samples in response to MeJA treatment over a time course. Transcript abundance was measured by real-time qPCR, normalized to reference genes *eIF4E* and *H3*. Samples analyzed were: (A) young needles, (B) mature needles, (C) bark/phloem, (D) wood/xylem, (E) young stems. Data are means of 3-4 biological replicates at each time point; error bars represent standard error of the mean. Data was statistically analyzed and means were separated using Kruskal-Wallis test statistic ($\alpha=0.05$), see Table 4.7.

Table 4.7. Relative transcript abundance of *PgDXS2B* in control or MeJA-treated samples from white spruce. Contents are expressed as relative transcript abundance to reference genes *eIF4E* and *H3* (\pm SEM). Different letters within control and MeJA columns indicate significantly different means separated by the Kruskal-Wallis test statistic ($\alpha=0.05$); p-values indicate significance of interaction between time and treatment.

Gene of Interest	Sample	Day	Control	MeJA
<i>PgDXS2B</i>	Young Needles ($P=0.001$)	0	0.580 \pm 0.162 <i>cde</i>	
		2	0.657 \pm 0.108 <i>cde</i>	1.930 \pm 0.347 <i>ab</i>
		4	1.538 \pm 0.277 <i>abc</i>	1.504 \pm 0.369 <i>abcd</i>
		6	2.120 \pm 0.460 <i>a</i>	2.328 \pm 1.311 <i>abc</i>
		8	2.240 \pm 0.981 <i>abcd</i>	0.692 \pm 0.161 <i>bcde</i>
		16	0.636 \pm 0.203 <i>cde</i>	0.522 \pm 0.159 <i>de</i>
		30	0.234 \pm 0.060 <i>e</i>	0.513 \pm 0.046 <i>de</i>
	Mature Needles ($P=0.063$)	0	0.339 \pm 0.217	
		2	0.706 \pm 0.276	0.897 \pm 0.202
		4	0.493 \pm 0.055	0.339 \pm 0.064
		6	1.079 \pm 0.409	0.697 \pm 0.259
		8	0.691 \pm 0.129	0.556 \pm 0.099
		16	1.194 \pm 0.114	0.272 \pm 0.037
		30	0.444 \pm 0.106	0.508 \pm 0.051
	Bark/Phloem ($P<0.0005$)	0	0.244 \pm 0.036 <i>e</i>	
		2	0.324 \pm 0.048 <i>e</i>	11.583 \pm 3.115 <i>a</i>
		4	1.202 \pm 0.482 <i>bcde</i>	3.713 \pm 0.288 <i>ab</i>
		6	0.337 \pm 0.068 <i>e</i>	5.077 \pm 1.290 <i>ab</i>
		8	0.757 \pm 0.227 <i>cde</i>	3.333 \pm 0.870 <i>abc</i>
		16	0.485 \pm 0.091 <i>de</i>	1.815 \pm 0.120 <i>abcd</i>
		30	0.845 \pm 0.317 <i>cde</i>	1.743 \pm 0.339 <i>abcd</i>
	Wood/Xylem ($P<0.0005$)	0	0.089 \pm 0.023 <i>e</i>	
		2	0.118 \pm 0.038 <i>de</i>	1.119 \pm 0.170 <i>abc</i>
		4	0.150 \pm 0.039 <i>cde</i>	0.637 \pm 0.132 <i>abcd</i>
		6	0.183 \pm 0.022 <i>bcde</i>	3.899 \pm 0.590 <i>a</i>
		8	0.139 \pm 0.058 <i>cde</i>	6.248 \pm 1.166 <i>a</i>
		16	0.122 \pm 0.021 <i>de</i>	3.565 \pm 0.722 <i>ab</i>
		30	0.143 \pm 0.022 <i>cde</i>	2.791 \pm 0.847 <i>ab</i>
	Young Stems ($P=0.141$)	2	3.760 \pm 0.990	17.772 \pm 3.867
		4	3.821 \pm 0.722	4.833 \pm 0.387
		6	4.892 \pm 1.302	4.408 \pm 0.592
		8	2.753 \pm 0.569	3.801 \pm 1.048
		16	5.061 \pm 1.466	3.236 \pm 0.938
		30	4.482 \pm 1.048	3.652 \pm 0.280

4.3. Discussion

Gymnosperm *DXS* genes have been studied previously (Phillips et al., 2007: *Picea abies*; Kim et al., 2009: *Pinus densiflora*) but not within the context of either a long term growth time course or with respect to their responses to MeJA in multiple sample types. Hence, the present work with white spruce contributes new knowledge about *DXS* genes in relation to downstream GA or DRA pathways over seasonal time, within different tree samples, and in response to stress signaling.

Three *DXS* genes, *PgDXS1*, *PgDXS2A* and *PgDXS2B* (named for their sequence similarity and phylogenetic distance to Norway spruce orthologs; Figure 4.2) were cloned and functionally characterized from white spruce. These represent the small *DXS* family in white spruce and showed conserved functionality and product profiles with previously characterized angiosperm orthologs, producing DXP as the product when incubated with pyruvate and G3P as substrates and the co-factor TPP (Figure 4.4) (Cordoba et al., 2011; Battilana et al., 2011). The present characterization of *P. glauca* *DXS*s represents the first use of *in vitro* assays to functionally characterize *DXS* enzymes in a conifer species whereas previous studies in Norway spruce, *P. densiflora* and *Ginkgo biloba* used *E.coli* complementation assays (Phillips et al., 2007; Kim et al., 2009; Kim et al., 2006) to prove conserved *DXS* function. The characterized *PgDXS* proteins fit well into proposed clades, clustering with gymnosperm sequences (Figure 4.2) and showing clear separation between type I and type II sequences. *PgDXS* enzymes also contained characteristic TPP-binding domains and all conserved residues known to be catalytically relevant to the active site (Figure 4.1) (Xiang et al., 2007). No *DXS* type III sequences were found after examination of the PG29 white spruce genome (Birol et al., 2013; Warren et al., 2015), suggesting that type

III *DXS* genes may not exist in white spruce. Type III *DXS* genes are not ubiquitous in all plant genomes and therefore it was not unusual that none were found in white spruce.

White spruce *DXS* genes show specific changes in transcript abundance through apical bud and apical shoot development

Transcript changes in three white spruce *DXS* genes were compared in apical buds and developing apical shoots over a year-long time course (Figure 4.5). Apical buds and shoots showed changing overall trends, with transcript levels of *DXS* genes peaking in late spring / early summer (May to June) during the time of fast growth and major stem elongation (Supplemental Table S1). A clear and statistically significant pattern was seen for *PgDXS1*; transcript levels peaked over a week in late May (time points 14-15) and remained elevated for the entire month of June (time points 16-20). Elevated transcripts at this time correlated well with fast apical bud growth. While there were clear patterns of up-regulated *PgDXS* type II transcripts during the growing season (summer months), there was also a clear phenomenon of oscillation of transcript abundance that cannot be easily explained. A similar oscillation of transcript abundance, over this same time period was not seen in any of the diTPS or CYP450 transcripts (Figure 3.18-3.19). It is also important to note that the qPCR analysis was performed with the same RNA samples for the *DXS*, diTPS and CYP450 genes; hence the transcript oscillation observed with the *DXS* genes cannot be tied to technical issues with the biological materials or data collection and processing. Instead, it may be that *PgDXS* type II expression is episodic and also possibly responsive to additional factors, beyond those that affect the downstream DRA pathways. While a positive correlation of *PgDXS1* expression and apical bud and shoot development was apparent, correlations of

expression of the two *PgDXS* type II genes remained unclear, and required a shift of focus to a spatially more refined analysis of transcript expression in needles, stems and emerging buds of the developing apical shoot over a narrower time frame of the growing season.

Expression levels of all *PgDXS* genes varied by sample part (Figure 4.6). *PgDXS1* showed highest expression in needles in late June, with transcript levels increasing steadily from near zero in late April; notably *PgDXS1* was the only *DXS* family member whose expression levels in needles remained elevated throughout the time course. In stems, *PgDXS1* transcripts peaked earlier than in needles in May but fell to steady levels similar to what was seen in new bud samples for the remainder of the time course. The up-regulated expression profile of *PgDXS1* in needles is similar to the results for characterized angiosperm *DXS* orthologs. In *Arabidopsis thaliana*, tomato, maize and *Medicago truncatula* (Estévez et al., 2000; Lois et al., 2000; Cordoba et al., 2011; Walter et al., 2002) *DXS1* gene transcripts are highly expressed in photosynthetic tissues and plant samples undergoing development, such as young leaves, stems and seedlings. This profile of expression is in agreement with the idea that *DXS* type I genes, including *PgDXS1*, are committed to primary metabolism pathways and are mainly found where photosynthetic structures develop.

Expression of *PgDXS2A* and *PgDXS2B* share some spatial commonalities, but are not identical in their timing (Figure 4.6). Transcript levels of both *PgDXS* type II genes were up-regulated in needles early in the time course, *PgDXS2B* peaking first in late May, two weeks before *PgDXS2A*. By late June transcript levels of both genes dropped dramatically in needles showing a clear change in allocation. Notably for *PgDXS2B*, during this time period when transcript levels in needles drop dramatically, transcript levels in stem and new buds are at their highest; hence, sample part specific gene expression at this growth stage seems

tightly defined and was not resolved in the complex whole apical shoot sample. Transcript levels of both *PgDXS* type II genes were similar in new bud samples, being highest at emergence and dropping sharply as growth continued. In other plants, such as *Medicago truncatula* and maize, *DXS* type II genes localized with high expression in roots, particularly when responding to mycorrhizal treatment (Walter et al., 2002). In conifers, information on the patterns of expression of *DXS* type II transcripts or proteins is limited. Kim et al. (2009) found transcripts of *P. densiflora DXS2* mainly in wood (xylem), whereas other studies focused on sample types known to provide high oleoresin content such as stems that were treated with MeJA or wounded (Phillips et al., 2007; Zulak et al., 2009). No comparable study locating a *DXS2* in developing gymnosperm samples existed in the literature prior to the present work.

There are clear spatial and temporal differences between the expression of white spruce *DXS* type I and II genes, as well as between the two *DXS* type II genes. *PgDXS1* showed the most sustained expression in photosynthetic tissue, whereas *PgDXS* type II genes were expressed for only a short duration in needles, both dropping to low levels when *PgDXS1* was at its peak.

Accumulation of DRA through apical bud and shoot development shows relationships to *PgDXS* expression

Comparing DRA accumulation to transcript levels of *PgDXS* genes could add another layer of definition to the potential relationship between general or specialized terpenoid pathways in addition to the gene expression patterns of the GA and DRA pathways discussed in Chapter 3. In developing apical buds, DRA levels (Figure 3.15) showed a significant

increase in concentration in mid-May (time points 13-14), corresponding to the final stages of bud flush where the stem and needles are rapidly growing and expanding. Before this rise in the DRA levels in mid-May, all *PgDXS* gene transcripts were up-regulated (Figure 3.15; Figure 4.5). Specifically, transcripts levels of *PgDXS2B* were increasing as early as March and *PgDXS2A* transcripts were apparent in April, both suggesting that *PgDXS* type II protein levels and enzymatic activities were rising at these times.

Examining the shortened time course focused on different sample parts of the fast growing apical buds and shoots (Figure 3.16), all *PgDXS* gene transcripts were induced and rising sharply in needles at the time of peak DRA accumulation in late May (Figure 4.6). Furthermore, shortly after DRA levels peaked there was a steep drop in *PgDXS* type II transcript levels, alluding to their participation in DRA formation. By contrast, *PgDXS1* transcript levels in needles were elevated for most of the time course, and their expression did not match that of DRA accumulation as closely as did the expression patterns of the *PgDXS* type II genes. This fits well with the probable primary role of *PgDXS1* in the formation of photosynthetic pigments or gibberellins needed in the fast growing needle samples during this developmental time frame. In stem and new buds, DRA levels peaked in July and August, respectively, a time when *PgDXS* type II transcript levels were relatively stable (*PgDXS2A*) or slowly declining from peak levels a few weeks prior (*PgDXS2B*). In either case *DXS* type II gene expression was active during the production of DRA in stem and new buds. By contrast, in stems, *PgDXS1* levels peaked much earlier in the time course when DRA concentration was significantly lower and stems were rapidly elongating during bud flush and possibly exhibiting photosynthetic activity.

Transcript abundances of *DXS* genes in white spruce samples show specific patterns of change with MeJA treatment

As with genes involved in GA and DRA metabolism discussed in Chapter 3, responses of *DXS* gene expression to MeJA treatment were assessed with a refined set of five distinct sample types to identify the spatial and temporal differences in expression of these MEP pathway genes. The study spanned both growing and mature white spruce samples as well as those that are known to hold large volumes of resin and those that are integral to photosynthetic activity.

The expression pattern of *PgDXS1* in response to MeJA treatment differed somewhat by sample type (Figure 4.9). In bark and young stems *PgDXS1* transcripts exhibited a short and fast response to the treatment with MeJA, quickly dropping significantly after 2 days and remained at control levels for the rest of the time course. Zulak et al. (2009) observed a similar pattern to the MeJA-induced expression of *PaDXS1* in Norway spruce bark samples, finding a spike in transcript abundance at 2 days post treatment, followed by a sharp decline. This also agrees with previous work by Phillips et al. (2007) which showed a slight response by *PaDXS1* three days post MeJA or wounding treatment in the bark of Norway spruce saplings. Notably in wood/xylem samples, *PgDXS1* was also significantly induced by MeJA treatment but it showed a delayed induction when compared to bark or young stems, peaking at day 8. In *P. densiflora*, *PdDXS1* was induced in wood (Kim et al., 2009), and in *Ginkgo biloba* *GbDXS1* expression showed a short and fast response over 2 days to MeJA treatment in young leaf derived callus cultures (Gong et al., 2006). *PgDXS1* remained consistent and unchanged in both young and mature needles when exposed to MeJA treatment.

Interestingly, mean transcript control values (Figure 4.8A) were similar throughout in needle

and wood samples, pointing towards a consistent need for the type I *DXS* through multiple sample types. In young stems, the mean control value of *PgDXS1* was significantly higher than in other sample types which could point to young stems being the fastest growing and developing tissue at this time.

Overall, *PgDXS1* expression is more evenly distributed over sample types and shows less dramatic changes when treated with MeJA than *PgDXS2A* or *PgDXS2B* (Figure 4.8). However, *PgDXS1* does exhibit multiple iterations of up-regulation in response to MeJA treatment in bark, wood and young stems (Figure 4.9). This could possibly indicate that, in response to a stress signal, all forms of *DXS* may be up-regulated and utilized for synthesis of DXP for the production of defensive chemicals or that MeJA treatment may be triggering other downstream processes or pathways, not identified, that require the participation of a type I *DXS* gene.

In general, both *PgDXS* type II genes showed similar expression patterns across multiple sample types, perhaps best visualized in Figure 4.8B and C. Specifically, in known resin-rich sample types (bark, wood) both *PgDXS2A* and *PgDXS2B* showed significant up-regulation when exposed to MeJA treatment. Both *PgDXS2A* and *PgDXS2B* also showed high mean transcript abundance in young stems but their mean expression was dramatically lower in needles.

The expression patterns of *PgDXS2A* and *PgDXS2B* were most similar in wood/xylem samples over time (Figure 4.10, 4.11); transcript levels in the MeJA treatment peaked at day 8 following a steep rise. *PgDXS2A*, however, had a much stronger induction; at its peak the fold change in transcript levels was more than double that of *PgDXS2B*. When

comparing the two *PgDXS* type II genes, transcript changes were noticeably different in bark, specifically their induction was separated by time. In bark samples, *PgDXS2A* was significantly induced as early as 2 days post MeJA treatment and exhibited a prolonged up-regulation until day 16. On the other hand, *PgDXS2B* transcript levels in MeJA-treated bark were induced quickly at day 2 and dissipated to control levels after 6 days. In a similar experiment, Zulak et al. (2009) found that in *P. abies*, *PaDXS2A* and *PaDXS2B* transcripts followed similar trends in MeJA-treated bark samples, both experiencing a peak in abundance at day 8 which agrees well with the timing of *PgDXS2A* but not *PgDXS2B*. This deviation in temporal allocation of the *DXS* type II genes in white spruce bark could indicate a difference in function between the two.

One very noticeable difference between *PgDXS2A* and *PgDXS2B* was their expression in young stems. In this sample type, *PgDXS2B* expression mirrored that of *PgDXS1*, exhibiting a fast response to the MeJA treatment and dropping quickly after 2 days to control levels whereas *PgDXS2A* was down-regulated in young stems 16 days post MeJA treatment. One may reason that at this developmental point young stem samples are in the process of differentiating towards what was previously specified in this experiment as bark/phloem (containing cork, cortex, and primary and secondary phloem) and wood/xylem (consisting of primary and secondary xylem, pith, and the vascular cambium). Extrapolating from this, it should be possible to compare young stems, which represent new growth of the year, to bark and wood samples, which were produced in the previous year. From this comparison it is easily seen that the mean control levels of both *PgDXS* type II gene transcripts were significantly higher in young stems when compared to bark and wood (Figure 4.8B, C). This points to the age of the white spruce sample type as being a

considerable factor in transcript expression. In young stems, a quick growing tissue, it is possible that *PgDXS2A* and *PgDXS2B* could be diverted from their assumed roles in traumatic resin biosynthesis to roles more befitting growth, development or even the production of resin in constitutive ducts.

DRA accumulation in spruce samples treated with MeJA and relationships to *DXS* expression

DRA levels were measured as a part of the study of MeJA treatment on five distinct sample types to determine whether a correlation can be made with the changes in transcript levels of the *PgDXS* genes. In response to MeJA treatment, DRA levels increased significantly in wood/xylem and young stems over time, in both sample types DRA levels were noticeably higher than control measurements at day 16 post treatment and beyond (Figure 3.23). All *PgDXS* genes exhibited significantly up-regulated transcript levels in MeJA-treated wood/xylem by day 8, with transcript levels of the *DXS* type II genes beginning to increase at day 6 (Figure 4.9, 4.10, 4.11). As well, in this sample type, *PgDXS2A* transcripts showed the most powerful induction with an over 100-fold increase over control at day 8. *PgDXS2B* transcripts reacted more moderately with an approximately 45-fold increase whereas *PgDXS1* showed only a 3-fold increase with the MeJA treatment at day 8. This large transcriptional reaction by the *DXS* type II genes correlates well with the timing of resin accumulation in wood samples, and infers their role in this specialized metabolic process.

The accumulation of DRAs was also significantly different over time in young stems (Figure 3.23). In both MeJA-treated and control samples DRA production increased over

time. *PgDXS1* and *PgDXS2B* showed very similar expression patterns in young stems, both were quickly up-regulated in response to MeJA with their transcription levels falling back to control levels after 2 days (Figure 4.9, 4.11). *PgDXS2A* expression was high at the beginning of the time course, but was down-regulated by 16 days post MeJA treatment (Figure 4.10). When examining mean transcript abundances in Figure 4.8, it is clear that expression of all *PgDXSs* was quite high in control and MeJA-treated young stems alike. Because of the fast-growing and developing nature of this tissue it is unclear if this broad increase in *DXS* transcription is tied exclusively to DRA production.

Chapter 5: Concluding discussion

5.1. Overview of thesis work

In conifers two diterpenoid biosynthetic pathways, GA biosynthesis and DRA biosynthesis, serve disparate roles centered in general and specialized metabolism, respectively. During normal plant function, both pathways are present and are important to the tree's success – GAs are phytohormones that serve purposes in growth and reproduction, whereas DRAs are a main component of oleoresin that provide anti-microbial activities as well as a physical defense against pests. Figure 1.1 illustrates the pathway of GA biosynthesis in comparison with a simplified linear pathway of DRA biosynthesis (note that as a specialized metabolism pathway it is best described as a metabolic system with multiple nodes, many genes involved, and a range of end point metabolites produced; i.e. see Hamberger et al., 2011). Both pathways utilize a similar pattern of enzymes types, primarily diTPSs and CYP450s. During conifer evolution it appears that the monofunctional diTPSs of GA biosynthesis and bifunctional diTPSs of DRA biosynthesis evolved through duplication and sub- or neofunctionalization from a common bifunctional CPS/KS enzyme ancestor (Keeling et al., 2010; Trapp and Croteau, 2001; Bohlmann et al., 1998). The evolutionary origins of the CYP450 enzymes of these two pathways are not as clear, the *CYP720B* genes of DRA synthesis and the *CYP701* genes of GA biosynthesis fall into different clans of the P450 gene family, indicating a convergent evolution of function (Hamberger and Bohlmann, 2006; Hamberger and Bak, 2013; Hamberger et al., 2011). The GA and DRA pathways are also mechanistically similar, using two monofunctional or one bifunctional diTPS to cyclize GGPP to a diterpene olefin intermediate and a CYP450 to perform a 3-step hydroxylation reaction on a methyl group of the diterpenoid substrate to produce a structurally similar

diterpene acid product. Chapter 3 of this thesis focused on characterizing the spatial and temporal expression of the central genes of the similar GA and DRA pathways in white spruce apical buds and shoots over a seasonal timeframe and with respect to MeJA challenge.

Building on the analysis carried out in Chapter 3, it was important to also characterize the *DXS* family of genes, to evaluate their potential roles as they relate to the downstream GA and DRA pathways. *DXS* enzymes catalyze the first rate-limiting step in the MEP pathway, ultimately producing isoprenoid precursors for diterpenoids. Changes in *DXS* gene expression in some angiosperms such as *Arabidopsis thaliana*, tomato and lavender correlate with changes in multiple isoprenoid metabolite profiles, and are associated with increased production of carotenoids, abscisic acid, volatile monoterpenoids and gibberellins (Estévez et al., 2001; Enfissi et al., 2005; Muñoz-Bertomeu et al., 2006). *DXS* genes exist in small families and the genes typically divide into two types, type I associated with general metabolism and type II which are more likely to be induced by stressors and are associated with specialized metabolic pathways. Chapter 4 of this thesis explored the influences on the expression of the *DXS* family of genes in white spruce apical buds and shoots as well as in response to MeJA treatment and correlated these gene expression data with information about downstream GA and DRA pathway expression.

Before undertaking comparative studies of gene expression over time and treatment courses, previously uncharacterized genes from *DXS*, diTPS and CYP450 families of white and Sitka spruce were functionally characterized using *in vivo* or *in vitro* assays in *E.coli* or yeast systems. This functional characterization provided the first full and direct comparison of core GA and DRA pathway genes of white spruce. This ultimately supported the first

hypothesis posed in this thesis which was that spruce *DXS* genes as well as diTPS and CYP450 genes from the GA pathway would be functionally conserved in comparison with their orthologs in angiosperm and other gymnosperm species, whereas white spruce genes involved in DRA synthesis would show specialized functions similar to other conifer species. After characterization, the expression profiles of these pathway genes were measured via different experiments that were hypothesized to provide scenarios where both growth and defense pathways would be present and potentially competing.

5.1.1 Development of apical buds and apical shoots over a calendar year of growth

The first experiment was designed to provide a comparison of expression profiles of GA and DRA related genes by following the development of apical buds and apical shoots over a year-long time course. Expression of the *DXS* family genes and central GA and DRA diTPS and CYP450 genes was analyzed and compared to DRA levels as a measure of a metabolite product that could be affected by changes in expression of pathway genes. In this work, the hypothesis presented was that expression of genes associated with the specialized DRA pathway would show markedly different expression patterns than those of the general GA biosynthesis pathway, with maximal expression in times and places when defensive chemicals were needed.

This hypothesis was supported based on the analysis of the individual sample parts (e.g. needles, stem and new buds) that were dissected from apical buds/shoots. Clear differences were seen in the patterns and levels of expression of DRA versus GA associated genes when separated into the various sample parts (Figure 3.19, Figure 4.6). However, when

examining transcript abundances of *DXS*, *diTPS* and *CYP450* genes in whole apical bud or shoot samples (Figure 3.18, Figure 4.5) what was seen was a more generalized trend of upregulation over the spring and summer, correlated with active growth and need for defenses against pathogen/pest attack, with transcript levels falling in the autumn and winter months which is consistent with a period of dormancy. Hence, it is clear that different sample parts (needles, stem, new buds) follow different trajectories and have different needs for GA (growth) versus DRA (defense) pathways that could only be fully discerned by examining the individual sample parts.

The GA related genes, *PgCPS* and *PgDXS1*, shared a similar timeline of expression as well as high transcript levels in needle samples over the narrow time frame of apical bud and shoot development (Figure 3.19A, Figure 4.6A). It is clear that GA associated genes in white spruce were most prevalently allocated spatially to the photosynthetic tissues. Thus, mean transcript levels of GA genes were significantly higher in needles than other sample parts (Figure 3.20F, G, H, Figure 4.7D).

When examining the DRA pathway genes, clear patterns were associated with DRA accumulation and sample type allocation. *PgLAS*, *PgCYP720B4* and both *PgDXS* type II genes shared an early rise in transcript levels in needle samples followed by a sudden drop in expression in the month of June, identifying a very short time frame in which DRA synthesis and accumulation occurs in needles (Figure 3.19, Figure 4.6). After this increase in expression in needles, spatial allocation of DRA associated genes moved towards stem and new young bud samples which corresponds well with where and when DRAs were accumulated in white spruce over the narrowed time frame (Figure 3.16).

Overall, the GA and DRA pathways seem to be spatially separated; e.g., where DRA levels are lowest in needles, GA pathway genes are most highly expressed. Within samples, the overlap between the pathway genes can also be temporally separated; for example, in needles *PgCPS* abundance peaked 2 weeks after transcripts of *PgLAS* and *PgCYP720B4* and DRA levels were at their highest

DXS transcript levels did not exactly mirror what was seen for the central GA and DRA diTPS and CYP450 genes. However, trends relating *PgDXS1* gene expression with GA gene expression occurred whereas *DXS* type II expression more closely aligned with DRA associated genes with respect to both sample part allocation and the general timing of expression. This loose correlation is most likely due to the fact that *DXS* enzymes, as a rate-limiting step of the MEP pathway, are associated with several different downstream isoprenoid biosynthetic pathways and therefore *DXS* regulation or organization would not be tied exclusively to GA or DRA metabolism.

5.1.2. Response of GA and DRA biosynthetic pathways to MeJA

The second experiment aimed to provide an analysis of the GA and DRA pathway genes in response to stress, emulated by MeJA treatment. The treatment time course measured up to 30 days post-MeJA application over five sample types spanning young and older tissues known to potentially contain large amounts of resin or to be photosynthetically active. Transcript levels of *DXS* family genes and diTPS and CYP450s associated with GA and DRA biosynthesis were analyzed and compared to DRA levels over the span of the time course. Here the hypothesis put forward stated that the MeJA treatment would affect gene

expression of enzymes involved in the specialized DRA pathway but have little or no effect on genes involved in GA biosynthesis.

Expression changes in response to MeJA treatment were observed to be the most considerable for DRA associated genes. Both *PgLAS* and *PgCYP720B4* showed similar responses, with transcript levels induced to varying degrees in all sample types (Figure 3.27, Figure 3.29). *PgLAS* and *PgCYP720B4* also showed similar patterns in response to differences in ages of the sample, with transcript levels peaking several days earlier in young or fast growing sample types versus older or more mature sample types. Both *PgDXS2A* and *PgDXS2B* showed similar high transcript levels in samples with high DRA content (e.g. wood/xylem and bark) (Figure 3.23, Figure 4.10, Figure 4.11). However, unexpected results were seen in young stem samples with mean transcript levels of both *PgDXS* type II genes being high in the control treatment (Figure 4.8). This suggests that DXS type II enzymes could possibly have roles outside of DRA biosynthesis in this sample type.

Contrary to the initial hypothesis, MeJA treatment did in fact have some effects on the GA related genes. *PgCPS* transcripts generally were downregulated in the presence of MeJA in the majority of sample types, but interestingly, transcript levels proved to be unaffected by MeJA in the fast growing young stems (Figure 3.25). *PgKS* transcript levels in MeJA-treated trees were upregulated in all sample types, mirroring what was seen for DRA associated genes with the exception that high *PgKS* transcript levels occurred in both young and mature needles which was not true for the expression of *PgLAS* and *PgCYP720B4* (Figure 3.26, Figure 3.24). The response to MeJA by a *KS* gene was unexpected and is usually just seen for *KS-like* genes that have evolved functions in specialized metabolic pathways through neofunctionalization. Furthermore, *PgCYP701* also showed a mixed

response to MeJA treatment with transcripts downregulated in photosynthetic samples and upregulated in bark and wood towards the later part of the time course (Figure 3.28). This response of *PgCYP701* was similar to that of *PgCPS*, but together with the expression profile of *PgKS* these results did not support the original hypothesis that MeJA treatment would have little to no effect on the expression of GA pathway genes.

5.2. Future research

The work done in this thesis contributed to the knowledge of conifer GA and DRA pathway functionality and organization in white spruce. The results of this research, generally speaking, broaden our understanding of the tree's spatial and temporal allocation of resources towards growth and producing vegetative buds for next year's growth versus oleoresin production and storage. As questions and hypotheses were answered throughout the research, there could easily be more avenues of research that emerge out of the foundation of this project. Some examples are discussed below.

1. As part of my data collection I explored the BAC resources (Hamberger et al., 2009) and PG29 white spruce genome (Birol et al., 2013; Warren et al., 2015) to seek the promoter region sequences of the *DXS*, *diTPS* and *CYP450* genes explored in this thesis. While the promoter regions for the majority of genes were found and analyzed using online resources like PLACE (Plant Cis-acting Regulatory DNA Elements; Higo et al., 1999) and MatInspector (Cartharius et al., 2005); others were too short in length or missing entirely from the white spruce genome resources at the time. However, as the white spruce genome resources grow, a project that analyzes the promoter regions of each specific gene could provide additional valuable insights into

the regulatory control of GA versus DRA pathway gene expression. For example, identification of response elements that are associated with transcription factors that mediate methyl jasmonate, gibberellins, temperature or light sensing could complement the research carried out in this thesis and potentially help explain some of the unexpected responses, for example the strong upregulation of *PgKS* expression in response to methyl jasmonate application in certain sample types.

2. To better understand the mechanics and relationship between the GA and DRA pathways it would be ideal to more thoroughly explore some of the unexpected differences noted between samples types, expanding studies to include additional spruce samples, as well as focus on specific tissues types. It became clear during data analysis that different ages of samples had an effect on the expression of some GA and DRA pathway genes that was not initially expected. For example, the different expression patterns of *PgCPS*, and both *PgDXS* type II genes in young stems versus older bark/phloem and wood/xylem tissue, could be the basis for a broader study that revolves around a larger range of ages in specific samples to determine if the pathways show comparable responses to stress (e.g. MeJA) at all ages or if there are critical times of the year when stress responses are particularly robust. Expansion of sampling to include other circumstances where it could be surmised that we would observe a difference between the GA and DRA pathways, for example during cone bud development, would be an interesting and potentially beneficial future direction in which to expand the current study. Furthermore, the application of laser microdissection (LMD) technology to target single tissue types in developing apical

buds or in young versus older stem samples, as described in Abbott et al. (2010), could potentially add further clarification to the spatial differences observed between GA and DRA pathways in this thesis.

3. This thesis measured DRA metabolites and thus was able to correlate changes in end product levels with the expression levels of DRA and GA pathway genes.

Comparable measurements of gibberellin levels would certainly have benefited the project. Indeed, outside collaborations with Dr. Hitoshi Sakakibara of the RIKEN Plant Science Center (Japan), and Dr. Thomas Moritz of the Umeå Plant Science Center (Sweden) were set up to analyze GA metabolites but unfortunately no measurable GA levels were detected in samples spanning the apical bud and shoot developmental time course. Hence, the hoped-for comparison of end point metabolite levels for both of GA and DRA pathways, that would have added another layer of information to the project, was ultimately impossible. To supplement this missing information in future research, a potential approach would be to analyze the GA and DRA pathways at the protein level, measuring *in vivo* protein amounts using a technique called selected reaction monitoring. Similar studies have been performed in other conifer species, to give a multi-leveled approach combining transcripts, protein levels and metabolite end products to better map the spatial and temporal distribution of pathway activity (Zulak et al., 2009; Hall et al., 2011). Furthermore, detailed kinetic characterization of certain pathway enzymes could lead to a better understanding of their specific roles. For example, an understanding of the kinetic differences between the DXS type II enzymes in white spruce could help differentiate

the potential magnitude of their contributions in selected sample types where transcript levels are similar.

4. Analysis of the *DXS* gene family proved insightful to the analysis set forth in this thesis. Expanding on the importance of the MEP pathway in the production of GA and DRA metabolites, there is experimental evidence that two other enzymes from the MEP pathway, DXP reductoisomerase (*DXR*) and hydroxymethyl-butenyl 4-diphosphate reductase (*HDR*), perform rate-limiting roles in some bacterial and plant species (Cordoba et al., 2009; Rodríguez-Concepción, 2006). Indeed, Phillips et al. (2007) found that *DXR* and *HDR* in Norway spruce responded to fungal inoculation and wounding in concert with *DXS* type II gene transcripts. *DXR* and *HDR* exist in single or small member families; functional characterization of these genes and analysis of transcript and/or protein levels in white spruce would further contribute to the knowledge of how downstream GA and DRA pathways are organized.

References

- Abbott E, Hall D, Hamberger B, Bohlmann J** (2010) Laser microdissection of conifer stem tissues: isolation and analysis of high quality RNA, terpene synthase enzyme activity and terpenoid metabolites from resin ducts and cambial zone tissue of white spruce (*Picea glauca*). *BMC Plant Biology* **10**: 106
- Adams RP** (2007) Identification of essential oil components by gas chromatography-quadrupole mass spectroscopy, 4th Edition, Carol Stream, IL: Allured Pub Corp.
- Alfaro RI, Kornelia GL, King JN, El-Kassaby YA, Brown G, Smith LD** (2000) Budburst phenology of Sitka spruce and its relationship to white pine weevil attack. *Forest Ecology and Management* **127**: 19-29
- Araki N, Kusumi K, Masamoto K, Iba K** (2000) Temperature-sensitive Arabidopsis mutant defective in 1-deoxy- D-xylulose 5-phosphate synthase within the plastid non-mevalonate pathway of isoprenoid biosynthesis. *Physiologia Plantarum* **108**: 19-24
- Bak S, Beisson F, Bishop G, Hamberger B, Höfer R, Paquette S, Werck-Reichhart D** (2011) Cytochromes P450. *Arabidopsis Book* **9**: e0144
- Battilana J, Emanuelli F, Gambino G, Gribaudo I, Gasperi F, Boss PK, Grando MS** (2011) Functional effect of grapevine 1-deoxy-D-xylulose 5-phosphate synthase substitution K284N on Muscat flavour formation. *Journal of Experimental Botany* **62(15)**: 5497-5508
- Beaulieu J, Giguère I, Deslauriers M, Boyle B, MacKay J** (2013) Differential gene expression patterns in white spruce newly formed tissue on board the International Space Station. *Advances in Space Research* **52**: 760-772
- Bernhardt R** (2006) Cytochromes P450 as versatile biocatalysts. *Journal of Biotechnology* **124**:128-145
- Birol I, Raymond A, Jackman SD, Pleasance S, Coope R, Taylor GA, Yuen MM, Keeling CI, Brand D, Vandervalk BP, Kirk H, Pandoh P, Moore RA, Zhao Y, Mungall AJ, Jaquish B, Yanchuk A, Ritland C, Boyle B, Bousquet J, Ritland K, Mackay J, Bohlmann J, Jones SJ** (2013) Assembling the 20 Gb white spruce (*Picea glauca*) genome from whole-genome shotgun sequencing data. *Bioinformatics* **29(12)**: 1492-1497
- Bohlmann J, Keeling CI** (2008) Terpenoid biomaterials. *The Plant Journal* **54**: 656-669.
- Bohlmann J, Meyer-Gauen G, Croteau R** (1998) Plant terpenoid synthases: Molecular biology and phylogenetic analysis. *Proceedings of the National Academy of Sciences* **95**: 4126-4133
- Boronat A** (2010) The methylerythritol 4-phosphate pathway: regulatory role in plastid isoprenoid biosynthesis. *In* The Chloroplast: Basics and Applications, Vol 31 (Rebeiz CA, Benning C, Bohnert HJ, Daniell H, Hooper JK, Lichtenthaler HK, Portis AR, Tripathy BC, eds) Springer, the Netherlands, pp 119-126

Brachmann CB, Davies A, Cost GJ, Caputo E, Li J, Hieter P, Boeke JD (1998) Designer deletion strains derived from *Saccharomyces cerevisiae* S288C: a useful set of strains and plasmids for PCR-mediated gene disruption and other applications. *Yeast* **14**(2): 115-132

Buckingham, J (2011) Dictionary of Natural Products [Online]. Available: <http://www.chemnetbase.com> [Accessed 10 November 2015]

Carretero-Paulet L, Cairó A, Talavera D, Saura A, Imperial S, Rodríguez-Concepción M, Campos N, Boronat A (2013) Functional and evolutionary analysis of *DXLI*, a non-essential gene encoding a 1-deoxy-D-xylulose 5-phosphate synthase like protein in *Arabidopsis thaliana*. *Gene* **524**(1): 40-53

Cartharius K, Frech K, Grote K, Klocke B, Haltmeier M, Klingenhoff A, Frisch M, Bayerlein M, Werner T (2005) **MatInspector and beyond: promoter analysis based on transcription factor binding sites.** *Bioinformatics* **21**: 2933-2942

Chahed K, Oudin A, Guivarc'h N, Hamdi S, Chenieux JC, Rideau M, Clastre M (2000) 1-deoxy-D-xylulose 5-phosphate synthase from periwinkle: cDNA identification and induced gene expression in terpenoid indole alkaloid-producing cells. *Plant Physiology and Biochemistry* **38**: 559-566.

Chen F, Tholl D, Bohlmann J, Pichersky E (2011) The family of terpene synthases in plants: a mid-size family of genes for specialized metabolism that is highly diversified throughout the kingdom. *The Plant Journal* **66**: 212-229

Christianson DW (2006) Structural Biology and Chemistry of the Terpenoid Cyclases. *Chemical Reviews* **106**(8): 3412-3442

Cooke JE, Eriksson ME, Junttila O (2012) The dynamic nature of bud dormancy in trees: environmental control and molecular mechanisms. *Plant, Cell and Environment* **35**: 1707-1728

Cordoba E, Porta H, Arroyo A, San Román C, Medina L, Rodríguez-Concepción M, León P (2011) Functional characterization of the three genes encoding 1-deoxy-D-xylulose 5-phosphate synthase in maize. *Journal of Experimental Botany* **62**: 2023-2038

Cordoba E, Salmi M, León P (2009) Unravelling the regulatory mechanisms that modulate the MEP pathway in higher plants. *Journal of Experimental Botany* **60**: 2933-2943

Danielson PB (2002) The cytochrome P450 superfamily: Biochemistry, evolution and drug metabolism in humans. *Current Drug Metabolism* **3**(6): 3561-3597

Davidson SE, Smith JJ, Helliwell CA, Poole AT, Reid JB (2004) The pea gene *LH* encodes *ent*-kaurene oxidase. *Plant Physiology* **134**(3): 1123-1134.

Diaz-Chavez ML, Moniodis J, Madilao LL, Jancsik S, Keeling CI, Barbour EL, Ghisalberti EL, Plummer JA, Jones CG, Bohlmann J (2013) Biosynthesis of sandalwood oil: *Santalum album* CYP76F cytochromes P450 produce santalols and bergamotol. *PLoS One* **8**(9): e75053

- Durst F, Nelson DR** (1995) Diversity and evolution of plant P450 and P450-reductases. *Drug Metabolism and Drug Interactions* **12**: 189-206
- Edgar RC** (2004) MUSCLE: multiple sequence alignment with high accuracy and high throughput. *Nucleic Acids Research* **32(5)**: 1792-1797
- Eisenreich W, Bacher A, Arigoni D, Rohdich F** (2004) Biosynthesis of isoprenoids via the non-mevalonate pathway. *Cellular and Molecular Life Sciences* **61**: 1401-1426
- Eisenreich W, Rohdich F, Bacher A** (2001) Deoxyxylulose phosphate pathway to terpenoids. *Trends in Plant Sciences* **6**: 78-84
- Emanuelsson O, Nielsen H, Brunak S, von Heijne G** (2000) Predicting subcellular localization of proteins based on their N-terminal amino acid sequence. *Journal of Molecular Biology* **300(4)**: 1005-1016
- Emanuelsson O, Nielsen H, von Heijne G** (1999) ChloroP, a neural network-based method for predicting chloroplast transit peptides and their cleavage sites. *Protein Science* **8(5)**: 978-984
- Enfissi EMA, Fraser PD, Lois LM, Boronat A, Schuch W, Bramley PM** (2005) Metabolic engineering of the mevalonate and non-mevalonate isopentenyl diphosphate-forming pathways for the production of health-promoting isoprenoids in tomato. *Plant Biotechnology Journal* **3(1)**: 17-27
- Eriksson ME, Moritz T** (2002) Daylength and spatial expression of a gibberellin 20-oxidase isolated from hybrid aspen (*Populus tremula* L. x *P. tremuloides* Michx.). *Planta* **214**: 920-930
- Estévez JM, Cantero A, Reindl A, Reichler S, León P** (2001) 1-Deoxy-D-xylulose-5-phosphate synthase, a limiting enzyme for plastidic isoprenoid biosynthesis in plants. *Journal of Biological Chemistry* **276**: 22901-22909
- Estévez JM, Cantero A, Romero C, Kawaide H, Jiménez LF, Kuzuyama T, Seto H, Kamiya Y, León P** (2000) Analysis of the expression of CLA1, a gene that encodes the 1-deoxy-D-xylulose 5-phosphate synthase of the 2-C-methyl-D-erythritol-4-phosphate pathway in Arabidopsis. *Plant Physiology* **124(1)**: 95-104
- Fäldt J, Martin D, Miller B, Rawat S, Bohlmann J** (2003) Traumatic resin defense in Norway spruce (*Picea abies*): methyl jasmonate-induced terpene synthase gene expression, and cDNA cloning and functional characterization of (+)-3-carene synthase. *Plant Molecular Biology* **51**: 119-133
- Fleet CM, Sun TP** (2005) A DELLAcate balance: the role of gibberellin in plant morphogenesis. *Current Opinions in Plant Biology* **8**: 77-85
- Fleet CM, Yamaguchi S, Hanada A, Kawaide H, David CJ, Kamiya Y, Sun TP** (2003) Overexpression of *AtCPS* and *AtKS* in Arabidopsis confers increased *ent*-kaurene production but no increase in bioactive gibberellins. *Plant Physiology* **132**: 830-839

- Franceschi VR, Krekling T, Christiansen E** (2002) Application of methyl jasmonate on *Picea abies* (Pinaceae) stems induces defense-related responses in phloem and xylem. *American Journal of Botany* **89**: 578-586
- Franceschi VR, Krokene P, Christiansen E, Krekling T** (2005) Anatomical and chemical defenses of conifer bark against bark beetles and other pests. *New Phytologist* **167**: 353-376
- Gershenzon J, Dudareva N** (2007) The function of terpene natural products in the natural world. *Nature Chemical Biology* **3**: 408-414
- Gietz RD, Schiestl RH** (2007) High-efficiency yeast transformation using the LiAc/SS carrier DNA/PEG method. *Nature Protocols* **2**(1): 31-34
- Gong YF, Liao ZH, Guo BH, Sun XF, Tang KX** (2006) Molecular cloning and expression profile analysis of *Ginkgo biloba* DXS gene encoding 1-deoxy-D-xylulose 5-phosphate synthase, the first committed enzyme of the 2-C-methyl-D-erythritol 4-phosphate pathway. *Planta Medica* **72**: 329-335
- Gotoh O** (1992) Substrate recognition sites in cytochrome P450 family 2 (CYP2) proteins inferred from comparative analyses of amino acid and coding nucleotide sequences. *Journal of Biological Chemistry* **267**(1): 83-90
- Graham SE, Peterson JA** (1999) How similar are P450s and what can their differences teach us? *Archives of Biochemistry and Biophysics* **369**(1): 24-29
- Guengerich FP, Martin MV, Sohl CD, Cheng Q** (2009) Measurement of cytochrome P450 and NADPH-cytochrome P450 reductase. *Nature Protocols* **4**(9): 1245-1251
- Guindon S, Dufayard JF, Lefort V, Anisimova M, Hordijk W, Gascuel O** (2010) New algorithms and methods to estimate maximum-likelihood phylogenies: assessing the performance of PhyML 3.0. *Systematic Biology* **59**(3): 307-321
- Hall DE, Robert JA, Keeling CI, Domanski D, Quesada AL, Jancsik S, Kuzyk M, Hamberger Br, Borchers CH, Bohlmann J** (2011) An integrated genomic, proteomic and biochemical analysis of (+)-3-carene biosynthesis in Sitka spruce (*Picea sitchensis*) genotypes that are resistant or susceptible to white pine weevil. *The Plant Journal* **65**(6): 936-948
- Hall DE, Zerbe P, Jancsik S, Quesada AL, Dullat H, Madilao LL, Yuen M, Bohlmann J** (2013) Evolution of conifer diterpene synthases: diterpene resin acid biosynthesis in lodgepole pine and jack pine involves monofunctional and bifunctional diterpene synthases. *Plant Physiology* **161**: 600-616
- Hamberger B, Bohlmann J** (2006) Cytochrome P450 mono-oxygenases in conifer genomes: discovery of members of the terpenoid oxygenase superfamily in spruce and pine. *Biochemistry Society Transactions* **34**(6): 1209-1214
- Hamberger B, Hall D, Yuen M, Oddy C, Hamberger B, Keeling CI, Ritland C, Ritland K, Bohlmann J** (2009) Targeted isolation, sequence assembly and characterization of two

white spruce (*Picea glauca*) BAC clones for terpenoid synthase and cytochrome P450 genes involved in conifer defence reveal insights into a conifer genome. *BMC Plant Biology* **9**: 106

Hamberger B, Ohnishi T, Hamberger B, Séguin A, Bohlmann J (2011) Evolution of diterpene metabolism: Sitka spruce CYP720B4 catalyzes multiple oxidations in resin acid biosynthesis of conifer defense against insects. *Plant Physiology* **157**: 1677-1695

Hamberger B, Bak S (2013) Plant P450s as versatile drivers for evolution of species-specific chemical diversity. *Philosophical Transactions of The Royal Society Biological Sciences* 2013; **368**(1612): 20120426

Han M, Heppel SC, Su T, Bogs J, Zu Y, An Z, Rausch T (2013) Enzyme inhibitor studies reveal complex control of methyl-D-erythritol 4-phosphate (MEP) pathway enzyme expression in *Catharanthus roseus*. *PLoS ONE* **8**(5): E62467

Hao X, Shi M, Cui L, Xu C, Zhang Y, Kai G (2014) Effects of methyl jasmonate and salicylic acid on tanshinone production and biosynthetic gene expression in transgenic *Salvia miltiorrhiza* hairy roots. *Biotechnology and Applied Biochemistry* **62**(1): 24-31

Harris LJ, Saparno A, Johnston A, Prsic S, Xu M, Allard S, Kathiresan A, Ouellet T, Peters RJ (2005) The maize An2 gene is induced by Fusarium attack and encodes an *ent*-copalyl diphosphate synthase. *Plant Molecular Biology* **59**: 881-894

Hawkins CF, Borges A, Perham RN (1989) A common structural motif in thiamin pyrophosphate-binding enzymes. *FEBS Letters* **255**: 77-82

Hayashi K, Kawaide H, Notomi M, Sakigi Y, Matsuo A, Nozaki, H (2006) Identification and functional analysis of bifunctional *ent*-kaurene synthase from the moss *Physcomitrella patens*. *FEBS Letters* **580**: 6175-6181

Hedden P, Phillips AL (2000) Gibberellin metabolism: New insights revealed by the genes. *Trends in Plant Science* **5**: 523-530

Heide OM (1993) Daylength and thermal time responses of bud burst during dormancy release in some northern deciduous trees. *Physiologia Plantarum* **88**(4): 531-540

Hellemans J, Mortier G, De Paepe A, Speleman F, Vandesompele J (2007) qBase relative quantification framework and software for management and automated analysis of real-time quantitative PCR data. *Genome Biology* **8**(2): R19

Helliwell CA, Poole A, Peacock WJ, Dennis ES (1999) Arabidopsis *ent*-kaurene oxidase catalyzes three steps of gibberellin biosynthesis. *Plant Physiology* **119**(2): 507-510

Higo K, Ugawa Y, Iwamoto M, Korenaga T (1999) Plant cis-acting regulatory DNA elements (PLACE) database. *Nucleic Acids Research* **27**(1): 297-300

Hochmuth DH (2007) MassFinder 3. Hochmuth Scientific Consulting, Hamburg, Germany

Horvath DP, Anderson JV, Chao WS, Foley ME (2003) Knowing when to grow: signals regulating bud dormancy. *Trends in Plant Science* **8**(11): 534-540

- Howe GT, Aitken SN, Neale DB, Jermstad KD, Wheeler NC, Chen THH** (2003) From genotype to phenotype: unraveling the complexities of cold adaptation in forest trees. *Canadian Journal of Botany* **81**: 1247-1266
- Humphrey TV, Richman AS, Menassa R, Brandle JE** (2006) Spatial organisation of four enzymes from *Stevia rebaudiana* that are involved in steviol glycoside synthesis. *Plant Molecular Biology* **61**(1-2): 47-62
- Kato H, Kodama O, Akatsuka T** (1994) Oryzalexin F, a diterpene phytoalexin from UV-irradiated rice leaves. *Phytochemistry* **36**: 299-301
- Kato-Noguchi H, Ino T** (2003) Rice seedlings release momilactone B into the environment. *Phytochemistry* **63**: 551-554
- Kawaide H, Hayashi K, Kawanabe R, Sakigi Y, Matsuo A, Natsume M, Nozaki H** (2011) Identification of the single amino acid involved in quenching the entkauranyl cation by a water molecule in *ent*-kaurene synthase of *Physcomitrella patens*. *FEBS Journal* **278**: 123-133
- Kayal WE, Allen CC, Ju CJ, Adams E, King-Jones S, Zaharia LI, Abrams SR, Cooke JE** (2011) Molecular events of apical bud formation in white spruce, *Picea glauca*. *Plant, Cell and Environment* **34**(3): 480-500
- Keeling CI, Bohlmann J** (2006) Genes, enzymes and chemicals of terpenoid diversity in the constitutive and induced defense of conifers against insects and pathogens. *New Phytologist* **170**: 657-675
- Keeling CI, Dullat HK, Yuen M, Ralph SG, Jancsik S, Bohlmann J** (2010) Identification and functional characterization of monofunctional *ent*-copalyl diphosphate and *ent*-kaurene synthases in white spruce (*Picea glauca*) reveal different patterns for diterpene synthase evolution for primary and secondary metabolism in gymnosperms. *Plant Physiology* **152**: 1197-1208
- Keeling CI, Madilao LL, Zerbe P, Dullat HK, Bohlmann J** (2011a) The primary diterpene synthase products of *Picea abies* levopimaradiene/abietadiene synthase (*PaLAS*) are epimers of a thermally unstable diterpenol. *Journal of Biological Chemistry* **286**(24): 21145-21153
- Keeling CI, Weisshaar S, Lin RPC, Bohlmann J** (2008) Functional plasticity of paralogous diterpene synthases involved in conifer defense. *Proceedings of the National Academy of Sciences* **105**: 1085-1090
- Keeling CI, Weisshaar S, Ralph SG, Jancsik S, Hamberger B, Dullat HK., Bohlmann J** (2011b) Transcriptome mining, functional characterization, and phylogeny of a large terpene synthase gene family in spruce (*Picea spp.*). *BMC Plant Biology* **11**:43
- Kim BR, Kim SU, Chang YJ** (2005) Differential expression of three 1-deoxy-D-xylulose-5-phosphate synthase genes in rice. *Biotechnology Letters* **27**: 997-1001
- Kim SM, Kuzuyama T, Chang YJ, Song KS, Kim SU** (2006) Identification of class 2 1-deoxy-D-xylulose 5-phosphate synthase and 1-deoxy-D -xylulose 5-phosphate

reductoisomerase genes from *Ginkgo biloba* and their transcription in embryo culture with respect to ginkgolide biosynthesis. *Planta Medica* **72**: 234-240

Kim YB, Kim SM, Kang MK, Kuzuyama T, Lee JK, Park SC, Shin SC, Kim SU (2009) Regulation of resin acid synthesis in *Pinus densiflora* by differential transcription of genes encoding multiple 1-deoxy-D-xylulose 5-phosphate synthase and 1-hydroxy-2-methyl-2-(E)-butenyl 4-diphosphate reductase genes. *Tree Physiology* **29**: 737-749

Köksal M, Hu H, Coates RM, Peters RJ, Christianson DW (2011) Structure and mechanism of the diterpene cyclase *ent*-copalyl diphosphate synthase. *Nature Chemical Biology* **7**: 431-433

Kong L, Abrams SR, Owen SJ, Graham H, Aderkas PV (2008) Phytohormones and their metabolites during long shoot development in Douglas-fir following cone induction by gibberellin injection. *Tree Physiology* **28**: 1357-1364

Kooper BJ, Illman, BL, Kersten PJ, Klepzig KD, Raffa KF (2005) Effects of diterpene acids on components of a conifer bark beetle-fungal interaction: tolerance by *Ips pini* and sensitivity by its associate *Ophiostoma ips*. *Environmental entomology* **34**(2): 486-493

Kozlowski TT, Pallardy SG (1997) Vegetative growth. In *Physiology of Woody Plants*, 2nd edn (Kozlowski TT, Pallardy SG, eds), Academic Press, San Diego, CA. pp 34-67

Kurosawa E (1926) Experimental studies on the nature of the substance secreted by the “bakanae” fungus. *Natural Historical Society of Formosa* **16**: 213-227

Laemmli UK (1970) Cleavage of structural proteins during the assembly of the head of bacteriophage T4. *Nature* **227**(5259): 680-685

Lange BM, Croteau R (1999) Genetic engineering of essential oil production in mint. *Current Opinion in Plant Biology* **2**: 139-144

Leal I, White EE, Sahota TS, Manville JF (1997) Differential expression of vitellogenin gene in the spruce terminal weevil feeding on resistant versus susceptible host trees. *Insect Biochemistry and Molecular Biology* **27**: 569-575

Letunic I, Bork P (2011) Interactive Tree Of Life v2: online annotation and display of phylogenetic trees made easy. *Nucleic Acids Research* **39**: W475-W478

Lewinsohn E, Gijzen M, Muzika RM, Barton K, Croteau R (1993) Oleoresinosis in grand fir (*Abies grandis*) saplings and mature trees. *Plant Physiology* **101**(3): 1021-1028

Lichtenthaler HK (1999) The 1-deoxy-D-xylulose-5-phosphate pathway of isoprenoid biosynthesis in plants. *Annual Review of Plant Physiology and Plant Molecular Biology* **50**: 47-65

Lichtenthaler HK (2010) The non-mevalonate DOXP/MEP (deoxyxylulose 5-phosphate/methylerythritol 4-phosphate) pathway of chloroplast isoprenoid and pigment biosynthesis. In *The Chloroplast: Basics and Applications*, Vol 31 (Rebeiz CA, Benning C,

Bohnert HJ, Daniell H, Hooper JK, Lichtenthaler HK, Portis AR, Tripathy BC, eds) Springer, the Netherlands, pp 95-118

Lindgren BS, Nordlander G, Birgersson G (1996) Feeding deterrence of verbenone to the pine weevil, *Hylobius abietis* (L.) (Col., Curculionidae). Journal of Applied Entomology **120**: 397-403

Little CHA, Macdonald JE (2003) Effects of exogenous gibberellin and auxin on shoot elongation and vegetative bud development in seedlings of *Pinus sylvestris* and *Picea glauca*. Tree Physiology **23**: 73-83

Livak KJ, Schmittgen TD (2001) Analysis of relative gene expression data using real-time quantitative PCR and the 2(-Delta Delta C(T)) method. Methods **25(4)**: 402-408

Lois LM, Rodríguez-Concepción M, Gallego F, Campos N, and Boronat A (2000) Carotenoid biosynthesis during tomato fruit development: regulatory role of 1-deoxy-D-xylulose 5-phosphate synthase. The Plant Journal **22**: 503-513

Martin D, Gershenzon J, Bohlmann J (2003) Induction of volatile terpene biosynthesis and diurnal emission by methyl jasmonate in foliage of Norway spruce. Plant Physiology **132**: 1586-1599

Martin D, Tholl D, Gershenzon J, Bohlmann J (2002) Methyl jasmonate induces traumatic resin ducts, terpenoid resin biosynthesis, and terpenoid accumulation in developing xylem of Norway spruce stems. Plant Physiology **129**: 1003-1018

Martin DM, Fäldt J, Bohlmann J (2004) Functional characterization of nine Norway spruce TPS genes and evolution of gymnosperm terpene synthases of the TPS-d subfamily. Plant Physiology **135**: 1908-1927

McKay SAB, Hunter WL, Godard KA, Wang SX, Martin DM, Bohlmann J, Plant AL (2003) Insect attack and wounding induce traumatic resin duct development and gene expression of (-)-pinene synthase in Sitka spruce. Plant Physiology **133**: 600-616

Miller B, Madilao LL, Ralph S, Bohlmann J (2005) Insect-induced conifer defense. White pine weevil and methyl jasmonate induce traumatic resinosis, de novo formed volatile emissions, and accumulation of terpenoid synthase and putative octadecanoid pathway transcripts in Sitka spruce. Plant Physiology **137**: 369-382

Mizutani M (2012) Impacts of diversification of cytochrome P450 on plant metabolism. Biological and Pharmaceutical Bulletin **35(6)**: 824-832

Mizutani M, Sato F (2011) Unusual P450 reactions in plant secondary metabolism. Archives of Biochemistry and Biophysics **507(1)**: 194-203

Moritz T (1995) Biological activity, identification and quantification of gibberellins in seedlings of Norway spruce (*Picea abies*) grown under different photoperiods. Physiologia Plantarum **95**: 67-72

Moritz T, Philipson JJ, Odén PC (1990) Quantitation of gibberellins A1, A3, A4, A9 and a putative A9-conjugate in grafts of Sitka spruce (*Picea sitchensis*) during the period of shoot elongation. *Plant Physiology* **93**: 1476-1481

Morris WL, Ducreux LJ, Hedden P, Millam S, Taylor MA (2006) Overexpression of a bacterial 1-deoxy-D-xylulose 5-phosphate synthase gene in potato tubers perturbs the isoprenoid metabolic network: implications for the control of the tuber life cycle. *Journal of Experimental Botany* **57**(12): 3007-3018

Morrone D, Xu M, Fulton B, Determan MK, Peters RJ (2008) Increasing complexity of a diterpene synthase reaction with a single residue switch. *Journal of the American Chemical Society* **130**: 5400-5401

Muñoz-Bertomeu J, Arrillaga I, Ros R, Sequera J (2006) Up-regulation of 1-deoxy-D-xylulose-5-phosphate synthase enhances production of essential oils in transgenic spike lavender. *Plant Physiology* **142**(3): 890-900

Nelson DR (2006) Cytochrome P450 nomenclature, 2004. *Methods in Molecular Biology* **320**: 1-10

Nelson DR, Ming R, Alam M, Schuler MA (2008) Comparison of cytochrome P450 genes from six plant genomes. *Tropical Plant Biology*, **1**: 216-235

Nelson DR, Schuler MA, Paquette SM, Werck-Reichhart D, Bak S (2004) Comparative genomics of rice and Arabidopsis. Analysis of 727 cytochrome P450 genes and pseudogenes from a monocot and a dicot. *Plant Physiology* **135**: 756-772

Nienstaedt H (1966) Dormancy and dormancy release in white spruce. *Forest Science* **12**(3): 374-384

O'Maille PE, Chappell J, Noel JP (2004) A single-vial analytical and quantitative gas chromatography-mass spectrometry assay for terpene synthases. *Analytical Biochemistry* **335**: 210-217

Odén PC, Wang Q, Hogberg K-L, Werner M (1995) Transport and metabolism of gibberellins in relation to flower bud differentiation in Norway spruce (*Picea abies*). *Tree Physiology* **15**: 451-456

Olsen JE, Jensen E, Junttila O, Moritz T (1995a) Photoperiodic control of endogenous gibberellins in seedlings of *Salix pentandra*. *Physiologia Plantarum* **93**(4): 639-644

Olsen JE, Junttila O, Moritz T (1995b) A localised decrease of GA₁ in shoot tips of *Salix pentandra* seedlings precedes cessation of shoot elongation under short photoperiod. *Physiologia Plantarum* **95**(4): 627-632

Olsen JE, Junttila O, Moritz T (1997) Long-day induced bud break in *Salix pentandra* is associated with transiently elevated levels of GA₁ and gradual increase in indole-3-acetic acid. *Plant and Cell Physiology* **38**: 536-540

Olszewski N, Sun TP, Gubler F (2002) Gibberellin signaling: Biosynthesis, catabolism, and response pathways. *Plant Cell* **14**(Suppl.): S61-S80

Omura T, Sato R (1964) The carbon monoxide-binding pigment of liver microsomes. I. Evidence for its hemoprotein nature. *The Journal of Biological Chemistry* **239**: 2370-2378

Peters RJ (2006) Uncovering the complex metabolic network underlying diterpenoid phytoalexin biosynthesis in rice and other cereal crop plants. *Phytochemistry* **67**(21): 2307-2317

Peters RJ (2010) Two rings in them all: the labdane-related diterpenoids. *Natural Products Report* **27**: 1521-1530

Peters RJ, Flory JE, Jetter R, Ravn MM, Lee HJ, Coates RM, Croteau RB (2000) Abietadiene synthase from grand fir (*Abies grandis*): characterization and mechanism of action of the “pseudomature” recombinant enzyme. *Biochemistry* **39**: 15592-15602

Phillips MA, Walter MH, Ralph SG, Dabrowska P, Luck K, Uro EM, Boland W, Strack D, Rodriguez-Concepcion M, Bohlmann J, and Gershenzon J (2007) Functional identification and differential expression of 1-deoxy-D-xylulose 5-phosphate synthase in induced terpenoid resin formation of Norway spruce (*Picea abies*). *Plant Molecular Biology* **65**: 243-257

Phinney BO (1983) The history of gibberellins. *In* *The Biochemistry and Physiology of Gibberellins*, Vol 1 (Crozier A, ed), Praeger Press, New York, NY, pp 19-52

Pompon D, Louerat B, Bronine A, Urban P (1996) Yeast expression of animal and plant P450s in optimized redox environments. *Methods in Enzymology* **272**: 51-64

Prisic S and Peters RJ (2007) Synergistic substrate inhibition of *ent*-copalyl diphosphate synthase: a potential feed-forward inhibition mechanism limiting gibberellin metabolism. *Plant Physiology* **144**: 445-454

Prisic S, Xu M, Wilderman PR, Peters RJ (2004) Rice contains two disparate *ent*-copalyl diphosphate synthases with distinct metabolic functions. *Plant Physiology* **136**(4): 4228-4236

Prisic S, Xu J, Coates RM, Peters RJ (2007) Probing the role of the DXDD motif in Class II diterpene cyclases. *Chembiochem* **8**(8): 869-874

Raffa KF, Aukema BH, Erbilgin N, Klepzig KD, Wallin KF (2005) Interactions among conifer terpenoids and bark beetles across multiple levels of scale: an attempt to understand links between population patterns and physiological processes. *Recent Advances in Phytochemistry* **39**: 80-118

Richman AS, Gijzen M, Starratt AN, Yang Z-Y, Brandle JE (1999) Diterpene synthesis in *Stevia rebaudiana*: recruitment and up-regulation of key enzymes from the gibberellin biosynthetic pathway. *The Plant Journal* **19**: 411-421

Ro DK, Arimura G, Lau SY, Piers E, Bohlmann J (2005) Loblolly pine abietadienol/abietadienal oxidase *PtAO* (CYP720B1) is a multifunctional, multisubstrate

cytochrome P450 monooxygenase. Proceedings of the National Academy of Sciences **102**: 8060-8065

Ro DK, Bohlmann J (2006) Diterpene resin acid biosynthesis in loblolly pine (*Pinus taeda*): functional characterization of abietadiene/levopimaradiene synthase (*PtTPS-LAS*) cDNA and subcellular targeting of *PtTPS-LAS* and abietadienol/abietadienal oxidase (*PtAO*, CYP720B1). *Phytochemistry* **67(15)**: 1572-1578

Roach CR, Hall DE, Zerbe P, Bohlmann J (2014) Plasticity and evolution of (+)-3-carene synthase and (-)-sabinene synthase functions of a Sitka spruce monoterpene synthase gene family associated with weevil resistance. *Journal of Biological Chemistry* **289(34)**: 23859-23869

Rodríguez-Concepción M (2006) Early steps in isoprenoid biosynthesis: multilevel regulation of the supply of common precursors in plant cells. *Phytochemistry Reviews* **5(1)**: 1-15

Rohde A, Bhalerao RP (2007) Plant dormancy in the perennial context. *Trends in Plant Science* **12**: 217-223

Rohde A, Howe GT, Olsen JE, Moritz T, Van Montagu M, Junttila O, Boerjan W (2000) Molecular aspects of bud dormancy in trees. *In* *Molecular Biology of Woody Plants*, Vol 1 (Jain SM, Minocha SC, eds), Kluwer Academic Publishers, Dordrecht, the Netherlands, pp 89-134

Romanos MA, Scorer CA, Clare JJ (1992) Foreign gene expression in yeast: a review. *Yeast* **8**: 423-488

Rupasinghe S, Baudry J, Schuler MA (2003) Common active site architecture and binding strategy of four phenylpropanoid P450s from *Arabidopsis thaliana* as revealed by molecular modeling. *Protein Engineering* **16(10)**: 721-731

Ruttink T, Arend M, Morreel K, Storme V, Rombauts S, Fromm J, Bhalerao RP, Boerjan W, Rohde A (2007) A molecular timetable for apical bud formation and dormancy induction in poplar. *Plant Cell* **19**: 2370-2390

Sakamoto T, Miura K, Itoh H, Tatsumi T, Ueguchi-Tanaka M, Ishiyama K, Kobayashi M, Agrawal GK, Takeda S, Abe K, Miyao A, Hirochika H, Kitano H, Ashikari M, Matsuoka M (2004) An overview of gibberellin metabolism enzyme genes and their related mutants in rice. *Plant Physiology* **134**: 1642-1653

Silverstone A, Chang CW, Krol E, Sun TP (1997) Developmental regulation of the gibberellin biosynthetic gene *GA1* in *Arabidopsis thaliana*. *The Plant Journal* **12**: 9-19

Smith MW, Yamaguchi S, Ait-Ali T, Kamiya Y (1998) The first step of gibberellin biosynthesis in pumpkin is catalyzed by at least two copalyl diphosphate synthases encoded by differentially regulated genes. *Plant Physiology* **118(4)**: 1411-1419

Stofer Vogel B, Wildung MR, Vogel G, Croteau R (1996) Abietadiene synthase from grand fir (*Abies grandis*): cDNA isolation, characterization, and bacterial expression of a

bifunctional diterpene cyclase involved in resin acid biosynthesis. *Journal of Biological Chemistry* **271**: 23262-23268

Sun TP, Kamiya Y (1994) The *Arabidopsis* GA1 locus encodes the cyclase *ent*-kaurene synthetase A of gibberellin biosynthesis. *The Plant Cell* **6(10)**: 1509-1518

Theologis A, Ecker JR, Palm CJ, Federspiel NA, Kaul S, White O, Alonso J, Altafi H, Araujo R, Bowman CL, Brooks SY, Buehler E, Chan A, Chao Q, Chen H, Cheuk RF, Chin CW, Chung MK, Conn L, Conway AB, Conway AR, Creasy TH, Dewar K, Dunn P, Etgu P, Feldblyum TV, Feng J, Fong B, Fujii CY, Gill JE, Goldsmith AD, Haas B, Hansen NF, Hughes B, Huizar L, Hunter JL, Jenkins J, Johnson-Hopson C, Khan S, Khaykin E, Kim CJ, Koo HL, Kremenetskaia I, Kurtz DB, Kwan A, Lam B, Langin-Hooper S, Lee A, Lee JM, Lenz CA, Li JH, Li Y, Lin X, Liu SX, Liu ZA, Luros JS, Maiti R, Marzali A, Militscher J, Miranda M, Nguyen M, Nierman WC, Osborne BI, Pai G, Peterson J, Pham PK, Rizzo M, Rooney T, Rowley D, Sakano H, Salzberg SL, Schwartz JR, Shinn P, Southwick AM, Sun H, Tallon LJ, Tambunga G, Toriumi MJ, Town CD, Utterback T, Van Aken S, Vaysberg M, Vysotskaia VS, Walker M, Wu D, Yu G, Fraser CM, Venter JC, Davis RW (2000) Sequence and analysis of chromosome 1 of the plant *Arabidopsis thaliana*. *Nature* **408(6814)**: 816-820

Towbin H, Staehelin T, Gordon J (1979) Electrophoretic transfer of proteins from polyacrylamide gels to nitrocellulose sheets: procedure and some applications. *Proceedings of the National Academy of Sciences* **76(9)**: 4350-4354

Toyomasu T, Usui M, Sugawara C, Kanno Y, Sakai A, Takahashi H, Nakazono M, Kuroda M, Miyamoto K, Morimoto Y, Mitsunashi W, Okada K, Yamaguchi S, Yamane H (2015) Transcripts of two *ent*-copalyl diphosphate synthase genes differentially localize in rice plants according to their distinct biological roles. *Journal of Experimental Botany* **66(1)**: 369-376

Trapp SC, Croteau RB (2001) Genomic organization of plant terpene synthases and molecular evolutionary implications. *Genetics* **158**: 811-832

Vandesompele J, De Preter K, Pattyn F, Poppe B, Van Roy N, De Paepe A, Speleman F (2002) Accurate normalization of real-time quantitative RT-PCR data by geometric averaging of multiple internal control genes. *Genome Biology* **3(7)**: research0034

Walter MH, Hans J, Strack D (2002) Two distantly related genes encoding 1-deoxy-d-xylulose 5-phosphate synthases: differential regulation in shoots and apocarotenoid-accumulating mycorrhizal roots. *The Plant Journal* **31**: 243-254

Walter M, Fester T, Strack D (2000) Arbuscular mycorrhizal fungi induce the non-mevalonate methylerythritol phosphate pathway of isoprenoid biosynthesis correlated with accumulation of the 'yellow pigment' and the other apocarotenoids. *The Plant Journal* **21(6)**: 571-578

- Wang Q, Hillwig ML, Wu Y, Peters RJ** (2012) CYP701A8: a rice *ent*-kaurene oxidase paralog diverted to more specialized diterpenoid metabolism. *Plant Physiology* **158**(3): 1418-1425
- Wang Q, Little CHA, Moritz T, Odén PC** (1996) Identification of endogenous gibberellins, and metabolism of tritiated and deuterated GA4, GA9 and GA20, in Scots pine (*Pinus sylvestris*) shoots. *Physiologia Plantarum* **97**: 764-771
- Warren RL, Keeling CI, Yuen MMS, Raymond A, Taylor GA, Vandervalk BP, Mohamadi H, Paulino D, Chiu Readman, Jackman SD, Robertson G, Yang C, Hoffmann M, Weigel D, Nelson DR, Ritland C, Isabel N, Jaquish B, Yanchuk A, Bousquet J, Jones SJM, MacKay J, Birol I, Bohlmann J** (2015) Improved white spruce (*Picea glauca*) genome assemblies and annotation of large gene families of conifer terpenoid and phenolic defense metabolism. *The Plant Journal* **83**(2): 189-212
- Wendt KU, Poralla K, Schulz GE** (1997) Structure and function of a squalene cyclase. *Science* **277**(5333): 1811-1815
- Werck-Reichhart D, Feyereisen R** (2000) Cytochromes P450: a success story. *Genome Biology* **1**(6): REVIEWS3003
- Winter D, Vinegar B, Nahal H, Ammar R, Wilson GV, Provart NJ** (2007) An “Electronic Fluorescent Pictograph” Browser for Exploring and Analyzing Large-Scale Biological Data Sets. *PLoS One* **2**(8): e718
- Wright LP, Rohwer JM, Ghirardo A, Hammerbacher A, Ortiz-Alcaide M, Raguschke B, Schnitzler JP, Gershenzon J, Phillips MA** (2014) Deoxyxylulose 5-phosphate synthase controls flux through the methylerythritol 4-phosphate pathway in Arabidopsis. *Plant Physiology* **165**: 1488-1504
- Xiang S, Usunow G, Lange G, Busch M, Tong L** (2007) Crystal structure of 1-deoxy-D-xylulose 5-phosphate synthase, a crucial enzyme for isoprenoids biosynthesis. *Journal of Biological Chemistry* **282**: 2676-2682
- Xu M, Hillwig ML, Pristic S, Coates RM, Peters RJ** (2004) Functional identification of rice syn-copalyl diphosphate synthase and its role in initiating biosynthesis of diterpenoid phytoalexin/allelopathic natural products. *The Plant Journal* **39**: 309-318
- Xu M, Wilderman R, Peters RJ** (2007a) Following evolution’s lead to a single residue switch for diterpene synthase product outcome. *Proceedings of the National Academy of Sciences* **104**(18): 7397-7401
- Xu MM, Wilderman PR, Morrone D, Xu J, Margis-Pinheiro M, Upadhyaya NM, Coates RM, Peters RJ** (2007b) Functional characterization of the rice kaurene synthase-like gene family. *Phytochemistry*, **68**(3): 312-326
- Yamaguchi S** (2006) Gibberellin Biosynthesis in Arabidopsis. *Phytochemistry Reviews* **5**(1): 39-47.

Yamaguchi S (2008) Gibberellin metabolism and its regulation. *Annual Reviews of Plant Biology* **59**: 225-251

Yamaguchi S, Kamiya U (2000) Gibberellin biosynthesis: its regulation by endogenous and environmental signals. *Plant and Cell Physiology* **41**: 251-257

Yamaguchi S, Kamiya Y, Sun TP (2001) Distinct cell-specific expression patterns of early and late gibberellin biosynthetic genes during *Arabidopsis* seed germination. *The Plant Journal* **28**(4): 443-453

Yamaguchi S, Saito T, Abe H, Yamane H, Murofushi N, Kamiya Y (1996) Molecular cloning and characterisation of a cDNA encoding the gibberellin biosynthetic enzyme *ent*-kaurene synthase B from pumpkin (*Cucurbita maxima* L.). *The Plant Journal* **10**: 203-213

Yamaguchi S, Sun TP, Kawaide H, Kamiya Y (1998) The GA2 locus of *Arabidopsis thaliana* encodes *ent*-kaurene synthase of gibberellin biosynthesis. *Plant Physiology* **116**(4): 1271-1278

Zawaski C, Kadmiel M, Pickens J, Ma C, Strauss S, Busov V (2011) Repression of gibberellin biosynthesis or signaling produces striking alterations in poplar growth, morphology, and flowering. *Planta* **234**: 1285-1298

Zerbe P, Chiang A, Bohlmann J (2012) Mutational analysis of white spruce (*Picea glauca*) *ent*-kaurene synthase (*PgKS*) reveals common and distinct mechanisms of conifer diterpene synthases of general and specialized metabolism *Phytochemistry* **74**: 30-39

Zhao YJ, Cheng QQ, Su P, Chen X, Wang XJ, Gao W, Huang LQ (2014) Research progress relating to the role of cytochrome P450 in the biosynthesis of terpenoids in medicinal plants. *Applied Microbiology and Biotechnology* **98**(6): 2371-2383

Zhou K, Gao Y, Hoy JA, Mann FM, Honzatko RB, Peters RJ (2012) Insights into diterpene cyclization from structure of bifunctional abietadiene synthase from *Abies grandis*. *Journal of Biological Chemistry* **287**(9): 6840-6850

Zulak KG, Bohlmann J (2010) Terpenoid biosynthesis and specialized vascular cells of conifer defense. *Journal of Integrative Plant Biology* **52**: 86-97

Zulak KG, Dullat HK, Keeling CI, Lippert D, Bohlmann J (2010) Immunofluorescence localization of levopimaradiene/abietadiene synthase in methyl jasmonate treated stems of Sitka spruce (*Picea sitchensis*) shows activation of diterpenoid biosynthesis in cortical and developing traumatic resin ducts. *Phytochemistry* **71**: 1695-1699








Zulak KG, Lippert DN, Kuzyk MA, Domanski D, Chou T, Borchers CH, Bohlmann J (2009) Targeted proteomics using selected reaction monitoring reveals the induction of specific terpene synthases in a multi-level study of methyl jasmonate-treated Norway spruce (*Picea abies*). *The Plant Journal* **60**: 1015-1030









Appendix 1.








Collection of apical buds and apical shoots in the experiment “Vegetative white spruce apical bud development time course” (Section 2.5) was designed to include landmark developmental growth stages based on previously described Sitka spruce vegetative bud growth stages described by Alfaro et al. (2000). These stages were modified to fit white spruce growth, and are as follows:










Stage 1 “shiny conical”	buds are conical in shape with bud scales beginning to peel back
Stage 2 “shiny/swollen”	buds are more swollen than stage 1
Stage 3 “yellow/swollen”	buds are considerably swollen and appear yellowish in colour due to bud cap becoming translucent
Stage 4 “columnar”	shoots are starting to elongate, bud scales at tip of bud cap are translucent with needles clearly visible underneath
Stage 5 “split”	shoot continues to elongate, bud cap is substantially splitting and in some cases has become detached at tip of shoot
Stage 6 “brush”	bud cap is usually no longer present, needles are tightly packed and appear to originate from one point, shoot continues to elongate
Stage 7 “feather”	needle bases begin to separate, shoot continues to elongate
Stage 8 “growing shoot”	needles widely separate out from expanding shoot

Supplemental Table S1. Phenotypic observations of white spruce (*Pg653*) apical buds and shoots sampled during a year-long period of vegetative bud development. Images shown are of apical leader with 1 being the first time point collected in 2011 and 31 the last in that same year. Photos by K.M. Storey.

Month	Time point	Date		
January	1	Jan 19		<ul style="list-style-type: none"> • Apical bud is dark brown in color, with black tips on bud scales. • Apical bud is quite hard to the touch and is covered with dried oleoresin that is a white-ash color. • Apical bud width ~3-4 mm.
February	2	Feb 16		<ul style="list-style-type: none"> • Same as above
March	3	Mar 2		<ul style="list-style-type: none"> • Same as above
	4	Mar 9		<ul style="list-style-type: none"> • Bud scales are slightly peeling away from bud center. • Apical bud is in phenological stage 1 or 2. • Apical bud is dark brown in color, hard to the touch, and is covered with dried oleoresin that is a white-ash color. • Apical bud width ~3-4 mm.
	5	Mar 16		<ul style="list-style-type: none"> • Same as above
	6	Mar 23		<ul style="list-style-type: none"> • Same as above
	7	Mar 30		<ul style="list-style-type: none"> • Same as above

Month	Time point	Date		
April	8	Apr 6		<ul style="list-style-type: none"> • Apical bud cap appears slightly translucent, is yellow in color, and is soft and pliable to the touch. • Apical bud is in phenological stage 3. • The base of the apical bud is dark brown in color and is covered with dried oleoresin that is a white-ash color.
	9	Apr 13		<ul style="list-style-type: none"> • Apical bud cap appears very translucent, some new needles are visible underneath. • Apical bud is in phenological stage 4. • Apical bud is soft and pliable to the touch. • The base of the apical bud is covered with dried oleoresin that is a white-ash color.
	10	Apr 20		<ul style="list-style-type: none"> • Apical bud cap is either missing or completely transparent. • Apical bud is between phenological stages 4 and 5. • New needles are visible, light green in color, with some red needles at the center of the bud.
	11	Apr 27		<ul style="list-style-type: none"> • Apical bud has flushed, in some cases the bud cap still very loosely attached. • Apical bud is in phenological stage 5. • New bundles of needles have red needles at their center.
May	12	May 4		<ul style="list-style-type: none"> • Apical bud/shoot is actively elongating. • Apical shoot is in phenological stage 5 or 6. • Red needles once visible at the center of the bud are fading in color.
	13	May 11		<ul style="list-style-type: none"> • Apical shoot continues growth/elongation. • Apical shoot in phenological stage 6.
	14	May 18		<ul style="list-style-type: none"> • Apical shoot appears to be in phenological stage 7. • Bud scales once present at base of shoot have fallen away.
	15	May 25		<ul style="list-style-type: none"> • Apical shoot is in phenological stage 7, needle bases separate. • Color of the new needle growth is darkening but is lighter than mature needles (last year's growth).

Month	Time point	Date		
June	16	June 1		<ul style="list-style-type: none"> • Apical shoot is in phenological stage 8, needles are widely separated from growing shoot. • The apical shoot/leader has very small new buds growing along the stem, they appear as small red nodules.
	17	June 08		<ul style="list-style-type: none"> • Apical shoot is in phenological stage 8. • Color of the new needle growth continues to darken to more closely resemble mature needles. • Newly set buds along length of apical shoot are white in color with faint red color at their center. No bud scales are apparent.
	18	June 15		<ul style="list-style-type: none"> • Needles along apical shoot have characteristic sharpened point, resembling those of mature needles • Newly set buds on apical shoot are light yellow in color with darkening bud scales appearing on their outsides. • Newly set apical bud measures ~3 mm in width, whorl buds measure ~2-2.5 mm in width.
	19	June 22		<ul style="list-style-type: none"> • Color of needles along apical shoot are the same shade as mature needles. • Newly set buds on apical shoot are light yellow or green in color with darkening bud scales appearing on their outsides. • Newly set apical bud measures ~3-3.5 mm in width, whorl buds measure ~2-2.5 mm in width.
	20	June 29		<ul style="list-style-type: none"> • Newly set buds on apical shoot are a light brown color. • Newly set apical bud measures ~3.5 mm in width, whorl buds measure ~2.5-3 mm in width.
July	21	July 13		<ul style="list-style-type: none"> • Same as above
	22	July 27		<ul style="list-style-type: none"> • Newly set buds on apical shoot are a darkening red/brown color. • Newly set apical bud measures ~3-4 mm in width, whorl buds measure ~3-3.5 mm in width.

Month	Time point	Date		
August	23	Aug 10		<ul style="list-style-type: none"> Same as above
	24	Aug 24		<ul style="list-style-type: none"> Newly set apical bud measures ~4-4.5 mm in width, whorl buds measure ~3.5 mm in width.
September	25	Sept 7		<ul style="list-style-type: none"> Newly set buds on apical shoot are a dark red/brown color. Newly set apical bud measures ~4-4.5 mm in width, whorl buds measure ~3.5 mm in width.
	26	Sept 21		<ul style="list-style-type: none"> Same as above
October	27	Oct 5		<ul style="list-style-type: none"> Color of bark on stem of apical shoot is darkening, though still slightly lighter brown than that of mature bark.
	28	Oct		<ul style="list-style-type: none"> Newly set apical and whorl buds have accumulated dried oleoresin along the edges of bud scales.
November	29	Nov 2		<ul style="list-style-type: none"> Newly set apical and whorl buds have accumulated dried oleoresin covering their surface, is a white-ash color.
	30	Nov 16		<ul style="list-style-type: none"> Color of bark on stem of apical shoot has darkened to match that of mature bark. Some old growth needles (last year and beyond) have turned reddish in color, no insects are present.
December	31	Dec 14		<ul style="list-style-type: none"> Same as above